An-Najah National University

Faculty of Graduate Studies

DESIGN, SYNTHESIS, BIOACTIVITY AND MOLECULAR DOCKING OF IMIDAZOLONE DERIVATIVES HAVING HYDROPHILIC AND LIPOPHILIC FUNCTIONALITIES

By

Oswa Marwan Fares

Supervisor

Prof. Othman Hamed

This Thesis is Submitted in Partial Fulfillment of the Requirements for the Degree of PhD of Chemistry, Faculty of Graduate Studies, at An-Najah National University, Nablus, Palestine.

2025

DESIGN, SYNTHESIS, BIOACTIVITY AND MOLECULAR DOCKING OF IMIDAZOLONE DERIVATIVES HAVING HYDROPHILIC AND LIPOPHILIC FUNCTIONALITIES

By

Oswa Marwan Fares

This Dissertation was Defended Successfully on 07/ 05 / 2025 and approved by:

Prof. Othman Hamed	
Supervisor	Signature
Prof. Orwa Houshia	
External Examiner	Signature
Prof. Nidal Jaradat	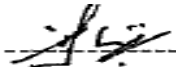
Internal Examiner	Signature
Dr. Mohyeddin Assali	
Internal Examiner	Signature

An-Najah National University

Faculty of Graduate Studies

DESIGN, SYNTHESIS, BIOACTIVITY AND MOLECULAR DOCKING OF IMIDAZOLONE DERIVATIVES HAVING HYDROPHILIC AND LIPOPHILIC FUNCTIONALITIES

By

Oswa Marwan Fares

Supervisor

Prof. Othman Hamed

In Accordance with An-Najah National University Deans Council Regulations for the award of Doctor of Philosophy, the following papers have been published after their extraction from the dissertation:

1. **Design, synthesis, anticancer properties, and molecular docking of imidazolone derivatives with lipophilic moiety.**

Dedication

To my esteemed supervisor, Prof. Othman Hamed for his unwavering guidance and support throughout this journey.

To my loving parents, Kareema and Marwan Fares, my brothers Dr. Anas, Dr. Osaid and Osama for their constant encouragement and belief in me that fueled my determination to see this thesis through. In particular, my mother who encouraged me to start this journey with inspiration and took care of my kids all along. To my husband for unending love, continuous support and help. To both of my sons, Omar and Wisam who really tried to help me sometimes and told me to study harder.

Finally, I would like to dedicate this thesis to everyone who has helped, supported, and encouraged me throughout my studies.

Acknowledgment

I extend my deepest gratitude to my supervisor, Professor Othman Hamed, for his unwavering support and insightful critiques throughout my research journey. His deep commitment to academic excellence and meticulous attention to detail have significantly shaped this dissertation.

I am grateful to Prof. Avni Berisha (Department of Chemistry, Faculty of Natural and Mathematics Science, University of Prishtina) for running the molecular docking.

Great thanks to Prof. Mohyeddin Assali (Pharmaceutical Chemistry and Technology Department, An-Najah National University) for performing the anticancer analysis. In addition to Prof. Ghaleb Adwan (Biology Department, An-Najah National University) for his huge help in the antibacterial study of the prepared compounds, and all the laboratory technicians for their great help.

I'm also very thankful to Prof. Haythem Saadeh (Chemistry Department, University of Jordan, Amman) for running the NMR characterization of the prepared compounds.

I am grateful to Prof. Mohammed Sabbah, for helping me in transferring the chemicals needed for my theses work from Nablus to the Faculty of Agriculture and Veterinary Medicine of An-Najah National University in Tulkarm to complete the laboratory work, as a result of Israeli attacks and hard checkpoints.

I would like to thank all the professors and teachers who taught me everything I know about chemistry from the bachelor's level up to the PhD.

Declaration

I, the undersigned, declare that I submitted the thesis entitled:

DESIGN, SYNTHESIS, BIOACTIVITY AND MOLECULAR DOCKING OF IMIDAZOLONE DERIVATIVES HAVING HYDROPHILIC AND LIPOPHILIC FUNCTIONALITIES

I declare that the work provided in this thesis, unless otherwise referenced, is the researcher's own work, and has not been submitted elsewhere for any other degree or qualification.

Student's Name: Oswa Marwan Hasan Fares

Signature: 

Date: 7/5/2025

List of Contents

List of Tables

List of Figures

List of Appendices

DESIGN, SYNTHESIS, BIOACTIVITY AND MOLECULAR DOCKING OF IMIDAZOLONE DERIVATIVES HAVING HYDROPHILIC AND LIPOPHILIC FUNCTIONALITIES

By

Oswa Marwan Fares

Supervisor

Prof. Othman Hamed

Abstract

The current chemotherapies available showed negative side effects leading to permanent damage to human organs. Therefore, finding an effective anticancer therapy with minimum side effects is a major challenge. In this work, two new series of imidazolones, one containing phenyl group (3a-g) and the other containing thiophene group (5a-g), were synthesized by a condensation cyclization of vanillin-based oxazolones with various amines.

The anticancer activity of the synthesized imidazolones was analyzed against four different cancer cell lines: liver cancer (HepG2), cervical adenocarcinoma (HeLa), colon cancer (CaCo-2) and breast cancer (MCF-7) cells. Imidazolone 3f with dodecyl chain exhibited the highest anticancer activity with IC_{50} value of 65.26 ± 3.2 µM against HepG2 and 20.02 ± 3.5 µM against MCF-7. Imidazolone 5g with thiophene and pyridyl group showed the highest efficiency among all tested derivatives with an IC_{50} value of 18.44 ± 2.3 µM and 5.96 ± 2.3 µM against Hela and CaCo-2 cells, respectively. Imidazolone 5b with chlorophenyl moiety displayed an IC_{50} value of 2.18 ± 0.7 µM and 5.51 ± 1.1 µM against HepG2 and Hela cells, respectively.

The pharmacokinetics and antitumor potential of the most active imidazolones were assessed through ADME and molecular docking. ADME properties emphasize favorable drug-likeness under Lipinski's guidelines, with molecular weights ranging from 357.43 (5d) to 468.65 g/mol (5f). Molecules 3g, 3f, and 5f show optimal hydrogen bonding, moderate bioavailability (0.55), and synthetic accessibility scores from 3.78 to 4.76. Docking studies with proteins 4MAN and 1HNJ highlight strong interactions for 3g, 3f, and 5f, with molecule 3g showing the best binding for 4MAN (-52.13 kcal/mol)

and 5f for 1HNJ (-38.63 kcal/mol). These results recognize 3g and 5f imidazolones as promising candidates for targeted cancer therapy.

In addition, antibacterial activity of the prepared oxazolones were examined. Oxazolone 8 containing 2-thiophenyl moiety was the most potent with an MIC of 500 µg/mL against all tested bacterial strains, including the most resistant *Staphylococcus aureus.* A combination of these oxazolones with commercial antibiotics can provide a synergetic effect to inhibit the bacterial growth at lower MIC values.

Keywords: Vanillin; Antitumor; Antimicrobial; Lipophilic; Imidazolone; Thiophene; ADME.

Chapter One

Introduction

1.1 Heterocycle Structures and Bioactivities

Heterocyclic compounds are defined as organic compounds having at least one ring with one or more heteroatom atom(s) such as nitrogen, sulfur, oxygen or phosphorous. The ring can be five- or six or seven-membered. The most common five-membered heterocyclic compounds are shown in Figure A1A of the appendix A including imidazole (1), pyrrole (2), furan (3) and thiophene (4) are composed of five-membered rings with one or two heteroatoms included.

Heterocyclic compounds represent about two-thirds of all the known organic compounds, and they gained special attention from chemists who generate selective synthetic methods to the huge variations of structural features related to this class (1). Heterocycles are also present in nature and produced by many plants. They are also found in nucleic acids, hormones, drugs, cellulose and related materials, in addition to many natural and synthetic dyes (2).

Chemists have shown that nitrogen and oxygen-containing heterocyclic compounds are the most famous compounds used in pharmacology as scaffolds for biologically interesting compounds. These heterocyclic compounds can be vitamins, herbicides, antifungals, antibiotics, and anti-cancer drugs (3). In fact, a large percentage of heterocycles are found in various medications, especially chiral heterocyclic compounds, which are intermediates for a number of chiral drugs (4).

Many interesting heterocycles can prevail in potential biological and pharmacological activities such as substituted indole, quinoxaline, pyridine, imidazopyridine, imidazolones, coumarin, imidazole, pyrimidines, pyrazines, quinolines, O-alkylated chromones and azaindoles derivatives.

For instance, pyridine derivatives like Tacrine are used for Alzheimer's disease; Enpiroline used as an antimalarial, Tedizolid and Ceftazidime act as antibiotics, also Axitinib, Imatinib and Lorlatinib are anticancer agents (5). Moreover, indole derivatives such as tryptophan, Vincristine, Serotonin, Bufotenine, Psilocybin, and Vinblastine have antipsychotic, antiviral and anticancer activities (6). The quinoxaline derivatives

provide antitumoral activity like Chlorosulfaquinoxaline, antiglaucoma activity like Brimonidine, and antibacterial activity such as Quinacillin activity (7). In addition, azaindole derivatives show cytotoxic activity as Variolins, and anti-HIV agents like Temsavir (8). Commercial drugs derived from imidazoles such as Alpidem, and Zolpidem provide anxiolytic and hypnotic activity (9). Derivatives of pyrimidine are potent anticancer agents like Doxazosin, antimicrobials like Rilpivirine, and antiretroviral agents such as Etravirine (10).

1.2 Nitrogen-based heterocycles

Nitrogen heterocyclic systems are cyclic compounds containing nitrogen as the main heteroatom of the ring. For example, pyridine is a six-membered ring which has one nitrogen atom. Nitrogen-containing heterocycles can be five-membered rings with two nitrogen atoms, such as imidazolones (5), or oxazolones (6) with nitrogen and oxygen atoms (Figure A1B, appendix A).

Nitrogen-containing heterocyclic compounds are very interesting for synthetic organic chemists as they occur in different natural products such as imidazole which is found in purine, histamine, histidine, and DNA structures (11). The nitrogen atoms in these heterocyclic molecules are the reason for their biological activity. They tend to allow them to interact firmly through H-bonding with biological macromolecules like proteins, enzymes and DNA (12, 13). These strong interactions ensure the significant biological and therapeutic properties of imidazole derivatives, leading to a diverse range of therapeutic drugs used for inflammation, cancer and infections. For instance, nitrogen-based heterocycles are used in synthetic drugs because of their ability to offer many pharmacological activities, such as anticancer, antimicrobial, antiviral, and anti-inflammatory properties (14).

In recent years, literature has shown a sharp growth on heterocycles emphasizing their increasing importance in the pharmaceutical field.

Imidazolone, which is the base of the present research, a unique class of nitrogen-containing heterocycles having various biological properties. Due to the pharmacological importance of imidazolones, this work has been planned to synthesize novel imidazolone derivatives and test their bioactivity. A brief account of oxazolones,

which are the starting material in imidazolones synthesis, in addition to imidazolones chemistry and biological importance have been highlighted in the following sections.

1.3 Oxazolones

1.3.1 Structure and chemistry of oxazolones

Oxazolone (6) or azlactone (Figure A1B, appendix A) is a five-membered heterocycle that consists of two oxygen atoms and one nitrogen atom as heteroatoms. They are classified as saturated 7 or unsaturated 8, like those shown in Figure A1C of appendix A. In general, the numbering the ring follows the Hantzsch–Widman rules, where the priority is for the oxygen atom, and the numbering direction continues toward the nitrogen atom.

Oxazolones can present in five structural isomeric forms (Figure A1D, appendix A), based on the location of a carbonyl group and the double bonds; these isomers include: 5(4H)-oxazolones (9), 5(2H)–oxazolones (10), 4(5H)-oxazolones (11), 2(5H)-oxazolones (12) and 2(3H)-oxazolones (13). The most significant isomer is the 5(4H)-oxazolones (15).

The 5(2H)-oxazolones have recently been discovered and are called "Pseudo oxazolones". Several research on 2(3H)- and 4(5H)-systems have also been reported. However, the 2(5H)-oxazolones were unknown. The main core of the oxazolone structure has been examined by X-ray diffraction, where the bond length within the ring are illustrated in Figure A1E of appendix A.

The core oxazole ring has six π-electrons in its aromaticity; all of its features illustrate that the electron delocalization is not complete, so it has little aromatic character. The oxazolone ring-opening is dominant in its chemistry rather than maintaining its type. 5(4H)- Oxazolones, the saturated isomers also known as 2,4-disubstituted 5-oxo-4,5-dihydro-1,3-oxazole, have been studied heavily. They show carbonyl and C=N absorptions at 1820 and 1660 cm^{-1} regions, respectively. Oxazolones derived from chiral α- amino acids can be obtained in optically active forms that can racemize readily.

The chemistry of oxazolones is amazing, focusing on 5(4H)–oxazolones illustrated in Figure A1F of appendix A. The nucleophiles can attack oxazolones at C-2 (imine carbon), but attacking the carbonyl carbon leads to fission of the carbonyl-oxygen link

and producing a-amino acid derivatives, which is more common. By way of the resonance stabilized anions, 5(4H)-oxazolones react with electrophiles at C-4 or, less commonly, at C-2, and they are considered as tautomeric 1,3-dipoles in cycloadditions (15).

1.3.2 Synthesis of oxazolones

Many different methods are available for oxazolones synthesis, the most common includes:

1.3.2.1 Erlenmeyer Synthesis

Friedrich Gustav Carl Emil Erlenmeyer performed the first Erlenmeyer reaction in 1893. A condensation occurred between benzaldehyde and N-acetyl glycine in the presence of acetic anhydride and sodium acetate. After the initial cyclization of this glycine, a Perkin condensation occurs, giving the desired azlactones (Figure A2A, appendix A) (16). The general mechanism of oxazolone formation is illustrated in Figure A2B of appendix A (17).

The earliest method to prepare oxazolone is the cyclodehydration condensation, where the reaction of a carbonyl compound with acyl glycine, and acetic anhydride can form the 5(4)-oxazolone (14) (Figure A2C, appendix A).

Various acyl glycines were used to form oxazolone including acetyl, benzoyl, and phenyl acetyl groups, but hippuric acid (N-benzoyl glycines) gave the highest yield and more stable compounds among all of them (18).

1.3.2.2 The Bergmann Synthesis

In this method, oxazolones are produced by the action of acetic anhydride on certain *α*--α-haloacyl amino acids. Bergmann and Stem found that acetic anhydride and pyridine react with N-chloroacetyl phenylalanines to give the 5(4)-oxazolone (15) like shown in Figure A2D of appendix A (19).

1.3.2.3 Dicyclohexyl carbodiimide (DCC) Method

The DCC method is carried out in chloroform, which causes a compound with amide and acid functionality to undergo cyclization to form oxazolone with a loss of water

molecule (Figure A3A, appendix A). This procedure has been used to prepare many optically active oxazolones (15).

1.3.2.4 Diversified Methods

As an example, the preparation of 2-oxazolin-5-one (17) is shown in Figure A3B of the appendix. The preparation was performed via reaction of isothiazolidinone derivative (16) with acetic anhydride-pyridine combination (20). Also, acid-catalyzed rearrangement of 2-azetidinone (18) yielded the 2-oxazolin-5-one (19) (Figure A3C, appendix A) (21).

1.3.3 Reactivity of oxazolones

The oxazolone ring has many reactive sites causing various transformation possibilities (Figure A4A, appendix A). The acidic proton(s) at C-4 (pK_a value about 9.0) of the oxazolone can react with a base to form the enolate of oxazole which can interact with different electrophiles. Alternatively, using Lewis acids with oxazolones form either the 1,3-dipole or the reactive ketene intermediate, each can be used in cycloaddition reactions for synthesizing new heterocyclic compounds. In addition, nucleophilic attack can open the oxazolone ring from the carbonyl group to give protected amino acids (22, 23).

According to literature, the ring opening of 2-phenyl-5(4H)-oxazolone using a nucleophile like water or simple alcohols happens in which an enzyme catalyzes the reaction. This oxazolone ring-opening formed the corresponding ester. The ring opening of oxazolones depends on the type of substituents at the C-2 and C-4 positions and on the nucleophilic alcohol used (24). Increasing the power of electron donating groups on the phenyl ring at C-2 position of oxazolones decreases the rate of ring opening (25). As a result, oxazolones are vital intermediates for preparing different compounds. Some of the most important examples are listed below:

1.3.3.1 Hydrolysis of azlactones

Oxazolones hydrolysis produces α-acylaminoacrylic acids, and this can be reduced to form α-amino acids (Figure A4B, appendix A). This method was commonly used to synthesize phenyl amines with 85% yield (26).

Hydrolysis of azlactones with amines and amino acids yields amides and dipeptide derivatives. The 2-oxazolin-5-one derivatives react more easily with primary amines than with secondary amines through ring opening at C5 of oxazolone, producing the amides with a good yield (Figure A4C, appendix A) (27).

1.3.3.2 Aminolysis of oxazolones

Generally, oxazolones react with amines at C-5, except for some 4-hetero methylene oxazolones. Most 5(4)-oxazolones react more readily with primary amines than secondary amines (28, 29). It was found that aminolysis (splitting the molecule to two smaller molecules using ammonia or amine) of 5(4)- oxazolone (20) with aromatic amines in benzene produced N-substituted cinnamides (21) (Figure A4D, appendix A) (15).

In addition, Kandile *et al* reported that the aminolysis of oxazolone with primary amines (H_2NR where R = NHPh, CH_2-Ph or Ph) can give the desired amides as shown in Figure A4E of the appendix (30).

1.3.3.3 Reaction with amino acids

Mohr and other researchers focused on using oxazolones in peptide synthesis producing compounds with antibiotics and antitumor activities (25). Oxazolones react with amino acids like acid anhydrides in behavior, using aqueous acetone as a solvent and sodium hydroxide to neutralize the released acid (Figure A5A, appendix A) (31-33).

1.3.3.4 Reaction with hydroxylamine hydrochloride

Hydroxylamine hydrochloride reaction with oxazolones occurs via carbonyl oxygen fission, then by cyclization. For example, the derivatives of 5(4)-oxazolone (22) were used to synthesize the 5-imidazolones (23) when reacting them with hydroxylamine hydrochloride as shown in Figure A5B of appendix A (34).

1.3.3.5 Alkylation reactions

Alkylation of saturated oxazolones was performed in anhydrous dimethylformamide or any aprotic solvent producing disubstituted oxazolones at position 4 (Figure A5C, appendix A) (35).

1.3.3.6 Friedel-Crafts reaction

The interaction of the derivative 5(4)-oxazolone (24) with benzene, m-xylene, chlorobenzene or toluene and using anhydrous aluminum chloride, produced the 2-Amino-3,3-diphenylpropanoic acid shown in Figure A5D, appendix A) (36, 37).

1.3.3.7 Oxazolones in synthesis of imidazolones

One of the most important applications of the oxazolone nucleus is converting it to heterocyclic compounds, specifically imidazolones (38). This synthesis can be done by reacting the oxazolone with various nitriles or nitrile derivatives. Many researchers follow this route like Huisgen and coworkers (39) also Bilodeau and Cunningham (40). For instance, oxazolones can react with alcoholic ammonia using potassium carbonate to prepare imidazolones (Figure A5E, appendix A).

1.3.4 Biological activities of oxazolones

Functionally substituted oxazolones have been reported as effective pharmacophores (41-44). Their bioactivities are influenced by the substituents on C-2 and C-4 positions (45, 46). For instance, the presence of a substituted (p-nitro) exocyclic phenyl group at C-4 position of the oxazolone ring has significantly increased the immunosuppressive activity (47).

In general, the biological activities of oxazolones include antibacterial activity (48), antidiabetic activity (49), anticancer activity (50), fungicidal activity (51), antifungal activity (52), urease inhibition activity (46), cardioprotective activity (53), immunomodulatory activity (54), anti-inflammatory and analgesic activity (55).

Some new synthesized oxazolone derivatives were reported as potent inhibitors of COX-2 enzyme but not so good against COX-1. Especially, compound 25 in Figure A6 of appendix A, which can inhibit the enzyme comparably to celecoxib, is used as a reference drug in the analysis. This study emphasized the fact that oxazolones can be studied for developing new effective anti-inflammatory agents (56).

Kus et al. synthesized and tested the antioxidant efficiency of 4-(substituted benzylidene)-2-(substitutedphenyl)oxazol-5(4H)-one derivative. The study focused on combating oxidative cellular damage, which contributes to the onset of cancers, cardiovascular diseases, and aging. The *in vitro* evaluation was done to estimate lipid

peroxidation inhibition and its impacts on hepatic cytochrome P450-dependent ethoxyresorufin-O-deethylase (EROD) enzyme in rats. They discovered that oxazol-5(4H)-one (26) (Figure A6, appendix A) as the most potent compound affecting microsomal EROD activity, surpassing the specific inhibitor caffeine.

In a separate investigation, Zhang and colleagues identified novel oxazolone derivatives functioning as insecticides that can stimulate nicotinic acetylcholine receptors. These N-substituted amino2(5H)-oxazolones, serving as agonists for nicotinic acetylcholine receptors (nAChR), demonstrated significant efficacy against hemipteran insect species. The most potent compound was 27, as illustrated in Figure 1.3K of the appendix, due to its comparable action with the standard imidacloprid that was used in the study. This work confirmed that compounds containing a small alkyl group, like ethyl, cyclopropyl and methyl exhibited maximum activity. The 2,2-difluoroethyl derivative showed less activity, but compounds with larger alkyl groups such as cyclobutyl, n-propyl and cyclopropylmethyl, had a severe loss of activity. The neonicotinoid class of chemistry is common for having physical properties that allow uptake into plants through systemic delivery, either by soil treatment or seed treatment. This study used a soil application of the prepared oxazolones and resulted in a comparable activity to the foliar application of these compounds (57).

Many commercially available effective drugs contain the oxazolone nucleus as the core of their activity. For example, the oxazolidinone antibiotic Posizolid works against phase 2 Tuberculosis (58). Also, Deflazacort has oxazolone moiety which showed immunosuppressive and anti-inflammatory properties (47). The ZHD-0501, a metabolite of the staurosporine (STA) analog which contain an oxazolone group that inhibits the proliferation of many murine and human tumor cell types (59). In addition, Jadomycin B is an antifungal antibiotic containing the 8H-benz[b]oxazolo[3,2]-phenanthridine pentacyclic scaffold formed from Streptomyces venezuelae bacterium ISP 5230 (60). Moreover, Phenacyl oxazolone involves the intramolecular Diels- Alder reaction, is used in preparation of pancratistatin which is an anticancer drug (61).

1.3.4.1 Antimicrobial activity of oxazolones

Bacterial infections have serious effects on health, which increase diseases and mortality. In particular, multidrug-resistant bacteria like VRE (vancomycin-resistant Enterococcus faecium), MRSA (methicillin-resistant Staphylococcus aureus), and b-lactamase-resistant Streptococcus pneumoniae (62). The severe infections resulting from these types of bacteria are considered a major issue in healthcare, and their treatment became a challenge because of antibiotic resistance dissemination (63). Therefore, discovering novel antimicrobial agents is essential in decreasing the spread of infections caused by drug-resistant bacteria.

Because of many different pharmaceutical activities of oxazolones, and since substituents changes are common procedures in medicinal chemistry for novel drug designs, many researchers had focused on synthesis and antibacterial studies of new oxazolone derivatives. Among these is the preparation of 4-(arylmethylidene)-2-phenyl/methyl-5(4H)-oxazolone derivatives and screening for antibacterial properties and the ability of urease inhibition. It was found that compound 28 (Figure A6, appendix A) demonstrated strong effectiveness, achieving 80% inhibition of Staphylococcus aureus and 70% inhibition of Salmonella typhi. However, the urease inhibition was not exhibited by all the compounds The SAR study found that the presence of phenyl group instead of a methyl group at C-2 plays a vital role in increasing the activity. Also, electron withdrawing groups at C-4 position are very good way to enhance the activity (46).

In addition, it was reported in the literature that the 2-phenyloxazol-5(4H)-one (29) (Figure A6, appendix A), in which using the groups 4-F, 4-Cl, 4-CH_3 and 3-Cl as substituents on the benzyl moiety showed amazing anti-bacterial properties on Escherichia coli and Bacillus subtilis (25).

In a recent study, a group of oxazolone derivatives were prepared by condensation of hippuric acid derivative and aromatic aldehydes with different substituents. After testing the antibacterial activity, it was observed that using hydroxy or nitro groups on the para position of benzene ring in 30 (Figure A6, appendix A) highly increased the antibacterial activity against *E. coli,* the same effect was found when the methoxy group was placed at the meta-position (64).

Lately, the literature reported the preparation and investigation of oxazoline-5-one (31) (Figure A6, appendix A), against the microbial strains *S. aureu*s, *E. coli, P. aeruginosa* and others. It revealed a notable efficacy against the Gram-positive and Gram-negative bacteria and exhibited inhibitory effects on biofilm formation in 42% of the microorganisms. The derivative has both bacteriostatic bactericidal effects with Minimum Inhibitor Concentration (MIC) values ranging from 6.25-3.12 mg/ml, and Minimum Bactericidal Concentration (MBC) values of 12.5-3.12 mg/ml (65).

1.4 Imidazoles and imidazolones

The most known bioactive nitrogen-containing heterocycles are the alkaloids of imidazoles (1) and imidazolones (5). The five-membered ring of imidazole ($C_3N_2H_4$) contains two nitrogen atoms at 1 and 3 positions that can also be named 1,3-diazoles. This imidazole ring occurs in many essential biological structures like histidine (32) and histamine related hormone (33) in Figure A7A of appendix A.

The imidazole ring is aromatic according to Huckel's rule as it has a planar structure, also the electron pair in p unhybridized orbital on nitrogen and 4 electrons of the remaining four atoms in the ring form a conjugated 6-electron system.

There are two tautomeric forms of imidazole, the 1*H*-imidazole and the 3*H*-imidazole, according to the position of protons on each nitrogen atom. Figure A7B in appendix A shows the imidazole resonance structures (66).

Imidazoline compounds that have an oxygen- nitrogen double bond at positions 1 and 3 and a carbon-oxygen double bond in positions 2, 4, or 5 are the keto dihydroimidazoles, known as oxoimidazolines or imidazolinone. They are highly polar and amphoteric compounds, having acid and base characters, leading to good solubility in aqueous media. Moreover, the electron-rich core of imidazolones causes them to easily accept and donate electrons, providing strong biochemical interactions with multiple targets within a cell (67).

According to the position of C=O (keto) groups, three isomers of imidazolinone can exist, which are given in Figure A7C of the appendix. The isomer 1-imidazol-5(4*H*)-one is a 5 membered heterocyclic ring system having N atoms at the first and third positions and a carbonyl group at the fifth position. It is also known as 5-oxo-imidazoline and can

exist in various bioactive natural products such as biotin, histamine, histidine, alkaloids and nucleic acids. This isomer is the most common structure due to its broad bioactivity (68). They have recently obtained a lot of attention due to their various uses in pharmaceuticals and metabolites (69).

1.4.1 Synthesis of imidazolones

In 1988, Hoffmann discovered the synthesis of 2-substituted-5-imidazolones, when heating *N*'-diacetyl-ethylene-diamine in the presence of a stream of dry HCl, he prepared 2-methyl-5-imidazoline (70). Ladenburg followed by reacting two equivalents of sodium acetate and one equivalent of ethylene diamine dihydrochloride to prepare the imidazolone derivatives (71).

As mentioned before, oxazolones are reactive heterocycles that can bind with different compounds like water, alcohols, thiophenols, hydrazinehydrates, phenyl hydrazines, aromatic aminoacids and ammonia. Oxazolones represent the intermediate stage in synthesizing imidazolones. Specifically, the oxazolones reactions with various substituted amines, hydrazines and amino acids. Various procedures have reported the preparation of imidazolines (72, 73). The most common method is the condens ation of substituted oxazolones with primary amines in dry media like pyridine, the preparation of different amides of acylamino acrylic acids were done (Figure A8A, appendix A).

It is worth noting that different factors can influence the imidazolone ring closure. For example, when R'=H, sodium hydroxide alone can turn the amide into the imidazolone (74). But when R'= $-CH_2R$, heating above the melting point is essential (75). In addition, substituted anilides where R'= $-C_6H_4R$ have been transformed to imidazolones by using phosphorus oxychloride. Benzoylphenylamine amide produces a very low yield, but benzoyl aminoisobutyric acid amide produces a good yield of imidazolone (76).

One of these reactions is when the derivative of oxazol-5(4*H*)-one (34) reacted with 5-(furan-2-yl)-1,3,4-oxadiazol-2-amine to synthesize eight compounds containing 1,3,4-oxadiazole ring binding with imidazole-5-one nucleus (Figure A8B, appendix A) (77).

The common method for the synthesis of N-amino-imidazol-5-one (35) compounds is by using hydrazine in pyridine. N. Kais Abood et al. used this procedure to prepare three imidazol-5-ones, which were then further used in the synthesis of 1,3,4-thiadiazole derivatives (Figure A8C, appendix A) (78).

Another method to prepare imidazolones is the aminolysis of azalactones, in acetic acid with suitable amines like shown in Figure A9A of appendix A (79).

Moreover, R. Suthakaran et al. synthesized imidazolone derivatives (36) in glacial acetic acid, by reacting the corresponding 5-oxazolones with ethane-1,2-diamine and heating the mixture (Figure A9B, appendix A) (80).

Srivastava et al. synthesized a biologically active group of 5- imidazolones by mixing equimolar quantities of substituted 5-oxazolinones with heterocyclic primary amines at 140 ºC (81). In another research, heterocyclic amines including pyridin-4-amine and pyrimidin-4-amine were reacted with oxazol-5(4*H*)-ones (37), preparing imidazol-5(4*H*)-one derivatives with pyridine (38) and pyrimidine rings (39), respectively like shown in Figure A9C of appendix A (82). In the work of S. Moorkoth, five novel imidazolones were prepared from 2-aminochromone and oxazol-5(4*H*)-one derivatives (40) (Figure A10A, appendix A) (83).

Novel oxazolones were successfully synthesized in good yield using benzoyl glycine and appropriate aldehydes, combined with a mixture of acetic anhydride and anhydrous sodium acetate. These oxazolones were then transformed into 5-oxo-imidazolines through fusion with substituted cinnamoyl hydrazine (Figure A10B in appendix A). (79).

1.4.2 Biological activities of imidazolones

Imidazolones have electronic-rich properties that enable them to bind with various enzymes, proteins, and receptors more effectively than other heterocycles (84). Moreover, the structural characteristics of the imidazole ring induce their capacity to make multiple drug-ligand interactions through hydrogen bonding, van der Waals forces, and hydrophobic interactions (85).

The 5-oxo-imidazolone derivatives are reported in the literature as biologically active compounds, either as rings for replacement of other rings or as substituent groups. The wide spectra of 5-oxo-imidazolones biological activity includes analgesic and anti-inflammatory (86-89), antibacterial (90-92), anticonvulsant (93), antimicrobial (94), antifungal and immunomodulatory (95), anthelmintic (96) and anticancer activities (97).

1.4.2.1 Antimicrobial activity

The sharp increase in multidrug-resistant microorganisms over recent years has emerged as a critical health concern. As a result, imidazolone derivatives were provided as possible candidates for new antibacterial and antifungal drugs due to their extensive range of biological activities. The antimicrobial effect of 5-imidazolones includes different levels of inhibition against both Gram-positive and Gram-negative bacteria. Specifically, 5-oxo-imidazoline derivatives containing electron-withdrawing groups on the aromatic ring at the C-1 and C-4 positions had achieved inhibition ranges of the standard drugs (Figure A11A, appendix A)(66).

Metha et al. reported in the literature the *in-vitro* antimicrobial study of newly prepared imidazolinones having benzimidazole moiety (Figure A11B, appendix A). The antibacterial analysis was conducted against Escherichia coli, Bacillus megaterium, Salmonella typhosa, Streptococcus citreus and Ampicillin, using norfloxacin and chloramphenicol standards. The antifungal activity was assessed against Aspergillus niger, with griseofulvin serving as the standard. The results confirmed that the most effective compounds contained 2-furyl, p-bromophenyl, p-chlorophenyl and 3,4-dimethoxy functionalities on the imidazolone heterocycle (98).

In addition, green synthesis and evaluation of antimicrobial activity for novel quinoline based imidazolone compounds were done by N.C. Desai *et* al. When these compounds were assessed against various bacterial strains, they found that compounds with electron withdrawing groups shown in Figure A11C of appendix A exhibited potent antibacterial activity in which their MIC values were 25 μg/mL) against the Gram-negative bacteria *E. coli*. Also, the hydroxy, nitro and phenyl containing analogues were discovered to have good effects comparable to the reference drug against *E. coli* (99).

In the work of Harshad *et al*., preparation of a novel series of 3'- quinolinyl substituted imidazole-5-one derivatives and studying the antimicrobial effects against *E.coli, B. Subtilis, B. Cereus, A. Parasiticus*, *S. rolfsii* was performed. Most of the derivatives in Figure A12A of appendix A showed moderate to strong antibacterial inhibition against the tested strains when compared to the reference drug ampicillin, while the derivative having R_1 = OCH3, R_2 = Ph, and X = N–CH_2CH_3 was noticed to exhibited potent influence against the bacterial species *E. coli* (100).

1.4.2.2 Anticonvulsant Activity

Sudha *et al*. illustrated the synthesis of a new substituted imidazolones group shown in Figure A12B of appendix A. They evaluated the *in vivo* anticonvulsant activity for these derivatives using the maximal electroshock (M.E.S) model with the standard phenytoin. The results indicated that compounds with electron withdrawing groups such as the nitro group at the para location of the aromatic ring showed excellent anticonvulsant activities close to the standard phenytoin (101).

Moorthy *et al* published novel imidazolinone analogues and studied their *in silico* metabolic and toxicity as effective anticonvulsant factors. It was noticed that the two compounds with maximal protection were compound 41 which has p-OCH_3 , p-OH on phenyl ring at the 4th positions of imidazolinone, in addition to compound 42 with p-OCH_3, o-Cl (Figure A12C, appendix A) (102).

In another research where Mohamad *et al*. prepared Imidazol-5(4*H*)-one (43) (Figure A13A, appendix A) with low neurotoxicity. They emphasized that compounds with benzylidene and furfurylidene groups at R^1 have potent protection versus seizures, while the anticonvulsant activity was less affected by substitutions of R^2 group (103).

1.4.2.3 Anti-Inflammatory and Analgesic Activity

Moustafa *et al*. observed the synthesis of a group of 5-4*H*-imidazolones with anti-inflammatory action close to the reference NSAIDs, but with low ulcerogenic side effects. Amazingly, compound 44 in Figure A13B of appendix A featuring a fluoro group at 4th position of the aryl ring was a strong anti-inflammatory agent similar to the meloxicam reference, and with lower ulcerogenic side effects at 10mg/kg on rats (87).

Moreover, novel compounds of imidazol-5(4H)-one revealed efficacy in carrageenan-induced paw and rats pleurisy edema models of acute inflammation. In particular, the derivative 45 (Figure A13C, appendix A) which has two methoxy groups showed the highest activity in comparison with other analogues. The inhibition percent value was very close to the standard drug ibuprofen (67.14%) (83).

1.4.2.4 Anthelmintic Activity

Yellasubbaiah *et al*. noticed the synthesis and *in vitro* anthelmintic activity of some new imidazolidinone derivatives (46) illustrated in Figure A13D of appendix A. Most compounds showed significant dose dependent anthelmintic activity at concentrations of 62.5 μg/ml, 125 μg/ml, 250 μg/ml, 500 μg/ml and 1000 μg/ml for the death of worms at a time comparable to albendazole standard (96).

Another anthelmintic investigation was done by Maneshwar *et al*. with derivatives 47 (Figure A13E, appendix A) that exhibited interesting stereoselective anthelmintic activities on earthworms by an *in vitro* study. It was concluded that compounds having electron-withdrawing moieties at the para position of the aryl ring, such as Cl, NO_2 had showed higher *in vitro* efficiency as anthelmintic agents (104).

1.5 Literature review, 5-imidazolones as anticancer agents

Cancer is a cellular disease that disrupts the normal mechanisms regulating growth and maintaining homeostasis. It is a significant public health issue, classified as the world's second leading cause of death, following cardiovascular disease. In 2015, approximately 8.8 million people died from cancer, according to the World Health Organization.

Continuous advancements in chemotherapy have led to an increase in the number of cancer survivors. However, these treatments can have damaging effects, as many survivors experience long-term negative medical side effects and psychological consequences related to their disease or treatment. In other words, they must cope with the physical side effects of cancer and its treatment, which can cause functional impairments, mental health challenges, and psychological as well as financial burdens. (105).

From 1949 to 2014, there have been 150 chemotherapeutic drugs approved by US FDA (106). More than 55% of these chemotherapies are composed of nitrogen-based heterocycles (azole) (107), like oxadiazole (108), quinoline (109), pyrimidines (110), imidazole (111) and imidazolones (112) and other more exhibited amazing anticancer activities. Currently, cancer treatments combine two or more of chemotherapeutic agents, surgery, radiotherapy, or hormonal therapy (113).

One of the common chemotherapeutic agents having the imidazolone nuclei is methotrexate (Figure A14A, appendix A), which is used to treat acute lymphoblastic leukemia, acute myeloid non-Hodgkin's lymphoma, leukemia, breast and bladder cancer. It acts by inhibiting DNA synthesis through stopping folate metabolism (114).

Despite the fact that the mechanism for initiating cancer is available, successful cancer therapies are not widely known. Consequently, effective treatments are essential to lower the deaths caused by cancer. Imidazole and imidazolone derivatives with multiple substitutions have various biological importance and chemical interest as well. To prepare safer anticancer molecules, chemists studied the possibilities of further changes to the heterocyclic structure of imidazolines and their effects on cancer cells, which is important as a result of their use in biological research.

Starting with pyridyl imidazolidinone derivatives which were synthesized and tested against Enterovirus 71 (EV71). It was found that compounds 48 and 49 in Figure A14B of appendix A are medically qualified as anti-EV71 agents (115).

It was reported in another study that the imidazolone derivative (50) (Figure A14C, appendix A) revealed a high anti-cancer efficiency with an inhibition percentage ranging from 30 to 98% (116). After that, a group of 5,5-diphenylimidazolidine-2,4-dione derivatives were created and evaluated as anticancer compounds. They identified that the cytotoxicity on HeLa cells was close to that of the chemotherapy medication Docetaxel (117).

Heba *et al*. worked on synthesizing and testing a group of imidazol-5(4H)-ones (51) for cytotoxicity in breast (MCF-7) and liver (HepG2) tumor cell lines. It was found that these compounds are moderately effective against HepG2 cells (IC_{50}= 10.9 to 15.8 μg/ml). However, their acetate derivatives (52) were less effective against MCF-7 and

HepG2 cells compared to the standard drug of vinblastine (Figure A15A, appendix A) (118).

In another study, 2- aminochromones imidazolones were prepared and studied by Sudheer *et al*. The *in vitro* cytotoxicity test on two cell lines showed that conversion to imidazolidinones raised the cytotoxic activity of aminochromone. Specifically, compound 53 (Figure A15B, appendix B) revealed a high activity with an IC_{50} value of 19.76 µg/ml. This work indicated that the compound which has two methoxy groups in its structure was the most promising (83).

Sudheer *et al*. presented the synthesis and cytotoxic activity of 2-aminoflavone analogues and their derivatives. The *in vitro* cytotoxicity studies on two different cell lines showed that these imidazolidinones generally increased the cytotoxic activity of the aminoflavone. Compound 54 in Figure A15C of appendix A revealed the most promising activity with an IC_{50} of 9.87 µg/mL (119). It is important to mention that the most dynamic compound is the one with two methoxy substituents in its structure.

New derivatives of 5-imidazolones were synthesized by Solankee *et al*. and their anticancer activity was tested. The structure of the most promising compound (55) is shown in Figure A15D of appendix A (120).

Pai and his group observed the synthesis and anticancer activity of different imidazolones. It was found that the *in vitro* anticancer activity of the compounds against cervical cancer cell lines (HeLa) has IC_{50} value of around 100. More precisely, compound 56 in Figure A16A of appendix A presented an IC_{50} value of 14.56 µg/mL compared to the standard Cisplatin (6.58 µg/ml). This good inhibitory influence was related to the presence of halogen-substituted thiazole ring on the imidazolone (121).

Recently, S. Abu-Jabal and coworkers had synthesized a new series of imidazolones that were tested against Hep3B and Hela cells. They found that the majority of the prepared imidazolones 57 with the substituents $-NH_2$, $-NO_2$, -COOH, -OH, -Br, -Cl (Figure A16B, appendix A) on the 4-position of a benzene ring revealed good anti-cancer action with low viability against normal human cells. They emphasized that the derivative containing NO_2 group at the fourth position of the benzene ring was the best, with an IC_{50} value of 134 µM against Hep3B cells, while the derivative with the pyridyl group had the lowest IC_{50} value of 85 µM against Hela cells. Moreover, using alkyl

sulfonate functionality in the imidazolone structure (Figure A16C, appendix A) enhanced their solubility in water and improved their bioactivity on the analyzed cancer cells. A molecular docking study for some of the synthesized imidazolone and sulfonate exhibited a significant docking score between -6.8 and -8.7 kcal/mol for protein structures (122).

In more recent work, Y. Sheta and her coworkers had synthesized two groups of imidazolones. After analyzing the anticancer influence of these compounds, they found that five derivatives of compound 58 in Figure A17A of appendix A have a potent growth inhibition activity versus MDA-MB-468, breast MCF-7, and non-small cell lung EKVX with IC_{50} range of 0.045–0.137 μM. It was clear from their work that increasing the carbon chain length connected to the thiol group at C-2 of imidazolone had raised the anticancer effect. The mechanistic pathways were also studied, which led to the result that all the tested compounds exhibited their anticancer action via binding with Chk1 and Chk2 binding sites. The most active derivative is the one with the longest R= C_4H_9, was also promoted EKVX cell cycle arrest at S phase by stimulation of the apoptotic approach (123).

Moreover, a novel published work in the literature focused on synthesizing of imidazolone sulfonamide- pyrimidine compounds and analysis of their potential anticancer effects as modified analogs for some known EGFR inhibitors. The cytotoxicity of the prepared hybrids was evaluated against the breast MCF-7 cancer cell line using doxorubicin (Dox) as standard. The results indicated that the derivative 59 drawn in Figure A17B of appendix A had the highest potent activity with an IC_{50} value of 1.06 mM, super passing Dox (IC_{50} =1.92 mM). Also, the mechanistic studies illustrated the ability of this compound to inhibit EGFR kinase. In addition, this compound has a significant increase in the proportion of apoptotic cells in comparison to the untreated standard (124).

Lately, novel derivatives of imidazolone (60), shown in Figure A17C of appendix A were synthesized as candidates for anticancer effects as modified analogs of some known EGFR inhibitors. Among them, three compounds with Ar= 4-OH-C_6H_4-, 2-furyl and 2-thienyl groups, presented strong antiproliferative activity and selectivity against tested tumor cells including hepatic (HepG2), breast (MCF-7), and prostate (PC-3) tumor cells with IC_{50} range of 5.35–27.29 μM and SI range of 2.49–11.93. After that,

Subsequent biological assays were conducted to elucidate their mechanism of action, revealing high efficiency in EGFR suppression with an IC_{50} range of 0.137–0.507 μM. The most effective EGFR inhibitor, featuring the 2-thienyl aromatic substituent, arrested the MCF-7 cell cycle at the S phase by inducing the apoptotic pathway, as evidenced by increased expression of Caspases and Bax, along with a decline in Bcl-2. Moreover, molecular docking showed a strong interaction between this effective derivative and the EGFR binding pocket (125).

1.6 Vanillin as a starting material

Vanillin, which is known chemically as 4-hydroxy-3-methoxybenzaldehyde (Figure A17D of appendix A), is a white to mildly yellow crystalline phenolic compound with a delightful scent, commonly used as a flavor enhancer in various products. It serves as the primary aromatic component in natural vanilla items. The tropical vanilla plant's pod or bean is where vanillin is derived from (126).

Vanillin can originate from both synthetic and natural sources. When derived from the seedpods of vanilla planifolia, the compound is initially bound to β-D-glucose and does not exhibit its flavor characteristics. During production, hydrolytic enzymes release free vanillin from the glucoside. Vanillin can also be synthesized from small natural compounds. Clove oil provides eugenol, which, through the oxidation of a vinyl group attached to the aromatic ring, transforms into vanillin. Similarly, vanillin can be produced from coniferyl alcohol which is found in spruce tree lignin and from ferulic acid that is found in rice. Interestingly, the vanillin precursor guaiacol is present in petroleum (126).

Fragments resembling vanillin are likely to be present in larger molecules. Through processes like metabolism, radiation, heat, and decomposition, vanillin can be released. For example, irradiating a curcumin solution results in the formation of free vanillin, feruloylmethane, and acetone. Moreover, vanillin is one of the metabolic products of curcumin (127).

Many researches indicates that moderate consumption of vanillin can significantly reduce the risk of liver and heart diseases. Nevertheless, it is essential to regulate the daily intake of vanillin in foods to be less than 10 mg/kg as recommended by the United

Nations Food and Agriculture Organization. Excessive consumption may lead to adverse effects, such as kidney and liver damage (128).

The vanillin molecule is composed of a benzene ring connected to an ether group, an aldehyde group, and a hydroxyl group. This specific chemical structure is responsible for its distinctive bioactive properties and its potential to be altered or combined with other substances to create various derivatives (129). These derivatives reduce adverse effects while enhancing the targeted delivery and release of the bioactive substance, managing dosage, and improving stability and bioavailability (130).

Vanillin is designed to form a molecule that can be easily modified to produce a wide range of derivatives due to its several unique groups. The original molecule undergoes changes when the hydroxyl or aldehyde groups engage in typical organic chemical reactions.

There are three main transformations possible in vanillin reactions: the modification of the aldehyde group, the alkylation of the hydroxyl group, and the formation of fused rings. The oxidative ring opening reactions of the vanillin molecule are also possible (131).

Conversely, complex derivatives like vanillin–hydrazone derivatives, Schiff-base and Mannich-base derivatives, vanillin-based pyrazoline derivatives, triazole-based vanillin derivatives, and vanillin hybrids are synthesized when the compound interacts with other substances (132). Vanillin can be incorporated into an existing biopolymer, leading to the development of promising vanillin-based biopolymers.

1.6.1 Biological activity of vanillin derivatives

Various chemicals can be combined with vanillin to create new composites with anti-inflammatory and anti-cancer properties. Numerous derivatives have already been successfully tested, including metal particles, metal oxides, paramagnetic nanoparticles, phenolic compounds, plant extracts, biopolymers, medications, and more. Given that the synthesized materials exhibit low toxicity and are biocompatible, the potential combinations are virtually limitless. This is the main reason leading the derivatives of natural compounds, particularly vanillin, to be anticipated to play a significant role in the pharmaceutical field (133).

Vanillin derivatives can be categorized into two main groups based on their functionality when combined with other molecules or in complexes. The first group involves derivatives where vanillin is either bound to or enclosed by another substance, aiding its transport into biological systems and targeted action. The second group consists of vanillin combined with other compounds to form complexes that serve as carriers for other drugs or bioactive substances (134).

Vanillin is extensively utilized in pharmaceutical products, including dietary supplements and food items. While it is primarily known for its taste and aroma, vanillin also possesses multiple biological activities including anticancer (133), antidiabetic (135), antioxidant (136), antibacterial (137) and antidepressant properties (138) that can be advantageous for human health. These observations suggest the prospects of a dual role for vanillin in food technology and therapeutic uses. Moreover, these great features are good indications that a thorough and holistic view of the compound and some of its derivatives is warranted, especially for potential application as a main component of functional food for health promotion.

Both in vitro and in vivo studies indicate that the anti-inflammatory properties of vanillin and its derivatives are primarily due to their role in regulating the expression of various genes, leading to decreased secretion of pro-inflammatory cytokines (IL-1β, IL-8, IL-6, TNF-a), reduced activity of the COX-2 and inducible nitric oxide synthase (i-NOS) enzymes, resulting in lower production of NO and prostaglandins, and increased secretion of anti-inflammatory cytokines (IL-4, IL-10, TGF-B). Given the interconnected nature of chronic inflammation, neurodegeneration, and cancer, these mechanisms not only offer neuroprotective benefits but are also vital in combating cancer cells.

The anti-cancer potential of vanillin and its derivatives is evident in their use as anti-cancer agents across various cancer types. The antimutagenic effects of 4-hydroxy-3-methoxybenzaldehyde is due to its effect on cell redox homeostasis and DNA repair pathways (139).

Furthermore, vanillin disrupts the normal growth and reproduction of bacteria, making it and its derivatives effective antibacterial agents (140, 141), with promising applications in wound healing. Although existing research strongly supports the benefits of vanillin, its low bioavailability limits human clinical trials (131).

1.7 Scope of this work

This investigation aims to develop novel imidazolone derivatives that exhibit high activity against certain cancer cell lines. The overall objectives of the current study are:

1. Design and synthesize two new classes of imidazolone derivatives, especially those with lipophilic moiety.
2. Analyze the structures of the compounds by spectroscopic means such as FT-IR, NMR (^{1}H and ^{13}C) and MS.
3. Study the anticancer activity and *in vitro* cytotoxicity of the prepared compounds against several types of tumor cells.
4. Analyze the ADME and molecular docking of the most potent imidazolone derivatives.
5. Study the antimicrobial activity of the prepared oxazolones.

1.8 Long-term Objectives

Providing pharmaceutical companies with some amounts of synthesized imidazolone derivatives for full-scale testing in large animal models, clinical studies, and subsequent development on a commercial level.

1.9 Novelty of this work

In this project, a method of synthesizing two novel groups of vanillin and 2-thiophenecarboxaldehyde based imidazolones was presented. The method describes a multistep process that involves reacting each of the vanillin and the 2-thiophenecarboxaldehyde with different commercially available reagents and aliphatic amine compounds.

The produced oxazolones are expected to reveal antimicrobial activities. Moreover, the new imidazolone derivatives are expected to be valuable drugs with various biological activities. These derivatives will be evaluated as anticancer agents. From an economic

point of view, there is a great financial benefit from using low-cost, safe, natural, and biodegradable starting material and reactants in synthesizing drugs.

In this research, a new series of natural product vanillin and 2-thiophenecarboxaldehyde -based imidazolone derivatives were synthesized as versatile bioactive compounds. To the best of our knowledge, these kinds of imidazolones have never been presented in the literature.

Chapter Two

Materials and Methods

2.1 Materials and Instrumentations

All materials used in this work were of analytical grade. Glycine, 2-thiophene carbonyl chloride, ethanol amine, butyl amine, dodecyl amine, N-methyl ethylenediamine, 2-chlorophenyl hydrazine hydrochloride, 2-bromophenyl hydrazine hydrochloride, 4-flourophenyl hydrazine hydrochloride, L-arginine, 2-picolylamine, tetrahydrofuran, ethanol, methanol, diethyl ether, hexane, ethyl acetate, acetic acid, acetic anhydride, anhydrous sodium acetate, sodium bicarbonate and hydrochloric acid were all purchased from Sigma-Aldrich (USA). Benzoyl chloride was purchased from RiedeldeHaen company (Germany). Vanillin was purchased from ThermoFischer company (Waltham, MA, USA).

A Melting Point SMP3 equipment (Stuart Scientific) was used to determine all melting points in Celsius (°C). IR spectra were collected using Nicolet iS5 FT-IR by Thermo-Fisher Scientific (Waltham, MA, USA). All NMR analyses were conducted with Bruker Avance, 500 MHz spectrometers (Fällanden, Switzerland) at the Chemistry Department (University of Jordan, Amman, Jordan). Compounds molar masses were measured using MS/MS by Thermo-Fisher Scientific LCQ Fleet ion trap mass spectrometer (Waltham, MA, USA). This analysis was executed in positive electrospray mode using a voltage of 5.0 kV with a gas flow of 30.0 units, a capillary temperature of 295.0 °C and an ionization time of 250.0 ms. The purification of synthesized compounds was achieved through flash chromatography, employing an eluting solvent mixture of EtOAc/hexane (4:6).

The materials needed for the antibacterial activity study include Mueller-Hinton agar (MHA), Nutrient broth, Eosin methylene blue agar (EMB), 0.5Mcfarland standard, sterile normal saline and sterile 20% Dimethyl sulfoxide (DMSO) solution. The bacterial strains used in this study are: *Staphylococcus aureus* ATCC 6538P, *Staphylococcus epidermidis* ATCC 12228, *Pseudomonas aeruginosa* ATCC 9027, *Escherichia coli* ATCC 25922and *Klebsiella pneumonia* ATCC 13883.

As for the anticancer activity evaluation, Hepatocellular carcinoma cell line (Hep3B) cells (HB-8064), Cervical adenocarcinoma (Hela) cells (CCL-2), Breast cancer (MCF-7) cells (HTB-22) and Colorectal cancer (CaCo-2) cells (HTB-37) were purchased from ATCC (Manassas, Virginia, USA), whereas normal liver cells (LX2) cells (SCC064) were purchased from Sigma-Aldrich (Jerusalem, Israel). Dulbecco's free Ca^{+2} phosphate-saline buffer (REF # 02-023-1A), Pen-Strep Solution (catalog #030311B), and L-glutamine solution (REF # 03-020-1B) were obtained from the Biological Industries (Jerusalem, Israel). Sigma Life Science provided us with a Trizma base (Lot SLBF2864V). The viability of cells was determined by the Cell Tilter 96 Aqueous One Solution Cell Proliferation (MTS) Assay (Promega Corporation, Madison, WI, USA). The cell lines were incubated using Esco CO_2 cell culture incubator. Also, an Accumax Variable micropipette with normal and long narrow gel loading tips was used. Eppendorf Thermo mixer (Eppendorf, Hamburg, Germany), PH/ORP meter (Hanna Instruments, Woonsocket, RI, USA), XB-30 Flak Ice maker (MRC laboratory-instruments, Harlow, UK).

2.2 Chemical synthesis and characterization

2.2.1 Preparation of benzoyl glycine (1)

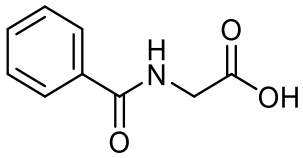

A mixture of benzoyl chloride (2.0 g, 14.2 mmol) and glycine (1.0 g, 13.2 mmol) was prepared in 10 mL water containing $NaHCO_3$ (10% by weight) using a 50 mL round bottom flask. Vigorous shaking of the mixture was conducted by a stirrer till the odor of the benzoyl chloride vanished. Then HCl (10%) was added dropwise to the reaction mixture to neutralize the $NaHCO_3$. The produced white solid material was collected by filtration under vacuum, rinsed with distilled water, and subjected to recrystallization in boiling water (30 mL). The produced solid was collected by vacuum filtration and dried at 65 °C in an oven under reduced pressure. Product weight was 1.68 g (yield 71.19%), m.p 187–189 °C (Lit m.p = 190.0 °C).

IR (ν cm^{-1}): 3340 (secondary amine, N-H stretching), 3068 (O-H stretching, carboxyl group), 2932–2780 (C-H, aliphatic), 1705 (C=O, carboxylic acid), 1665 (C=O, amide) 1602 (C=C, aromatic ring) Figure B1 (appendix B). ^{13}C NMR (500 MHz, DMSO) δ (ppm): 172.4 (O=C-OH), 166.8 (N-C=O), 131.4-127.5 (C_6H_5-), 41.6 (-C-NH). *m*/*z*: (M+) for $C_9H_9NO_3$ Calcd. 179.06, found 180.06.

2.2.2 Preparation of (Z)-4-(4-Hydroxy-3 Methoxybenzylidene)-2-Phenyloxazol-5-(4H)-One (2)

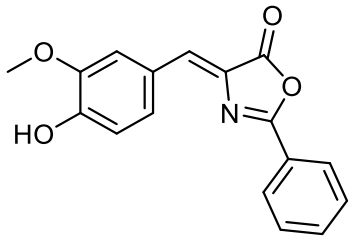

Vanillin (0.68 g, 4.46 mmol) and benzoyl glycine (prepared above, 0.8 g, 4.46 mmol) were suspended in a round bottom flask (25.0 mL) along with sodium acetate (0.4 g, 5.0 mmol) and acetic anhydride (6.0 mL, 14.0 mmol). The reaction mixture was stirred at 110 °C until vanillin disappeared as detected by TLC (2.5 h, then diluted with 15.0 mL ethanol and placed in a refrigerator for about 16.0 hr. The produced yellow precipitate was collected via suction filtration and dried under reduced pressure at 65 °C. The product mass was 0.90 g (yield 68.70%), m.p 190–192 °C (Lit m.p. 192–193 °C).

IR (ν cm^{-1}): 3632 (O-H, stretching, phenol), 1761 (C=O, lactone), 1655 (C=N, imine), 1606 (C=C, aryl**),** 1320–1270 (C-O and C-N) Figure B2 (appendix B). ^{1}H NMR (500 MHz, DMSO) δ (ppm): 9.80 (1H, s, OH), 8.11 (1H, s, vinylic), 7.59-7.51 (5H, m, aromatic), 7.28–6.94 (3H, m, aromatic), 3.89 (3H, s, methoxy) Figure B26 (appendix B). ^{13}C NMR (500 MHz, DMSO) δ in ppm: 167.1 (C=O, ester), 163.2 (C=N), 151.1, 142.0, 132.4, (126.2–130.1) (aryl), 56.3 (methyl). *m*/*z*: (M+) for $C_{17}H_{13}NO_4$ Calcd. 295.08, found 295.13.

Synthesis of imidazolones (compounds 3a to 3g), general procedure

A solution of amino compound (10 mmol) in tetrahydrofuran (30 mL) containing 2 drops of acetic acid was prepared in a 50 mL round bottom flask. Oxazolone **2** (10 mmol) was added to the amine solution. The produced mixture was refluxed at 90 ºC until the complete disappearance of compound **2** as the reaction followed by TLC, then

placed in a refrigerator until the solid stopped precipitating (about 4h). The produced solid was collected by suction filtration, dried at 60 °C under vacuum, and purified by flash chromatography.

2.2.3 Synthesis of (Z)-3-((2- bromophenyl)amino)-5-(4-hydroxy-3-methoxybenzylidene)- 2-phenyl-3,5-dihydro-4H-imidazol-4-one (3a)

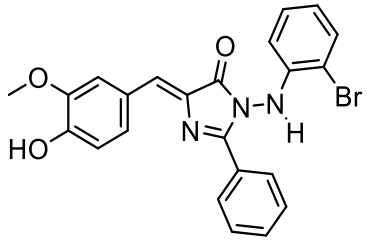

Following the general procedure for the synthesis of imidazolones, imidazolone 3a was prepared by reacting compound 2 with 2-bromophenylhydrazine, with a yield of 69.64%, m.p 98-101 °C and R_f 0.12 (Ethyl acetate).

IR (ν cm^{-1}): 3320 (O-H), 3055 (vinylic), 2930 (C-H, aliphatic), 1762 (C=O, amide), 1638 (C=N, imine), 1610 (C=C, aryl), 1320 (C-N), 1224 (C-O), 780 (C-Br) Figure B3 (appendix B). ^{1}H NMR (500 MHz, DMSO) δ (ppm) 9.48 (s, 1, OH), 9.27 (s, 1H, amine), 7.71 (2H, d), 7.6 (s, 1H, vinylic), 7.52-7.40 (m, 5H), 7.31-7.24 (m, 2H), 7.26 (m, 5H), 7.07 (d, 1H, J = 8.2 Hz), 6.9 (m, 2H), 3.87 (s, 3H, OMe) Figure B27 (appendix B). ^{13}C NMR (500 MHz, DMSO) δ (ppm): 169.2 (C=O, amide), 154.1 (C=N), 148.6 (Ar-OH), 148.0 (Ar-O), 141.7 (=C-N), 138.3 (N-C=O), 135.3-115.1 (C_6H_5-), 128.6 (Vinyl), 110.9 (C-Br), 56.2 (O-CH_3) Figure B28 (appendix B). *m/z*: (M+) for $C_{23}H_{17}BrN_2O_3$ Calcd.: 448.04, found: 448.12.

2.2.4 Synthesis of (Z)-3-((2-chlorophenyl)amino)-5-(4-hydroxy-3-methoxybenzylidene)-2-phenyl-3,5-dihydro-4H-imidazol-4-one (3b)

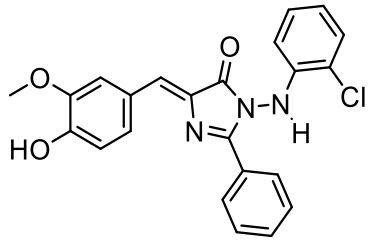

Following the general procedure for the preparation of imidazolones, imidazolone 3b was prepared by reacting compound 2 with 2-chlorophenylhydrazine. Brown product, yield of 74.63%, m.p =79.5-82 °C. R_f 0.36 (Hexane/Ethyl acetate, 6:4).

IR (ν in cm^{-1}): 3320 (O-H), 3053 (vinylic), 2930 (C-H, alipahtic), 1762 (C=O, amide), 1638 (C=N imine,), 1610 (C=C aryl), 1320 (C-N), 1224 (C-O), 760 (C-Cl) Figure B4 (appendix B). ^{1}H NMR (500 MHz, DMSO) δ (ppm) 9.51 (s, 1, OH), 8.71 (s, 1H, amine), 7.75 (2H, d), 7.6 (s, 1H, vinylic), 7.50-7.40 (m, 5H), 7.31-7.24 (m, 2H), 7.26 (m, 5H), 7.07 (d, 1H, J = 8.2 Hz), 6.5 (m, 2H), 3.90 (s, 3H, OMe) Figure B29 (appendix B). ^{13}C NMR (500 MHz, DMSO) δ (ppm): 165.5 (C=O, amide), 163.9 (N-C=N), 140.0 (C-OH, phenol), 150.9 (C, aryl), 134.1(Ar-Cl), 132.9–132.0 (=C-N), 132.3–128.4 (C_6H_5-), 56.1 (O-CH_3). *m/z*: (M+) for $C_{23}H_{17}ClN_2O_3$ Calcd.: 404.1, found: 444.3.

2.2.5 Synthesis of (Z)-5-(4-hydroxy-3-methoxybenzylidene)-3-(2- ydroxyethyl)-2-phenyl-3,5-dihydro-4H-imidazol-4-one (3c)

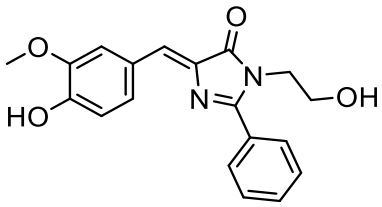

By following the general procedure for imidazolones synthesis, imidazolone 3c was prepared by reacting compound **2** with 2-aminoethanol. The beige-colored product was obtained in a yield of in a yield of 62.5%, m.p =167–169 °C. R_f 0.68 (Ethyl acetate).

IR (ν in cm^{-1}): 3340-3300 (O-H, aliphatic and phenol), 3045 (=C-H), 2932 and 2970 (C-H), 1766 (C=O, lactam), 1634 (C=N), 1610-1580 (C=C), 1320 (C-N), 1224 (C-O) Figure B5 (appendix B). ^{1}H NMR (500 MHz, DMSO) δ (ppm) 9.49 (s, 1H, OH), 7.7 (d,

2H), 7.6 (s, 1H, vinylic), 7.46 (m, 3H), 7.3 (m, 2H), 6.8 (d, 2H), 3.9 (d, 1H), 6.9 (m, 2H), 3.9 (t, 1H, OH), 3.82 (t, 2H), 3.7 (s, 3H, OMe), 3.6 (t, 2H) Figure B30a, B30b (appendix B). ^{13}C NMR (500 MHz, DMSO) δ (ppm): 169.9 (N-C=O), 156.0 (N-C=N), 148.5 (Ar-OH), 148.7 (Ar-O), 136.5 (=C-N), 134.2–116.7 (C_6H_5-), 59.4 (C-OH), 56.2 (O-CH_3), 45.0 (N-C-) Figure B31 (appendix B). *m*/*z*: (M+) for $C_{19}H_{18}N_2O_4$ Calcd.: 338.13, found: 338.36.

2.2.6 Synthesis of (Z)-5-(4-hydroxy-3-methoxybenzylidene)-3-(2-(methylamino)ethyl)-2-phenyl-3,5-dihydro-4H-imidazol-4-one (3d)

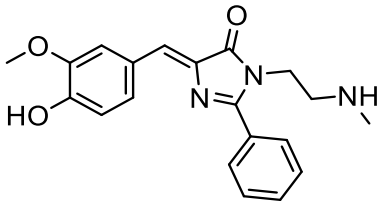

Following the general procedure for the synthesis of imidazolones, compound 3d was prepared by reacting compound **2** with N-methyl ethylenediamine. A pale-yellow product was formed in a 69.26% yield, m.p =116–118 °C. R_f 0.38 (Hexane/Ethyl acetate: 6:4).

IR (ν in cm^{-1}): 3345-3320 (O-H, and N-H, phenol and amine), 3052 (=C-H), 2938 and 2985 (C-H), 1766 (C=O, lactam), 1630 (C=N), 1610-1586 (C=C), 1322 (C-N), 1228 (C-O) Figure B6 (appendix B). ^{1}H NMR (500 MHz, DMSO) δ (ppm) 9.4 (s, 1H, OH), 7.75 (m, 3H), 7.5 (s, 1H, vinylic), 7.45 (m, 5H), 7.3 (m, 3H), 6.7 (d, 1H), 3.8 (s, 3H, OMe), 2.7 (t, 2H), 1.8 (t, 2H), 1.4 (m, 2H)., 1.05 (t, 3H) Figure B32 (appendix B). ^{13}C NMR (500 MHz, DMSO) δ (ppm): 169.5 (C=O, amide), 155.7 (C=N imine,), 148.7 (Ar-OH), 148.0 (C, Aryl), 136.6 (=C-N), 134.2–127.3 (Aryl), 56.2 (O-CH_3), 50.4 (C-N), 42.4 (Ar-C-N), 35.9 (N-CH_3) Figure B33 (appendix B). *m*/*z*: (M+) for $C_{21}H_{22}N_2O_3$ Calcd.: 350.16, found: 350.42.

2.2.7 Synthesis of (Z)-3-butyl-5-(4-hydroxy-3-methoxybenzylidene)-2-phenyl-3,5-dihydro-4H-imidazol-4-one (3e)

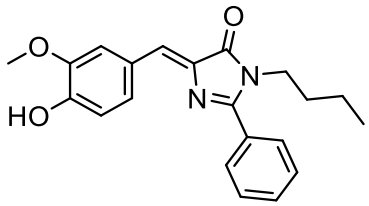

Appling the general procedure for preparing imidazolones, product 3e was prepared by reacting compound 2 with n-butylamine. A product with a beige color was formed 70.5% yield, m.p =177.5–180 °C. R_f 0.19 (Hexane/Ethyl acetate: 6:4).

IR (ν in cm^{-1}): 3335 (O-H, phenol), 3050 (vinylic), 2934 and 2975 (C-H, aliphatic), 1762 (C=O, amide), 1634 (C=N), 1612-1590 (C=C), 1320 (C-N), 1222 (C-O) Figure B7 (appendix B).^{1}H NMR (500 MHz, DMSO) δ (ppm) 9.35 (s, 1H, OH), 7.70 (m, 3H), 7.5 (s, 1H, vinylic), 7.5 (m, 5H), 7.3 (m, 3H), 6.7 (d, 1H), 3.8 (s, 3H, OMe), 3.3 (t, 2H), 1.7 (m, 2H), 1.5 (m, 18H), 0.8 (t, 3H) Figure 34a-34d (appendix B). ^{13}C NMR (500 MHz, DMSO) δ (ppm): 169.8 (N-C=O), 156.0 (N-C=N), 148.5 (Ar-OH), 148.8 (C-O, aryl), 136.4 (=C-N), 134.0–126.3 (Aryl), 56.1 (O-CH_3), 41.8 (-C-N), 30.4 (C-), 20.3 (-C-Methyl), 13.7 (CH_3) Figure B35 (appendix B). *m/z*: (M+) for $C_{20}H_{21}N_3O_3$ Calcd. 351.16, found: 351.41.

2.2.8 Synthesis of (Z)-3-dodecyl-5-(4-hydroxy-3-methoxybenzylidene)-2-phenyl-3,5-dihydro-4H-imidazol-4-one (3f)

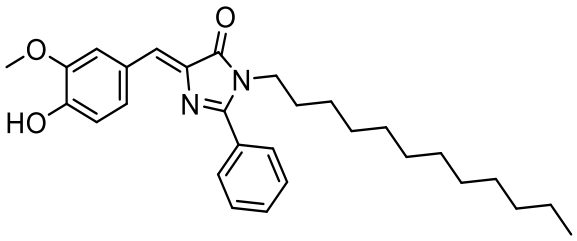

Following the general procedure for the synthesis of imidazolones, imidazolone 3f was prepared by reacting compound 2 with n-dodecyl amine. The orange product was formed in a 64.13% yield, m.p =109.5–111 °C. R_f 0.13 (Hexane/Ethyl acetate: 5:5).

IR (ν in cm^{-1}): 3330 (O-H, phenol), 3035 (vinylic), 2930 and 2982 strong (C-H, aliphatic), 1766 (C=O, amide), 1631 (C=N), 1610-1592 (C=C, aryl), 1326 (C-N), 1220 (C-O) Figure B8 (appendix B). ^{1}H NMR (500 MHz, DMSO) δ (ppm) 9.35 (s, 1H, OH), 7.70 (m, 3H), 7.5 (s, 1H, vinylic), 7.5 (m, 5H), 7.3 (m, 3H), 6.7 (d, 1H), 3.8 (s, 3H, OMe), 3.3 (t, 2H), 1.7 (m, 2H), 1.5 (m, 18H)., 0.8 (t, 3H) Figure B36a, B36b (appendix B). ^{13}C NMR (500 MHz, DMSO) δ (ppm): 175.8 (C=O), 168.6 (C=O, amide), 155.9 (C=N), 148.6 (Ar-OH), 147.8 (Ar-O), 135.5 (=C-N), 134.0–116.3 (C_6H_5-), 56.2 (O-CH_3), 41.5 (-C-N), 31.8-26.7 (-C-), 22.3 (-C-Methyl), 14.0 (CH_3) Figure B37 (appendix B). *m*/*z*: (M+) for $C_{29}H_{38}N_2O_3$ Calcd. 462.29, found: 462.63.

2.2.9 Synthesis of (Z)-2-amino-5-((amino(4-(4-hydroxy-3-methoxybenzylidene)-5-oxo-2-phenyl-4,5-dihydro-1H-imidazol-1-yl)methyl)amino)pentanoic acid (3g)

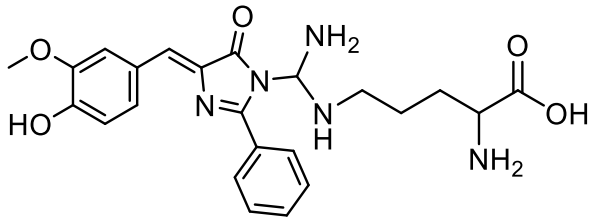

The amino acid L-arginine (3.0 mmol) was suspended in methanol (30 ml) followed by the addition oxazolone 2 (3.0 mmol). The mixture was stirred vigorously at room temperature for 24 hours. Then, the solvent was removed under a vacuum and the product was washed with water then, methanol, and diethyl ether. A beige-colored product was obtained a 61.76 % yield, m.p 160-162 °C. R_f 0.21(Ethyl acetate).

IR (ν in cm^{-1}): 3400 (O-H, acid), 3280 (O-H, phenol), 3035 (vinylic), 2930 and 2982 (C-H, aliphatic), 1716 (C=O, acid), 1638 (C=N), 1601-1509 (C=C, aryl), 1484 (C-N), 1220 (C-O) Figure B9 (appendix B). ^{1}H NMR (500 MHz, DMSO) δ (ppm) 11.82 (s, 1H, OH), 8.11 (s, 1H, NH), 7.64 (d, 1H), 7.5 (m, 5H), 7.23 (d, 1H), 7.17 (d, 1H), 3.96 (s, 2H) Figure B38 (appendix B). ^{13}C NMR (500 MHz, DMSO) δ (ppm): 171.0 (N-C=O), 158.4 (C=N), 148.9 (Ar-OH), 148.7 (Ar-O), 138.4 (=C-N), 134.1–125.3 (C_6H_5-), 82.9 (N-C-N), 55.95 (O-CH_3), 55.1 (-C-NH_2), 44.1 (-C-NH), 25.8 (-C-). *m*/*z*: (M+) for $C_{23}H_{27}N_5O_5$ Calcd. 453.20, found: 453.50.

2.2.10 Synthesis of 2-thiophenecarbonylglycine (4)

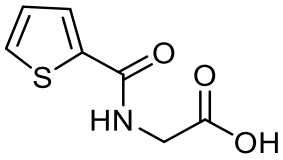

A mixture of 2-thiophenecarbonyl chloride (2.0 g, 13.7 mmol) and glycine (1.0 g, 13.2 mmol) was prepared in a 10% solution of sodium bicarbonate (10.0 mL). The reaction mixture was vigorously hand shaken until the odor of the 2-thiophenecarbonyl chloride disappeared. The reaction mixture was neutralized by the dropwise addition of HCl (10%). The produced solid material was collected by filtration under vacuum, rinsed with distilled water, and subjected to recrystallization in boiling water (30 mL). The white product of 2-thiophenecarbonylglycine was collected by suction filtration and dried at 65 °C in an oven under reduced pressure. The mass of the product was 1.7 g (yield 69.67%), m.p 121–123 °C.

IR (ν cm^{-1}): 3335 (N-H, stretching), 3268 (O-H, carboxyl group, stretching), 2932–2890 (C-H, aliphatic), 1704 (C=O, carboxylic acid), 1662 (C=O, amide), 1595 (C=C, thiophene ring) Figure B10 (appendix B). ^{13}C NMR (500 MHz, DMSO) δ (ppm): 172.8 (C=O, carboxyl), 164.3 (amide), 141.2 (=C-S),131.2-127.8 (Ar), 41.4 (-C-N) Figure B40a, B40b (appendix B).

- **General method for preparation of 2-thiophene oxazolone derivatives (compounds 5 to 10)**

A sample of specific aldehyde (5.0 mmol) was suspended in a round bottom flask (50.0 mL) containing acetic anhydride (6.1 mL, 15.0 mmol**)** and anhydrous sodium acetate (0.8 g, 10.0 mmol). 2-thiophenecarbonylglycine (4) (0.93 g, 5.0 mmol) was added to the suspension. The mixture was stirred at 110 °C until the aldehyde was consumed and the reaction was monitored by TLC (3.0 h). The reaction mixture was diluted with 15.0 mL ethanol and placed in a refrigerator for about 16.0 hr. The produced precipitate was collected by vacuum filtration, rinsed two times with ethyl ether and dried at 65 °C under vacuum.

2.2.11 Synthesis of (Z)-4-(4-Hydroxy-3-Methoxybenzylidene)-2- (thiophen-2-yl)oxazol-5-(4H)-One (5)

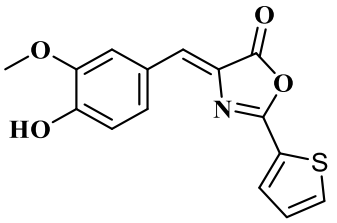

By following the general method for 2-thiophene oxazolones synthesis, a sample of vanillin (0.76 g, 5.0 mmol) was suspended in a 50 mL round bottom flask containing acetic anhydride (6.1 mL, 15.0 mmol**)** and sodium acetate anhydrous (0.8 g, 10.0 mmol). 2-thiophenecarbonylglycine (4) (0.93 g, 5.0 mmol) was added to the mixture. The reaction mixture was stirred at 110 °C until vanillin was consumed as shown by TLC (3.0 h). The reaction mixture was diluted with 15.0 mL ethanol and placed in in a refrigerator for about 16.0 hr. The produced yellow precipitate was filtered, rinsed two times with ethyl ether and dried at 65 °C under vacuum. The product mass was 1.02 g (yield 67.70%), m.p 199-201 °C. R_f 0.52 (Hexane/Ethyl acetate: 6:4).

IR (ν cm^{-1}): 3350 (O-H stretching, phenol), 1768 (C=O, lactone), 1652 (C=N), 1603 (C=C), 1318–1268 (C-O and C-N) Figure B11 (appendix B). ^{1}H NMR (500 MHz, DMSO) δ (ppm): 9.3 (s, 1H, OH), 7.76 (d, 1H), 7.6 (d, 1H), 7.40 (d, 1H), 7.38 (s, 1H), 7.30 (d, 1H), 7.30 (dd, 1H), 6.87 (d,1H), 3.72, (s, 3H). ^{13}C NMR (500 MHz, DMSO) δ (ppm): 167.1 (C=O, ester), 162.2 (C=N), 151.1 (Ar-O), 142.0 (Ar-OH), 134.4 (=C-N), (132.6–126.2) (aryl), 56.2 (O-CH_3). *m/z*: (M+) for $C_{15}H_{11}NO_4S$ Calcd. 301.3, Found 301.1, M+2 303.1.

- **Synthesis of 2-thiophene imidazolones (compounds 5a to 5g), general procedure**

In a round bottom flask (50.0 mL), a solution of compound 5 and an amine (10 mmol) in THF (25 mL) was prepared, and four drops of acetic acid were added to the solution and refluxed until the complete disappearance of compound 5 as shown by TLC. The reaction mixture was poured into 25 g ice and placed in the refrigerator until the solid stopped forming (2 hr). The reaction mixture was filtered and the collected solid was dried at 60 ^{o}C in an oven under vacuum and purified by flash chromatography.

2.2.12 Synthesis of (Z)-3-((2-bromophenyl)amino)-5-(4-hydroxy-3-methoxybenzylidene)-2-(thiophen-2-yl)-3,5-dihydro-4H-imidazol-4-one (5a)

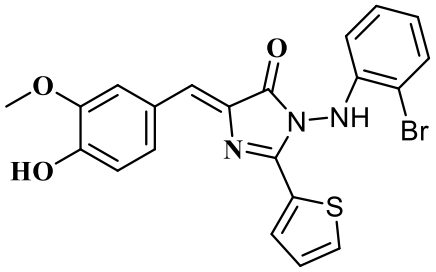

Following the general procedure for the synthesis of 2-thiophene imidazolone derivatives, imidazolone 5a was prepared by reacting compound 5 with 2-bromophenylhydrazine. The brown product was formed in 63.40% yield, m.p 160–162 °C. R_f 0.23 (Hexane/Ethyl acetate: 6:4).

IR (ν cm^{-1}): 3322 (O-H), 3057 (=C-H), 1763 (C=O, amide), 1641 (C=N, imine), 1604 (C=C, aryl), 1322 (C-N), 1227 (C-O), 782 (C-Br) Figure B12 (appendix B). ^{1}H NMR (500 MHz, DMSO) δ (ppm) 9.48 (s, 1, OH), 9.27 (s, 1H, N-H), 7.71 (2H, d, J = 8.6 Hz), 7.6 (s, 1H, vinylic), 7.5-7.4 (m, 5H), 7.3-7.2 (m, 2H), 7.26 (m, 5H), 7.1 (d, 1H), 6.9 (m, 2H), 3.87 (s, 3H, OMe) Figure B41a-B41c (appendix B). ^{13}C NMR (500 MHz, DMSO) δ (ppm): 167.7 (C=O, amide), 148.7 (Ar-OH), 148.5 (Ar-O), 146.7 (C=N), 142.4 (=C-NH), 138.5 (=C-S), 138.2 (C-N), 133.4-115.7 (Ar), 111.3 (C-Br), 56.3 (O-CH_3). *m*/*z*: (M+) for $C_{21}H_{16}BrN_2O_3S$ Calcd.: 469.01, Found: 462.21, (M+1 470.32).

2.2.13 Synthesis of (Z)-3-((2-chlorophenyl)amino)-5-(4-hydroxy-3-methoxybenzylidene)-2-(thiophen-2-yl)-3,5-dihydro-4H-imidazol-4-one (5b)

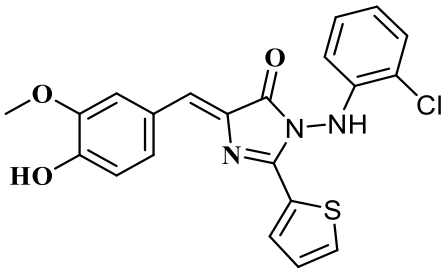

Following the general procedure for the synthesis of 2-thiophene imidazolones, compound 5b was prepared by reacting compound 5 with and 2-chlorophenylhydrazine. A brown colored product has a yield of 71.36%, m.p 92-94 °C. R_f 0.52 (Hexane/Ethyl acetate: 4:2).

IR (ν cm^{-1}): 3326 (O-H, phenol), 3057 (vinylic), 1761 (C=O, lactam), 1640 (C=N), 1603 (C=C), 1322 (C-N), 1218 (C-O) Figure B13 (appendix B). ^{1}H NMR (500 MHz, DMSO) δ (ppm) 9.48 (s, 1, OH), 9.27 (s, 1H, N-H), 7.71 (2H, d), 7.6 (s, 1H, vinylic), 7.5-7.4 (m, 5H), 7.3-7.2 (m, 2H), 7.26 (m, 5H), 7.07 (d, 1H), 6.9 (m, 2H), 3.87 (s, 3H, OMe) Figure B42a-B42d (appendix B). ^{13}C NMR (500 MHz, DMSO) δ (ppm): 167.8 (C=O, amide), 148.9 (Ar-OH), 148.1 (Ar-O), 146.7 (N-C=N), 138.5 (=C-S), 138.7 (=C-NH), 130.3-125.4 (Ar), 122.0 (C-Cl), 131.27–128.37 (C_6H_5-), 56.2 (O-CH_3). *m/z*: (M+) for $C_{21}H_{16}ClN_2O_3S$ Calcd.: 425.01, Found: 425.11, (M+2 427.32).

2.2.14 Synthesis of (Z)-5-(4-hydroxy-3-methoxybenzylidene)-3-(2-hydroxyethyl)-2-(thiophen-2-yl)-3,5-dihydro-4H-imidazol-4-one (5c)

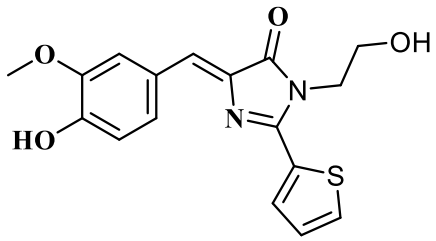

Following the general procedure for the synthesis of 2-thiophene imidazolone analogues, imidazolone 5c was prepared by reacting compound 5 with aminoethanol. The beige product was obtained in a 67.62% yield, m.p 117.5–119 °C. R_f 0.33 (Ethyl acetate).

IR (ν cm^{-1}): 3330 (O-H), 3051 (vinylic), 2932 (C-H, aliphatic), 1758 (C=O, amide), 1633 (C=N, imine), 1605 (C=C, aryl), 1322 (C-N), 1221 (C-O) Figure B14 (appendix B). ^{1}H NMR (500 MHz, DMSO) δ (ppm) 9.32 (s, 1, OH), 7.63 (d, 1H), 7.50 (s, 1H, vinylic), 7.45 (s, 1H), 7.38 (1H, d), 7.30 (m, 3H), 7.14 (dd, 1H), 4.12 (t, 2H), 3.84 (s, 3H, OMe), 3.78 (m, 2H), 3.54 9t, 1H, OH) Figure B43 (appendix B). ^{13}C NMR (500 MHz, DMSO) δ (ppm): 168.0 (N-C=O), amide, 161.8 (C=N, imine), 148.5 (Ar-OH), 148.7 (Ar-O), 136.9 (=C-S),136.4 (=C-N), 130.2–115.7 (Ar), 59.4 (C-OH), 56.2 (O-CH_3), 45.0 (N-C-) Figure B44 (appendix B). *m/z*: (M+) for $C_{17}H_{16}N_2O_4S$ Calcd.: 344.10, Found: 344.15.

2.2.15 Synthesis of (Z)-5-(4-hydroxy-3-methoxybenzylidene)-3-(2-(methylamino)ethyl)-2-(thiophen-2-yl)-3,5-dihydro-4H-imidazol-4-one (5d)

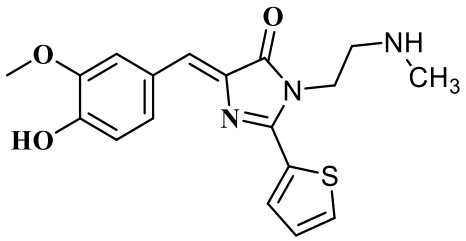

Following the general procedure for the synthesis of 2-thiophene imidazolones derivatives, imidazolone 5d was prepared by reacting compound 5 with N-methyl ethylenediamine. A brown solid was obtained in a 64.71% yield, m.p 79-81 °C. R_f 0.54 (Ethyl acetate).

IR (ν cm^{-1}): 3340-3330 (N-H and O-H), 3048 (vinylic), 2941 (C-H, aliphatic), 1756 (C=O, amide), 1631 (C=N, imine), 1604 (C=C), 1320 (C-N), 1220 (C-O) Figure B15 (appendix B). ^{1}H NMR (500 MHz, DMSO) δ (ppm) 9.32 (s, 1H, OH), 7.6 (d, 1H), 7.52 (s, 1H, vinylic), 7.43 (dd, 1H), 7.29 (m, 3H), 7.15 (t, 1H), 6.87 (d, 1H), 4.08 (t, 2H), 3.82 (s, 3H, OMe), 2.91 (t, 2H), 2.45 (d, H), 1.66, (t, 1H, NH) Figure B45a, B45b (appendix B). ^{13}C NMR (500 MHz, DMSO) δ (ppm): 167.7 (C=O, amide), 155.9 (C=N, imine), 148.7 (Ar-OH), 148.0 (Ar-O), 136.9 (=C-N), 136.4 (=C-S), 130.9–115.1 (Ar), 56.2 (O-CH_3), 50.4 (-C-N), 42.4 (Ar-**C**-N), 35.9 (N-CH_3). *m/z*: (M+) for $C_{18}H_{19}N_3O_3S$ Calcd.: 357.43, Found: 357.15.

2.2.16 Synthesis of (Z)-3-butyl-5-(4-hydroxy-3-methoxybenzylidene)-2-(thiophen-2-yl)-3,5-dihydro-4H-imidazol-4-one (5e)

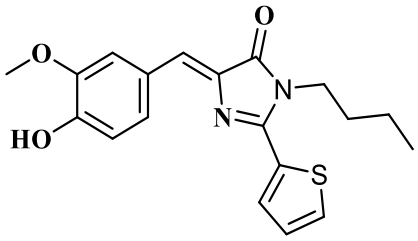

Following the general procedure for the synthesis of 2-thiophene imidazolones, compound 5e was prepared by reacting compound 5 with n-butyl amine. A white product was obtained in 68.17% yield, m.p 171-173 °C. R_f 0.16 (Hexane/Ethyl acetate: 6:4).

IR (ν cm^{-1}): 3334 (O-H), 3048 (=C-H, vinylic), 2942 (C-H, aryl), 1752 (C=O, amide), 1633 (C=N, imine), 1602 (C=C, aryl), 1321 (C-N), 1222 (C-O) Figure B16 (appendix B). ^{1}H NMR (500 MHz, DMSO) δ (ppm) 9.32 (s, 1, OH), 7.57 (d, 1H), 7.51 (s, 1H, vinylic), 7.42 (dd, 1H), 7.31 (m, 3H), 7.13 (t, 1H), 6.83 (d, 1H), 3.83 (s, 3H, OMe), 3.72 (t, 3H), 1.73 (t, 2H), 1.41 (m, 2H), 0.93 (t, 3H) Figure B46 (appendix B). ^{13}C NMR (500 MHz, DMSO) δ (ppm): 167.8 (C=O, amide), 156.1 (C=N), 148.5 (Ar-OH), 148.8 (Ar-O), 136.9 (=C-N), 136.3 (=C-S), 130.0–115.3 (Ar), 56.2 (O-CH_3), 41.8 (-C-N), 30.5 (-C-), 20.2 (-C-Methyl), 13.8 (CH_3) Figure B47 (appendix B). *m/z*: (M+) for $C_{19}H_{20}N_2O_3S$ Calcd.: 355.44, Found: 356.23.

2.2.17 Synthesis of (Z)-3-dodecyl-5-(4-hydroxy-3-methoxybenzylidene)-2-(thiophen-2-yl)-3,5-dihydro-4H-imidazol-4-one (5f)

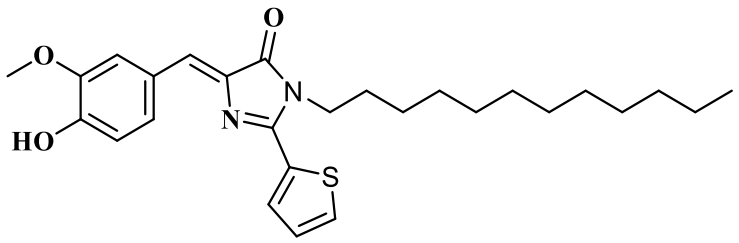

Following the general procedure for the synthesis of 2-thiophene imidazolone derivatives, imidazolone 5f was prepared by reacting compound 5 with n-dodecyl amine. The pale-yellow product was obtained in 72.55% yield, m.p 133–134.5 °C. R_f 0.21 (Hexane/Ethyl acetate: 6:4).

IR (ν cm^{-1}): 3330 (O-H, aryl), 3042 (vinylic), 2936 and 2868 (C-H, aliphatic), 1750 (C=O, amide), 1631 (C=N, imine), 1601 (C=C, aryl), 1323 (C-N), 1222 (C-O) Figure B17 (appendix B). ^{1}H NMR (500 MHz, DMSO) δ (ppm) 9.34 (s, 1, OH), 7.57 (d, 1H), 7.53 (s, 1H, vinylic), 7.42 (dd, 1H), 7.31 (m, 3H), 7.13 (t, 1H), 6.83 (d, 1H), 3.83 (s, 3H, OMe), 3.72 (t, 3H), 1.73 (t, 2H), 1.41 (m, 2H), 0.93 (t, 3H) Figure B48 (appendix B). ^{13}C NMR (500 MHz, DMSO) δ (ppm): 167.8 (O=C-N), 156.6 (N-C=N), 148.6 (Ar-OH), 147.8 (Ar-O), 136.9 (=C-N), 136.3 (=C-S), 130.9–115.3 (Ar), 56.2 (O-CH_3), 41.9 (-C-N), 31.8-26.5 (-C-), 22.7 (-C-Methyl), 14.1 (CH_3) Figure B49 (appendix B). *m/z*: (M+) for $C_{27}H_{36}N_2O_3S$ Calcd.: 368.66.44, Found: 368.78.

2.2.18 Synthesis of (Z)-5-(4-hydroxy-3-methoxybenzylidene)-3-(pyridin-3-ylmethyl)-2-(thiophen-2-yl)-3,5-dihydro-4H-imidazol-4-one (5g)

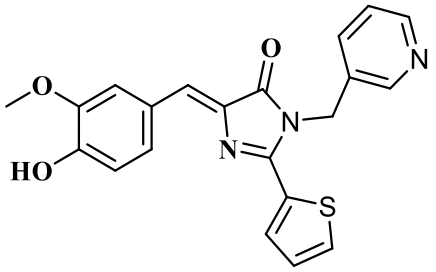

Following the general procedure for the synthesis of 2-thiophene imidazolones, compound 5g was prepared by reacting compound 5 with picolamine. The beige product was formed in a 73.06% yield, m.p 101–103 °C. R_f 0.71 (Ethyl acetate).

IR (ν cm^{-1}): 3332 (O-H), 3042 (vinylic), 2936 and 2868 (C-H, aliphatic), 1750 (C=O, amide), 1631 (C=N imine), 1601 (C=C, aryl), 1323 (C-N), 1222 (C-O) Figure B18 (appendix B). ^{1}H NMR (500 MHz, DMSO) δ (ppm) 9.36 (s, 1, OH), 8.50 (bs, 1H), 7.93 (bs, 1H), 7.54 (d, 1H), 7.44 (s, 1H, vinylic), 7.41 (dd, 1H), 7.25 (m, 3H), 6.85 (d, 1H), 5.27 (s, 2H), 3.85 (s, 3H, OMe) Figure B50 (appendix B). ^{13}C NMR (500 MHz, DMSO) δ (ppm): 168.6 (C=O, amide), 152.0 (C=N), 149.5 (C=N), 148.6 (Ar-OH), 147.8 (Ar-O), 136.9 (=C-N), 136.3 (=C-S), 130.9–115.3 (Ar), 56.2 (O-CH_3), 41.9 (-C-N), 31.8-26.5 (-C-), 22.7 (-C-Methyl), 14.1 (CH_3) Figure B51 (appendix B). *m*/*z*: (M+) for $C_{27}H_{36}N_2O_3S$ Calcd.: 391.45, Found: 391.76.

2.2.19 Synthesis of (Z)-4-(furan-2-ylmethylene)-2-(thiophen-2-yl)oxazol-5(4H)-one (6)

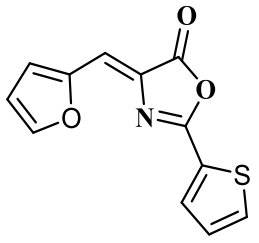

Following the general method for 2-thiophene oxazolones synthesis, product **6** was prepared by reacting furfural (0.48 g, 5.0 mmol) with compound 4. The produced precipitate was yellow with a yield of 68.29%, m.p 185-187 °C. R_f 0.77 (Hexane/Ethyl acetate: 4:2).

IR (ν cm^{-1}): 1770 (C=O, lactone), 1649 (C=N), 1603 (C=C), 1416-1313 (C-O and C-N), 1226 (C-S) Figure B19 (appendix B). ^{1}H NMR (500 MHz, DMSO) δ (ppm): 7.57 (d, 1H), 7.54 (d, 1H), 7.49 (d, 1H), 7.40 (d, 1H), 7.25 (dd, 1H), 7.11 (d, 1H), 7.09 (d, 1H), 6.87 (d,1H). ^{13}C NMR (500 MHz, DMSO) δ (ppm): 164.8 (C=O, ester), 152.5 (C=N), 145.4 (Ar-O), 134.3 (=C-N), (134.2–120.5) (aryl), 106.5 (-C=). *m*/*z*: (M+) for $C_{12}H_7NO_3S$ Calcd. 245.01, found 245.25.

2.2.20 Synthesis of (Z)-4-(pyridin-2-ylmethylene)-2-(thiophen-2-yl)oxazol-5(4H)-one (7)

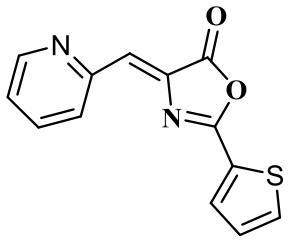

Following the general procedure for 2-thiophene oxazolones synthesis, product **7** was prepared by reacting 2-pyridinecarboxaldehyde (0.54 g, 5.0 mmol) with compound 4. The produced black precipitate was obtained in a yield of 71.09%, m.p 150-152 °C. R_f 0.76 (Hexane/Ethyl acetate: 4:2).

IR (ν cm^{-1}): 1711 (C=O, lactone), 1639 (C=N), 1524 (C=C), 1417-1373 (C-O and C-N), 1259 (C-S) Figure B20 (appendix B). ^{1}H NMR (500 MHz, DMSO) δ (ppm): 8.57 (dd, 1H), 7.80 (m, 2H), 7.72 (s, 1H, vinylic), 7.54 (d, 1H), 7.4 (d, 1H), 7.25 (m,2H). ^{13}C NMR (500 MHz, DMSO) δ (ppm): 166.5 (C=O, ester), 153.8 (C=N), 149.2 (=C-N), (137.3–121.7) (aryl). *m*/*z*: (M+) for $C_{13}H_8N_2O_2S$ Calcd. 256.03, found 256.28.

2.2.21 Synthesis of (Z)-2-(thiophen-2-yl)-4-(thiophen-2-ylmethylene)oxazol-5(4H)-one (8)

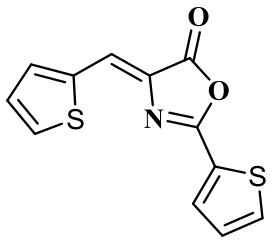

Following the general procedure for 2-thiophene oxazolones synthesis, product 8 was prepared via reacting 2-thiophenecarboxaldehyde (0.57 g, 5.0 mmol) with compound 4. The produced precipitate was greenish yellow with a yield of 70.23%, m.p 170-172 °C. R_f 0.70 (Hexane/Ethyl acetate: 4:2).

IR (ν cm^{-1}): 1795 (C=O, lactone), 1640 (C=N), 1564 (C=C), 1414-1372 (C-O and C-N), 1276 (C-S) Figure B21 (appendix B). ^{1}H NMR (500 MHz, DMSO) δ (ppm): 7.69 (dd, 1H), 7.64 (s, 1H, vinylic), 7.56 (dd, 1H), 7.50 (dd, 1H), 7.44 (dd, 1H), 7.26 (dd, 1H), 7,21(dd, 1H). ^{13}C NMR (500 MHz, DMSO) δ (ppm): 165.2 (C=O, ester), 152.5 (O-C=N), 141.1 (=C-S), 134.3 (=C-N), (136.3–128.4) (aryl), 124.9 (-C=). *m*/*z*: (M+) for $C_{12}H_7NO_2S_2$ Calcd. 260.99, found 261.31.

2.2.22 Synthesis of (Z)-2-(thiophen-2-yl)-4-(thiophen-3-ylmethylene)oxazol-5(4H)-one (9)

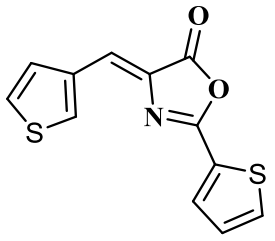

By following the general method for 2-thiophene oxazolones synthesis, product 9 was prepared by reacting 3-thiophenecarboxaldehyde (0.57 g, 5.0 mmol) with compound 4. The produced green precipitate has a yield of 72.52%, m.p 182-184°C. R_f 0.76 (Hexane/Ethyl acetate: 4:2).

IR (ν cm^{-1}): 1788 (C=O, lactone), 1648 (C=N), 1566 (C=C), 1414-1273 (C-O and C-N), 1248 (C-S) Figure B22 (appendix B). ^{1}H NMR (500 MHz, DMSO) δ (ppm): 7.69 (dd, 1H), 7.64 (s, 1H, vinylic), 7.56 (dd, 1H), 7.50 (dd, 1H), 7.44 (dd, 1H), 7.26 (dd, 1H),

7,21(dd, 1H). ^{13}C NMR (500 MHz, DMSO) δ in ppm: 165.8 (C=O, ester), 152.1 (O-C=N), 136.6 (=C-N), 130.7 (=C-S), (131.3–128.3) (aryl), 124.3 (-C=). *m*/*z*: (M+) for $C_{12}H_7NO_2S_2$ Calcd. 260.99, found 261.31.

2.2.23 Synthesis of (Z)-4-((4-bromothiophen-2-yl)methylene)-2-(thiophen-2-yl)oxazol-5(4H)-one (10)

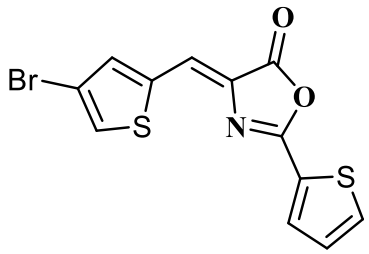

Following the general procedure for 2-thiophene oxazolones synthesis, product 10 was prepared via reacting 4-bromo-2-thiophenecarboxaldehyde (0.96 g, 5.0 mmol) with compound 4. The produced precipitate was greenish yellow with a yield of 64.71%, m.p 179-181 °C. R_f 0.54 (Hexane/Ethyl acetate: 4:2).

IR (ν cm^{-1}): 1780 (C=O, lactone), 1650 (C=N), 1568 (C=C), 1498-1359 (C-O and C-N), 1322 (C-S), 585 (C-Br) Figure B23 (appendix B). ^{1}H NMR (500 MHz, DMSO) δ (ppm): 7.83 (s, 1H), 7.7 (s, 1H, vinylic), 7.58 (d, 1H), 7.52 (d, 1H), 7.45 (dd, 1H), 7.26 (s, 1H), 7,23 (dd, 1H). ^{13}C NMR (500 MHz, DMSO) δ (ppm): 165.2 (C=O, ester), 152.6 (O-C=N), 134.6 (=C-N), 138.2 (=C-S), (134.1–128.4) (aryl), 124.1 (-C=), 115.6 (Ar-Br). *m*/*z*: (M+) for $C_{12}H_6BrNO_2S_2$ Calcd 338.90, found 340.21.

2.2.24 Synthesis of (Z)-2-phenyl-4-(thiophen-2-ylmethylene)oxazol-5(4H)-one (11)

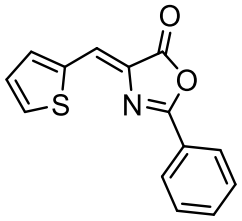

A sample of 2-thiophene carboxaldehyde (0.56g, 5.0 mmol) was suspended in a round bottom flask (50.0 mL) containing acetic anhydride (6.1 mL, 15.0 mmol**)** and anhydrous sodium acetate (0.8 g, 10.0 mmol). Benzoylglycine (1) (0.90 g, 5.0 mmol) was added to the suspension. The mixture was stirred at 110 °C until the aldehyde was consumed as the reaction was monitored by TLC (3.0 h). The reaction mixture was diluted with 15.0

mL ethanol and placed in in a refrigerator for about 16.0 hr. The yellow greenish precipitate was collected by vacuum filtration, rinsed two times with ethyl ether and dried at 65 °C under vacuum. The yield of the product is 60.94%, m.p 172-174 °C. R_f 0.74 (Hexane/Ethyl acetate: 4:2).

IR (ν cm^{-1}): 1789 (C=O, lactone), 1642 (C=N, imine), 1553 (C=C**),** 1326–1151 (C-O and C-N), 1051 (C-S) Figure B24 (appendix B). ^{1}H NMR (500 MHz, DMSO) δ (ppm): 7.85 (m, 2H), 7.70 (d, 1H), 7.66 (s, 1H, vinylic), 7.45 (m, 4H), 7.26 (dd, 2H).^{13}C NMR (500 MHz, DMSO) δ (ppm): 164.0 (C=O, ester), 161.6 (O-C=N), 141.0 (=C-S), (136.1–127.4) (aryl), 125.5 (-C=). *m*/*z*: (M+) for $C_{14}H_9NO_2S$ Calcd 255.04, found 255.29.

2.2.25 Synthesis of (Z)-2-phenyl-4-(thiophen-3-ylmethylene)oxazol-5(4H)-one (12)

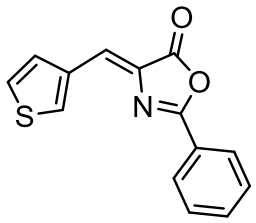

A sample of 3-thiophene carboxaldehyde (0.56g, 5.0 mmol) was suspended in a round bottom flask (50.0 mL) containing acetic anhydride (6.1 mL, 15.0 mmol**)** and anhydrous sodium acetate (0.8 g, 10.0 mmol). Benzoylglycine 1 (0.90 g, 5.0 mmol) was added to the suspension. The mixture was stirred at 110 °C until the aldehyde was consumed as the reaction was monitored by TLC (3.0 h). The reaction mixture was diluted with 15.0 mL ethanol and placed in in a refrigerator for about 16.0 hr. The yellow precipitate was collected by vacuum filtration, rinsed two times with ethyl ether and dried at 65 °C under vacuum. The yield of the product is 63.28%, m.p 180-182.5 °C. R_f 0.79 (Hexane/Ethyl acetate: 4:2).

IR (ν cm^{-1}): 1789 (C=O, lactone), 1649 (C=N, imine), 1554 (C=C), 1410–1338 (C-O and C-N), 1241 (C-S) Figure B25 (appendix B). ^{13}C NMR (500 MHz, DMSO) δ (ppm): 164.7 (C=O, ester), 161.6 (O-C=N), 136.0 (=C-N), 130.7 (=C-S), (131.1–127.4) (aryl), 125.5 (-C=). *m*/*z*: (M+) for $C_{14}H_9NO_2S$ Calcd 255.04, found 255.29. *m*/*z*: (M+) for C $C_{14}H_9NO_2S$ Calcd 255.04, found 255.29.

2.3 Antibacterial activity

The antibacterial activity of oxazolone derivatives (5 to 12) and the two promising imidazolones (3f and 3g) were tested using five bacterial strands. Two are gram-positive, which are *Staphylococcus aureus* and *Staphylococcus epidermidis*, and three gram-negative bacteria which are *Pseudomonas aeruginosa*, *Escherichia coli* and *Klebsiella pneumonia*.

2.3.1 Preparation of McFarland turbidity standard No. 0.5

In terms of barium sulfate standards, a 0.5 McFarland Standard corresponds to a bacterial suspension of 1.5 X 10^8 colony-forming units (CFU)/ml (142). A standard McFarland 0.5 turbidity was prepared by mixing 50 µl of a 1.175% (w/v) barium chloride dihydrate ($BaCl_2 \bullet 2H_2O$) solution with 9.95 ml of 1% (v/v) sulfuric acid. Then, the tube containing 0.5 McFarland standard was closed tightly using parafilm to avoid any evaporation and kept at room temperature in the dark. Prior to usage, the 0.5 McFarland standard was mixed vigorously using vortex mixer.

Three to four colonies of each bacteria species were placed in tubes that had 5.0-10 mL of sterile normal saline, the turbidity of the bacterial suspensions was modified to be in a similar turbidity of 0.5 McFarland standard with bacterial suspension of almost 1.5 x10^8 cfu/mL.

2.3.2 Determination of Minimum Inhibitory Concentration (MIC)

The values of MIC of oxazolone derivatives (compounds 5 to 12) in addition to 3f and 3g imidazolones were assessed using the broth microdilution technique in sterile 96-well microtiter plates, following the CLSI guidelines (143).

The compounds (800 µg/ml of 20% DMSO) and 20% DMSO (negative control) were two-fold serially diluted in nutrient broth in the wells of the plates in a final volume of 100µL. Then, a bacterial inoculum size of 10^4CFU/ml was added to each well. Negative control wells containing either 100µL NB only, or 100µL DMSO with bacterial inoculum, or the derivatives and nutrient broth without bacteria were included in these experiments. Each compound was analyzed in duplicate. After that, the microtiter plates were covered and kept in the incubator at 37°C for 24 h.

The MIC was considered as the lowest concentration of the compound that inhibited the bacterial growth. The values of MIC (μg/ml) are shown in Tables 4.5-4.9 (chapter four).

2.3.3 Determination of Minimum Bactericidal Concentration (MBC)

MBC was run only for the compounds whose wells showed inhibition to bacterial growth. In the MBC analysis, a 10 μL from these wells were taken by disposable inoculating loop and subcultured on MHA plates, followed by incubation at 37ºC for 24 hours.

The lowest concentration of these derivative that are needed to kill the bacterial strain was considered as MBC. Results of MBC are written in 4.3.2 (chapter four).

2.4 Anticancer activity

2.4.1 Cell lines and materials

The cytotoxicity of the prepared imidazolones (3a to g, and 5a to g) were evaluated on four various types of cancer cell lines including: liver cancer cells (HepG2), cervical adenocarcinoma cells (HeLa), colon cancer cells (CaCo-2), breast cancer cells (MCF-7) and normal liver cells (LX2). These cell lines were purchased from ATCC (Manassas, Virginia, USA). Dulbecco's free Ca^{+2} phosphate-saline buffer (REF # 02-023-1A), Pen-Strep Solution (catalogue #030311B), and L-glutamine solution (REF # 03-020-1B) were obtained from the Biological Industries. Sigma Life Science provided us with a Trizma base (Lot SLBF2864V). The viability of cells was determined by the Cell Tilter 96 Aqueous One Solution Cell Proliferation (MTS) Assay (Promega Corporation, Madison, WI, USA).

Esco CO_2 cell culture incubator was used to incubate the cell line. Also, an Accumax Variable micropipette with normal and long narrow gel loading tips was used. Eppendorf Thermo mixer (Eppendorf, Hamburg, Germany), PH/ORP meter (Hanna Instruments, Woonsocket, RI, USA), XB-30 Flak Ice maker (MRC laboratory-instruments, Harlow, UK).

2.4.2 Cell culture and cytotoxicity test

The cancer cells were cultured in 75 cm^2 plastic culture plates containing culture growth medium (CGM). The CGM consisted of Dulbecco's Modified Eagle Medium (DMEM) medium supplemented with 10% fetal bovine serum (FBS), l-glutamine, and penicillin/streptomycin. The plates were maintained at 37 °C in a humidified atmosphere containing 5% carbon dioxide (CO_2) to facilitate cell growth.

When the cells reached confluency in the 75 cm^2 culture plates, the CGM was aspirated. The cells were then rinsed twice with 15 mL of phosphate-buffered saline (PBS) devoid of Ca^{2+}. After that, 1 mL of trypsin was added to the cells, and the plate was incubated for approximately 3 min at 37 °C in a humidified atmosphere containing 5% CO_2.

After that, 10 mL of CGM was introduced to the plate in order to inactivate the trypsin. The cell suspension was then collected and diluted. The diluted cell suspension was distributed into a 96-well plate and allowed to adhere for 24 hours. Following the 24-hour adherence period, the cells in the 96-well plate were treated with 100 µL of a concentration range (62.5-2000 µM) dissolved in 1% DMSO solvent for all the compounds being studied, along with control and blank. The compounds were incubated with the cells for 48 hours.

After the incubation period, 20 µL of MTS (3-(4,5-dimethylthiazol-2-yl)-5-(3-carboxymethoxyphenyl)-2-(4-sulfophenyl)-2*H*-tetrazolium) solution was added to each well. The plate was then incubated for 2 h, and then, the absorbance of each well was measured using a plate reader.

Chapter Three

Results, Discussion and Conclusion

Imidazolone and its derivatives have garnered significant interest due to their varied pharmacological activities, especially their anti-tumor effects. The pharmacological activities include antimycobacterial, antifungal, anti-Parkinson, and antiviral. Several types of substituted imidazolones were synthesized and their bioactivities were evaluated and reported in the literature. But none of them reported imidazolone with lipophilic moiety. Motivated by these discoveries, we endeavored to create new imidazolones derivatives with various functionalities including those with fatty alkyl chain. These imidazolone were designed as anticancer agents, and their effectiveness against cervical cancer, breast cancer, and other cancer cell lines was assessed.

3.1 Synthesis of imidazolones (3a to 3g)

The method outlined in Figure 3.1 was followed in the synthesis of the imidazolones disclosed in this study. The synthetic route consisted of three steps, yielding between 61% and 74%. In the first step, glycine was reacted with benzoyl chloride, undergoing a condensation reaction to form hippuric acid (1). The second step of the synthesis route involved reacting hippuric acid with vanillin to produce oxazolone (2). The reaction was carried out using sodium acetate anhydrous and acetic anhydride as a dehydrating agent. The formation of oxazolone (2) occurs through condensation and cyclization that involves a loss of water molecule. The target imidazolones (3a to g) were synthesized from reacting oxazolone (2) with different primary amines. Amine compounds act as nucleophiles that perform a nucleophilic attack on the carbonyl group of oxazolone. This interaction leads to a series of reactions: first, the oxazolone undergoes ring opening, followed by condensation and dehydration, ultimately resulting in ring closure. The structures of oxazolone and imidazolones (3a to g) were confirmed using ^{1}H and ^{13}C NMR spectroscopy.

Figure 3.1

Synthesis of imidazolones (3a-g)

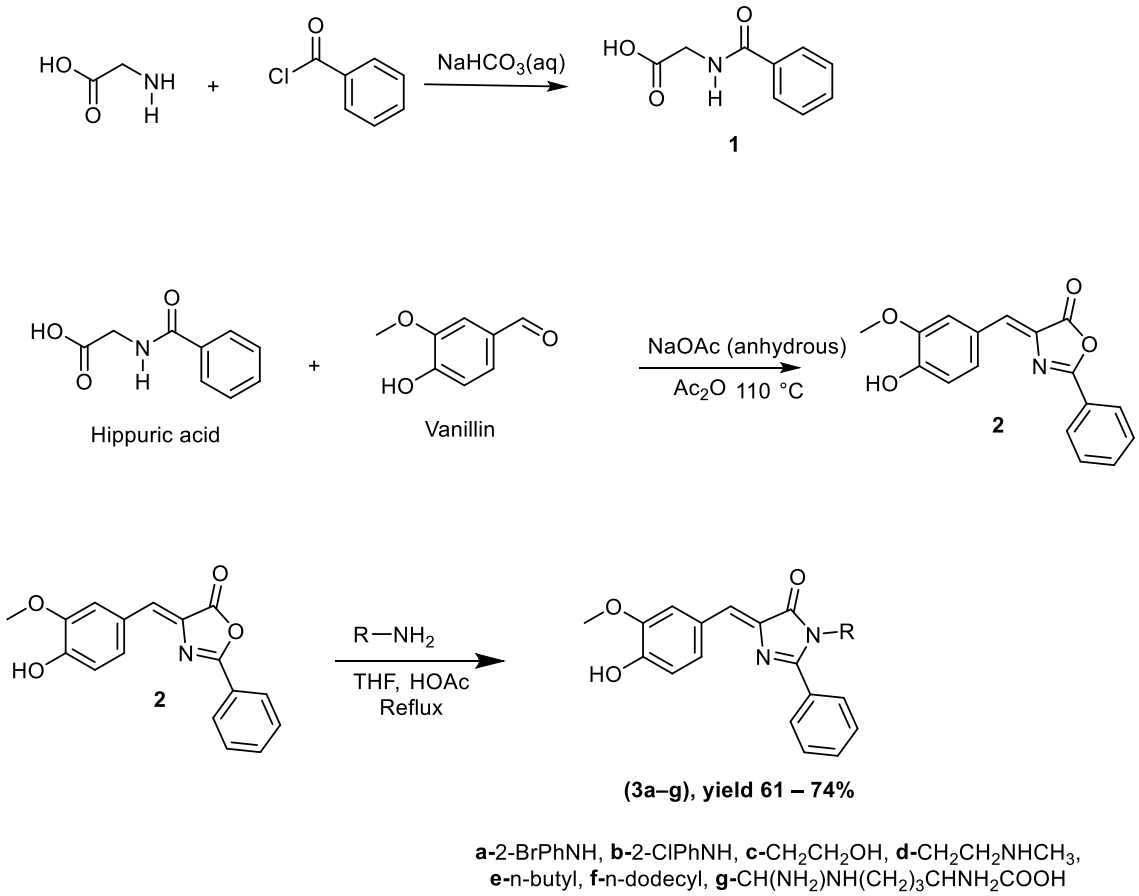

3.1.1 Reaction mechanisms

3.1.1.1 Preparation of benzoyl glycine (1)

The mechanism starts with a nucleophilic attack of glycine nitrogen at the electrophilic carbonyl carbon of benzoyl chloride. This forces the chloride (Cl^-) to leave as a good leaving group. The reaction is terminated by deprotonation to give the product 1 shown in Figure 3.2.

Figure 3.2

Mechanism of benzoylglycine (1) synthesis

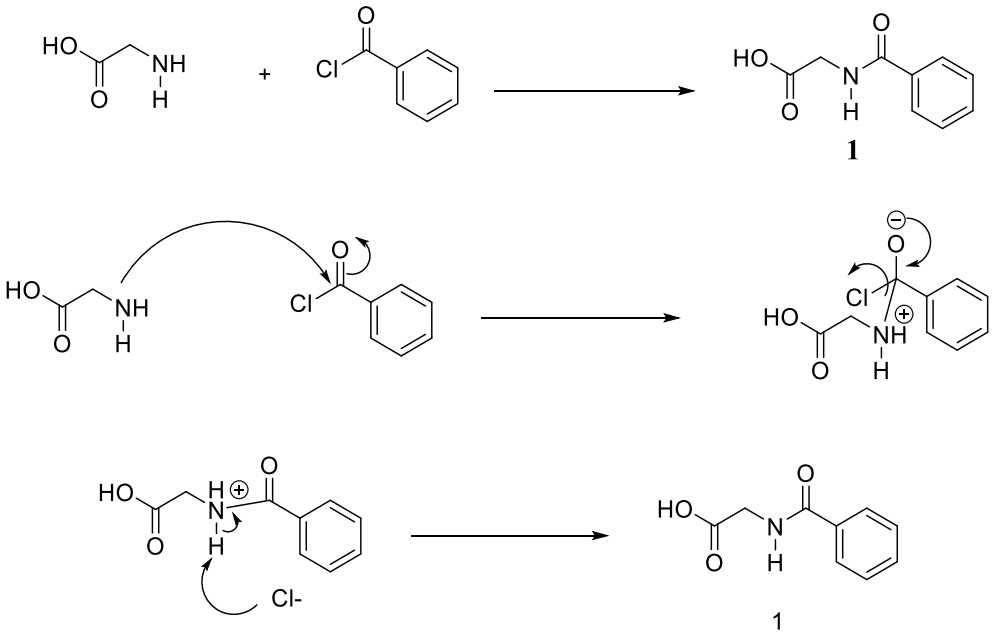

3.1.1.2 Chemical synthesis and characterization

In the first step, sodium acetate deprotonates the acid group in benzoylglycine to give carboxylate. The second step includes nucleophilic attack by carboxylate oxide on the carbonyl carbon of acetic anhydride and the leaving of the acetate group. After that, a proton transfer occurs to give the double bond (enol, tautomerization). Next, a condensation reaction occurs between the enol 13 and the aldehyde and a loss of water molecule forms the intermediate 14, which undergoes tautomerization to form imine-ol, which loses OH acidic proton producing 15, and undergoes intra S_N2 and form the final oxazolone product (Figure 3.3).

Figure 3.3

The mechanisms of oxazolone (2) synthesis

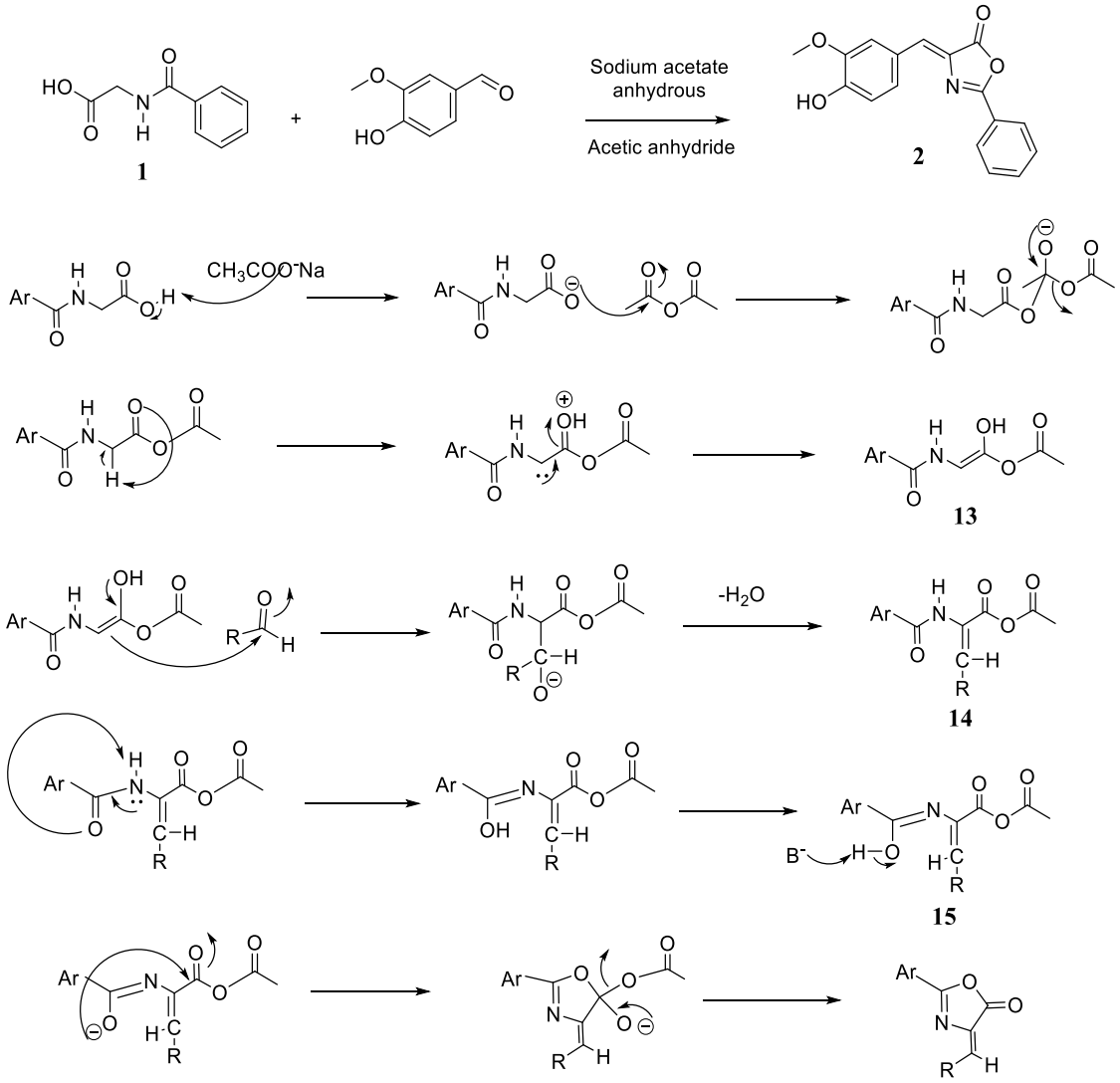

3.1.1.3 Synthesis of imidazolones (3a to 3g)

The mechanism starts with the lactone carbonyl protonation to give 16, the protonation creates stronger electrophilic carbon, where the nucleophile amine attacks this carbonyl group in 16 forcing it to undergo ring opening to form intermediate 17 having amide and hydroxyl groups. After that, a condensation cyclization occurs when the hydroxyl group of 17 is protonated causing a loss of water molecule to form 18. Next, the amide's nitrogen makes nucleophilic attack on *sp* carbon of 18 followed by deprotonation resulting in ring closure and producing the imidazolone as illustrated in Figure 3.4.

Figure 3.4

Mechanism of imidazolones (3a-g) synthesis

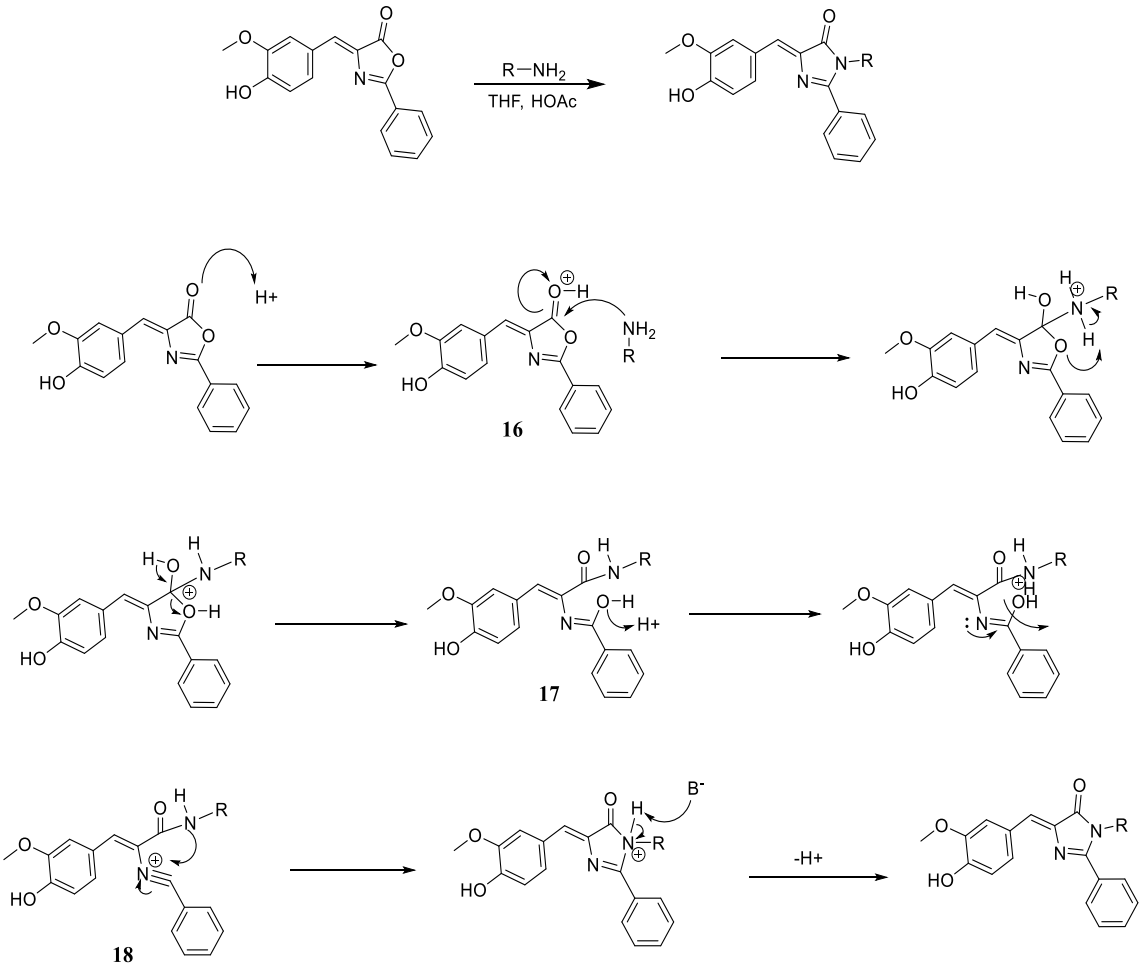

3.1.2 Anticancer activity

The synthesized imidazolones (3a-g) were submitted to the pharmaceutical department at An-Najah University (Nablus, Palestine) for analyzing their anticancer activity against four cancer cell lines which are: liver cancer cells (HepG2), cervical adenocarcinoma cells (HeLa), colon cancer cells (CaCo-2), breast cancer cells (MCF-7) and normal liver cells (LX2).

The *in vitro* anticancer screening involved testing four doses against the five selected cell lines using a concentration of imidazolones that is four series of two-fold dilutions from a stock solution with 1000 µg/mL (500.0, 250.0, 125.0 and 62.5 µg/mL). The tumor cell lines were incubated for 48 hours. All screening tests were performed in triplicate, and the average value was reported. The values of IC_{50} (concentration needed

to kill 50% of cancer cells) were determined for each cell line and summarized in Table 3.1.

Table 3.1

Values of IC_{50} (μg/mL) for imidazolones (3a-g) on various cancer cells (HepG2, MCF-7, CACO-2, HeLa) and LX-2 normal cell

Imidazolone	IC_{50} values (μg/mL)				
	HepG2	HeLa	CaCo-2	MCF-7	LX-2
3a	1484.73	292.44	57.91	115.28	238.81
3b	163.46	151.34	21.04	98.41	154.32
3c	175.41	768.70	50.83	427.25	183.18
3d	210.93	36.57	24.68	178.38	125.19
3e	449.57	125.36	109.75	574.18	54.29
3f	65.26	111.85	96.89	20.02	69.49
3g	461.82	251.79	261.75	715.27	124.23

The viability data for the four tested cancer cells and normal LX-2 cells was collected in Figure A18 of appendix A. It is observed that compounds 3a and 3b have selective activity on colorectal cancers (CaCo-2) with IC_{50} 57.91 and 21.04 μM, respectively. These two imidazolones have almost similar substituents which are the 2-chloro and 2-Bromophenyl amines. However, compound 3b with 2-chloro phenyl amine group provides a higher potency in comparison to the bromo derivative. Compound 3c with ethanol amine also showed selective activity on the CaCo-2 cells with IC_{50} equal to 50.83 μM. Compound 3d has the N-methyl ethylene diamine group exhibiting anticancer activity on both the colorectal cancer cells as well as cervical cancer cells with IC_{50} equal to 36.57 and 24.68 μM, respectively. The most potent derivative on all tested cancer cells was 3f with a dodecyl group and the highest activity was on the breast cancer cells (MCF-7) with IC_{50} 20.02 μM. This could be attributed to the hydrophobic nature of the dodecyl group that could enhance the cancer cell membrane penetration (144). Compound 3e with butylamine functionality showed moderate activity on HeLa and CaCo-2 cells. However, compound 3g showed the least anticancer activity against HeLa and CaCo-2 cells. This could be attributed to the high hydrophilic group substitution which could reduce the possibility of cancer cell penetration.

3.2 Preparation of imidazolones (5a to 5g)

Imidazolones (5a to 5g) were prepared using the method illustrated in Figure 3.5. The procedure includes three steps with a total yield ranging between 63% and 73%. It begins with a condensation reaction of glycine and 2-thiophenecarbonylchloride to produce 2-thiophenecarbonyl glycine (4). The second step involved reacting 2-thiophenecarbonyl glycine with vanillin in the presence of anhydrous sodium acetate and acetic anhydride as a dehydrating agent to produce the oxazolone (5). Different aldehydes were also used to prepare a series of various oxazolones in this study. The formation of oxazolone (5) occurs via condensation and cyclization that involves a loss of water molecule. The desired imidazolones (5a to 5g) were prepared by reacting oxazolone (5) with different hydrazines and primary amines. The amine compounds work as nucleophiles that make a nucleophilic attack on the carbonyl group of oxazolone causing it to undergo a ring opening, followed by condensation, dehydration and ring closure. The structures of oxazolones (5-10) and imidazolones (5a to g) were confirmed by ^{1}H and ^{13}C NMR.

Figure 3.5

Synthesis of imidazolones (5a-g)

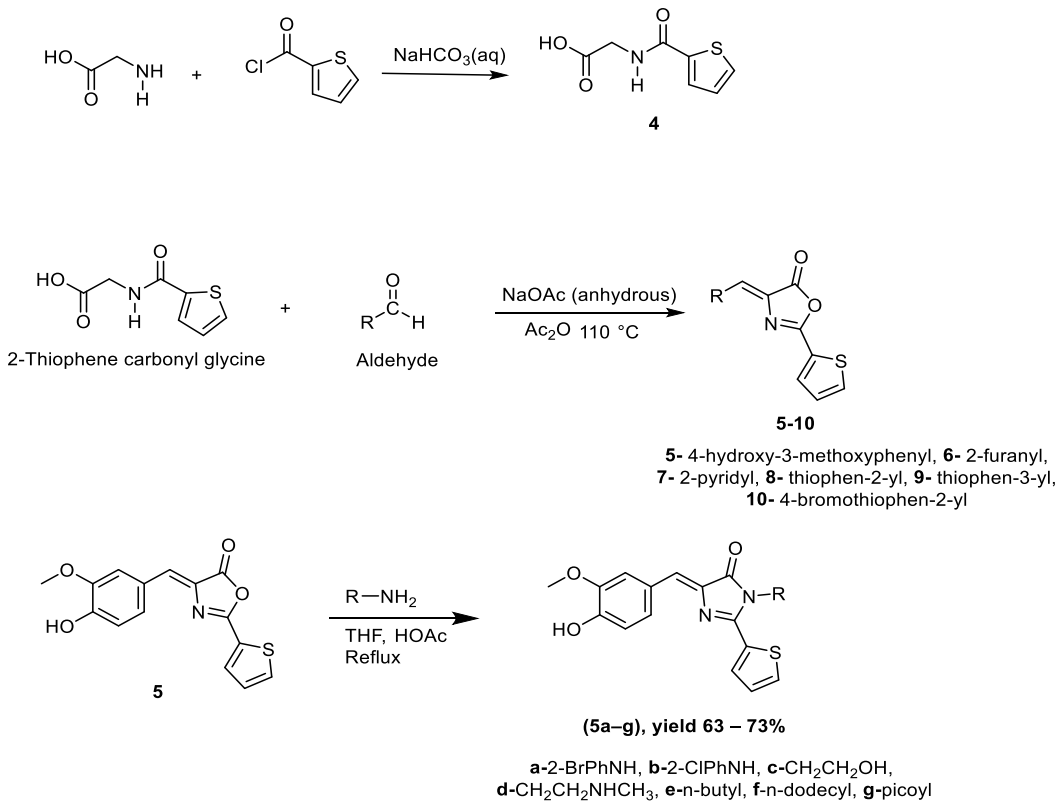

3.2.1 Mechanism of reactions

3.2.1.1 Synthesis of 2-thiophenecarbonyl glycine (4)

The first step is the nucleophilic attack of the glycine nitrogen on the electrophilic carbonyl carbon of 2-thiophenecarbonyl chloride, which causes the chloride (Cl^-) to act as a good leaving group. The reaction is finished by deprotonation which gives the product (4) (Figure 3.6).

Figure 3.6

Reaction mechanism for synthesis of 2-thiophenecarbonyl glycine (4)

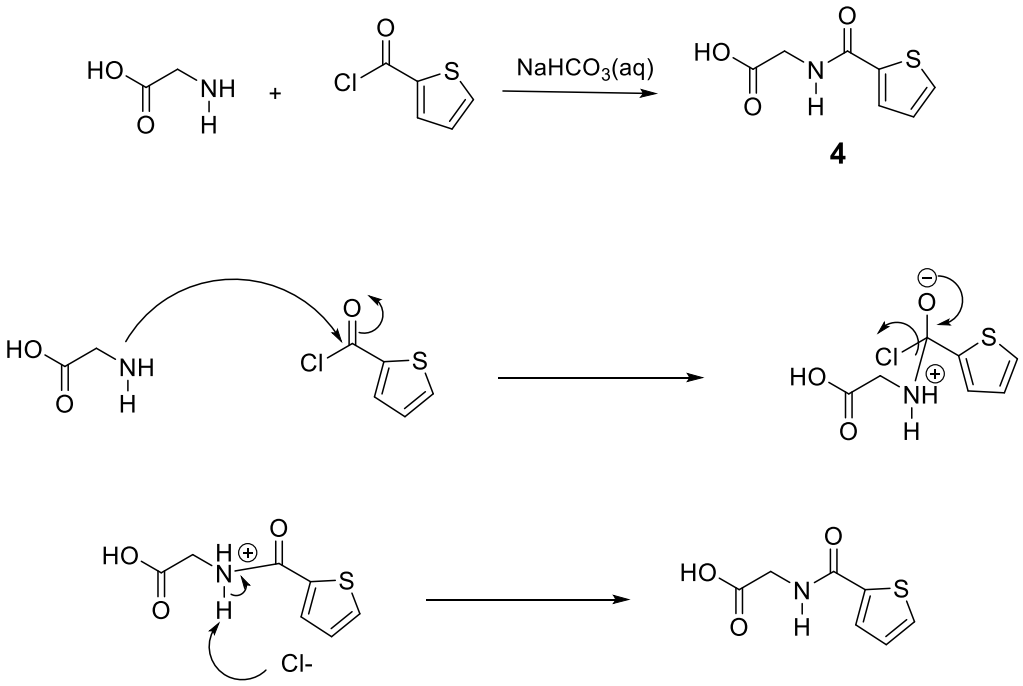

3.2.1.2 Synthesis of oxazolones (5 to 10)

First, sodium acetate deprotonates the acid group in 2-thiophenecarbonyl glycine to give an oxide. Second, the oxide makes a nucleophilic attack on the carbonyl carbon of acetic anhydride causing the acetate group to leave. After that, a proton transfer occurs to give the double bond (enol, Tautomerization). Then, a condensation reaction occurs between the enol 19 and the aldehyde followed by the loss of a water molecule forming the intermediate 20, which undergoes tautomerization to form imine-ol, which loses OH acidic proton producing 21, and undergoes intra S_N2 and form the final form the oxazolone derivatives (5 to 10) as described in Figure 3.7.

Figure 3.7

Mechanism for synthesis of oxazolones (5-10)

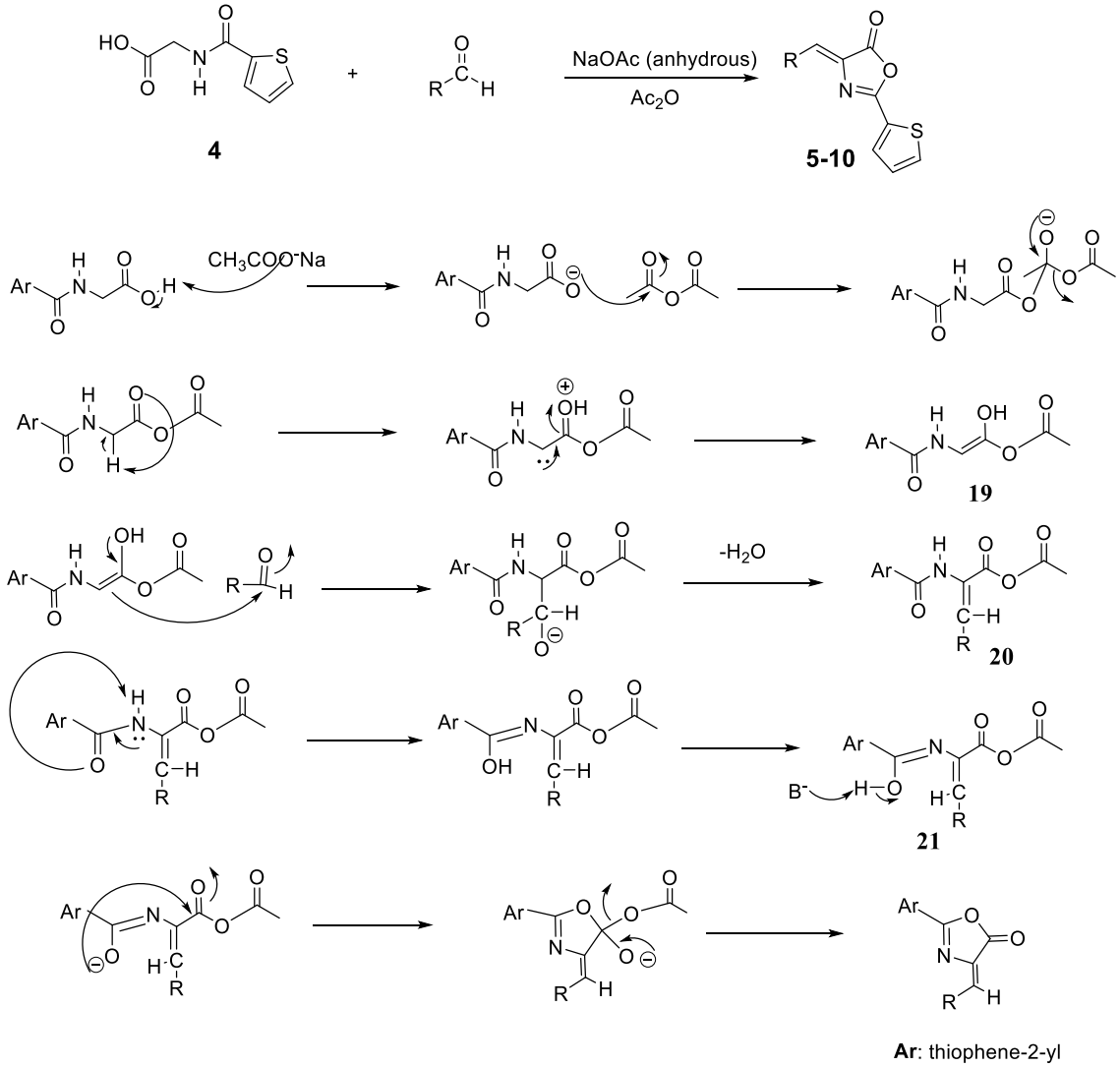

3.2.1.3 Preparation of imidazolones (5a to 5g)

In this mechanism, the first step is the protonation of the lactone carbonyl in oxazolone (5) to give 22, the protonation creates stronger electrophilic carbon, where the nucleophilic amine attacks this carbonyl group in 22 forcing it to undergo ring opening to form the intermediate 23 having amide and hydroxyl groups. Then, a condensation cyclization takes place when the hydroxyl group of 23 is protonated causing a loss of water molecule to form 24. After that, the amide's nitrogen attacks the *sp* carbon of 24 followed by deprotonation resulting in ring closure and producing the imidazolone as illustrated in Figure 3.8.

Figure 3.8

Reaction mechanism for preparing imidazolones (5a-g)

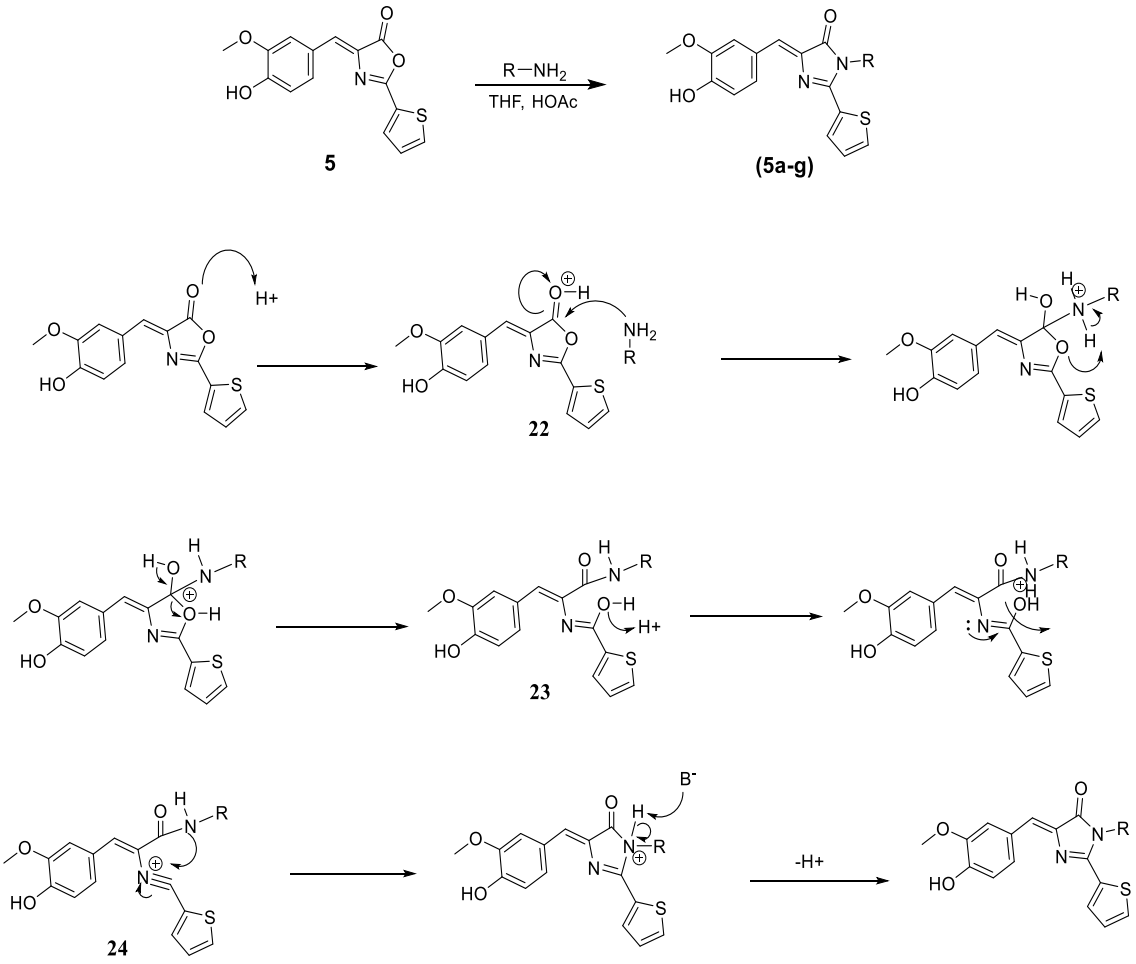

3.2.1.4 Synthesis of oxazolones (11) and (12)

The mechanism for synthesis of the two oxazolone derivatives (11) and (12) is the same as the one illustrated in Figure 3.3.

In the first step of the mechanism, sodium acetate deprotonates the acid group in benzoyl glycine (1) to give an oxide. The second step shows a nucleophilic attack of oxide on the carbonyl carbon of acetic anhydride followed by leaving of the acetate group. Then, a proton transfer takes place to give the double bond (enol). Finally, the nucleophilic double bond attacks the aldehyde's carbonyl followed by the loss of a water molecule to form the two oxazolone compounds (11) and (12).

3.2.2 Anticancer activity of imidazolones

Imidazolones (5a-g) were submitted to the pharmaceutical department at An-Najah University (Nablus, Palestine) to study the anticancer activity against four cancer cell lines which are: liver cancer cells (HepG2), cervical adenocarcinoma cells (HeLa), colon cancer cells (CaCo-2), breast cancer cells (MCF-7) and normal liver cells (LX-2).

The *in vitro* anticancer screening was performed four doses testing against the four selected cell lines using a four series of two-fold dilutions from a stock solution with 1000 µg/mL (500.0, 250.0, 125.0 and 62.5µg/mL). A 48 h of incubation with the tumor cell lines was conducted. The results were collected for each cell line from triplicate response parameters, IC_{50} values (concentration needed to kill 50% of cancer cells) were determined and described in Table 3.2.

Table 3.2

Values of IC_{50} (µg/mL) for imidazolones (5a-g) on different cancer cells (HepG2, MCF-7, CACO-2, HeLa) and LX-2 normal cell

Imidazolone	IC_{50} values (µg/mL)				
	HepG2	HeLa	CaCo-2	MCF-7	LX-2
5a	22.39	53.64	117.23	162.71	292.49
5b	2.18	5.51	1345.32	191.83	4.08
5c	239.91	97.68	13.17	184.34	602.59
5d	103.05	125.29	32.74	35.59	291.42
5e	1636.66	45.71	562.76	85.83	454.41
5f	67.67	78.01	68.45	114.15	72.87
5g	53.83	18.44	5.96	1316.49	175.79

The cytotoxicity of the second set of imidazolones against the tested cancer cells and normal LX-2 cells was collected in Figure A19 of appendix A. This second set of imidazolones showed a better anticancer activity in comparison to the first set due to the presence of the thiophene ring that could contributed to the extra interaction. Compound 5b with a chlorophenyl amine moiety exhibited the most potent anticancer activity on the HepG2 and HeLa cancer cells with a high selectivity as they showed a very low IC_{50} of 2.18 and 5.51 µM, respectively. Compound 5a with a bromophenyl amine substituent also showed good anticancer activity against the HepG2 and HeLa cancer cells with IC_{50} equal to 22.39 and 53.64 µM, respectively. While compound 5c with ethanol amine substitution and 5d with N-methyl ethylene amine demonstrated selective activity on CaCo-2 cells with potent IC_{50} equal to 13.17 µM for 5c and 32.74 µM for compound

5d. In the case of the butyl substituent in compound 5e, the compound displaced anticancer activity on HeLa and MCF-7 cancer cells with IC_{50} 45.71 μM and 85.83 μM, respectively. Regarding the dodecyl moiety, compound 5f showed moderate activity on all tested cancer cells ranging from 67.67-114.15 μM which emphasizes the capability of the hydrophobic group to increase the cell penetration. Finally, compound 5g with the picoyl moiety displayed very potent activity on the colorectal cancer cells and cervical cancer cells with IC_{50} equals to 5.96 μM and 18.44 μM, respectively. However, it has moderate activity on the liver cancer cells with IC_{50} 53.83 μM.

We could conclude that depending on the substituent of the imidazolone derivatives, the anticancer activity varies on the cancer cells as well as the potency of the compounds.

3.3 ADME and Molecular Docking

ADME and molecular docking were applied on four compounds that showed the highest cytotoxicity results against cancer cells. These compounds are the two imidazolones of the first set 3f and 3g, in addition to 5d and 5f of the second set.

ADME (Absorption, Distribution, Metabolism, and Excretion) properties for the molecules were computed via the use of the Swiss ADME server (145). The most important properties for the studied molecules are presented in Table 3.3. The molecular weights of the molecules range from 357.43 (5d) to 468.65 (5f). According to Lipinski's guidelines, MW ≤ 500 is optimal for drug-like molecules. All molecules fall within this range, making them potentially suitable for oral bioavailability (146). The number of H-bond acceptors varies from 4 (3f, 5f) to 9 (3g), while H-bond donors range from 1 (3f, 5f) to 5 (3g). Molecule 3g has the highest potential for hydrogen bonding, which might improve solubility but could affect permeability. Molecule 3f has one violation, whereas the other molecules comply fully with Lipinski's rules, indicating a higher likelihood of favorable pharmacokinetics for molecules 3g, 5f, and 5d (147, 148). All molecules share a bioavailability score of 0.55, which suggests moderate oral bioavailability. This is consistent across the dataset and aligns with the structural features of the compounds. Each molecule triggers at least one PAINS alert (149), highlighting potential suboptimal pharmacological properties.

Table 3.3

Some of the ADME (Absorption, Distribution, Metabolism, and Excretion) properties for molecules

Molecule	MW	#H-bond acceptors	#H-bond donors	Lipinski #violations	Bioavailability Score	PAINS #alerts	Brenk #alerts	Synthetic Accessibility
3f	462.62	4	1	1	0.55	1	1	4.49
3g	453.49	9	5	0	0.55	1	2	4.76
5f	468.65	4	1	0	0.55	1	1	4.61
5d	357.43	5	2	0	0.55	1	1	3.78

Molecule 3g has two Brenk alerts, suggesting a slightly higher risk of undesirable effects compared to others. The synthetic accessibility score ranges from 3.78 (5d) to 4.76 (3g). Lower scores indicate simpler synthesis. Molecule 5d is the easiest to synthesize, whereas 3g may present challenges due to its complex structure. In general, QSAR parameters indicate that all molecules exhibit reasonable drug-like properties, with variations in hydrogen bonding and synthetic complexity that may influence their development potential. Molecule 5d emerges as the most balanced candidate due to its compliance with Lipinski's rules, moderate H-bond properties, and favorable synthetic accessibility.

As for the molecular docking, virtual screening was conducted using the Maestro program, which incorporated receptor flexibility constraints to enhance accuracy. The program’s sophisticated algorithm effectively predicted the docking poses of the ligands. Three-dimensional coordinates of the target proteins, 4MAN and 1HNJ, were retrieved from the Protein Data Bank (PDB) (150). The 4MAN (151) entry, selected for its X-ray resolution of 2.07 Å, and the 1HNJ (151) entry, chosen for its superior X-ray resolution of 1.46 Å, provided detailed access to their respective active sites.

Each ligand was evaluated with 10 docked poses, and the model with the lowest binding free energy (dG) was selected for further analysis. This systematic approach identified the most favorable docking poses, emphasizing key interactions between the ligands and the proteins, thereby facilitating a deeper understanding of their binding mechanisms and potential antitumor activity.

Table 3.4

Molecular Docking results for the studied molecules

Molecule	Docking Score	MMGBSA dG Bind
	4MAN	
3g	-5.88	-52.13
5d	-4.75	-24.81
3f	-4.40	-44.52
5f	-3.71	-41.89
	1HNJ	
3g	-4.84	-35.88
5d	-2.05	-14.85
3f	-3.37	-38.01
5f	-4.75	-38.63

Figure 3.9

2D and 3D molecular docking poses for the interaction of molecules with 4MAN.

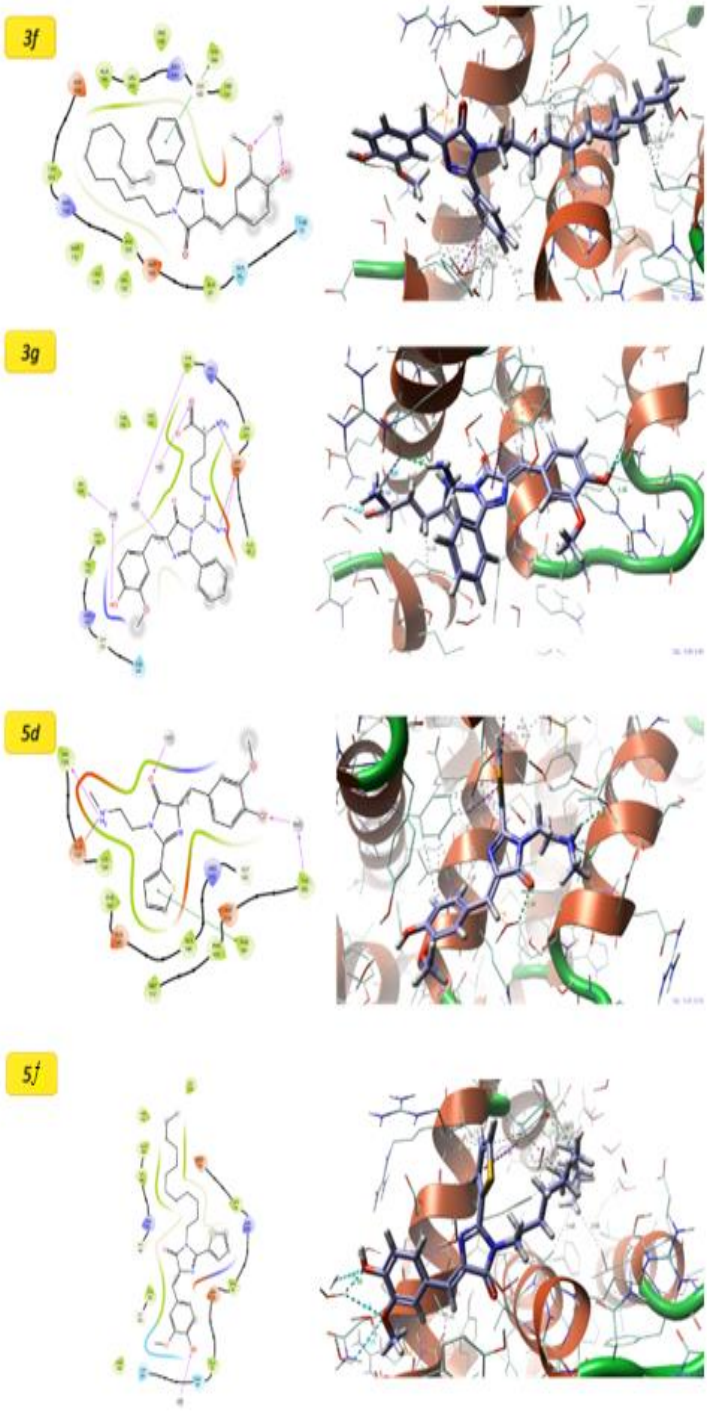

Figure 3.10

2D and 3D molecular docking poses for the interaction of molecules with 1HNJ.

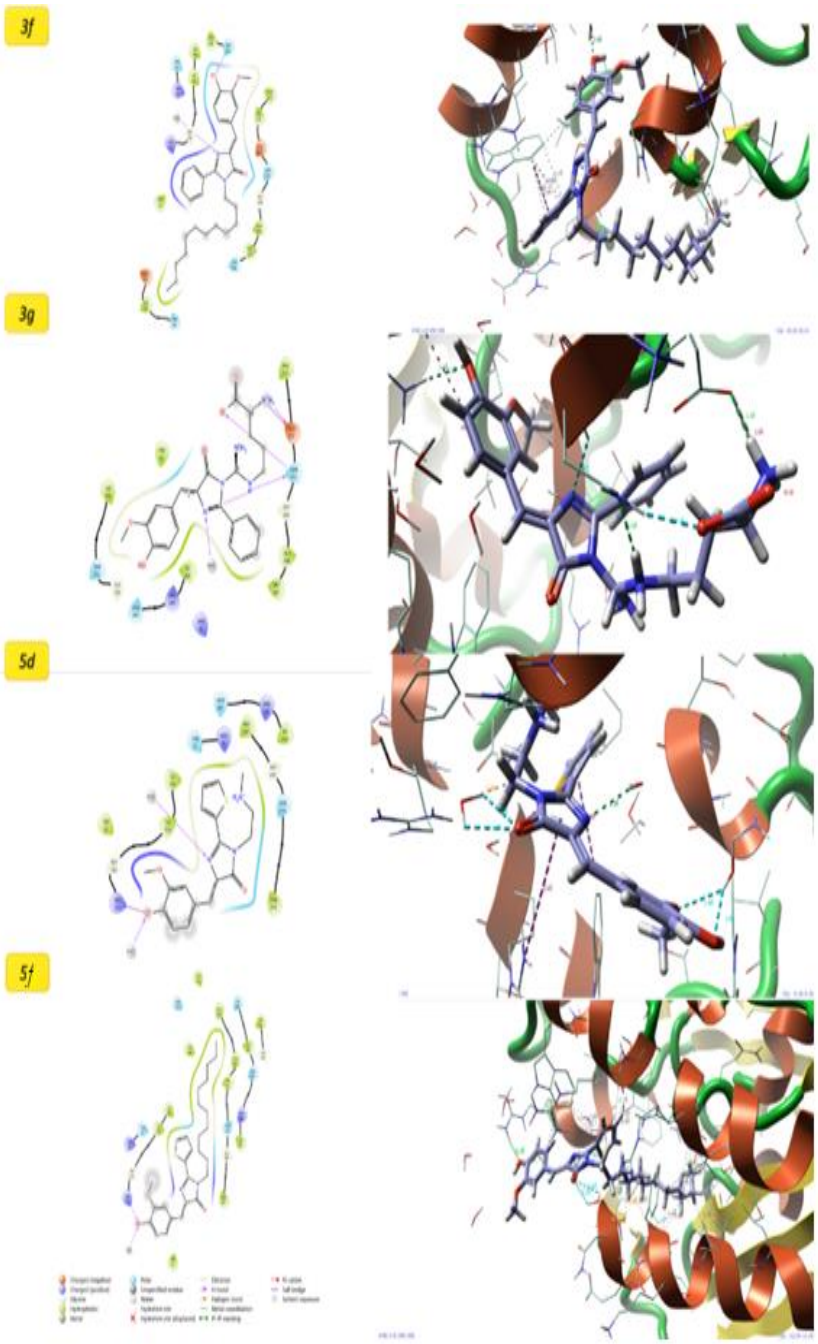

For the 4MAN protein (Figure 3.9), the molecule 3g exhibits the most favorable interaction, achieving the lowest docking score (-5.88) and the most negative MMGBSA binding free energy (-52.13 kcal/mol). The interactions observed for these molecules, as depicted in the 2D interaction poses (122, 152-154), are primarily categorized into three types: Hydrogen Bonding (H-bonding) – involving the formation

of directional and specific interactions between hydrogen donors and acceptors (amino acid side chains of proteins), contributing significantly to the stability and specificity of the ligand-protein complex. Salt Bridge Interactions - electrostatic interactions between positively and negatively charged groups, playing a crucial role in enhancing binding affinity and ensuring a robust attachment between the ligand and the protein and π-π stacking interactions that interactions occur between aromatic rings in the ligand and the protein, facilitating stable binding through overlap of π-electron clouds. This type of interaction is particularly important for ligands with aromatic moieties, as it enhances the overall binding strength and selectivity. These results strongly suggest high binding affinity and stability of the ligand-protein complex. In contrast, 5d, despite displaying a relatively moderate docking score (-4.75), demonstrates the least favorable MMGBSA binding energy (-24.81 kcal/mol), indicative of weaker overall interaction and stability. Molecule 3f achieves a docking score of -4.40 and a binding free energy of -44.52 kcal/mol, positioning it as a secondary strong candidate after 3g. On the other hand, 5f shows the weakest docking performance (-3.71) among the four tested ligands for 4MAN, but maintains a moderately favorable MMGBSA binding energy (-41.89 kcal/mol), indicating a reasonably stable interaction.

For 1HNJ protein, molecule 5f demonstrates the strongest interaction, characterized by a docking score of -4.75 and the most negative MMGBSA binding energy (-38.63 kcal/mol), highlighting its potential as the top candidate for this target. Molecule 3g, with a docking score of -4.84 and an MMGBSA binding energy of -35.88 kcal/mol, shows strong binding affinity and ranks as the second-best candidate. Similarly, molecule 3f achieves a moderate docking score (-3.37) and a relatively favorable MMGBSA binding energy (-38.01 kcal/mol), suggesting it as a viable alternative ligand. In contrast, 5d performs the weakest, as evidenced by its highest docking score (-2.05) and the least negative MMGBSA binding energy (-14.85 kcal/mol), indicating poor binding affinity and stability. Overall, for 4MAN, molecule 3g emerges as the most promising candidate, while 3f serves as a strong secondary option due to its favorable MMGBSA binding energy. For 1HNJ, molecule 5f is identified as the top-performing ligand, with 3g and 3f being suitable alternatives for further consideration. Across both targets, molecule 5d consistently shows the weakest binding performance, making it less favorable for further investigation.

The interaction data (Figure 3.10) for the protein 1HNJ with various molecules reveals significant variations in binding affinity, as indicated by both docking scores and MMGBSA ΔG Bind values. Among the molecules, 3g demonstrates a moderate docking score of -4.84 and an MMGBSA ΔG Bind value of -35.88, suggesting a relatively strong binding. Similarly, 5f shows a comparable docking score of -4.75 but exhibits the strongest MMGBSA ΔG Bind at -38.63, indicating the most stable interaction. In contrast, 5d has the weakest docking score of -2.05 and a significantly less favorable binding free energy of -14.85, implying a weaker interaction with the protein. The molecule 3f, while having a moderate docking score of -3.37, shows a notably strong MMGBSA ΔG Bind of -38.01, similar to 5f. Overall, 5f and 3f emerge as the top candidates with the strongest binding affinities, as indicated by their more negative MMGBSA ΔG Bind values.

The docking and MMGBSA ΔG Bind data strongly support potential antitumor activity, aligning closely with experimental results, for the molecules interacting with the proteins 4MAN and 1HNJ, which are likely involved in critical cancer-related pathways. Among these, molecules such as 3g, 3f, and 5f stand out due to their consistently strong binding across both proteins, demonstrated by highly favorable docking scores and ΔG Bind values. These interactions suggest their capacity to modulate protein functions or inhibit key pathways essential for tumor progression. Consequently, these molecules emerge as promising lead candidates for therapeutic development, warranting further investigation into their antitumor properties and potential for advancement into targeted cancer therapies.

3.4 Antimicrobial activity

Using the broth microdilution method, the oxazolones (5-12) in addition to imidazolones 3f and 3g were tested for a chance of having antibacterial activity. The antibacterial evaluation was done in the Biology Department at An-Najah University (Nablus, Palestine) against five bacterial strands. Two are gram positive, which are *Staphylococcus aureus* and *Staphylococcus epidermidis*, and three-gram negative bacteria which are *Pseudomonas aeruginosa*, *Escherichia coli* and *Klebsiella pneumonia*.

3.4.1 Interpretation of MIC results

The broth microdilution method was used to determine the minimal inhibitory concentration (MIC) of the prepared oxazolones (5-12) and the two imidazolones (3f) and (3g) against bacteria.

In this study, the results revealed that the synthesized derivatives showed almost similar degrees of inhibition against the tested bacteria. *Staphylococcus aureus* was the most resistant where compound 8 which has (2-thiophenyl) functionality was able to stop the bacterial growth with MIC of 500 µg/mL. *E. coli* was sensitive to most compounds at MIC 500 µg/mL except for compound (3g) that has the methylamino pentanoic acid moiety. As for *P*seudomonas *aeruginosa*, *Klebsiella pneumonia* and *Staphylococcus epidermidis* strains were found to be sensitive to all derivatives at MIC 500 µg/mL. These results indicate that the conversion of oxazolones to imidazolones did not significantly affect their antibacterial activities.

The MIC values of these compounds were high (500 µg/mL) for both gram-positive and gram-negative bacteria, where they cannot be used alone as an antibiotic drug. However, a combination of these derivatives with some commercial antibiotics can lead to a synergetic effect that can effectively stop bacterial growth at lower MIC values.

The 5% DMSO solution used as a negative control showed nonantibacterial activity against all tested bacterial strains. All MIC results of the derivatives against the five tested bacterial species are summarized in Tables 3.5-3.9.

Table 3.5

Values of MIC (µg/ml) for compounds (5-12, 3f and 3g) against Staphylococcus aureus, (+): Bacterial growth, (-): no bacterial growth

Concentration (µg/mL)	5	6	7	8	9	10	11	12	3f	3g
500	+	+	+	-	+	+	+	+	+	+
250	+	+	+	+	+	+	+	+	+	+
125	+	+	+	+	+	+	+	+	+	+
62.5	+	+	+	+	+	+	+	+	+	+
31.25	+	+	+	+	+	+	+	+	+	+
15.63	+	+	+	+	+	+	+	+	+	+
7.81	+	+	+	+	+	+	+	+	+	+
3.91	+	+	+	+	+	+	+	+	+	+

Table 3.6

Values of MIC (µg/ml) for compounds (5-12, 3f and 3g) against Escherichia coli, (+): Bacterial growth, (-): no bacterial growth

Concentration (µg/mL)	5	6	7	8	9	10	11	12	3f	3g
500	-	-	-	-	-	-	-	-	-	+
250	+	+	+	+	+	+	+	+	+	+
125	+	+	+	+	+	+	+	+	+	+
62.5	+	+	+	+	+	+	+	+	+	+
31.25	+	+	+	+	+	+	+	+	+	+
15.63	+	+	+	+	+	+	+	+	+	+
7.81	+	+	+	+	+	+	+	+	+	+
3.91	+	+	+	+	+	+	+	+	+	+

Table 3.7

Values of MIC (μg/ml) for compounds (5-12, 3f and 3g) against Klebsiella pneumonia, (+): Bacterial growth, (-): no bacterial growth

Concentration (μg/mL)	5	6	7	8	9	10	11	12	3f	3g
500	-	-	-	-	-	-	-	-	-	-
250	+	+	+	+	+	+	+	+	+	+
125	+	+	+	+	+	+	+	+	+	+
62.5	+	+	+	+	+	+	+	+	+	+
31.25	+	+	+	+	+	+	+	+	+	+
15.63	+	+	+	+	+	+	+	+	+	+
7.81	+	+	+	+	+	+	+	+	+	+
3.91	+	+	+	+	+	+	+	+	+	+

Table 3.8

Values of MIC (μg/ml) for compounds (5-12, 3f and 3g) against Pseudomonas aeruginosa, (+): Bacterial growth, (-): no bacterial growth

Concentration (μg/mL)	5	6	7	8	9	10	11	12	3f	3g
500	-	-	-	-	-	-	-	-	-	-
250	+	+	+	+	+	+	+	+	+	+
125	+	+	+	+	+	+	+	+	+	+
62.5	+	+	+	+	+	+	+	+	+	+
31.25	+	+	+	+	+	+	+	+	+	+
15.63	+	+	+	+	+	+	+	+	+	+
7.81	+	+	+	+	+	+	+	+	+	+
3.91	+	+	+	+	+	+	+	+	+	+

Table 3.9

Values of MIC (µg/ml) for compounds (5-12, 3f and 3g) against Staphylococcus epidermidis, (+): Bacterial growth, (-): no bacterial growth

Concentration (µg/mL)	5	6	7	8	9	10	11	12	3f	3g
500	-	-	-	-	-	-	-	-	-	-
250	+	+	+	+	+	+	+	+	+	+
125	+	+	+	+	+	+	+	+	+	+
62.5	+	+	+	+	+	+	+	+	+	+
31.25	+	+	+	+	+	+	+	+	+	+
15.63	+	+	+	+	+	+	+	+	+	+
7.81	+	+	+	+	+	+	+	+	+	+
3.91	+	+	+	+	+	+	+	+	+	+

3.4.2 MBC test

The minimum bactericidal concentration (MBC) values for each derivative were tested. At a concentration of 500 µg/mL, the prepared compounds were not able to kill either gram-positive or gram-negative bacteria. However, at higher concentrations, such as 1000 µg/mL, these compounds demonstrated a clear bactericidal effect.

3.5 Conclusion

Two new series of imidazolone derivatives were synthesized using vanillin and 2-thiophene carboxaldehyde as starting materials in a three-step process. The anticancer activities of the prepared imidazolones against four cancer cells, HepG2, Hela, CaCo-2 and MCF-7, in addition to a normal cell LX-2, were studied. Most of the prepared compounds showed some activity against the tested cells. Out of the first set, compound 3f with a dodecyl functionality showed exceptional activity against breast cancer cells (MCF-7) with IC_{50} 20.02 µM. This could be due to the hydrophobic nature of the dodecyl group which could enhance cancer cell membrane penetration. In addition, compound 5f having the dodecyl group showed the best activity on all tested cancer cells ranging from 67.67-114.15 µM which emphasizes the capability of the hydrophobic group to increase the cell penetration. ADME study validated drug-likeness and moderate bioavailability for all examined molecules, with molecule 5d exhibiting the most straightforward synthesis route. Molecular docking demonstrated

robust binding interactions, identifying molecules 3g and 5f as the most promising options for targeted cancer therapy owing to their elevated binding affinities and stability with both 4MAN and 1HNJ proteins. These results show the potential of the compounds as prospective anticancer drugs.

As for the antibacterial activity of oxazolones, oxazolone 8 containing 2-thiophenyl moiety was the most potent derivative able to stop the bacterial growth of all types of bacteria, even the most resistant *Staphylococcus aureus* with MIC of 500 µg/mL. A combination of these oxazolones with commercial antibiotics can provide a synergetic effect to stop bacterial growth at lower MIC values.

List of Abbreviations

Abbreviation	Meaning
FT-IR	Fourier -Transform Infrared Spectroscopy
NMR	Nuclear Magnetic Resonance
DMSO	Dimethyl Sulfoxide
mL	Milliliter
NB	Nutrient Broth
IC50	Molar concentration required to kill 50% of cancer cells was determined
MIC	Minimal Inhibitory Concentration
MBC	Minimum Bactericidal Concentration

References

(1) Brandi A, Cicchi S, Cordero FM, Goti AJCr. Heterocycles from alkylidenecyclopropanes. 2003;103(4):1213-70.

(2) Vitaku E, Smith DT, Njardarson JTJJomc. Analysis of the structural diversity, substitution patterns, and frequency of nitrogen heterocycles among US FDA approved pharmaceuticals: miniperspective. 2014;57(24):10257-74.

(3) Adhikari A, Bhakta S, Ghosh TJT. Microwave-assisted synthesis of bioactive heterocycles: An overview. 2022;126:133085.

(4) Qin L, Wu L, Nie Y, Xu YJCS, Technology. Biosynthesis of chiral cyclic and heterocyclic alcohols via C [double bond, length as m-dash] O/C–H/C–O asymmetric reactions. 2021;11(8):2637-51.

(5) Nan S, Wang P, Zhang Y, Fan J. Epigallocatechin-3-gallate provides protection against Alzheimer's disease-induced learning and memory impairments in rats. Drug Des Devel Ther 15: 2013–2024. 2021.

(6) Lim J, Kim JD, Choi HC, Lee SJJoOC. CNT-CuO catalyzed C–N bond formation for N-arylation of 2-phenylindoles. 2019;902:120970.

(7) Chen Q, Bryant VC, Lopez H, Kelly DL, Luo X, Natarajan AJB, et al. 2, 3-Substituted quinoxalin-6-amine analogs as antiproliferatives: a structure–activity relationship study. 2011;21(7):1929-32.

(8) Motati DR, Amaradhi R, Ganesh TJB, chemistry m. Azaindole therapeutic agents. 2020;28(24):115830.

(9) Zhang L, Peng XM, Damu GL, Geng RX, Zhou CHJMrr. Comprehensive review in current developments of imidazole-based medicinal chemistry. 2014;34(2): 340-437.

(10) Fulco PP, McNicholl IRJPTJoHP, Therapy D. Etravirine and rilpivirine: nonnucleoside reverse transcriptase inhibitors with activity against human immunodeficiency virus type 1 strains resistant to previous nonnucleoside agents. 2009;29(3):281-94.

(11) Siwach A, Verma PKJBc. Synthesis and therapeutic potential of imidazole containing compounds. 2021;15:1-69.

(12) Egbujor MC, Tucci P, Onyeije UC, Emeruwa CN, Saso LJM. NRF2 activation by nitrogen heterocycles: a review. 2023;28(6):2751.

(13) Peerzada MN, Hamel E, Bai R, Supuran CT, Azam AJP, Therapeutics. Deciphering the key heterocyclic scaffolds in targeting microtubules, kinases and carbonic anhydrases for cancer drug development. 2021;225:107860.

(14) Heravi MM, Zadsirjan VJRa. Prescribed drugs containing nitrogen heterocycles: an overview. 2020;10(72):44247-311.

(15) Kushwaha N, Kushwaha SJBRAC. Synthetic approaches and biological significance of oxazolone moieties: A review. 2022;12:6460-86.

(16) El-Mekabaty AJIJMOC. Erlenmeyer azlactones: synthesis, reactions and biological activity. 2013;2(1):40-66.

(17) Grzetic J, Oomens JJJotASfMS. Spectroscopic evidence for an oxazolone structure in anionic b-type peptide fragments. 2011;23(2):290-300.

(18) Avenoza A, Busto JH, Cativiela C, Peregrina JMJTl. Reactivity of (Z)-4-arylidene-5 (4H)-oxazolones:[4+ 2] cycloaddition versus [4+ 3] cycloaddition/nucleophilic trapping. 2002;43(23):4167-70.

(19) Nagamani C, Basavarajaiah S, Nagaraj S, Saraswathi DJIJoCER. Synthesis, characterization and biological evaluation of oxazolone derivatives. 2016;6:31-4.

(20) Sharada L, Aparna Y, Saba M, Sunitha S, Viveka LJIJoS, Publication R. A Review on Reactions and Applications of Oxazolones. 2015;5:1-9.

(21) Kildisheva O, Linkova M, Knunyants IJBotAoSotU, Division of chemical science. Structure and properties of oxazolones. 1957;6:737-47.

(22) Goodman M, Levine LJJotACS. Peptide synthesis via active esters. IV. Racemization and ring-opening reactions of opitcally active oxazolones. 1964;86(14):2918-22.

(23) Padwa A, Pearson W. Synthetic Applications of 1, 3-Dipolar Cycloaddition Chemistry Toward Heterocycles and Natural Products, 1st edn, 2002. John Wiley and Sons, Hoboken, NJ.

(24) Turner NJJCOC. The application of enzymes in the synthesis of amino acids, peptides and carbohydrates. 1997;1:21-36.

(25) Sharma N, Banerjee J, Shrestha N, Chaudhury DJEJBPS. A review on oxazolone, it's method of synthesis and biological activity. 2015;2(3):964-87.

(26) Tandel RJRJoPS. Synthesis and Study of Oxazolone derivatives showing biological activity. 2012;2319:555X.

(27) Khaidem S, Sarveswari S, Gupta R, Vijayakumar VJC. Synthesis and biological evaluation of some pyridazinone derivatives. 2012;43(39):no.

(28) Mulwad V, Satwe D. Synthesis of biologically active 4-[1-(2H-[1]-4-hydroxy-2-oxo-benzopyran-3-y1) methylidene]-2-phenyl-4H-oxazol-5-ones and [l, 2, 4] triazine-6-one and its derivatives. 2006.

(29) Fisk JS, Mosey RA, Tepe JJJCSR. The diverse chemistry of oxazol-5-(4 H)-ones. 2007;36(9):1432-40.

(30) Keni M, Tepe JJJTJoOC. One-Pot Friedel− Crafts/Robinson− Gabriel Synthesis of Oxazoles Using Oxazolone Templates. 2005;70(10):4211-3.

(31) Nagaraja O, Bodke YD, Pushpavathi I, Kumar SRJH. Synthesis, characterization and biological investigations of potentially bioactive heterocyclic compounds containing 4-hydroxy coumarin. 2020;6(6).

(32) Zaky HT, Mohamed MI, Kandile NGJAJoC. Efficient synthesis of new oxindol-based heterocyclic entities via indolin-2-one derivatives. 2014;7(5):630-8.

(33) Bentley TW, Llewellyn G, McAlister JAJTJooc. SN2 mechanism for alcoholysis, aminolysis, and hydrolysis of acetyl chloride. 1996;61(22):7927-32.

(34) Filler R, Rao YSJTJoOC. Chemistry of Lactones. VI. Reaction of Unsaturated Azlactones under Friedel-Crafts Conditions1, 2. 1962;27(7):2403-6.

(35) Sotelo E, Fraiz N, Yáñez M, Laguna R, Cano E, Raviña EJC, et al. Pyridazines. Part 31: synthesis and antiplatelet activity of 4, 5-disubstituted-6-phenyl-3 (2H)-pyridazinones. 2002;50(12):1574-7.

(36) Mukerjee AK, Rao L, Homami SS, Joseph KJCjoc. Reaction of unsaturated azlactones with sulfur nucleophiles: some observations. 1994;72(5):1383-7.

(37) Yan X, Wen J, Zhou L, Fan L, Wang X, Xu ZJCTiMC. Current scenario of 1, 3-oxazole derivatives for anticancer activity. 2020;20(21):1916-37.

(38) Kamneva I, Anis' kova T, Egorova AYJRJoC. Arylmethylidenefuranones: Reactions with C-and N-Nucleophiles. 2018;8:183-96.

(39) Brunn E, Funke E, Gotthardt H, Huisgen RJCB. 1.3-Dipolare Cycloadditionen, 61. Cycloadditionen von N-substituierten Oxazolium-5-olaten an Nitrile, Nitro-, Nitroso-und Azoverbindungen. 1971;104(5):1562-72.

(40) Bilodeau MT, Cunningham AMJTJoOC. Solid-supported synthesis of imidazoles: A strategy for direct resin-attachment to the imidazole core. 1998;63(9):2800-1.

(41) Vijaya P, Sundaraselvan GJMTP. Synthesis, characterization, PASS analysis and ADMET properties of oxazolone ring containing hydrazone derivatives. 2022;48:502-7.

(42) Fei T, Sun C, He C, Pang SJEMF. A comparative study of bridged 1, 2, 4-oxazolones and their derivatives. 2020;1(1):26-33.

(43) Marra IF, de Castro PP, Amarante GWJEJoOC. Recent advances in azlactone transformations. 2019;2019(34):5830-55.

(44) Bourotte M, Schmitt M, Follenius-Wund A, Pigault C, Haiech J, Bourguignon J-JJTl. Fluorophores related to the green fluorescent protein. 2004;45(33):6343-8.

(45) Bala S, Saini M, Kamboj SJIJCR. Methods for synthesis of Oxazolones: A Review. 2011;3(3):1102-18.

(46) Fareed G, Afza N, Versiani AM, Fareed N, Mughal RU, Kalhoro AM, et al. Synthesis, spectroscopic characterization and pharmacological evaluation of oxazolone derivatives. 2013;78(8):1127-34.

(47) Tandel R, Mammen D. Synthesis and study of some compounds containing oxazolone ring, showing biological activity. 2008.

(48) Olomola T, Akinboye A, Olasunkanmi O, Olasunkanmi LJIJoS. Synthesis, antimicrobial activities and computational studies of some oxazolone derivatives. 2018;20(1):1-14.

(49) Mariappan G, Saha B, Datta S, Kumar D, Haldar PJJoCS. Design, synthesis and antidiabetic evaluation of oxazolone derivatives. 2011;123:335-41.

(50) Jat L, Mishra R, Pathak DJIJPPS. Synthesis and anticancer activity of 4-Benzylidene-2-phenyloxazol-5 (4H)-one derivatives. 2012;4(1):378-80.

(51) Abdel-Aty ASJWJAS. Pesticidal effects of some imidazolidine and oxazolone derivatives. 2009;5:105-13.

(52) Bala S, Saini M, Kamboj S, Saini VJIJoP, Therapeutics. Synthesis of 2-[4-(substituted benzylidene)-5-Oxo-4, 5-dihydro-oxazol-2-ylmethyl]-isoindole-1, 3-dione Derivatives as Novel Potential Antimicrobial Agents. 2012;2012:45-52.

(53) Dobhal Y, Rawat R, Parcha V, Sharma R, Chaudhary RJWJoPS. Design, synthesis and evaluation of phenyl oxazolone derivatives as cardioprotective drugs. 2014:1712-22.

(54) Mesaik MA, Rahat S, Khan M, Ullah Z, Choudhary M, Murad S, et al. Atta-ur-Rahman and A. Ahmad. 2004;12:2049-57.

(55) Gökhan N, Köksal M, KÜPELİ E, YEŞİLADA E, ERDOĞAN HJTJoC. Some new Mannich bases of 5-methyl-2-benzoxazolinones with analgesis and anti-inflammatory activities. 2005;29(4):445-54.

(56) Mohamed LW, El-Badry OM, El-Ansary AK, Ismael AJBC. Design & synthesis of novel oxazolone & triazinone derivatives and their biological evaluation as COX-2 inhibitors. 2017;72:308-14.

(57) Zhang W, Barry JD, Cordova D, McCann SF, Benner EA, Hughes KAJB, et al. Discovery, synthesis, and evaluation of N-substituted amino-2 (5H)-oxazolones as novel insecticides activating nicotinic acetylcholine receptors. 2014;24(9): 2188-92.

(58) Wookey A, Turner P, Greenhalgh J, Eastwood M, Clarke J, Sefton CJCM, et al. AZD2563, a novel oxazolidinone: definition of antibacterial spectrum, assessment of bactericidal potential and the impact of miscellaneous factors on activity in vitro. 2004;10(3):247-54.

(59) Sánchez C, Méndez C, Salas JAJNpr. Indolocarbazole natural products: occurrence, biosynthesis, and biological activity. 2006;23(6):1007-45.

(60) Rix U, Zheng J, Remsing Rix LL, Greenwell L, Yang K, Rohr JJJotACS. The dynamic structure of jadomycin B and the amino acid incorporation step of its biosynthesis. 2004;126(14):4496-7.

(61) Gaenzler FC. Part I. A 2-nitroimidazole indocyanine green dye derivative tumor imaging agent. Part II. A dichlorination-reductive-dechlorination route to N-acetyl-2-oxazolone. Part III. Intramolecular Diels-Alder approach to the synthesis of pancratistatin. 2007.

(62) Hegazy WA, Rajab AA, Lila ASA, Abbas HAJWJoD. Anti-diabetics and antimicrobials: Harmony of mutual interplay. 2021;12(11):1832.

(63) Askoura M, Almalki AJ, Lila ASA, Almansour K, Alshammari F, Khafagy E-S, et al. Alteration of Salmonella enterica virulence and host pathogenesis through targeting sdiA by using the CRISPR-Cas9 system. 2021;9(12):2564.

(64) Saadi L, Adnan SJIJoC. Synthesis, Antibacterial and Antioxidant Evaluation of 2-Substituted-4-arylidene-5 (4 H)-oxazolone Derivatives.

(65) Mortazavi ZFA, Islami MR, Khaleghi MJJoGR. Antimicrobial and Antibiofilm Activity of 4-Benzylidene-2-methyl-oxazoline-5-one against Pathogen Bacteria. 2024;10(1):9-19.

(66) Nguyen CTJNIiC, Biochemistry. The Compounds Containing Imidazol-5-one Heterocycle: Synthesis and Biological Activities. 2022:97.

(67) Kerru N, Gummidi L, Maddila S, Gangu KK, Jonnalagadda SBJM. A review on recent advances in nitrogen-containing molecules and their biological applications. 2020;25(8):1909.

(68) Chawla A, Sharma A, Sharma AKJC. A convenient approach for the synthesis of imidazole derivatives using microwaves. 2012;43(24):no.

(69) Wall BJ, Sharma KK, O'Brien EA, Donovan A, VanVeller BJJotACS. General Installation of (4 H)-Imidazolone cis-Amide Bioisosteres Along the Peptide Backbone. 2024;146(17):11648-56.

(70) Kortiwala N, Patel J, Desai VAJJoC, Sciences C. Imidazolone and its various biological activities–a review. 2016;6(1):25-32.

(71) Scholz CJI, Chemistry E. Imidazole derivatives with sympathomimetic activity. 1945;37(2):120-5.

(72) Dhingra AK, Chopra B, Dua JS, Prasad DNJA-I, Chemistry A-AAiM. Therapeutic potential of N-heterocyclic analogs as anti-inflammatory agents. 2017;16(3): 136-52.

(73) Chatrabhuji P, Zala A, Undavia N. Synthesis, Characterization and antimicrobial studies on novel 1-[(4-chloro cinnamoyl) amino]-2-methyl-4-aryl methine-5-oxo-imidazolines.

(74) Erlenmeyer EJLAC. jun. und F. WITTENBERG. 1904;337:294.

(75) Behrens OK, Bergmann MJJoBC. Cosubstrates in proteolysis. 1939;129(2):587-602.

(76) Mohr E, Stroschein FJJfPC. Mitteilung über lactonähnliche Anhydride acylierter Aminosäuren. Über das Lacton des racemischen Benzoylphenylalanins. 1910;82(1):322-35.

(77) Kalpesh Patel KP, Jayachandran E, Ravi Shah RS, Vijaya Javali VJ, Sreenivasa G. Synthesis, characterization and anthelmintic activity (perituma posthuma) of new oxadiazole incorporated with imidazole and pyrazole. 2010.

(78) Abood NKJA-KUJfB. Synthesis And Characterization Of New Imidazole derivatives. 2013;5(1).

(79) Yellasubbaiah N, Velmurugan V, Nagasudha BJJoPRI. Recent Developments and Biological Activities of 5-Oxo-Imidazolones Derivatives: A Review. 2021;33(45A):287-305.

(80) Suthakaran R, Kavimani S, Venkaiaiah P, Suganthi KJRJoC. Synthesis and antimicrobial activity of 3-(2-(4z)-4-substituted benzylidene-4, 5-dihydro-5-oxo-2-phenyl imidazol-1-yl) ethyl)-6, 8-un/dibromo subtituted-2-substituted quinazoline-(3H)-one. 2008;1(1):22-9.

(81) SRIVASTAVA V, PANDEY B, GUPTA R, BARTHWAL J, KISHOR KJCI. MONOAMINE OXIDASE INHIBITORY AND ANTICONVULSANT ACTIVITY OF SOME NEW 1-(THIAZOL-2-YL)-2-METHYL-4-(SUBSTITUTED BENZYLIDENE)-5-IMIDAZOLONES. 1980;11(28):no-no.

(82) Koti D, Anupama B, Lakshmi KCJTPI. Microwave assisted synthesis and in vitro evaluation of some new imidazolin-5-one derivatives. 2013;3(9 Part A):4-11.

(83) Moorkoth S, Joseph A, Srinivasan K, Kutty GJIJPBT. Ynthesis and Evaluation of Biological Activity of Imidazolidinone Analogues of 2-Aminochromone. 2013;1:130-41.

(84) Alghamdi SS, Suliman RS, Almutairi K, Kahtani K, Aljatli DJDD, Development, Therapy. Imidazole as a promising medicinal scaffold: current status and future direction. 2021:3289-312.

(85) Molina P, Tárraga A, Otón FJO, Chemistry B. Imidazole derivatives: A comprehensive survey of their recognition properties. 2012;10(9):1711-24.

(86) BHALLA M, Naithani P, Bhalla T, Saxena A, Shanker KJC. Novel Imidazole Congeners as Anti-Inflammatory Agents. 1993;24(51):no-no.

(87) El-Araby M, Omar A, Hassanein HH, El-Helby A-GH, Abdel-Rahman AAJM. Design, synthesis and in vivo anti-inflammatory activities of 2, 4-diaryl-5-4 H-imidazolone derivatives. 2012;17(10):12262-75.

(88) Dhingra AK, Chopra B, Dass R, Mittal SKJCCL. Synthesis, antimicrobial and anti-inflammatory activities of some novel 5-substituted imidazolone analogs. 2016;27(5):707-10.

(89) Abdellatif KR, Fadaly WAJBC. New 1, 2-diaryl-4-substituted-benzylidene-5-4H-imidazolone derivatives: Design, synthesis and biological evaluation as potential anti-inflammatory and analgesic agents. 2017;72:123-9.

(90) Barakat A, Al-Majid AM, Al-Qahatany FM, Islam MS, Al-Agamy MHJBKCS. Synthesis, characterization and antimicrobial activity of novel pharmacophores incorporating imidazoline-oxazoline scaffold. 2014;35(2):563.

(91) Chatrabhuji P, Zala A, Undavia NJIJCA. Synthesis of 5-oxo-imidazolines derivatives as anti-microbial agents. 2015;4(1):44-8.

(92) Desai N, Joshi V, Rajpara K, Makwana AHJAJoC. A new synthetic approach and in vitro antimicrobial evaluation of novel imidazole incorporated 4-thiazolidinone motifs. 2017;10:S589-S99.

(93) Khalifa MM, Baset MA, El-Eraky WJMCR. Synthesis and anticonvulsant activity of novel imidazol “5 (4H)” one and 5-oxo-4, 5-dihydroimidazol-1-yl) propanamide derivatives. 2012;21:4447-54.

(94) Vagadiya G, Purohit D, Koradiya S. Synthesis and antimicrobial activity of 2-{[(4'-arylidine-5'oxo-2'phenyl) imidazolyl]-1'-Yl}-3-keto-1, 5-dimethyl-2-phenyl pyrazole. 2019.

(95) Khan KM, Mughal UR, Khan S, Khan S, Perveen S, Choudhary MIJLiDD, et al. Synthesis and antibacterial and antifungal activity of 5-substituted imidazolones. 2009;6(1):69-77.

(96) Yellasubbaiah N, Venumadhavi A, Sudha BN, Rajkumar T, Harika MS, Nagamani BJS. Synthesis, characterization and anthelmintic activity of some novel imidazolidinone derivatives. 2018;3(6).

(97) Johnson RA, Huong S-M, Huang E-SJAr. Inhibitory effect of 4-(4-fluorophenyl)-2-(4-hydroxyphenyl)-5-(4-pyridyl) 1H-imidazole on HCMV DNA replication and permissive infection. 1999;41(3):101-11.

(98) Mehta P, Davadra P, Shah N, Joshi HJILoC, Physics, Astronomy. Synthesis and antimicrobial activity of some new imidazolinone derivatives containing benzimidazole. 2014;10:74--80.

(99) Desai N, Maheta A, Rajpara K, Joshi V, Vaghani H, Satodiya HJJoSCS. Green synthesis of novel quinoline based imidazole derivatives and evaluation of their antimicrobial activity. 2014;18(6):963-71.

(100) Kathrotiya HG, Patel NA, Patel RG, Patel MPJCCL. An efficient synthesis of 3′-quinolinyl substituted imidazole-5-one derivatives catalyzed by zeolite and their antimicrobial activity. 2012;23(3):273-6.

(101) Sudha BN, Subbaiah NY, Raghavendra H, Srikanth A, Reddy CV, Manasa AJIJOHC. Synthesis, characterization and anticonvulsant activity of substituted imidazolinone derivatives. 2014;24(2):159-62.

(102) Hari Narayana Moorthy N, Saxena V, Karthikeyan C, Trivedi PJJoEI, Chemistry M. Synthesis, in silico metabolic and toxicity prediction of some novel imidazolinones derivatives as potent anticonvulsant agents. 2012;27(2):201-7.

(103) Mosaad Sayed M, Rehab Kamel M, Amira Ibrahim S, Moustafa E E-AJOJoMC. Potent Anticonvulsant 1H-Imidazol-5 (4H)-One Derivatives with Low Neurotoxicity. 2012;2012.

(104) Maneshwar T, Vijetha N, Balakrishna V, Kumar CV, Suresh MJIJP. Synthesis, characterization and anthelmintic activity of novel isatin substituted imidazoline derivatives. 2014;4(1):437-41.

(105) Spence RR, Heesch KC, Brown WJJCtr. Exercise and cancer rehabilitation: a systematic review. 2010;36(2):185-94.

(106) Sun J, Wei Q, Zhou Y, Wang J, Liu Q, Xu HJBsb. A systematic analysis of FDA-approved anticancer drugs. 2017;11:1-17.

(107) Lang DK, Kaur R, Arora R, Saini B, Arora SJA-CAiMC. Nitrogen-containing heterocycles as anticancer agents: An overview. 2020;20(18):2150-68.

(108) Benassi A, Doria F, Pirota VJIjoms. Groundbreaking anticancer activity of highly diversified oxadiazole scaffolds. 2020;21(22):8692.

(109) Jain S, Chandra V, Jain PK, Pathak K, Pathak D, Vaidya AJAJoC. Comprehensive review on current developments of quinoline-based anticancer agents. 2019;12(8):4920-46.

(110) Mahapatra A, Prasad T, Sharma TJFjopS. Pyrimidine: a review on anticancer activity with key emphasis on SAR. 2021;7(1):123.

(111) Ali I, Lone MN, Aboul-Enein HYJM. Imidazoles as potential anticancer agents. 2017;8(9):1742-73.

(112) Beloglazkina AA, Wobith B, Barskaia ES, Zefirov NA, Majouga AG, Beloglazkina EK, et al. Synthesis and biological testing of (5 Z)-2-aryl-5-arylmethylidene-3, 5-dihydro-4 H-imidazol-4-ones as antimitotic agents. 2016;25:1239-49.

(113) Khwaza V, Oyedeji OO, Aderibigbe BAJIjoms. Ursolic acid-based derivatives as potential anti-cancer agents: An update. 2020;21(16):5920.

(114) Chamorro-Petronacci C, García-García A, Lorenzo-Pouso A-I, Gómez-García FJ, Padín-Iruegas M-E, Gándara-Vila P, et al. Management options for low-dose methotrexate-induced oral ulcers: A systematic review. 2019;24(2):e181.

(115) Chang C-S, Lin Y-T, Shih S-R, Lee C-C, Lee Y-C, Tai C-L, et al. Design, synthesis, and antipicornavirus activity of 1-[5-(4-arylphenoxy) alkyl]-3-pyridin-4-ylimidazolidin-2-one derivatives. 2005;48(10):3522-35.

(116) Alaa A-M, El-Azab AS, Abou-Zeid LA, ElTahir KEH, Abdel-Aziz NI, Ayyad RR, et al. Synthesis, anti-inflammatory, analgesic and COX-1/2 inhibition activities of anilides based on 5, 5-diphenylimidazolidine-2, 4-dione scaffold: molecular docking studies. 2016;115:121-31.

(117) Alkahtani HM, Alanazi MM, Aleanizy FS, Alqahtani FY, Alhoshani A, Alanazi FE, et al. Synthesis, anticancer, apoptosis-inducing activities and EGFR and VEGFR2 assay mechanistic studies of 5, 5-diphenylimidazolidine-2, 4-dione derivatives: Molecular docking studies. 2019;27(5):682-93.

(118) El-Hady HA, Abubshait SAJRoci. Synthesis of imidazolinone and benzoxazole derivatives, and evaluation of their anticancer activity. 2015;41:1833-41.

(119) Moorkoth S, Srinivasan K, Gopalan Kutty N, Joseph A, Naseer MJMCR. Synthesis and evaluation of a series of novel imidazolidinone analogues of 6-aminoflavone as anticancer and anti-inflammatory agents. 2013;22:5066-75.

(120) Solankee A, Kapadia K, Upadhyay K, Patel JJOjoC. SYNTHESIS AND ANTICANCER ACTIVITY OF SOME 1-(2', 3'-DIMETHYL-1-PHENYL-3-PYRAZOLINE-S-ONE-4-YL)-2-PHENYL-4-(SUBSTITUTED BENZYLIDEN)-5-IMIDAZOLINES. 2001;17(2):315-8.

(121) Pai A, Singla RK, Joseph A, Kedar T, Thomas ATJP. Synthesis, invitro and invivo anticancer activity of substituted imidazolones. 2009;2:933-42.

(122) Abu-Jabal S, Ghareeb A, Smadi D, Hamed O, Assali M, Berisha A, et al. New Zwitterionic Imidazolones with Enhanced Water Solubility and Bioavailability: Synthesis, Anticancer Activity, and Molecular Docking. 2023;5(4):2613-29.

(123) Sheta YS, Sarg MT, Abdulrahman FG, Nossier ES, Husseiny EMJBC. Novel imidazolone derivatives as potential dual inhibitors of checkpoint kinases 1 and 2: Design, synthesis, cytotoxicity evaluation, and mechanistic insights. 2024;149:107471.

(124) Binjawhar DN, Katouah HA, Alshaye NA, Alharthi J, Alsharif G, Elsaid FG, et al. Synthesis and biological research of new imidazolone-sulphonamide-pyrimidine hybrids as potential EGFR-TK inhibitors and apoptosis-inducing agents. 2024;14(28):20120-9.

(125) Abdulrahman FG, Abulkhair HS, El Saeed HS, El-Dydamony NM, Husseiny EMJBC. Design, synthesis, and mechanistic insight of novel imidazolones as potential EGFR inhibitors and apoptosis inducers. 2024;144:107105.

(126) Walton NJ, Mayer MJ, Narbad AJP. Vanillin. 2003;63(5):505-15.

(127) Sinha AK, Sharma UK, Sharma NJIjofs, nutrition. A comprehensive review on vanilla flavor: extraction, isolation and quantification of vanillin and others constituents. 2008;59(4):299-326.

(128) Dehdashtian S, Wang S, Murray TA, Chegeni M, Rostamnia S, Fattahi NJSR. Determination of vanillin in different food samples by using SMM/Au@ ZIF-67 electrochemical sensor. 2023;13(1):17907.

(129) Gendron DJFiC. Vanillin: a promising biosourced building block for the preparation of various heterocycles. 2022;10:949355.

(130) Meghwar P, Saeed SMG, Tsoupras A, Aadil RM, Boateng IDJFB. Effect of electrolyzed watermelon rind flour on unleavened flatbread quality, techno-functional properties, minerals, bioactivities, and consumer preferences. 2024;61:104564.

(131) Olatunde A, Mohammed A, Ibrahim MA, Tajuddeen N, Shuaibu MNJEJoMCR. Vanillin: A food additive with multiple biological activities. 2022;5:100055.

(132) Raju SK, Sundhararajan N, Sekar P, Nagalingam YJJoDD, Therapeutics. Therapeutic aspects of biologically potent vanillin derivatives: A critical. 2023;13(7):177-89.

(133) Fache M, Boutevin B, Caillol SJEpj. Vanillin, a key-intermediate of biobased polymers. 2015;68:488-502.

(134) Arya SS, Rookes JE, Cahill DM, Lenka SKJAitm. Vanillin: A review on the therapeutic prospects of a popular flavouring molecule. 2021:1-17.

(135) Kanedi M, Nurhidayah S, Nurcahyani E, Widiastuti ELJEjop, research m. Fruit extract of vanilla (Vanilla planifolia Andrews) lowers total blood glucose in alloxan-induced hyperglycemic mice. 2019;6(9):314-6.

(136) Karathanos VT, Mourtzinos I, Yannakopoulou K, Andrikopoulos NKJFc. Study of the solubility, antioxidant activity and structure of inclusion complex of vanillin with β-cyclodextrin. 2007;101(2):652-8.

(137) Fuqua C, Greenberg EPJNrMcb. Listening in on bacteria: acyl-homoserine lactone signalling. 2002;3(9):685-95.

(138) Dinesh Dhingra DD, Amandeep Sharma AS. Evaluation of antidepressant-like activity of glycyrrhizin in mice. 2005.

(139) King AA, Shaughnessy DT, Mure K, Leszczynska J, Ward WO, Umbach DM, et al. Antimutagenicity of cinnamaldehyde and vanillin in human cells: Global gene expression and possible role of DNA damage and repair. 2007;616(1-2):60-9.

(140) Chen P, Liu Y, Li C, Hua S, Sun C, Huang LJH. Antibacterial mechanism of vanillin against Escherichia coli O157: H7. 2023;9(9).

(141) Fitzgerald D, Stratford M, Gasson M, Ueckert J, Bos A, Narbad AJJoam. Mode of antimicrobial action of vanillin against Escherichia coli, Lactobacillus plantarum and Listeria innocua. 2004;97(1):104-13.

(142) Cockerill FR, Wikler M, Bush K, Dudley M, Eliopoulos G, Hardy DJPsfastt-sis. Clinical and laboratory standards institute. 2012.

(143) Wayne AJPsfasttISCd. Clinical and Laboratory Standards Institute; CLSI. 2011. 2017.

(144) Hu M, Liu R, Castro N, Loza Sanchez L, Rueankham L, Learn JA, et al. A novel lipophilic amiloride derivative efficiently kills chemoresistant breast cancer cells. 2024;14(1):20263.

(145) Daina A, Michielin O, Zoete VJSr. SwissADME: a free web tool to evaluate pharmacokinetics, drug-likeness and medicinal chemistry friendliness of small molecules. 2017;7(1):42717.

(146) Martin YCJJomc. A bioavailability score. 2005;48(9):3164-70.

(147) Dulsat J, López-Nieto B, Estrada-Tejedor R, Borrell JIJM. Evaluation of free online ADMET tools for academic or small biotech environments. 2023;28(2):776.

(148) Daina A, Zoete VJC. A boiled-egg to predict gastrointestinal absorption and brain penetration of small molecules. 2016;11(11):1117-21.

(149) Baell JB, Holloway GAJJomc. New substructure filters for removal of pan assay interference compounds (PAINS) from screening libraries and for their exclusion in bioassays. 2010;53(7):2719-40.

(150) Berman H, Henrick K, Nakamura HJNs, biology m. Announcing the worldwide protein data bank. 2003;10(12):980-.

(151) Pon Nivedha R, Suryanarayanan V, Selvaraj C, Singh SK, Rajalakshmi MJMCR. Chemopreventive effect of saponin isolated from Gymnema sylevestre on prostate cancer through in silico and in vivo analysis. 2017;26:1915-25.

(152) Kaya Y, Kaya S, Berisha A, Erçağ AJJoMS. Cyclocondensation of 3, 4-diaminobenzophenone with glyoxal: Synthesis, X-ray structure, density functional theory calculation and molecular docking studies. 2023;1291:135973.

(153) Guclu G, Tas A, Dincer E, Ucar E, Kaya S, Berisha A, et al. Biological evaluation and in silico molecular docking studies of Abies cilicica (Antoine & Kotschy) Carrière) resin. 2023;1288:135740.

(154) Kumar A, Masroor S, Kaya S, Katin KP, Berisha A, Khan ME, et al. Synthesis of sustainable heterocyclic aryl sulfonamide derivatives: computational studies, molecular docking, and antibacterial assessment. 2024:1-14.

Appendices

Appendix A

Figures of Study

Figure A1

A: Some heterocyclic systems. B: 5-oxazolone and 5-imidazolone. C: Types of oxazolone. D: Isomers of oxazolone. E: Bonds length of oxazolone. F: Oxazolone chemistry

A

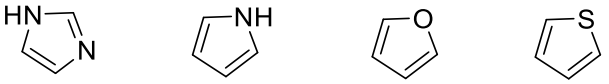

1 **2** **3** **4**

B

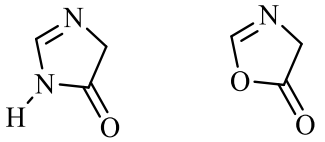

5 **6**

C

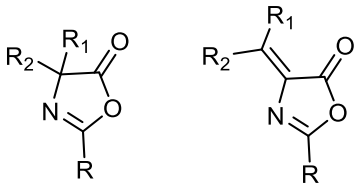

7 Saturated **8** Unsaturated

D

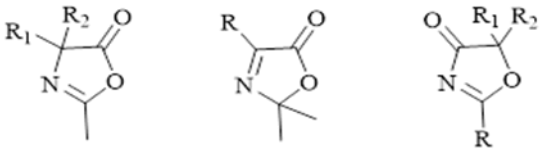

9 **10** **11**

12 **13**

E

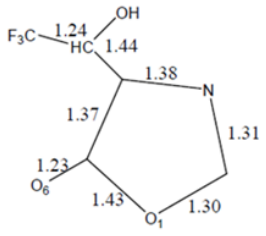

F

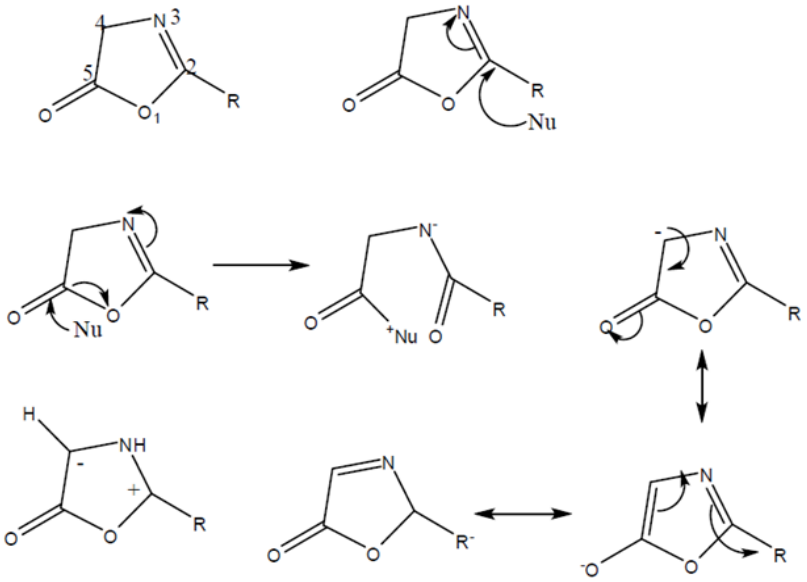

Figure A2

A: Erlenmeyer azlactones synthesis. B: Mechanism of oxazolone formation. C: Synthesis of oxazolone (14) by cyclohydration condensation. D: Using acetic anhydride and pyridine in 5(4)-oxazolone (15) synthesis

A

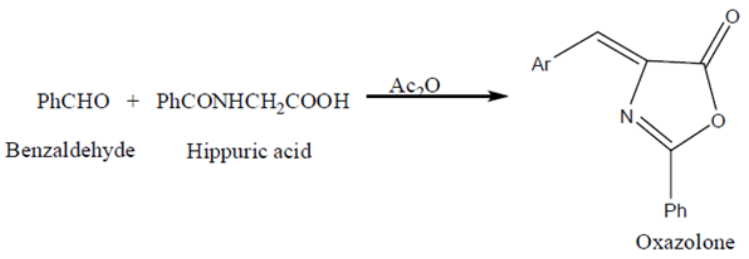

B

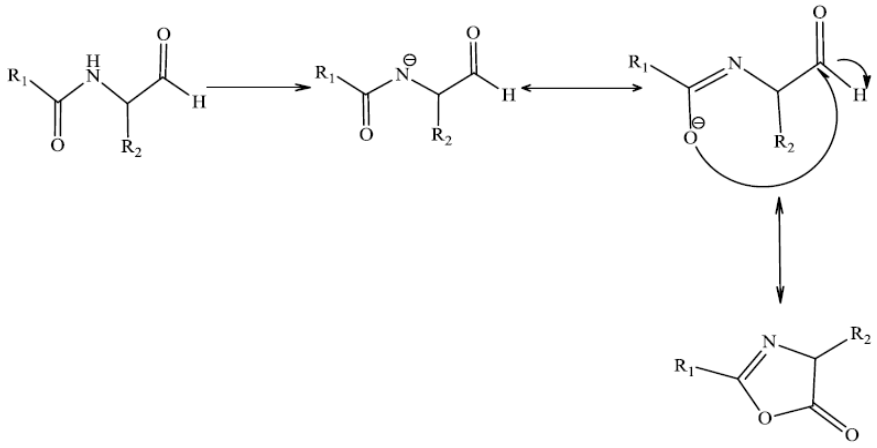

C

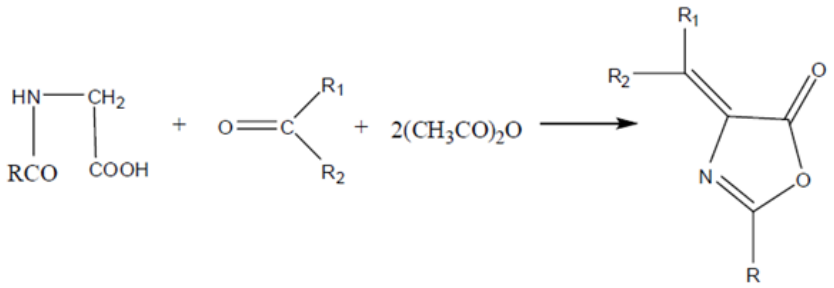

14

D

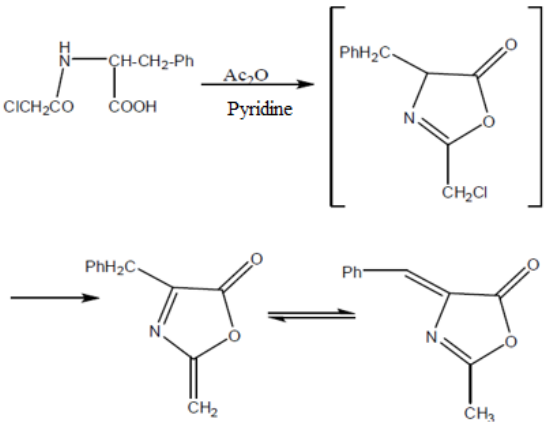

15

Figure A3

A: Preparation of azlactone by the DCC method. B: Preparation of 2-oxazolin-5-one (17) from acetic anhydride-pyridine mixture. C: Acid catalyzed preparation of 2-oxazolin-5-one (19)

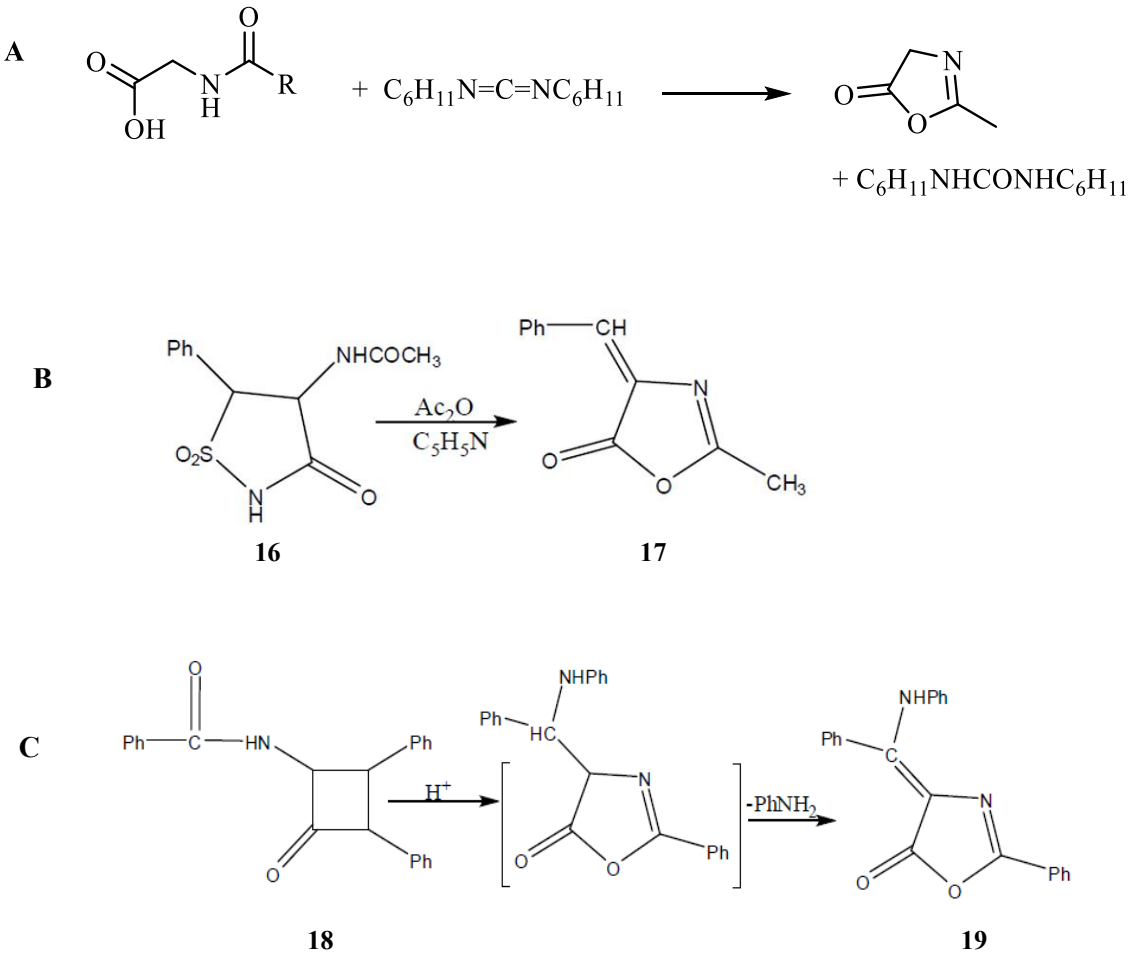

Figure A4

A: Reactivity of oxazolone. B: Oxazolone hydrolysis. C: Azlactone hydrolysis by amine and amino acid. D: Aminolysis of 5(4)-oxazolone (20). E: Aminolysis of oxazolone with primary amine H_2NR where R = NHPh, CH_2-Ph or Ph

A

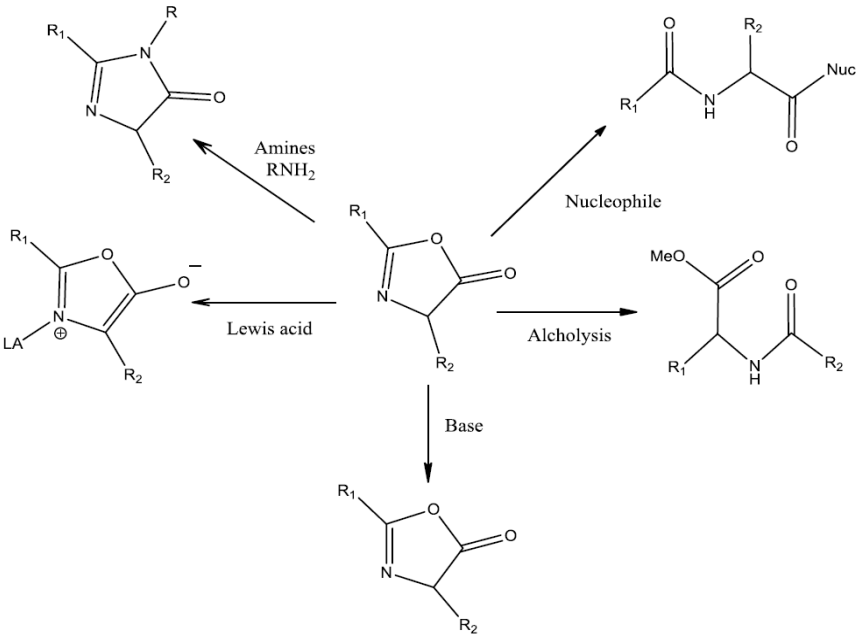

B

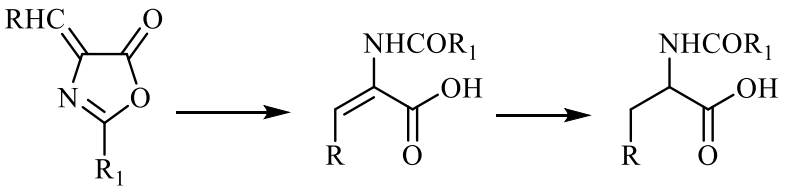

C

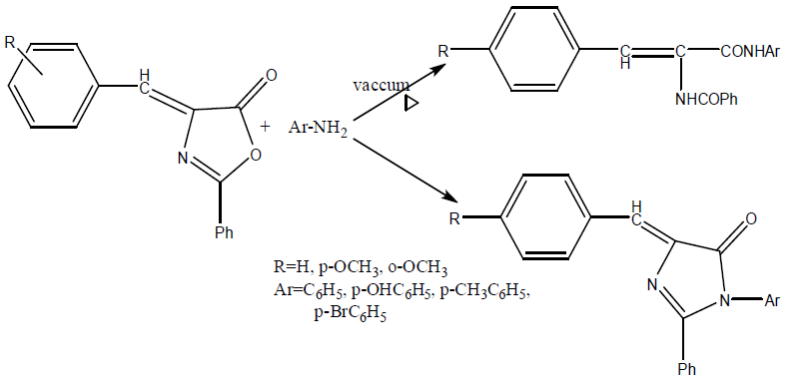

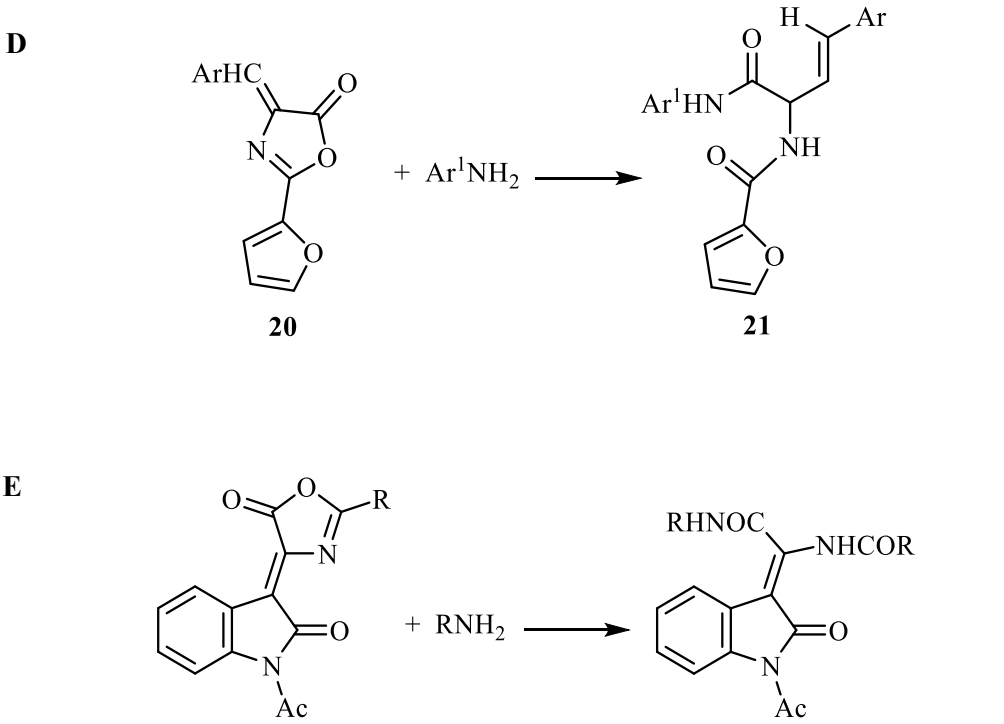

Figure A5

A: Acid anhydride behavior of oxazolone with amino acids. B: 5(4)-Oxazolone (22) reaction with hydroxylamine hydrochloride. C: Alkylation of oxazolones at C4. D: Friedel-Crafts reaction of 5(4)-oxazolone (24). E: Transferring unsaturated azlactones to imidazolones

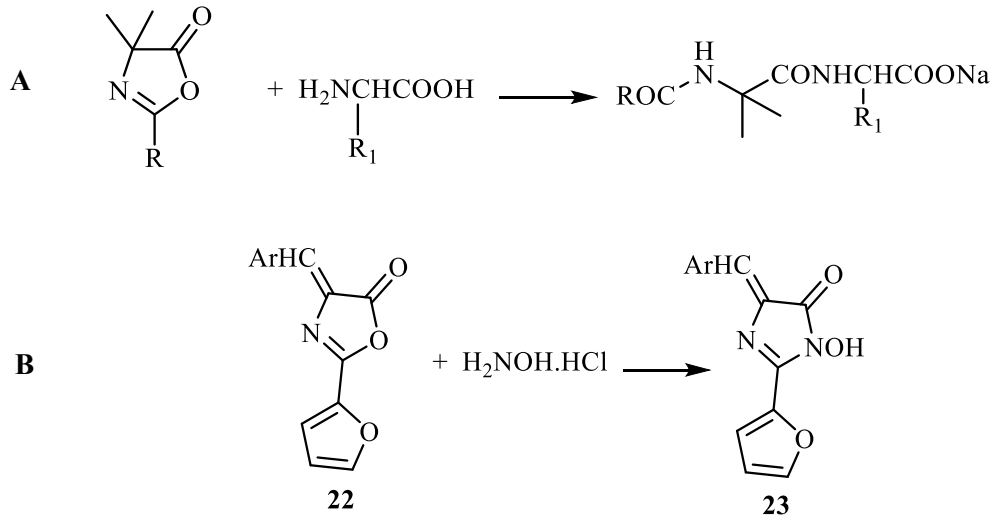

C

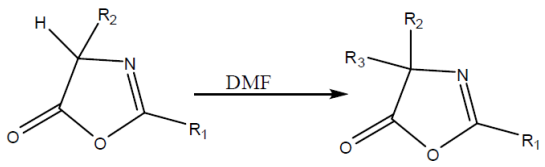

D

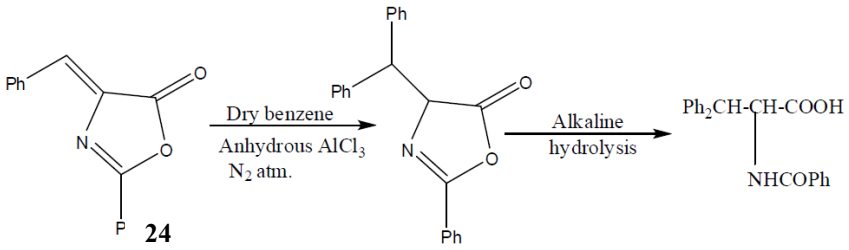

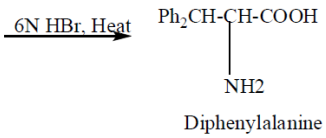

Diphenylalanine

E

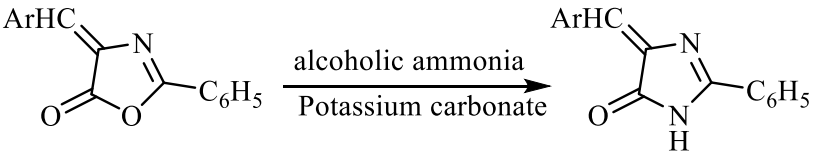

Figure A6

Structures of different oxazolone derivatives (25-31) with various biological activities

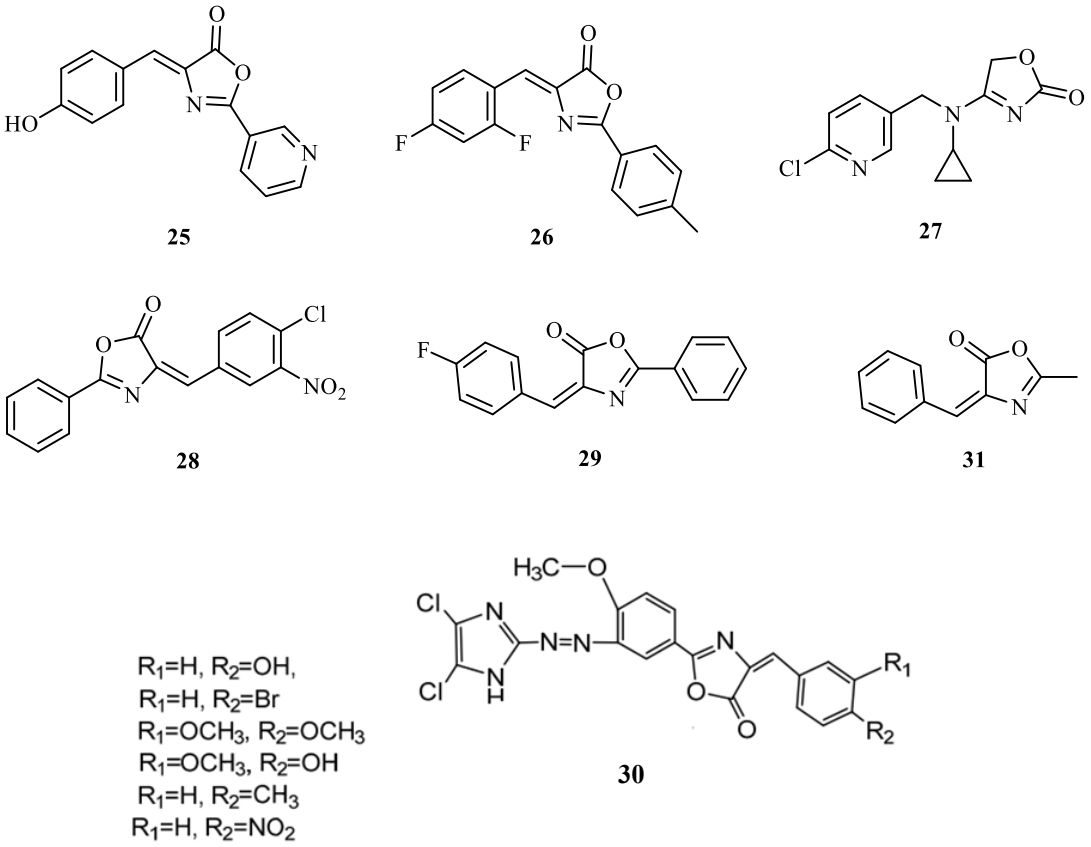

Figure A7

A: Structure of histidine and histamine-related hormone. B: Resonance structures of imidazoles. C: Isomers of imidazolinone

A

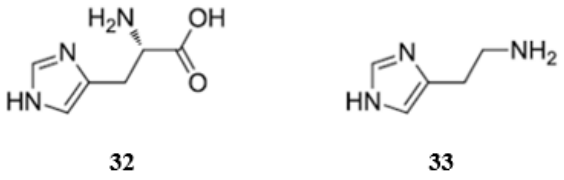

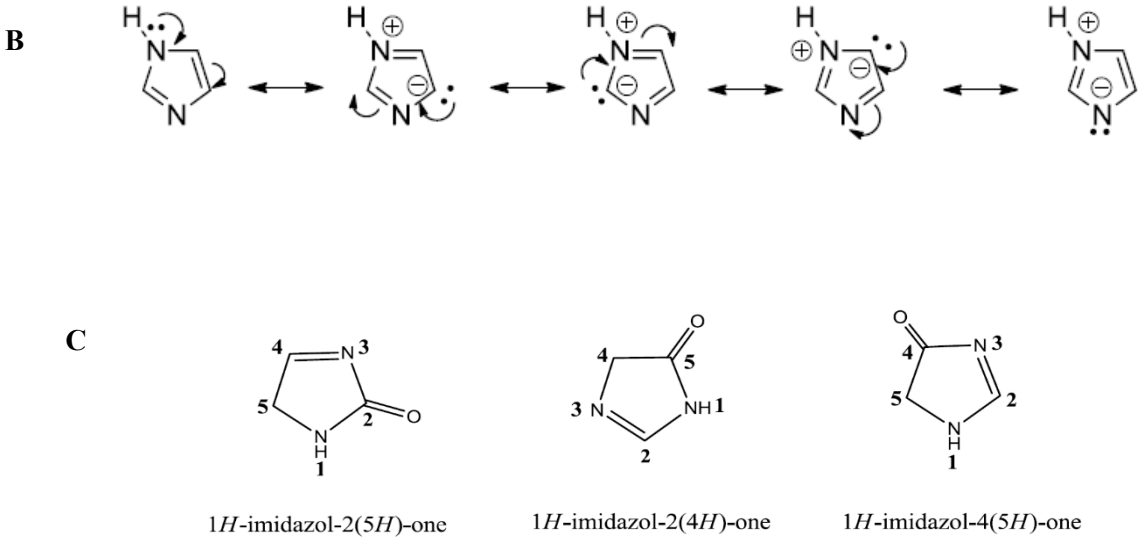

Figure A8

A: Imidazolone synthesis by oxazolone and primary amine condensation. B: Synthesis of 5-imidazolones containing1,3,4-oxadiazole group, X= H, 2-Cl, 4-$(CH_3)_2N$, 2-NO_2, 3-NO_2, 4-CH_3O or 2-HO. C: Synthesis of imidazol-5-one (35), R= Br, Cl or NO_2

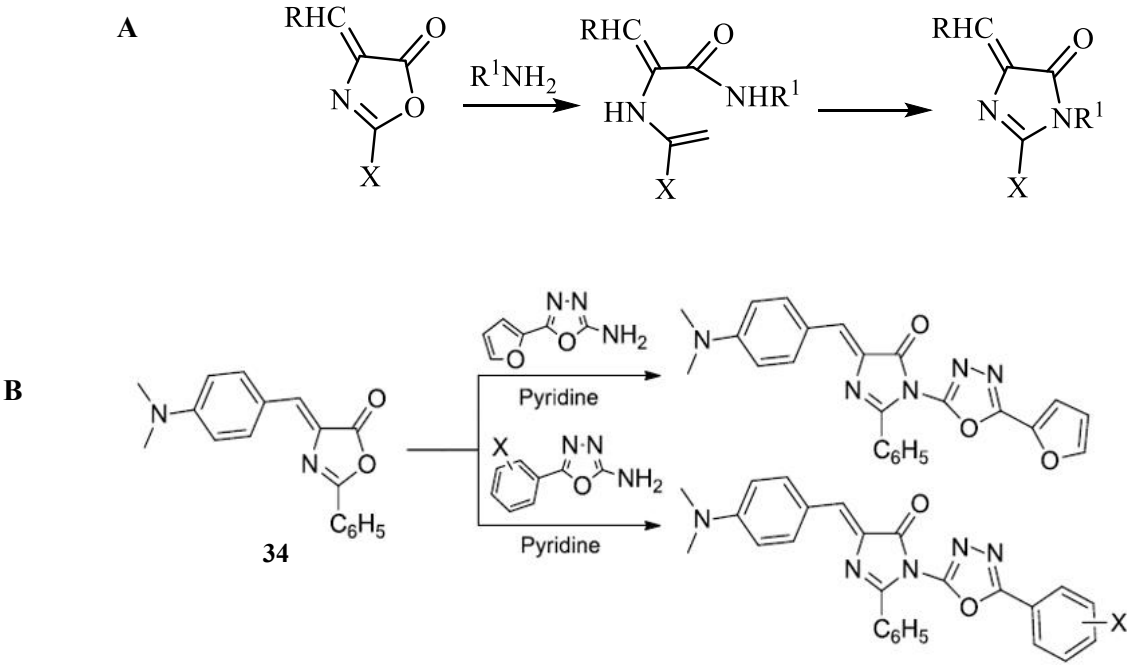

C

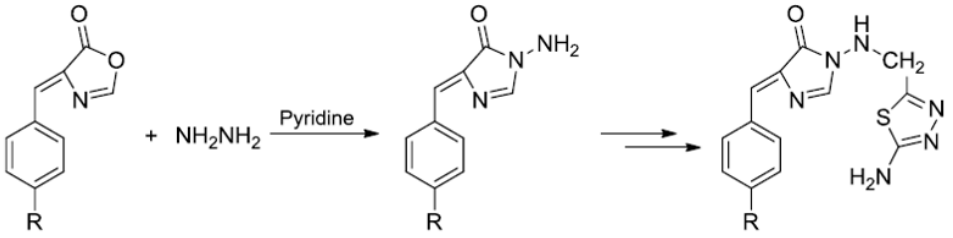

35

Figure A9

A: Aminolysis of oxazolone with ammonia. B: Reaction of oxazolone with ethane-1,2-diamine, where X= H, 2-Cl, 2-OH, 4-$(CH_3)_2N$ or 4-CH_3O. C: Preparation of imidazol-5(4H)-one derivatives (38) and (39) from 37

A

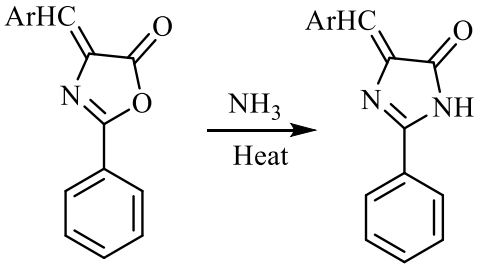

B

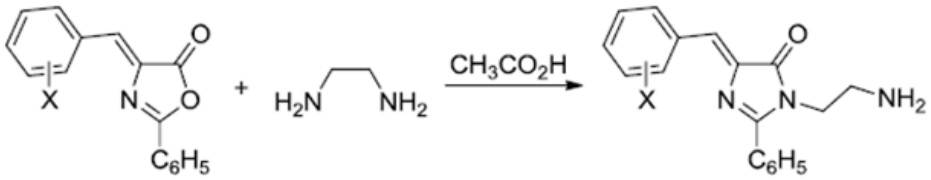

36

C

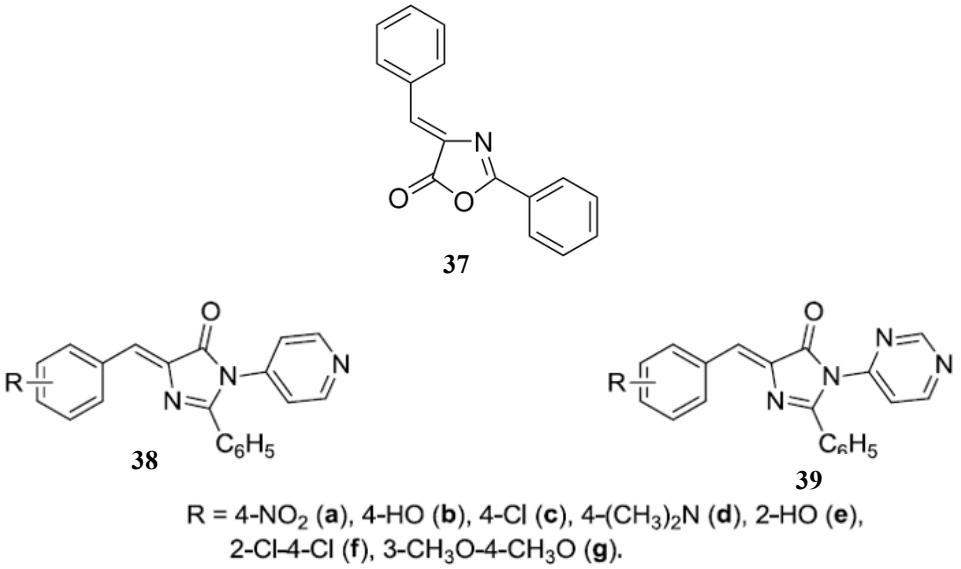

Figure A10

A: Reaction of 2- aminochromone and oxazol-5(4H)-ones (40). B: Structure of 5-oxo-imidazoline derivative after fusion with 4–methyl cinnamoyl hydrazine

A

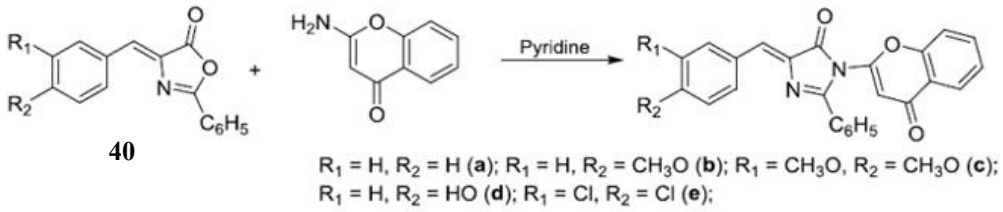

B

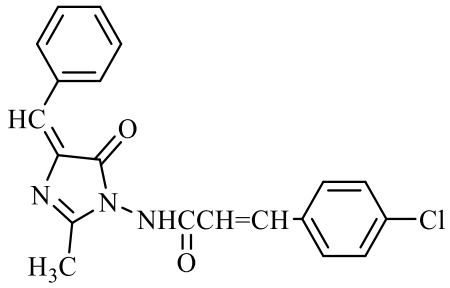

Figure A11

A: Effective antimicrobial imidazolone derivative. B: Antimicrobial imidazolinones with benzimidazole moiety. C: Imidazolones with antimicrobial effects prepared by N.C. Desai et al

A

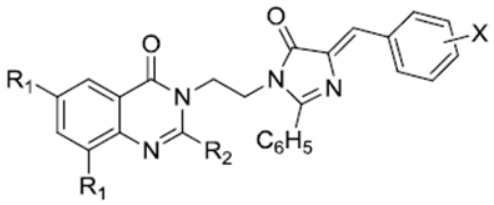

R_1 = H, Br; R_2 = CH_3, C_6H_5, CH_2Cl: X = H, 2-Cl, 2-OH, 4-$(CH_3)_2N$, 4-CH_3O

B

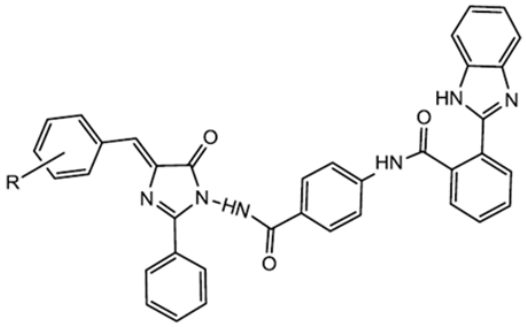

R= H, 4-NH_2, 2-Cl, 4-Cl, 3,4- di OCH_3, 4-OCH_3, 2-furyl, 2-OH, 4-OH, 4-Br

C

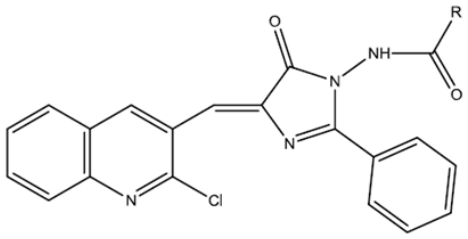

a = -C_6H_5
b = -C_6H_5-CH_2-
c = -3-Cl-C_6H_4
d = -4-Cl-C_6H_4
e = - 2,3-$(Cl)_2$-C_6H_3
f = -4-F-C_6H_4
g = -3-NO_2-C_6H_4
h = -4-NO_2-C_6H_4
i = -2-OH-C_6H_4
j = -3-OH-C_6H_4
k = -2-OH-4-Cl-C_6H_3
l = -C_5H_4N

Figure A12

A: Antimicrobial 3'- quinolinyl substituted imidazole-5-one derivatives. B: Anticonvulsant imidazolone derivative. C: Anticonvulsant imidazolones (41) and (42) prepared by Moorthy et al (R= H, p-dimethylamino, p-OH, p-OCH_3, o-Cl, o-OH)

A

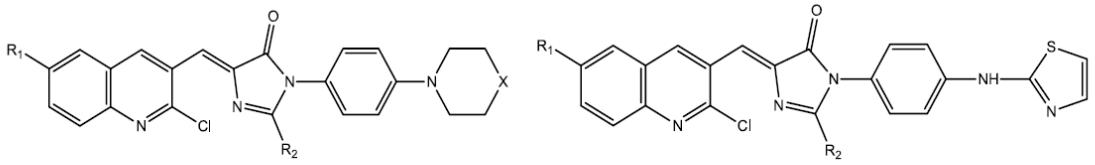

R_1 = H, CH_3, OCH_3
R_2 = CH_3, Phenyl
X = O, N-CH_2-CH_3, N-CH_3

B

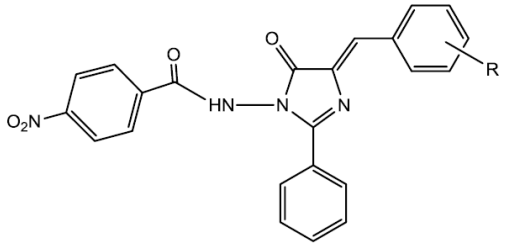

C

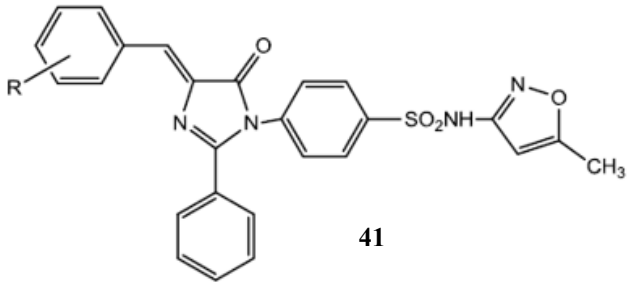

41

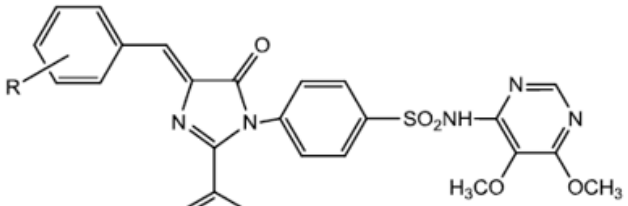

42

Figure A13

A: Structure of imidazol-5(4H)-one (43). B: Anti-inflammatory 5-4H-imidazolones (44). C: Structure of imidazol-5(4H)-one (45). D: Anthelmintic imidazol-5(4H)one (46). E: Anthelmintic imidazolone derivative (47)

A

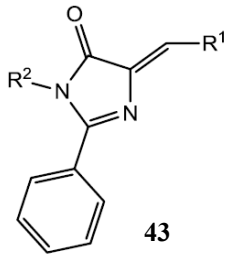

43

R^1 = Phenyl, 4-chlorophenyl, 4-methoxyphenyl, 2-furyl
R^2 = phenyl, 3-chlorophenyl, 4-chlorophenyl, 3,4-dichlorophenyl, 4-fluorophenyl, benzyl

B

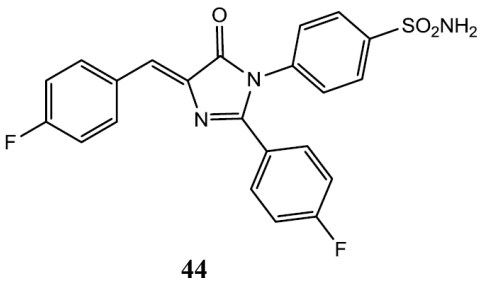

44

C

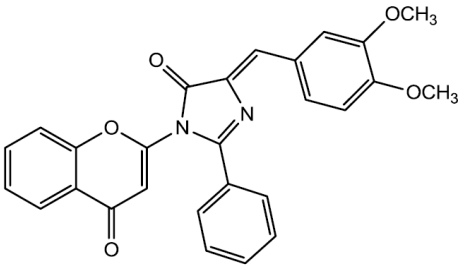

45

D

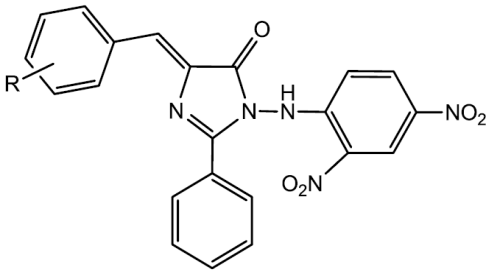

46

E

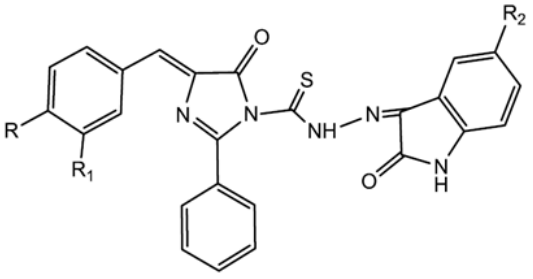

47

R = -H, -OCH_3, -Cl, -NO_2, -CH_3 **R_1** = H, -OCH_3 **R_2** = -H, -Cl

Figure A14

A: Structure of methotrexate. B: Structures of anticancer pyridyl imidazolidinones (48) and (49). C: Structure of imidazolone (50)

A

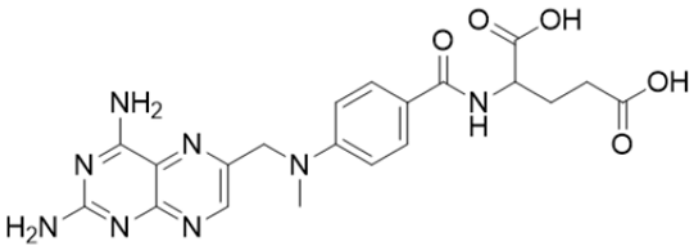

B

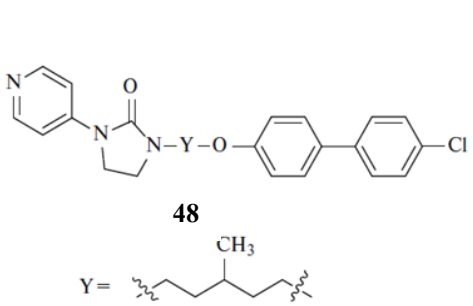

48

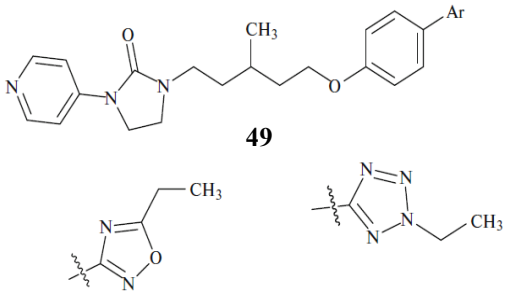

49

C

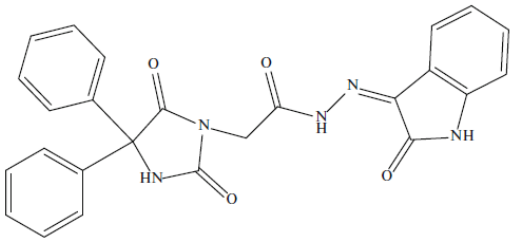

50

Figure A15

A: Structures of imidazol-5(4H)-one (51) and (52). B: Structure of the anticancer imidazol-5(4H)-one (53). C: Structure of imidazol-5-one (54). D: 5-imidazolone (55) structure

A

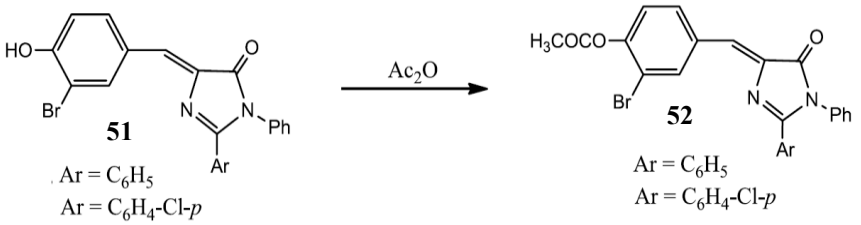

51

Ar = C_6H_5

Ar = C_6H_4-Cl-*p*

52

Ar = C_6H_5

Ar = C_6H_4-Cl-*p*

B

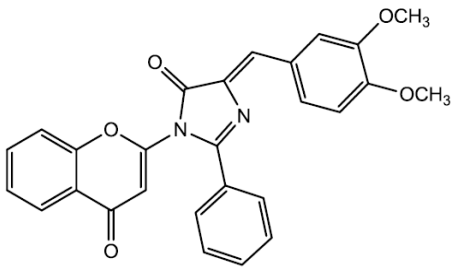

53

C

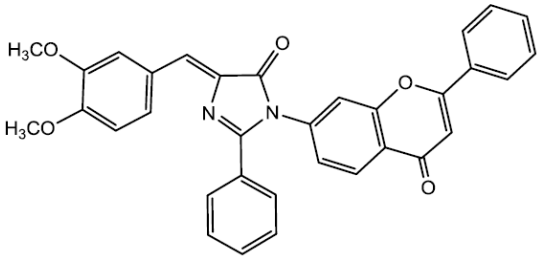

54

D

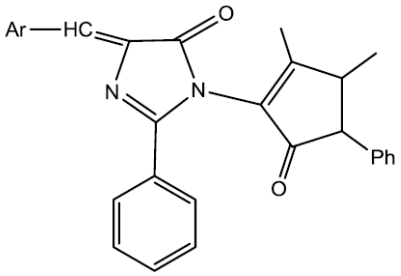

55

Figure A16

A: Structure of anticancer derivative 56 with the lowest IC_{50} value. B: General structure of aromatic substituted imidazolone 57. C: Preparation of zwitterionic imidazolones with alkyl sulfonate moiety

A

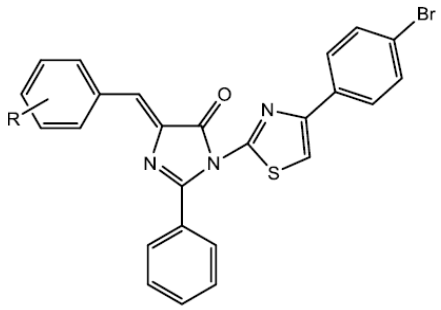

56

B

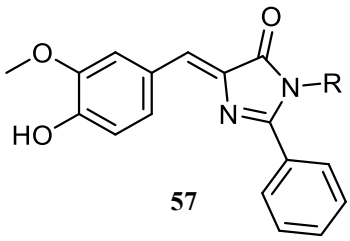

57

C

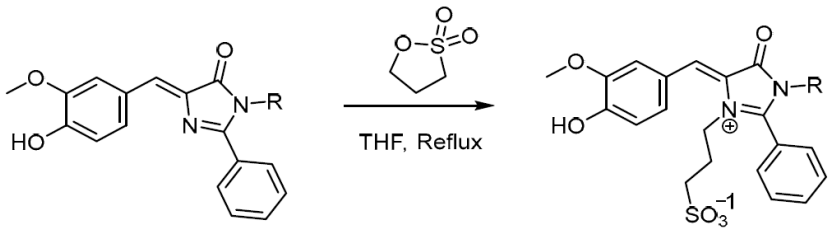

Figure A17

A: Anticancer imidazolone derivatives. B: Imidazolone (59) structure. C: Derivatives of imidazolone (60) with Ar: 4-CH_3-C_6H_4-, 4-Cl-C_6H_4-, 2,4-$(Cl)_2$-C_6H_3-, 4-OH-C_6H_4-, 2-furyl or 2-thienyl

A

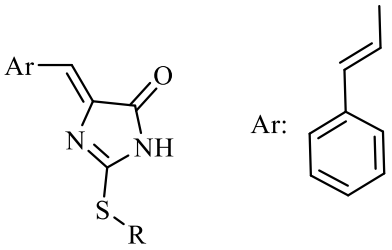

58

R: $-C_2H_5$, $-C_3H_7$, $-C_4H_9$

B

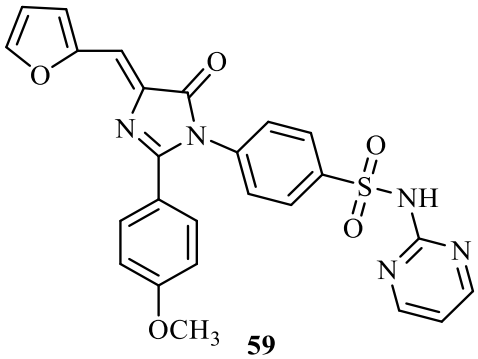

59

C

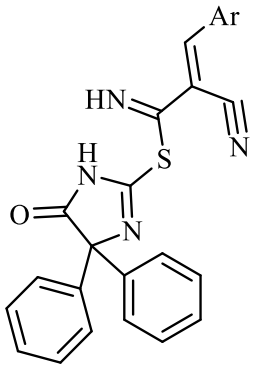

60

Figure A18

Imidazolones (3a-g) having viability against the five tested cells

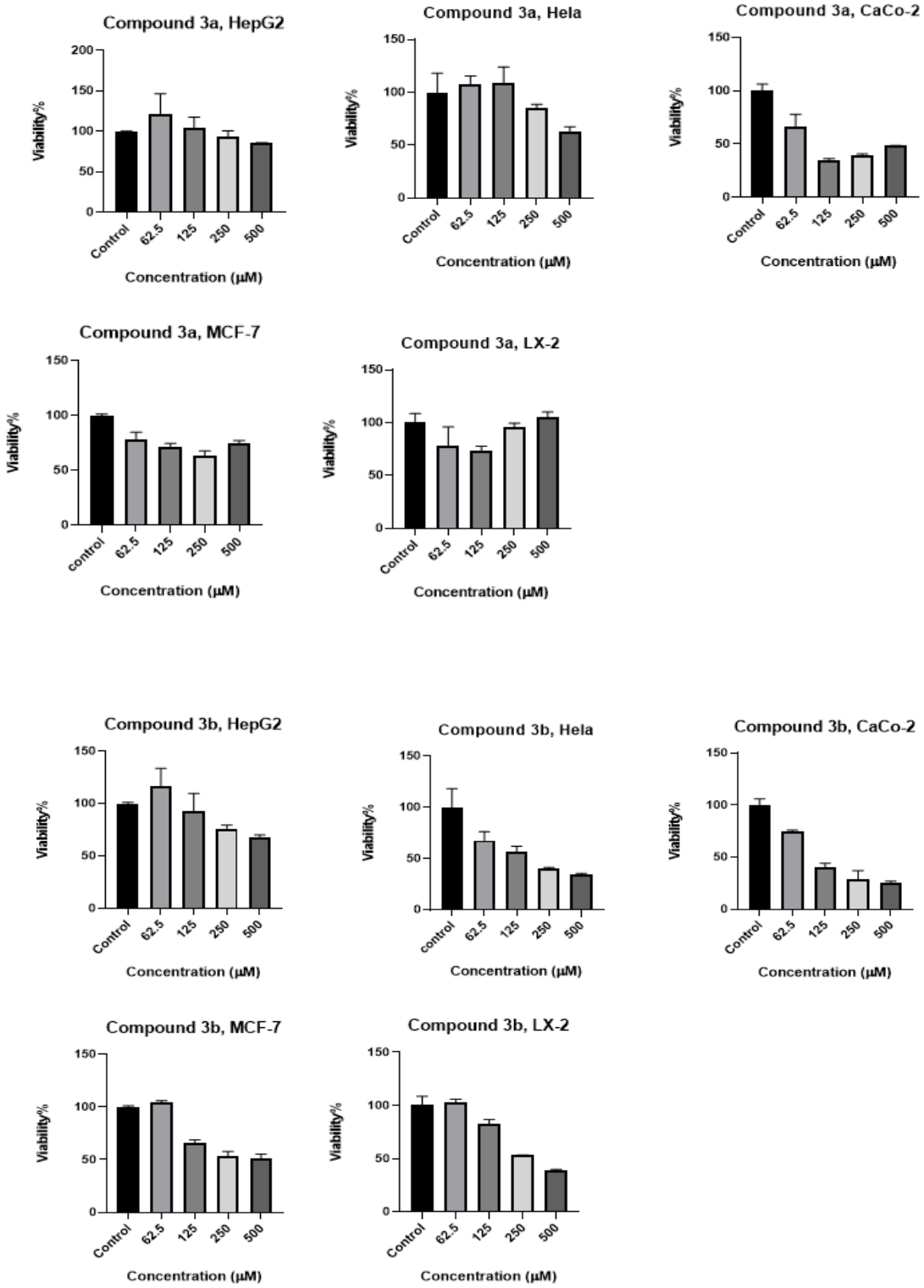

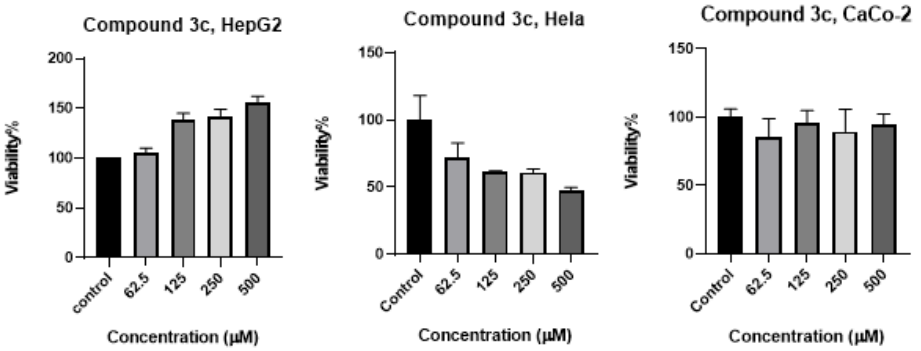
Compound 3c, HepG2
Viability%
200
150
100
50
0
control
62.5
125
250
500
Concentration (μM)
Compound 3c, Hela
Viability%
150
100
50
0
Control
62.5
125
250
500
Concentration (μM)
Compound 3c, CaCo-2
Viability%
150
100
50
0
Control
62.5
125
250
500
Concentration (μM)

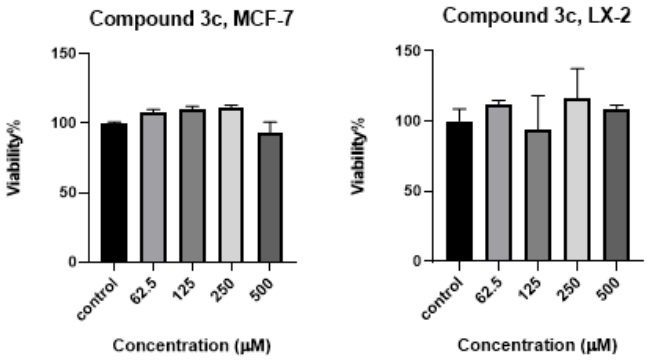
Compound 3c, MCF-7
Viability%
150
100
50
0
control
62.5
125
250
500
Concentration (μM)
Compound 3c, LX-2
Viability%
150
100
50
0
control
62.5
125
250
500
Concentration (μM)

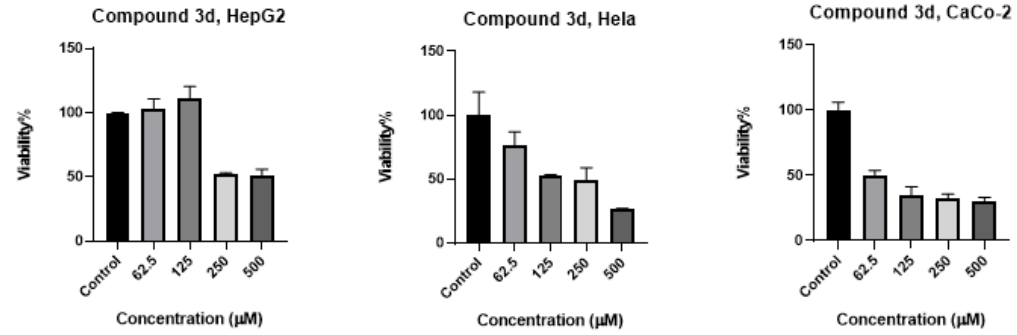
Compound 3d, HepG2
Viability%
150
100
50
0
Control
62.5
125
250
500
Concentration (μM)
Compound 3d, Hela
Viability%
150
100
50
0
Control
62.5
125
250
500
Concentration (μM)
Compound 3d, CaCo-2
Viability%
150
100
50
0
Control
62.5
125
250
500
Concentration (μM)

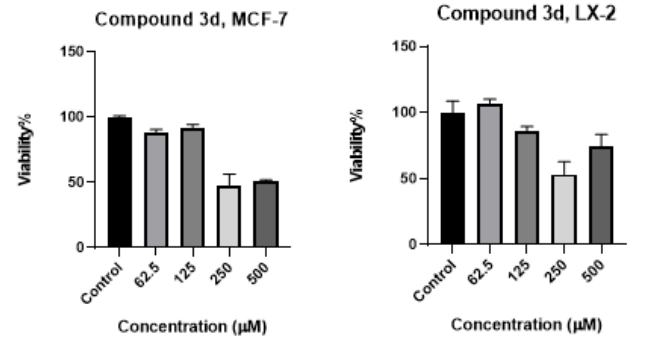
Compound 3d, MCF-7
Viability%
150
100
50
0
Control
62.5
125
250
500
Concentration (μM)
Compound 3d, LX-2
Viability%
150
100
50
0
Control
62.5
125
250
500
Concentration (μM)

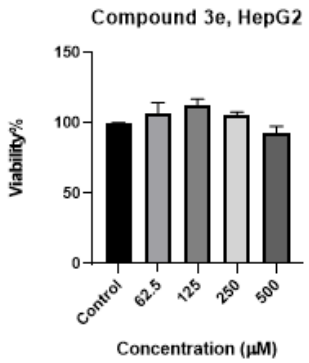
Compound 3e, HepG2
Viability%
150
100
50
0
Control
62.5
125
250
500
Concentration (μM)

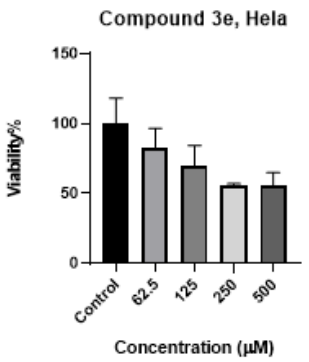
Compound 3e, Hela
Viability%
150
100
50
0
Control
62.5
125
250
500
Concentration (μM)

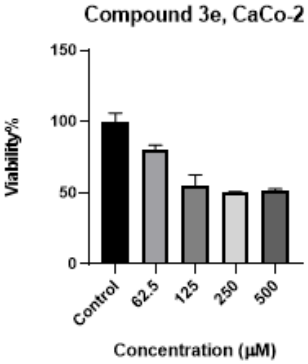
Compound 3e, CaCo-2
Viability%
150
100
50
0
Control
62.5
125
250
500
Concentration (μM)

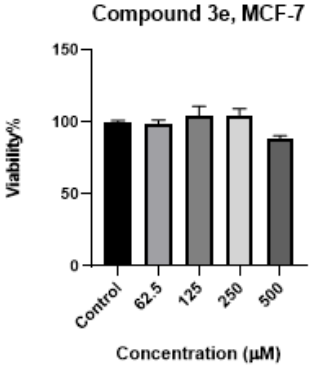
Compound 3e, MCF-7
Viability%
150
100
50
0
Control
62.5
125
250
500
Concentration (μM)

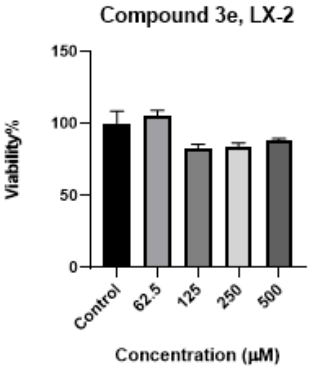
Compound 3e, LX-2
Viability%
150
100
50
0
Control
62.5
125
250
500
Concentration (μM)

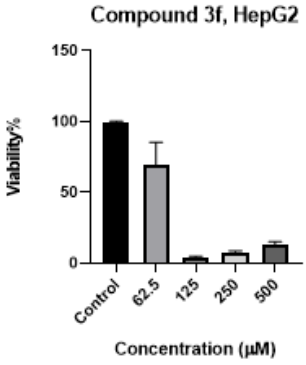
Compound 3f, HepG2
Viability%
150
100
50
0
Control
62.5
125
250
500
Concentration (μM)

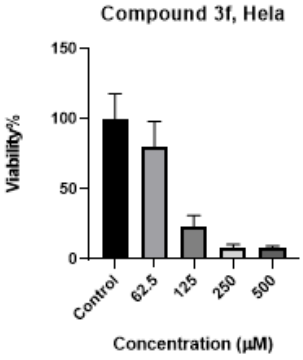
Compound 3f, Hela
Viability%
150
100
50
0
Control
62.5
125
250
500
Concentration (μM)

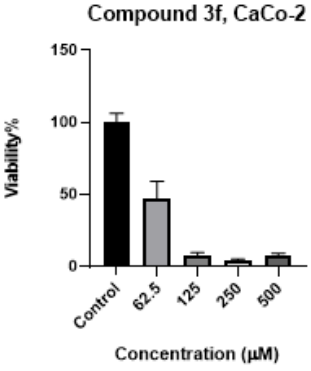
Compound 3f, CaCo-2
Viability%
150
100
50
0
Control
62.5
125
250
500
Concentration (μM)

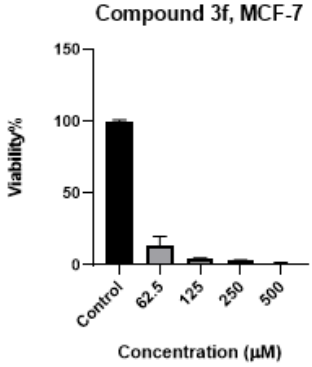
Compound 3f, MCF-7
Viability%
150
100
50
0
Control
62.5
125
250
500
Concentration (μM)

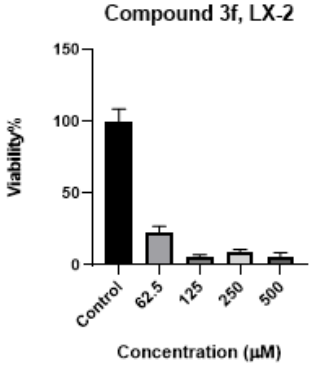
Compound 3f, LX-2
Viability%
150
100
50
0
Control
62.5
125
250
500
Concentration (μM)

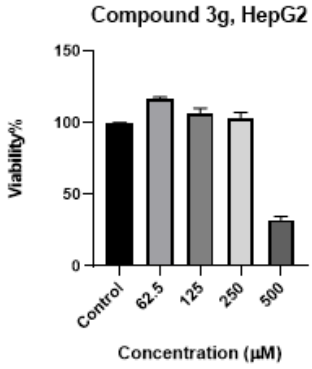
Compound 3g, HepG2
Viability%
150
100
50
0
Control
62.5
125
250
500
Concentration (μM)

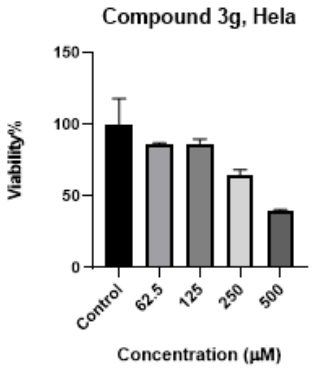
Compound 3g, Hela
Viability%
150
100
50
0
Control
62.5
125
250
500
Concentration (μM)

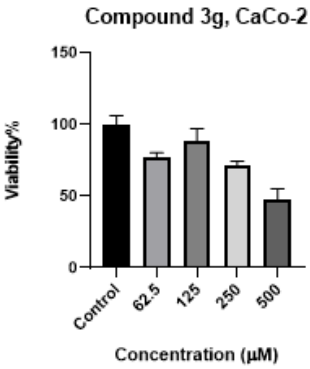
Compound 3g, CaCo-2
Viability%
150
100
50
0
Control
62.5
125
250
500
Concentration (μM)

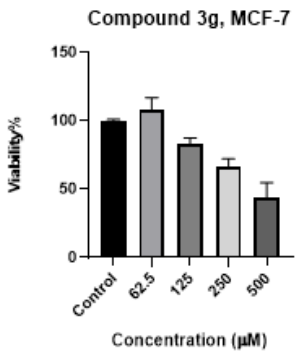
Compound 3g, MCF-7
Viability%
150
100
50
0
Control
62.5
125
250
500
Concentration (μM)

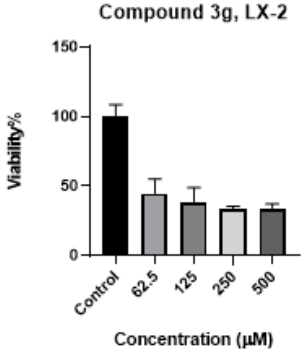
Compound 3g, LX-2
Viability%
150
100
50
0
Control
62.5
125
250
500
Concentration (μM)

Figure A19

The viability of compounds (5a-g) against tested cells

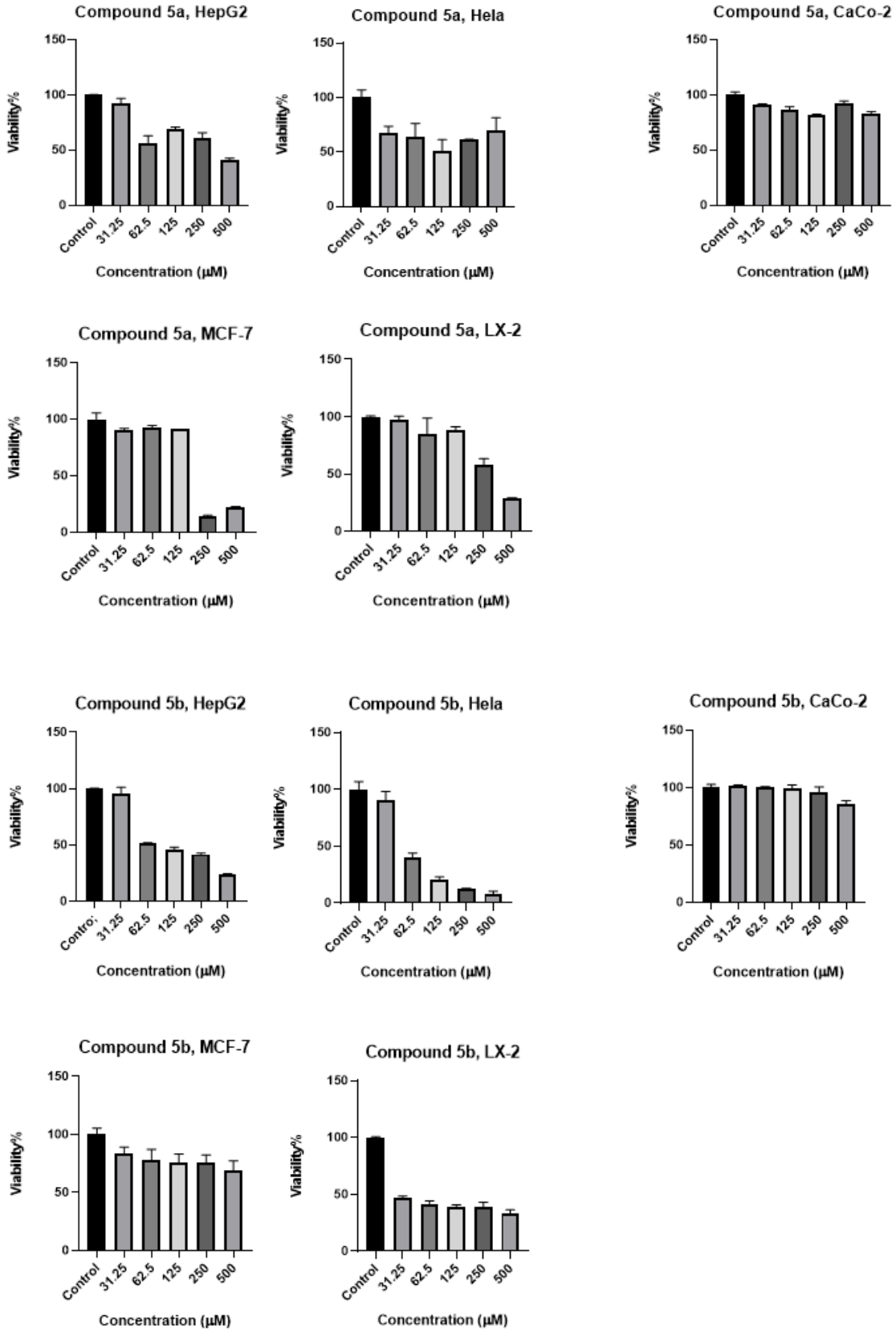

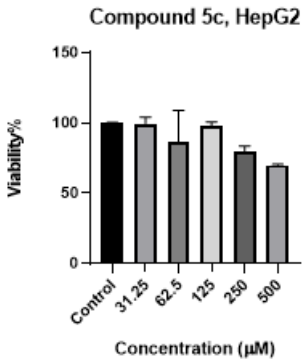
Compound 5c, HepG2
Viability%
150
100
50
0
Control
31.25
62.5
125
250
500
Concentration (μM)

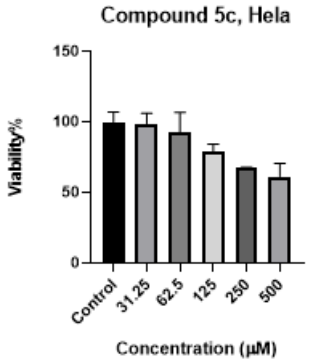
Compound 5c, Hela
Viability%
150
100
50
0
Control
31.25
62.5
125
250
500
Concentration (μM)

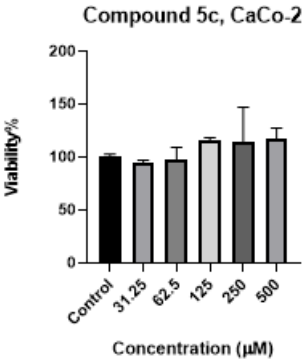
Compound 5c, CaCo-2
Viability%
200
150
100
50
0
Control
31.25
62.5
125
250
500
Concentration (μM)

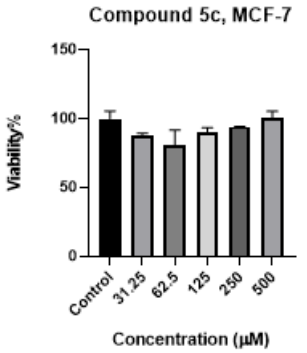
Compound 5c, MCF-7
Viability%
150
100
50
0
Control
31.25
62.5
125
250
500
Concentration (μM)

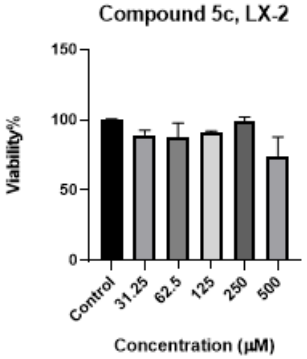
Compound 5c, LX-2
Viability%
150
100
50
0
Control
31.25
62.5
125
250
500
Concentration (μM)

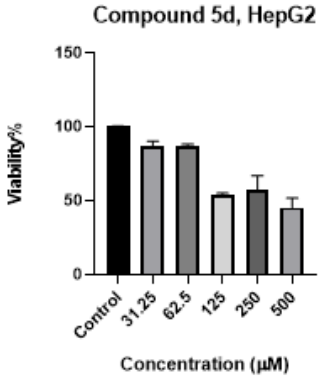
Compound 5d, HepG2
Viability%
150
100
50
0
Control
31.25
62.5
125
250
500
Concentration (μM)

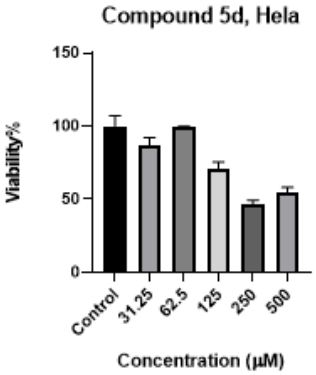
Compound 5d, Hela
Viability%
150
100
50
0
Control
31.25
62.5
125
250
500
Concentration (μM)

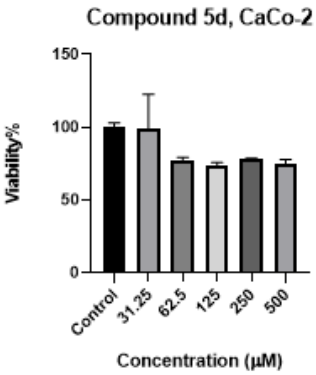
Compound 5d, CaCo-2
Viability%
150
100
50
0
Control
31.25
62.5
125
250
500
Concentration (μM)

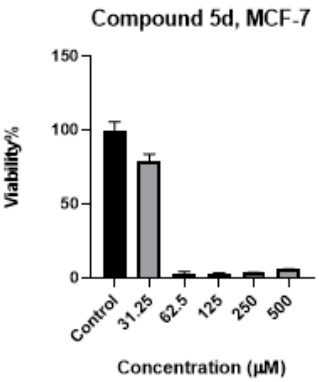
Compound 5d, MCF-7
Viability%
150
100
50
0
Control
31.25
62.5
125
250
500
Concentration (μM)

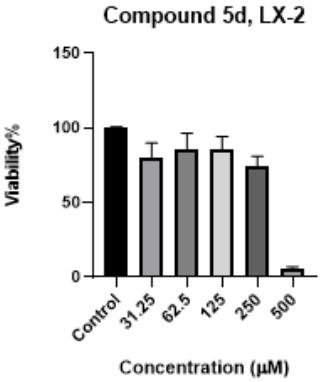
Compound 5d, LX-2
Viability%
150
100
50
0
Control
31.25
62.5
125
250
500
Concentration (μM)

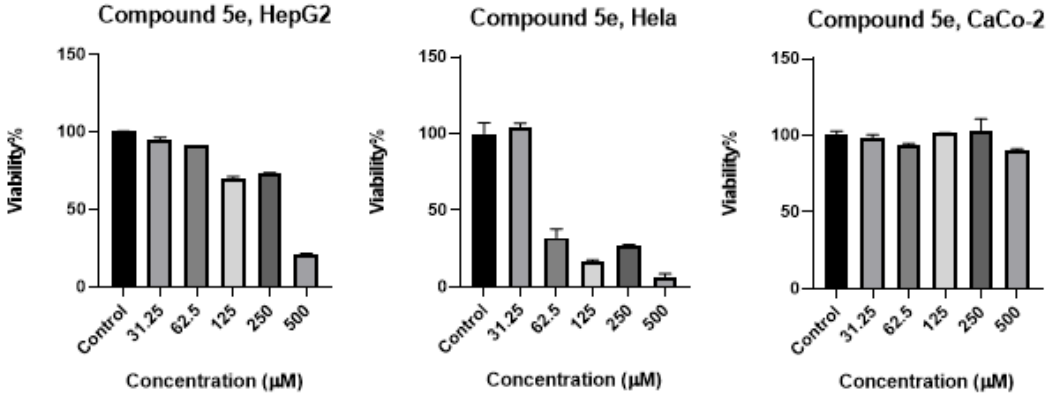
Compound 5e, HepG2
Compound 5e, Hela
Compound 5e, CaCo-2
Viability%
150
100
50
0
Control
31.25
62.5
125
250
500
Concentration (μM)

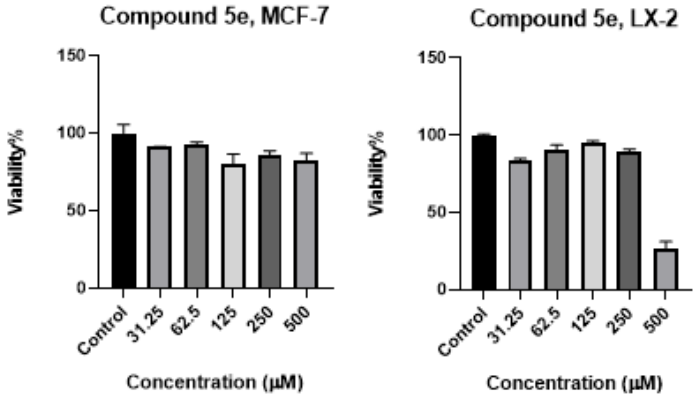
Compound 5e, MCF-7
Compound 5e, LX-2
Viability%
150
100
50
0
Control
31.25
62.5
125
250
500
Concentration (μM)

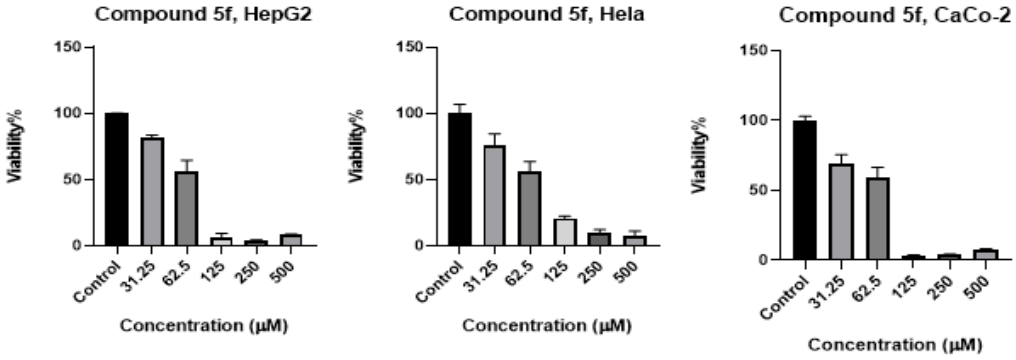
Compound 5f, HepG2
Compound 5f, Hela
Compound 5f, CaCo-2
Viability%
150
100
50
0
Control
31.25
62.5
125
250
500
Concentration (μM)

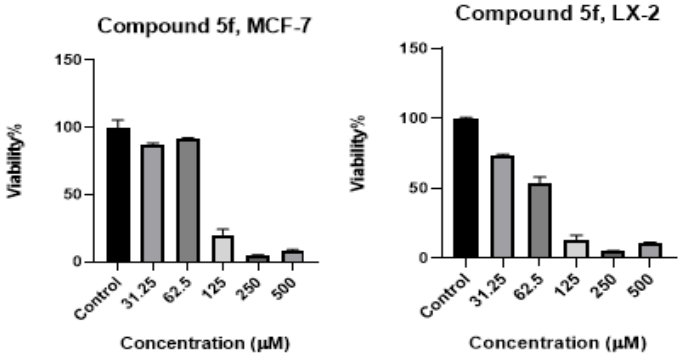
Compound 5f, MCF-7
Compound 5f, LX-2
Viability%
150
100
50
0
Control
31.25
62.5
125
250
500
Concentration (μM)

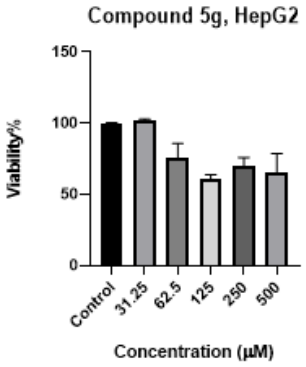
Compound 5g, HepG2
Viability%
150
100
50
0
Control
31.25
62.5
125
250
500
Concentration (μM)

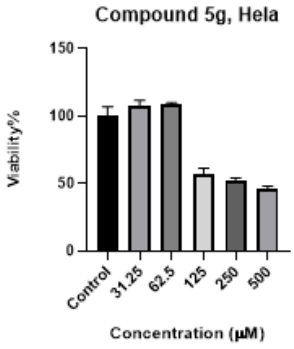
Compound 5g, Hela
Viability%
150
100
50
0
Control
31.25
62.5
125
250
500
Concentration (μM)

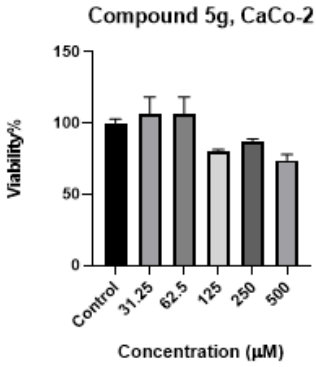
Compound 5g, CaCo-2
Viability%
150
100
50
0
Control
31.25
62.5
125
250
500
Concentration (μM)

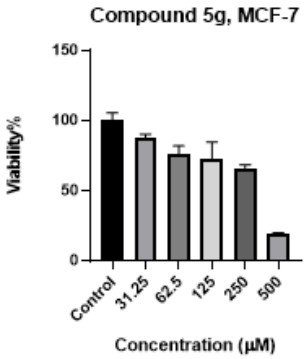
Compound 5g, MCF-7
Viability%
150
100
50
0
Control
31.25
62.5
125
250
500
Concentration (μM)

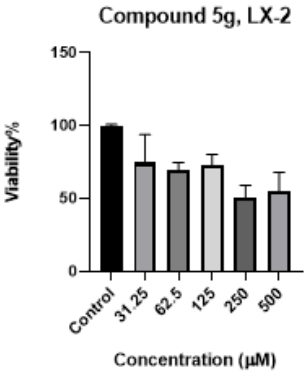
Compound 5g, LX-2
Viability%
150
100
50
0
Control
31.25
62.5
125
250
500
Concentration (μM)

Appendix B

Spectroscopic characterization graphs

Figure B1

FT-IR of benzoyl glycine (1)

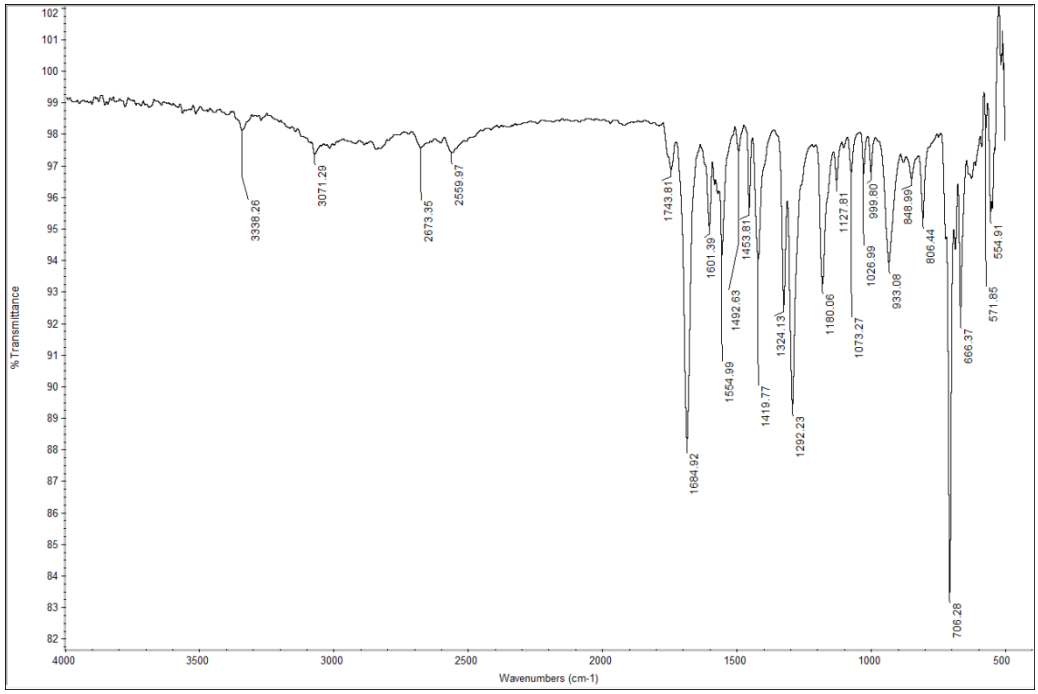

Figure B2

FT-IR of (Z)-4-(4-Hydroxy-3 Methoxybenzylidene)-2-Phenyloxazol-5-(4H)-One (2)

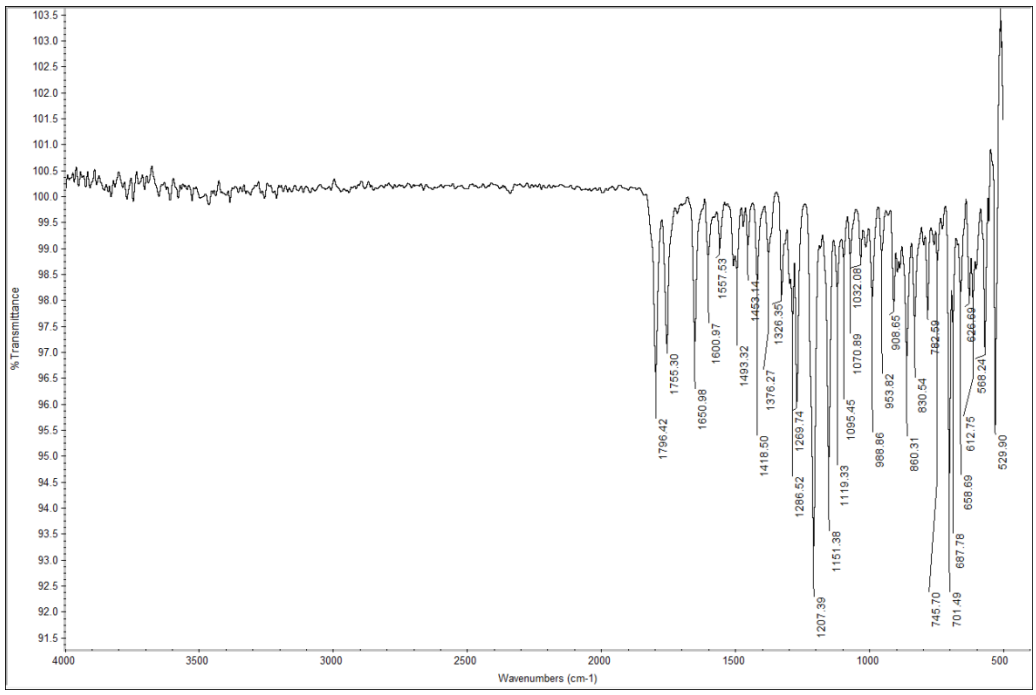

Figure B3

FT-IR of (Z)-3-((2-bromophenyl)amino)-5-(4-hydroxy-3-methoxybenzylidene)-2-phenyl-3,5-dihydro-4H-imidazol-4-one (3a)

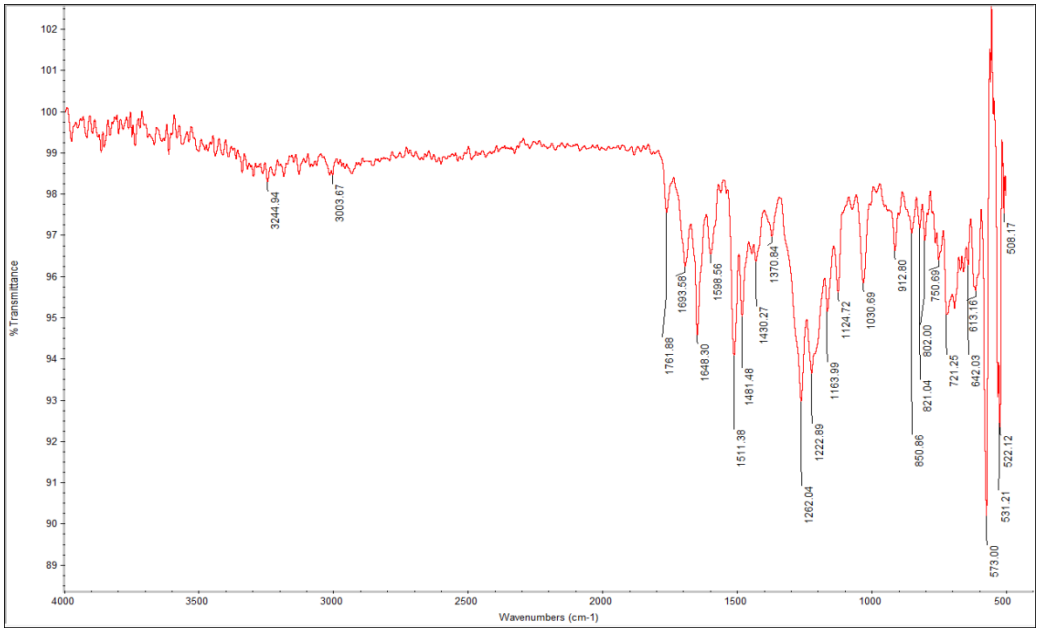

Figure B4

FT-IR of (Z)-3-((2-chlorophenyl)amino)-5-(4-hydroxy-3-methoxybenzylidene)-2-phenyl-3,5-dihydro-4H-imidazol-4-one (3b)

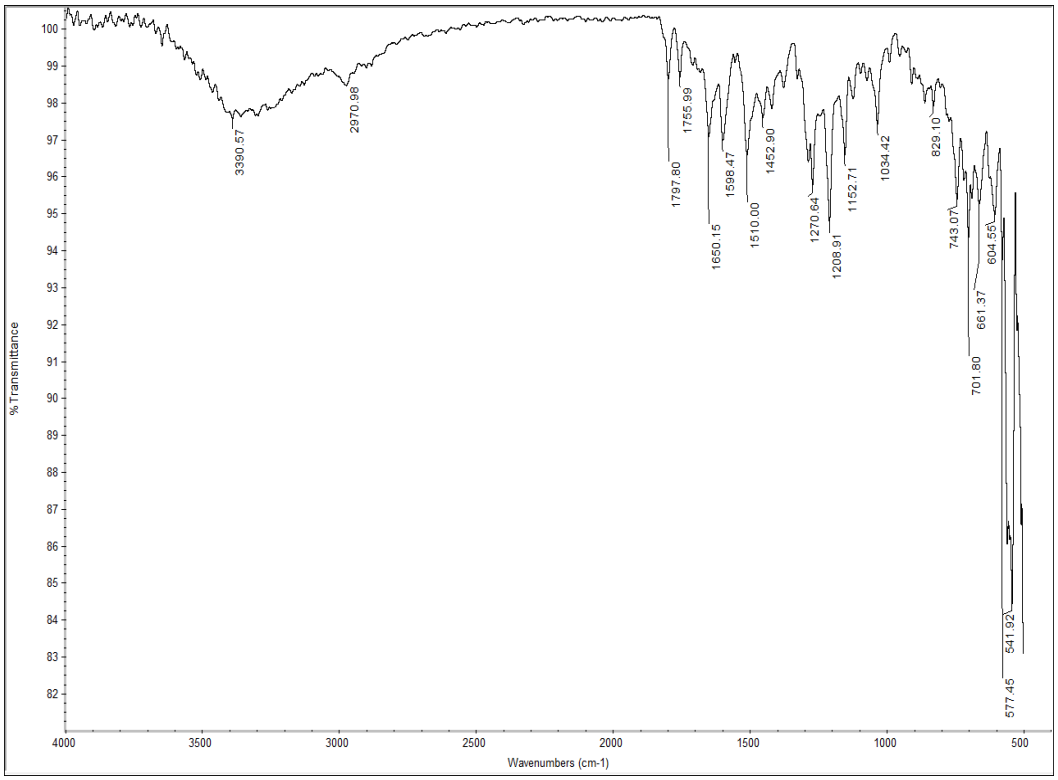

Figure B5

FT-IR of (Z)-5-(4-hydroxy-3-methoxybenzylidene)-3-(2-hydroxyethyl)-2-phenyl-3,5-dihydro-4H-imidazol-4-one (3c)

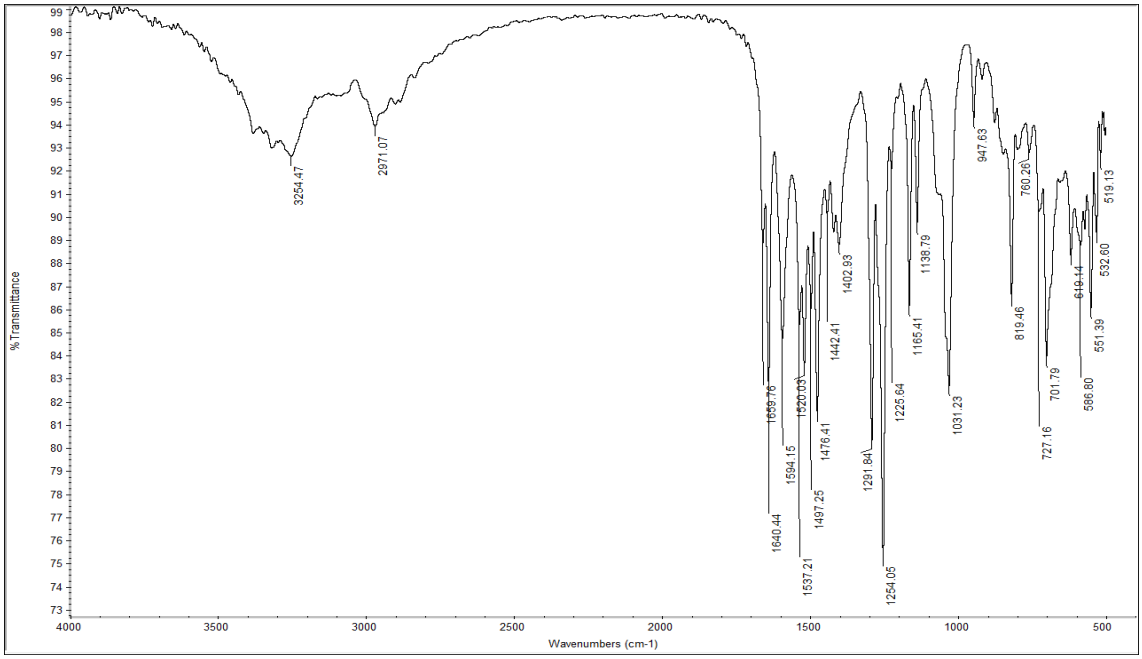

Figure B6

FT-IR of (Z)-5-(4-hydroxy-3-methoxybenzylidene)-3-(2-(methylamino)ethyl)-2-phenyl-3,5-dihydro-4H-imidazol-4-one (3d)

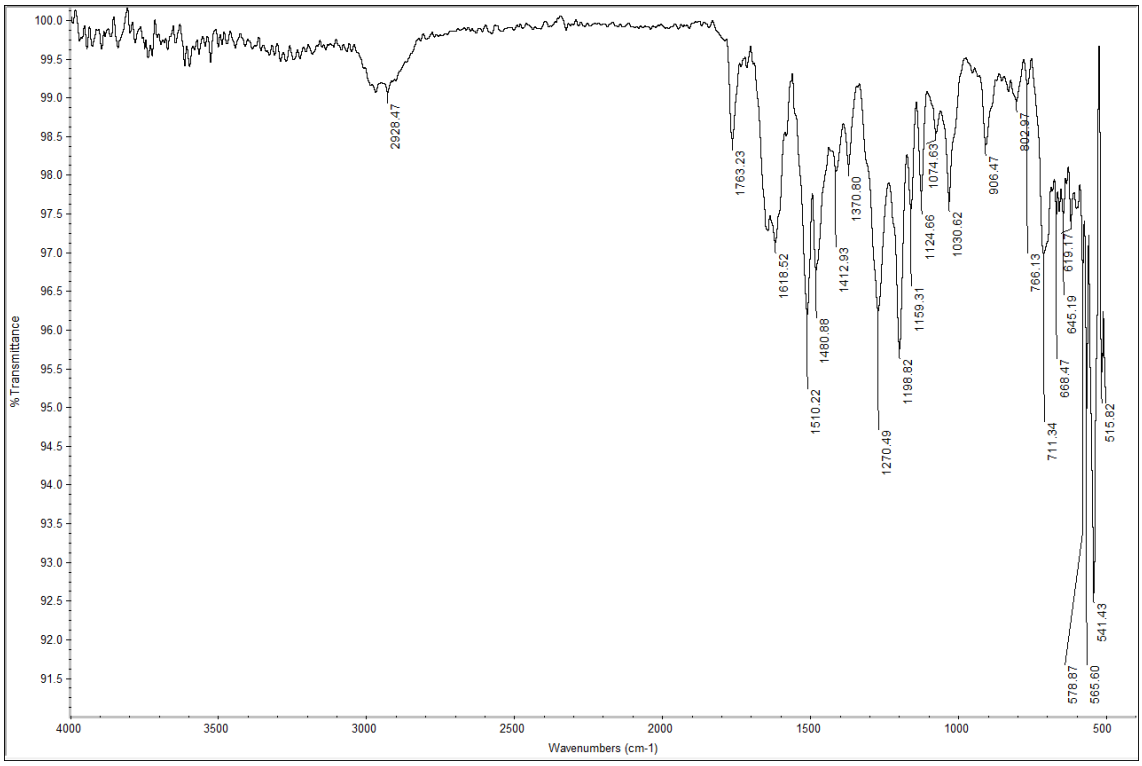

Figure B7

FT-IR of (Z)-3-butyl-5-(4-hydroxy-3-methoxybenzylidene)-2-phenyl-3,5-dihydro-4H-imidazol-4-one (3e)

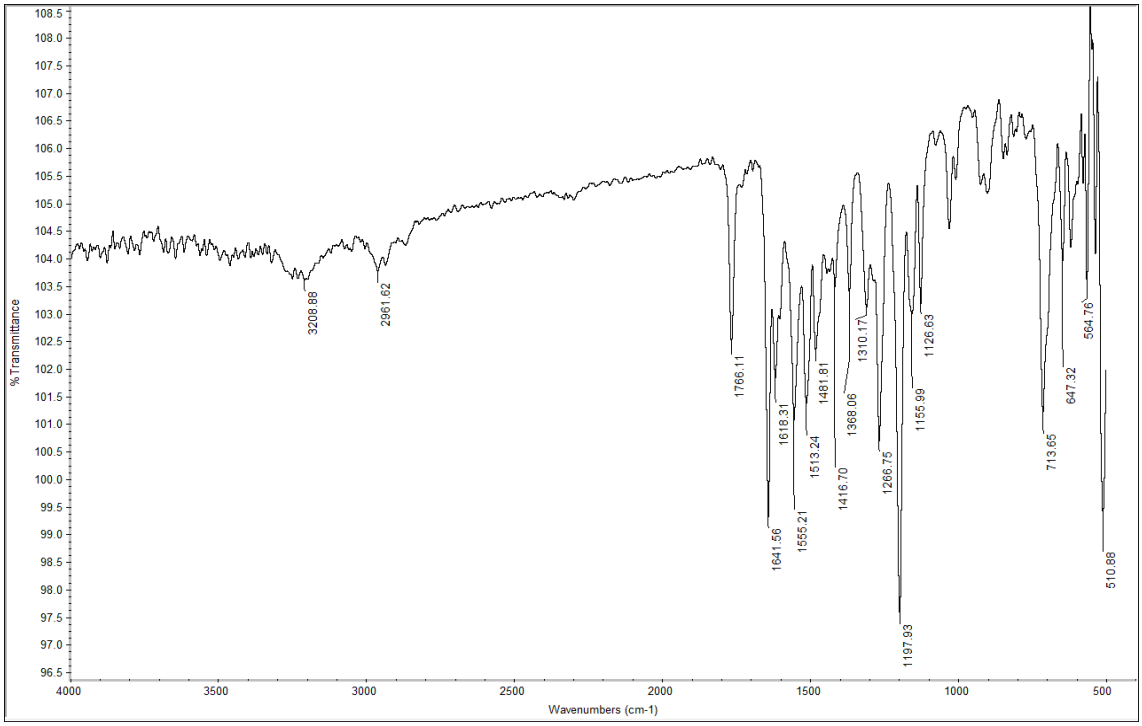

Figure B8

FT-IR of (Z)-3-dodecyl-5-(4-hydroxy-3-methoxybenzylidene)-2-phenyl-3,5-dihydro-4H-imidazol-4-one (3f)

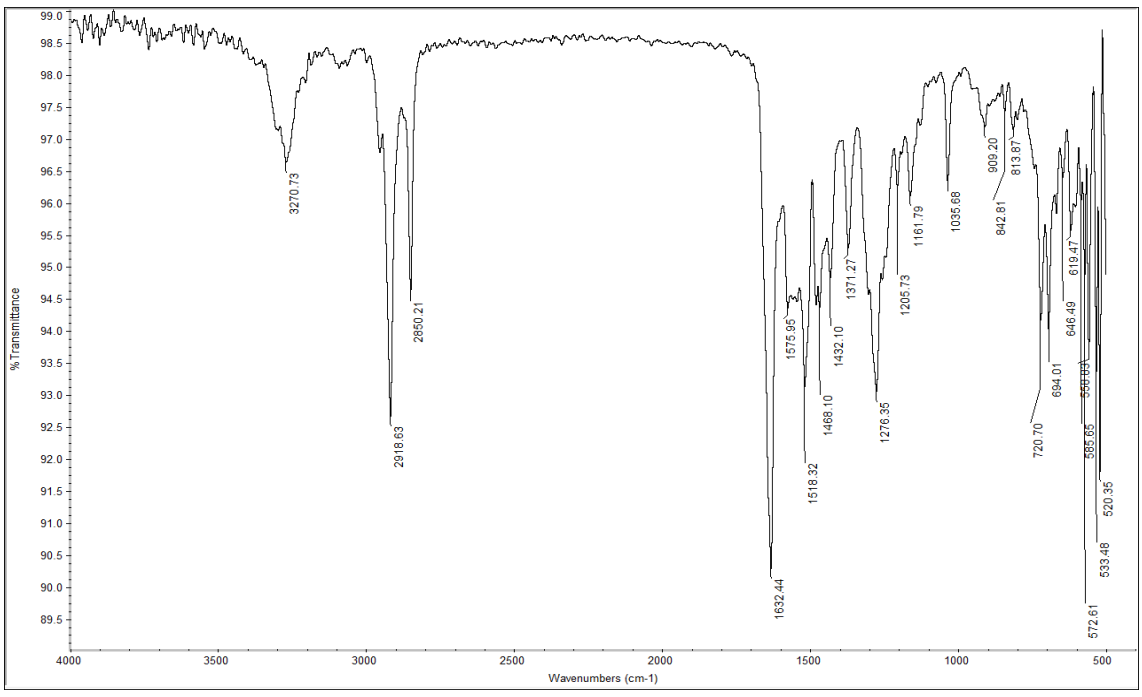

Figure B9

FT-IR of (Z)-2-amino-5-((amino(4-(4-hydroxy-3-methoxybenzylidene)-5-oxo-2-phenyl-4,5-dihydro-1H-imidazol-1-yl)methyl)amino)pentanoic acid (3g)

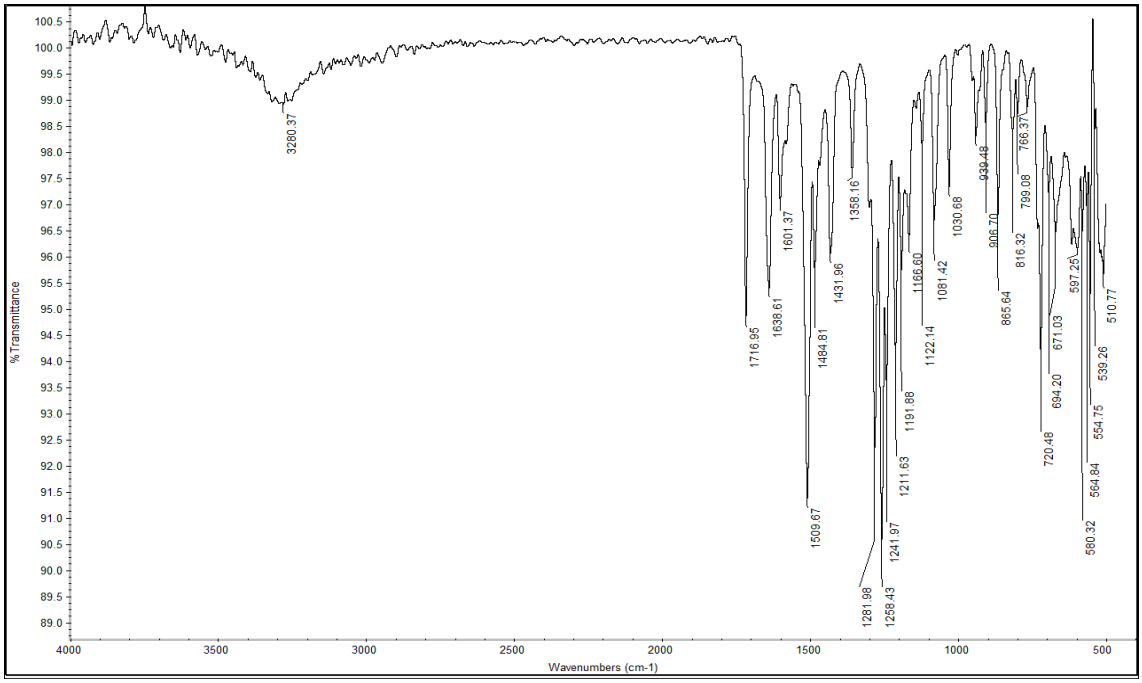

Figure B10

FT-IR of 2-thiophenecarbonylglycine (4)

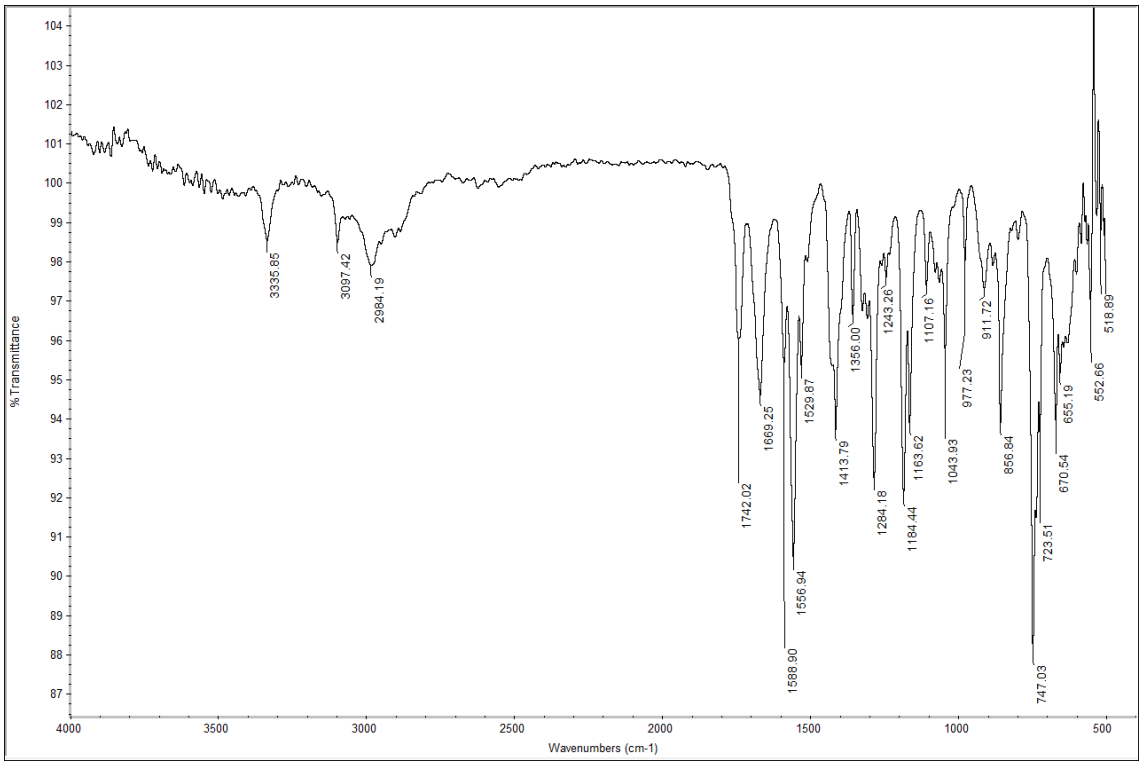

Figure B11

FT-IR of (Z)-4-(4-Hydroxy-3-Methoxybenzylidene)-2- (thiophen-2-yl)oxazol-5-(4H)-One (5)

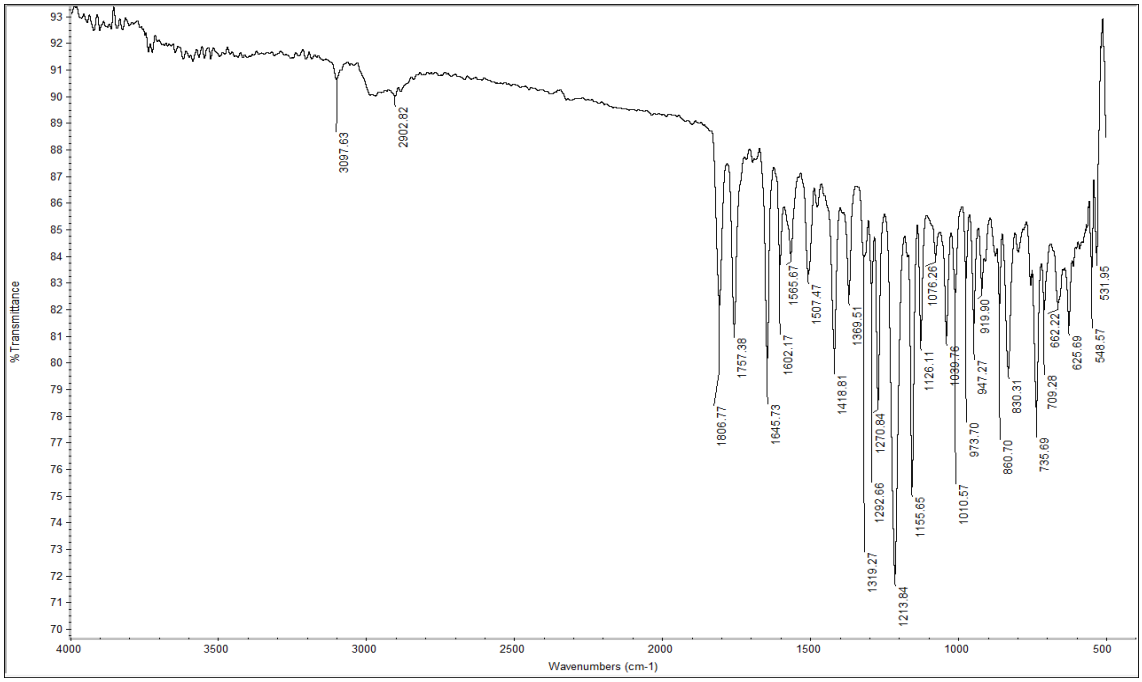

Figure B12

FT-IR of (Z)-3-((2-bromophenyl)amino)-5-(4-hydroxy-3-methoxybenzylidene)-2-(thiophen-2-yl)-3,5-dihydro-4H-imidazol-4-one (5a)

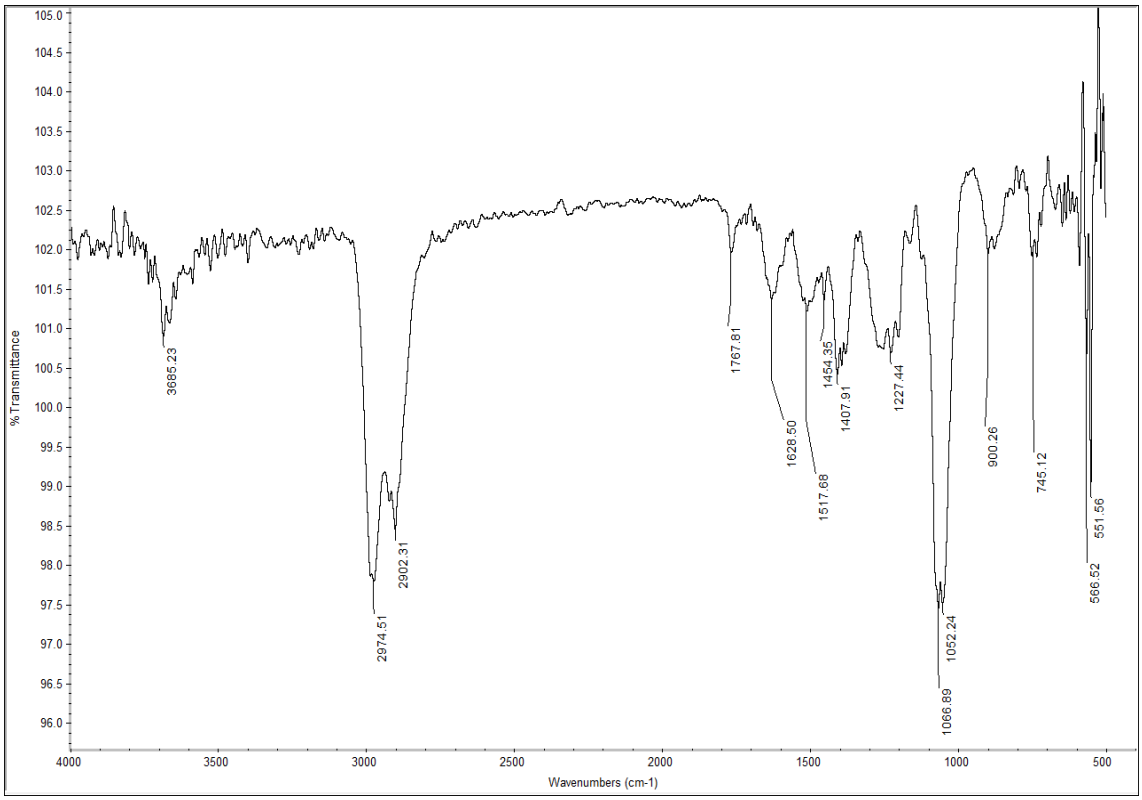

Figure B13

FT-IR of (Z)-3-((2-chlorophenyl)amino)-5-(4-hydroxy-3-methoxybenzylidene)-2-(thiophen-2-yl)-3,5-dihydro-4H-imidazol-4-one (5b)

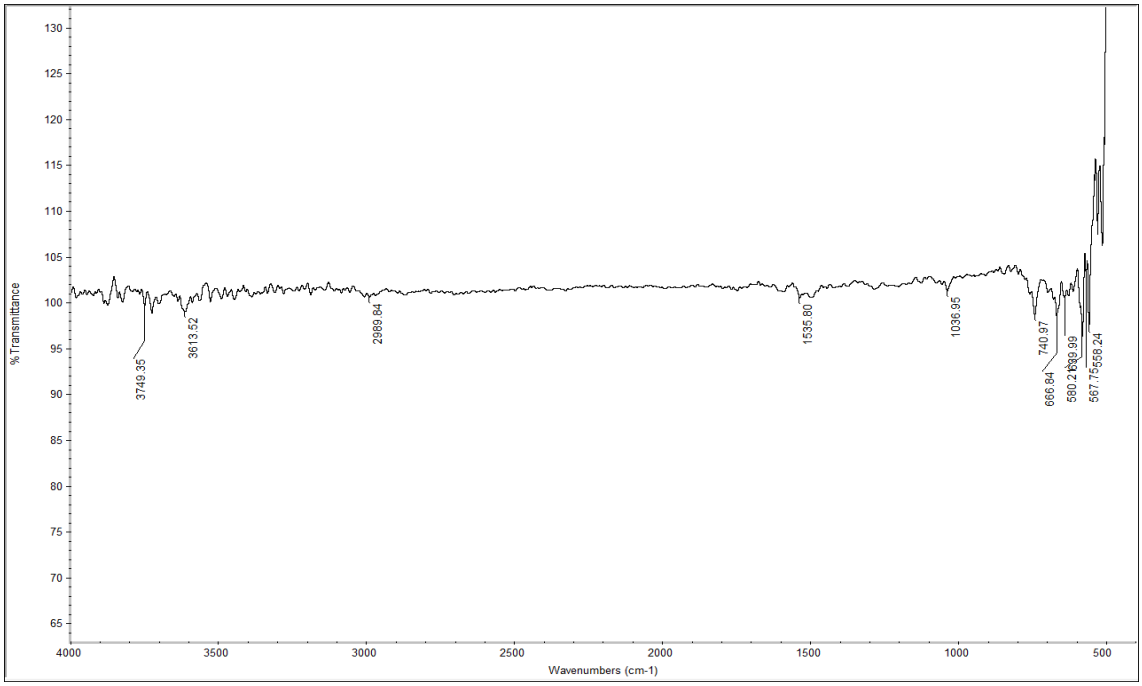

Figure B14

FT-IR of (Z)-5-(4-hydroxy-3-methoxybenzylidene)-3-(2-hydroxyethyl)-2-(thiophen-2-yl)-3,5-dihydro-4H-imidazol-4-one (5c)

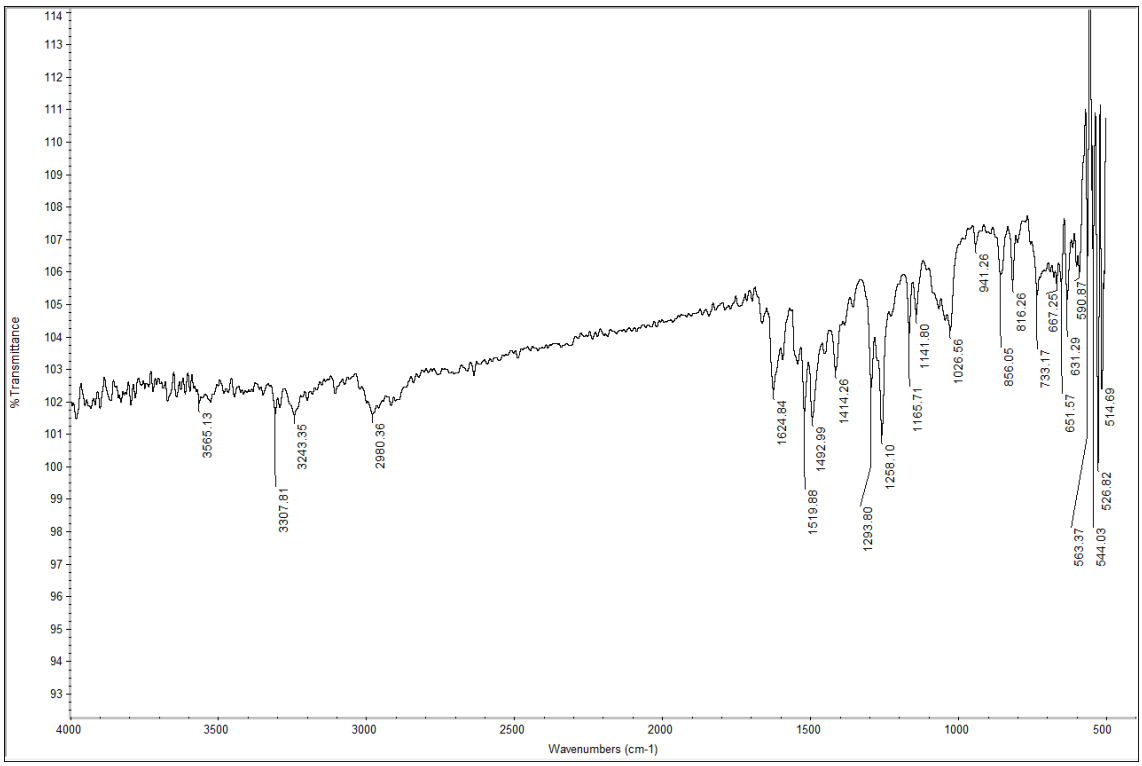

Figure B15

FT-IR of (Z)-5-(4-hydroxy-3-methoxybenzylidene)-3-(2-(methylamino)ethyl)-2-(thiophen-2-yl)-3,5-dihydro-4H-imidazol-4-one (5d)

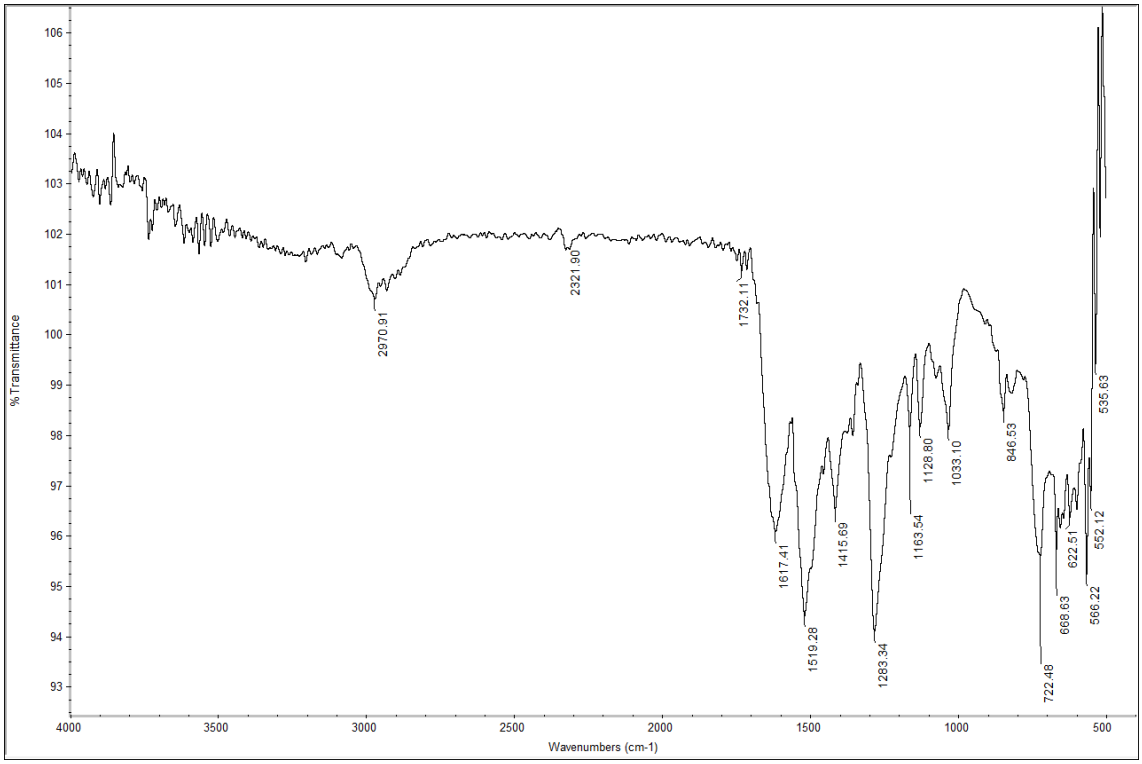

Figure B16

FT-IR of (Z)-3-butyl-5-(4-hydroxy-3-methoxybenzylidene)-2-(thiophen-2-yl)-3,5-dihydro-4H-imidazol-4-one (5e)

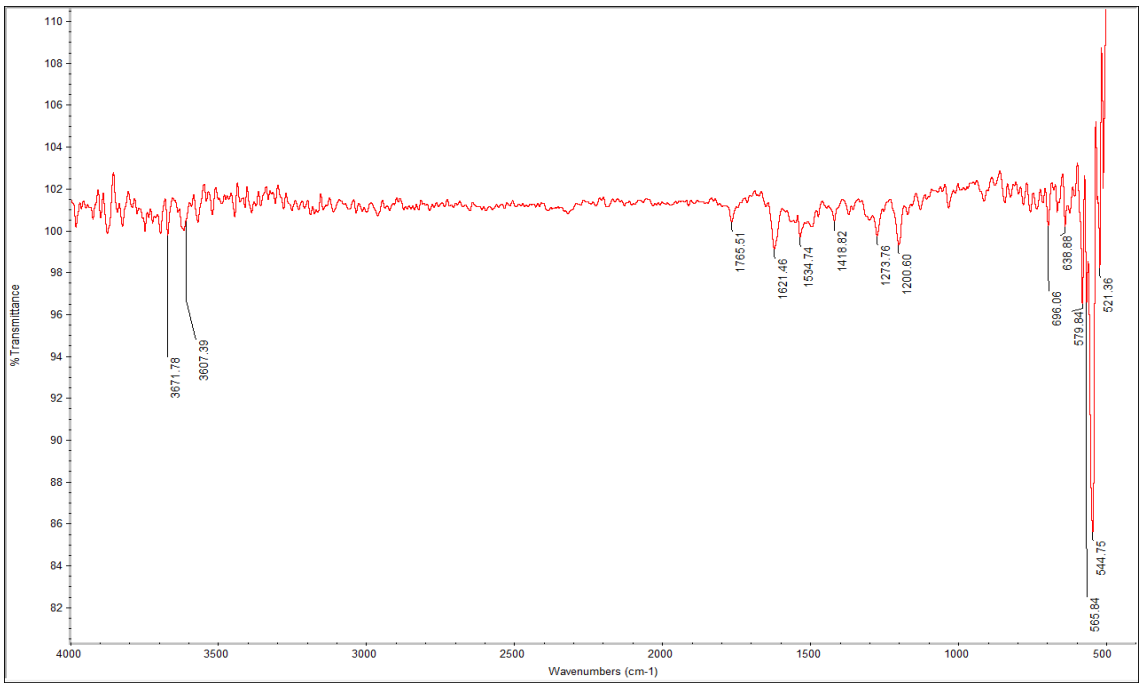

Figure B17

FT-IR of (Z)-3-dodecyl-5-(4-hydroxy-3-methoxybenzylidene)-2-(thiophen-2-yl)-3,5-dihydro-4H-imidazol-4-one (5f)

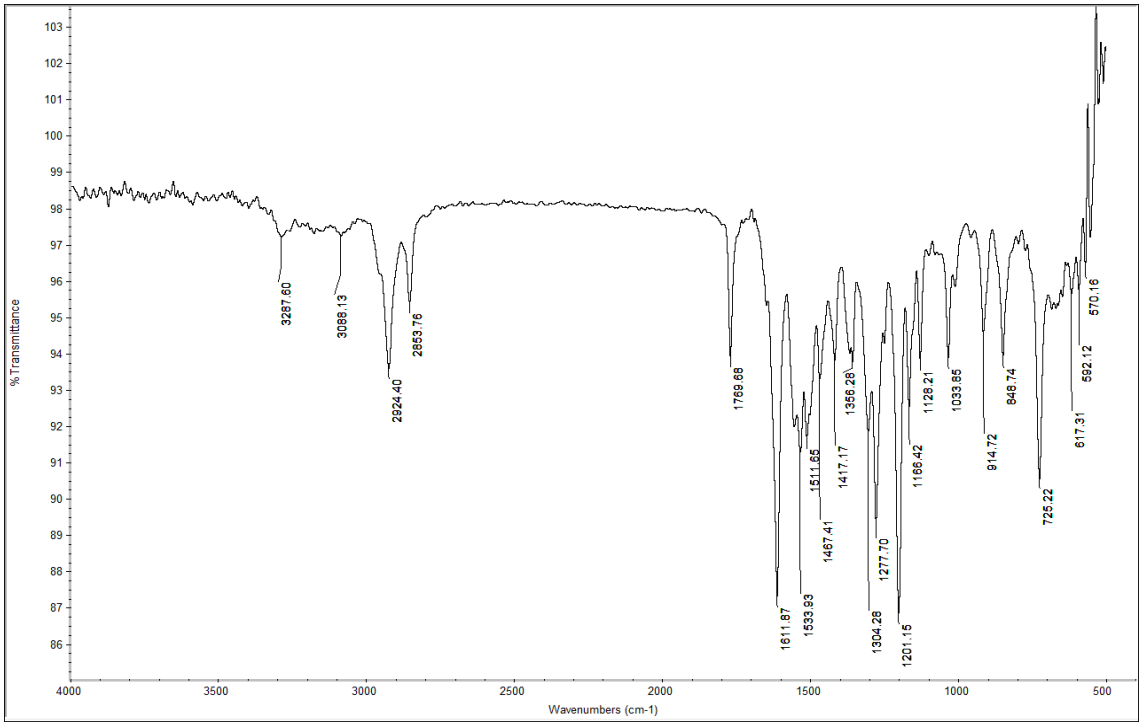

Figure B18

FT-IR of (Z)-5-(4-hydroxy-3-methoxybenzylidene)-3-(pyridin-3-ylmethyl)-2-(thiophen-2-yl)-3,5-dihydro-4H-imidazol-4-one (5g)

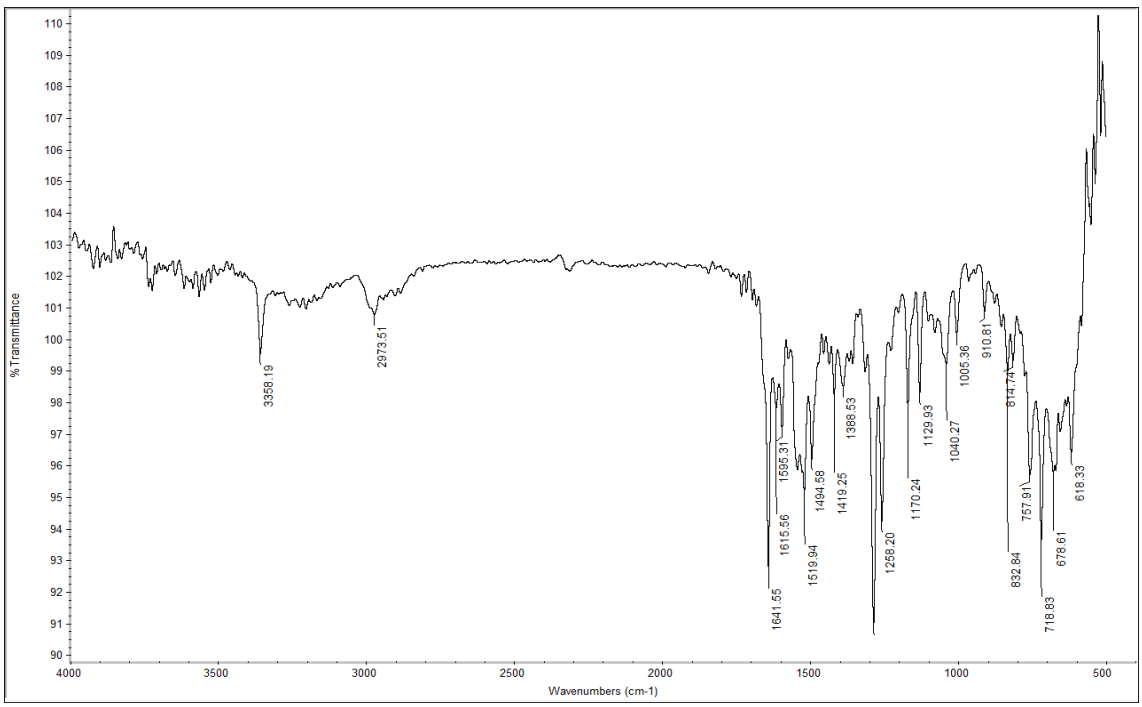

Figure B19

FT-IR of (Z)-4-(furan-2-ylmethylene)-2-(thiophen-2-yl)oxazol-5(4H)-one (6)

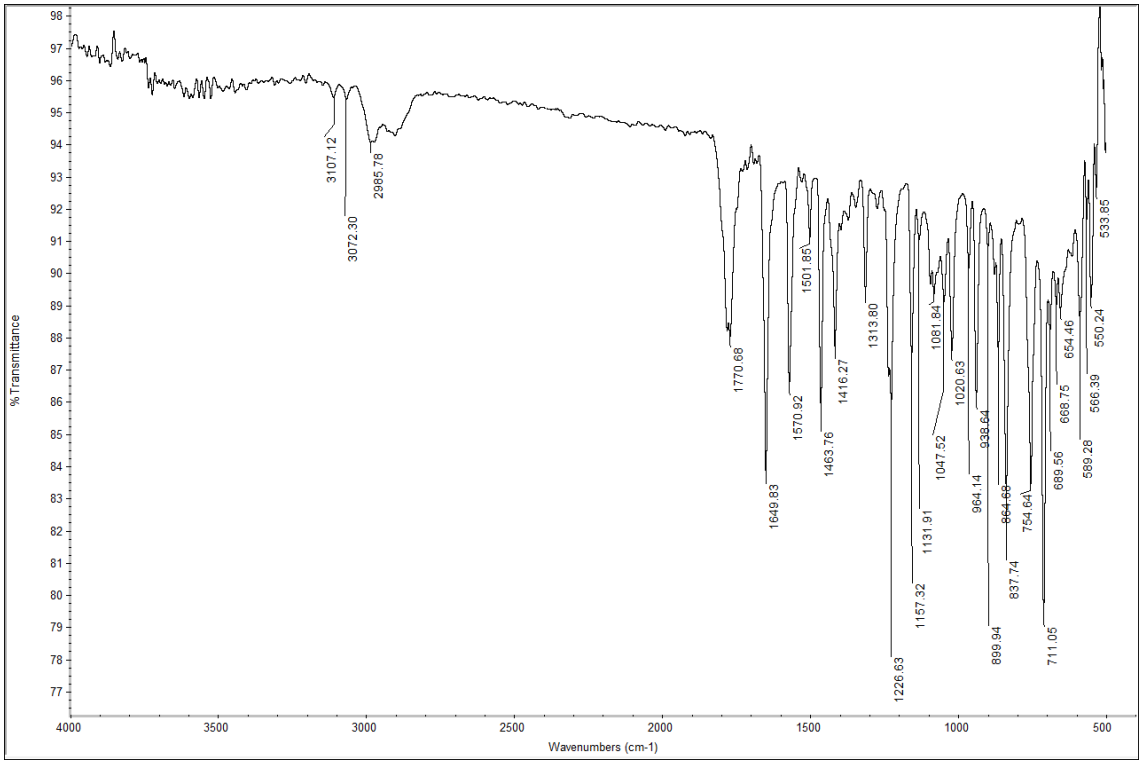

Figure B20

FT-IR of (Z)-4-(pyridin-2-ylmethylene)-2-(thiophen-2-yl)oxazol-5(4H)-one (7)

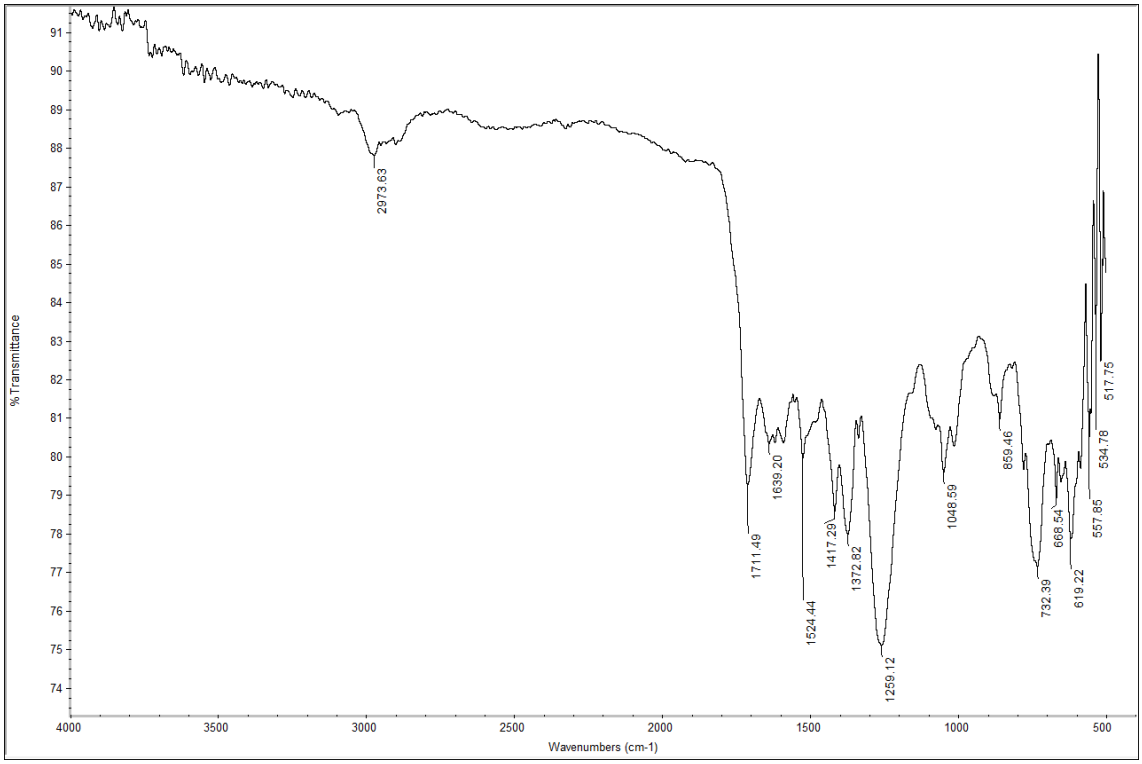

Figure B21

FT-IR of (Z)-2-(thiophen-2-yl)-4-(thiophen-2-ylmethylene)oxazol-5(4H)-one (8)

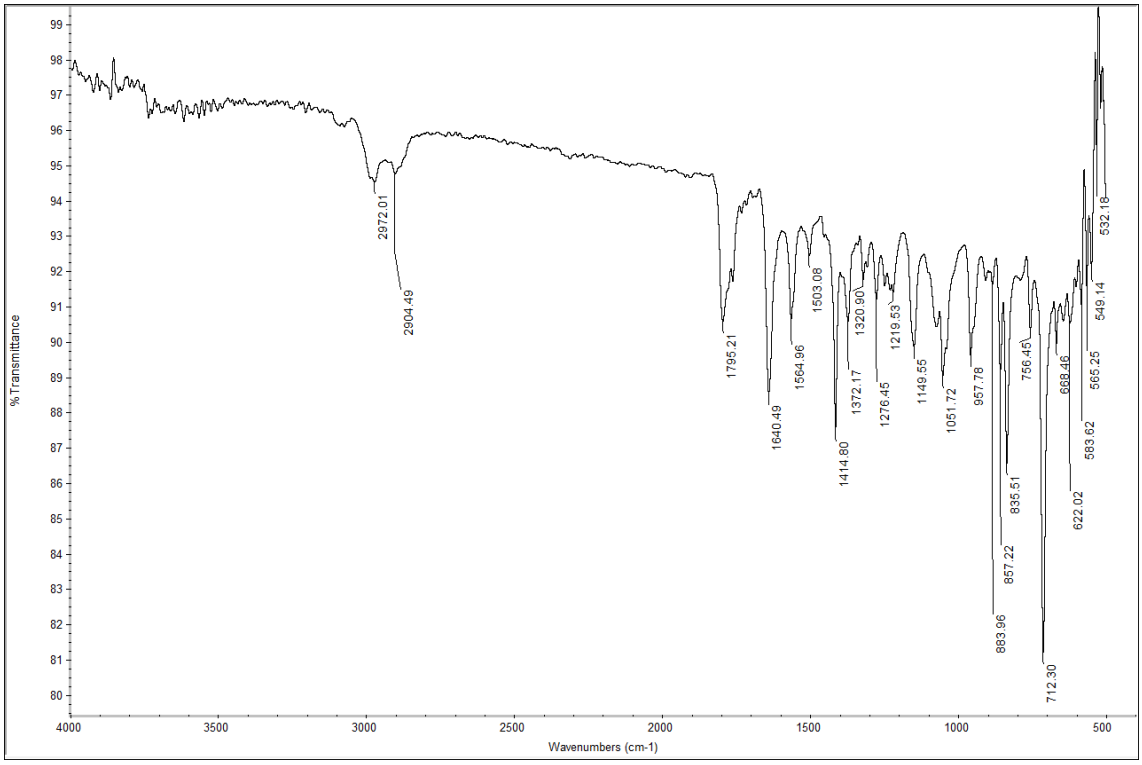

Figure B22

FT-IR of (Z)-2-(thiophen-2-yl)-4-(thiophen-3-ylmethylene)oxazol-5(4H)-one (9)

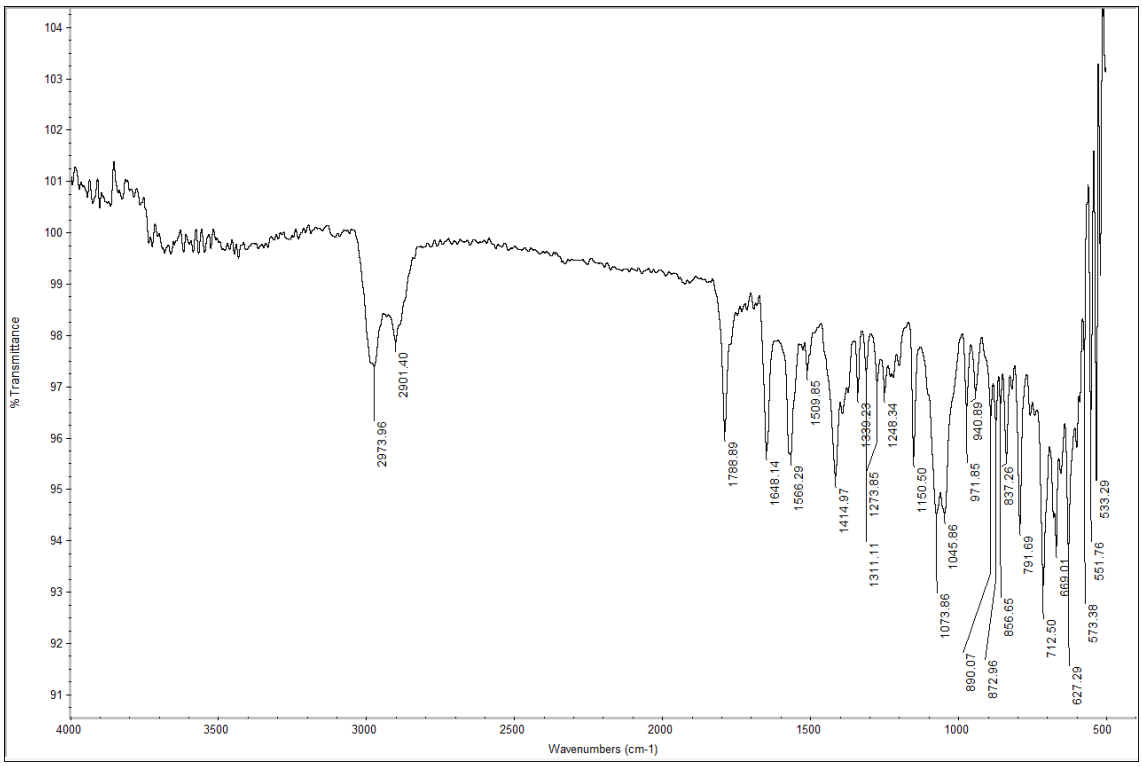

Figure B23

FT-IR of (Z)-4-((4-bromothiophen-2-yl)methylene)-2-(thiophen-2-yl)oxazol-5(4H)-one (10)

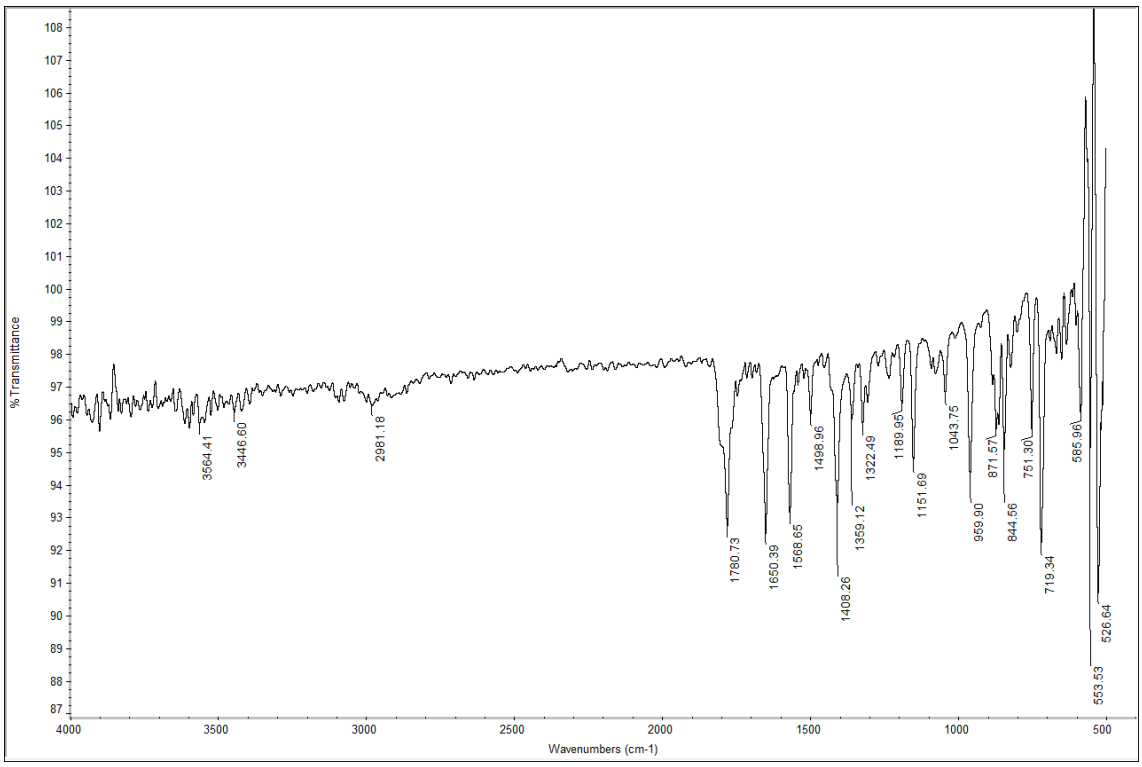

Figure B24

FT-IR of (Z)-2-phenyl-4-(thiophen-2-ylmethylene)oxazol-5(4H)-one (11)

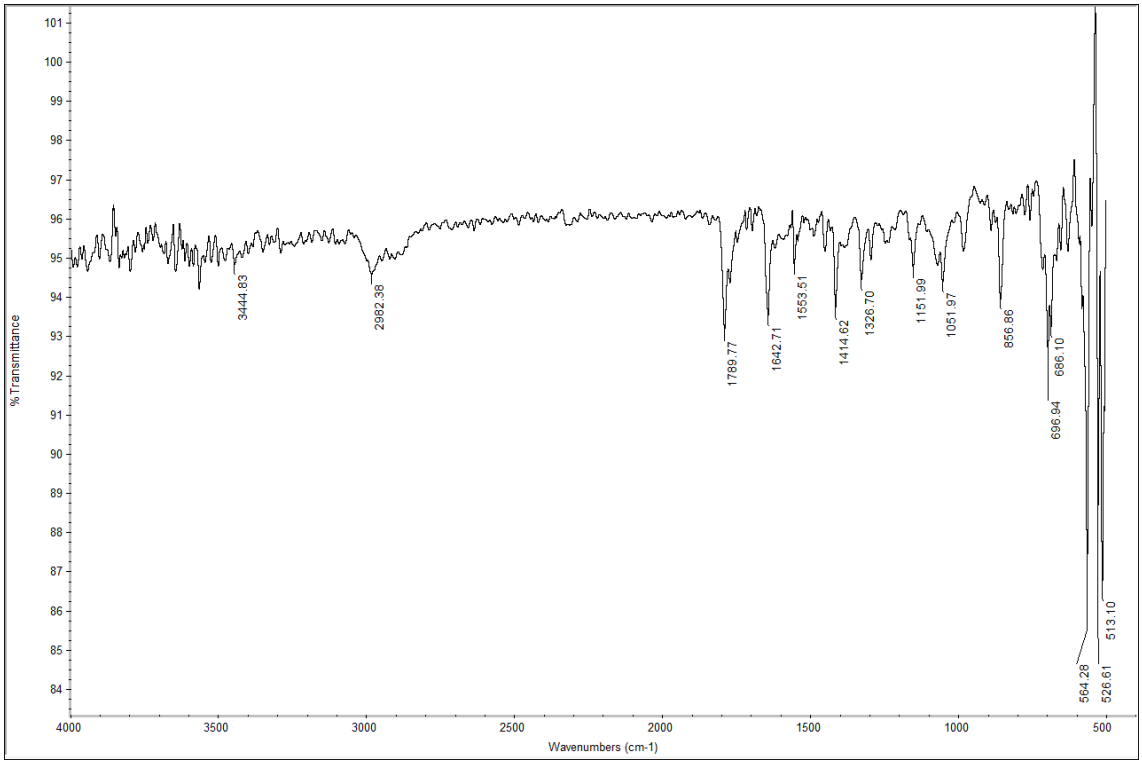

Figure B25

FT-IR of (Z)-2-phenyl-4-(thiophen-3-ylmethylene)oxazol-5(4H)-one (12)

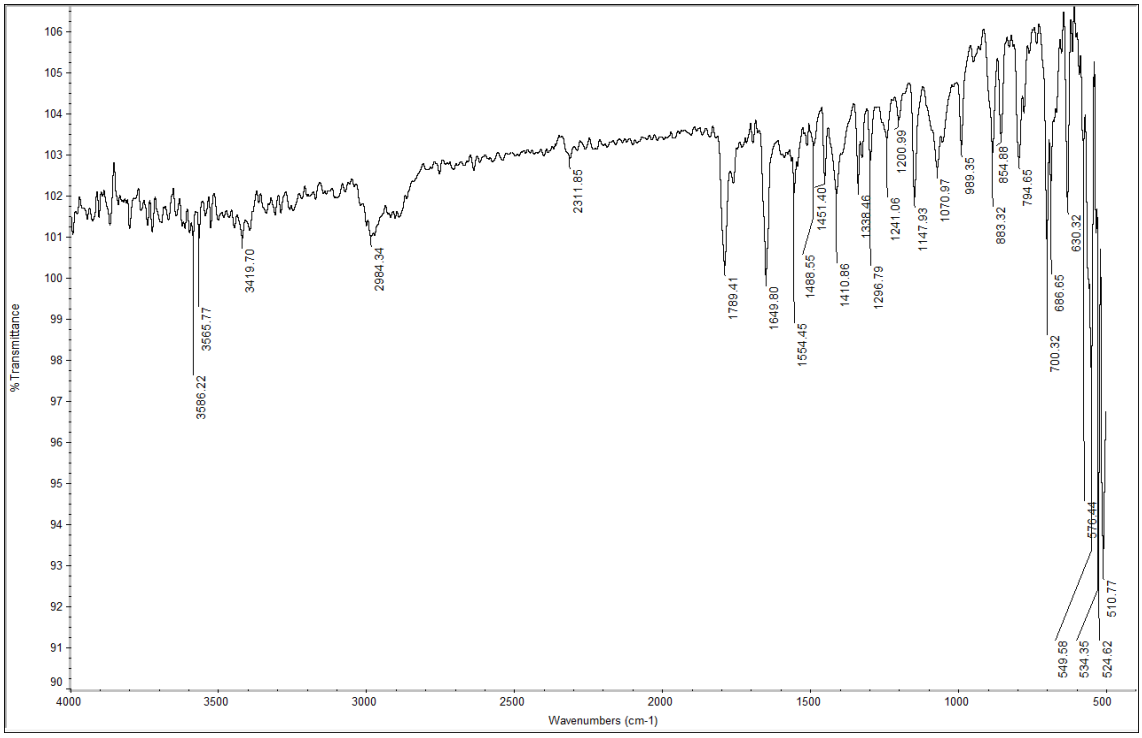

Figure B26

^{1}H NMR of (Z)-4-(4-hydroxy-3-methoxybenzylidene)-2-phenyloxazol-5(4H)-one (2)

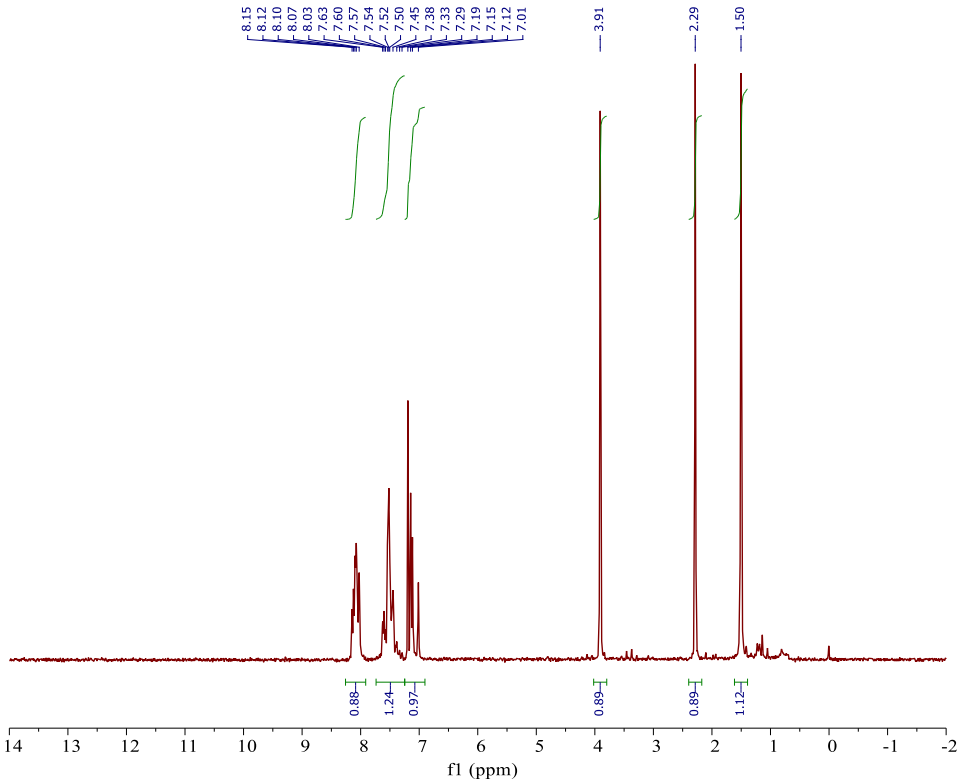

Figure B27

[1]H NMR of (Z)-3-((2-bromophenyl)amino)-5-(4-hydroxy-3-methoxybenzylidene)-2-phenyl-3,5-dihydro-4H-imidazol-4-one (3a)

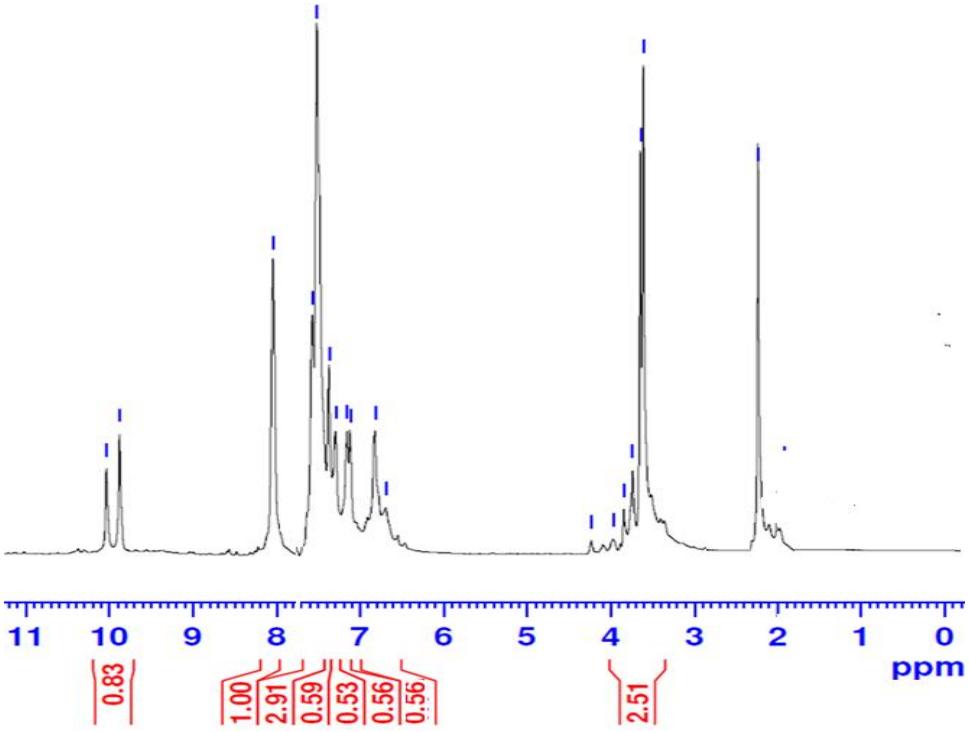

Figure B28

[13]C NMR of (Z)-3-((2-bromophenyl)amino)-5-(4-hydroxy-3-methoxybenzylidene)-2-phenyl-3,5-dihydro-4H-imidazol-4-one (3a)

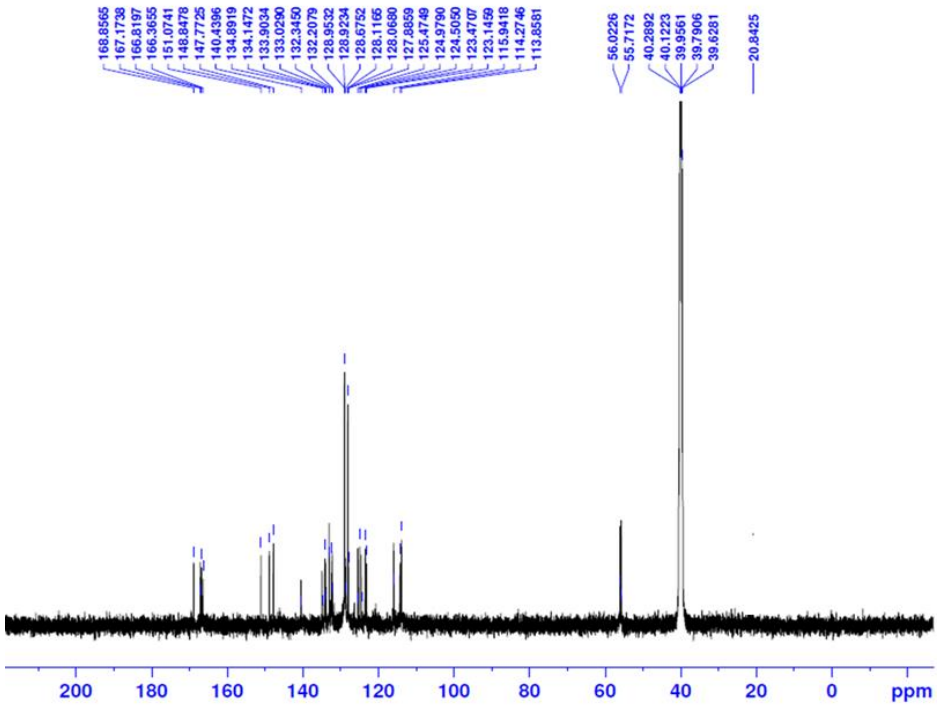

Figure B29

^{1}H NMR of (Z)-3-((2-chlorophenyl)amino)-5-(4-hydroxy-3-methoxybenzylidene)-2-phenyl-3,5-dihydro-4H-imidazol-4-one (3b)

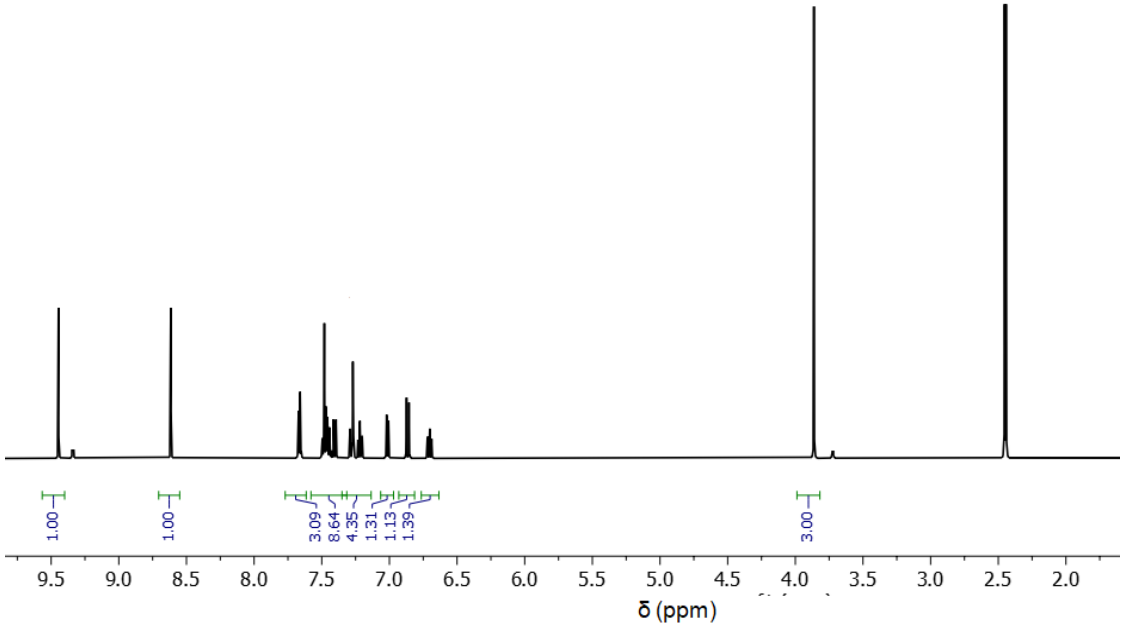

Figure B30a

^{1}H NMR of (Z)-5-(4-hydroxy-3-methoxybenzylidene)-3-(2-hydroxyethyl)-2-phenyl-3,5-dihydro-4H-imidazol-4-one (3c)

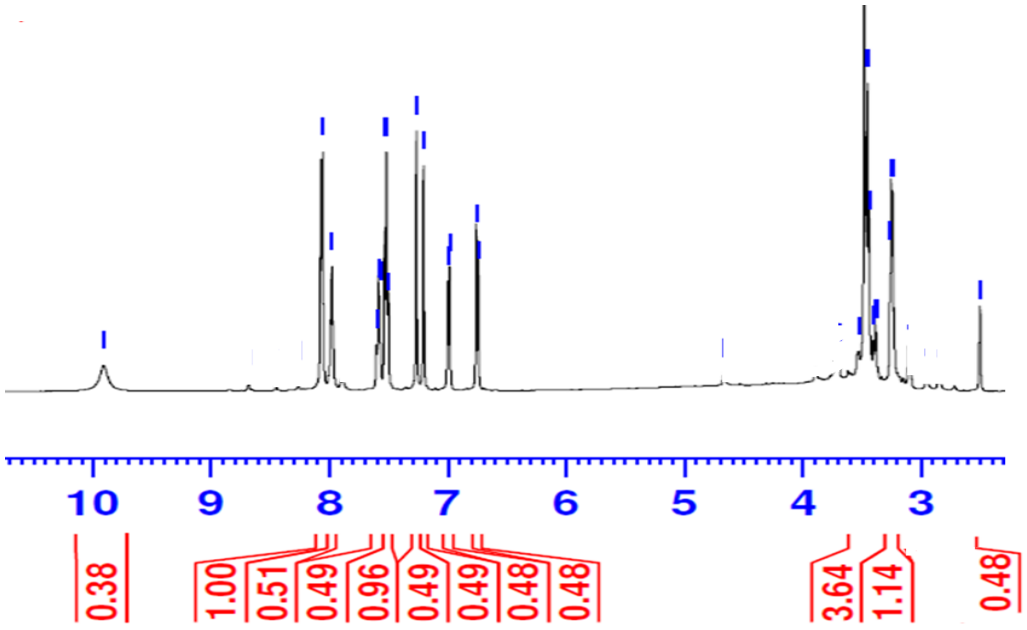

Figure B30b

[1]H NMR of (Z)-5-(4-hydroxy-3-methoxybenzylidene)-3-(2-hydroxyethyl)-2-phenyl-3,5-dihydro-4H-imidazol-4-one (3c)

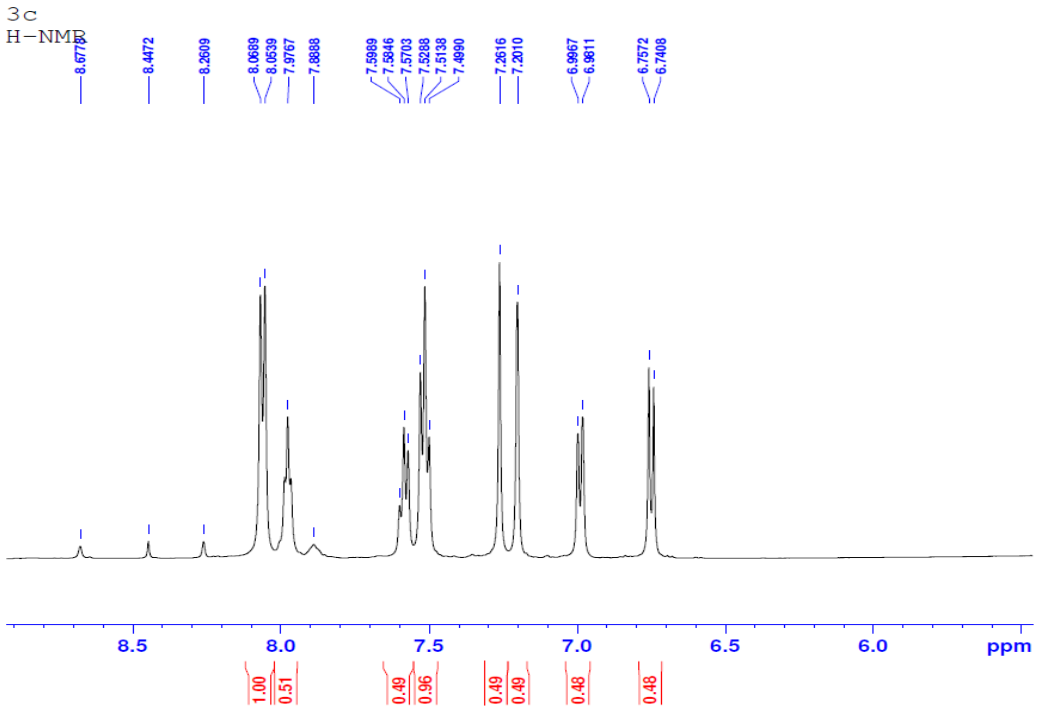

Figure B31

[13]C NMR of (Z)-5-(4-hydroxy-3-methoxybenzylidene)-3-(2-hydroxyethyl)-2-phenyl-3,5-dihydro-4H-imidazol-4-one (3c)

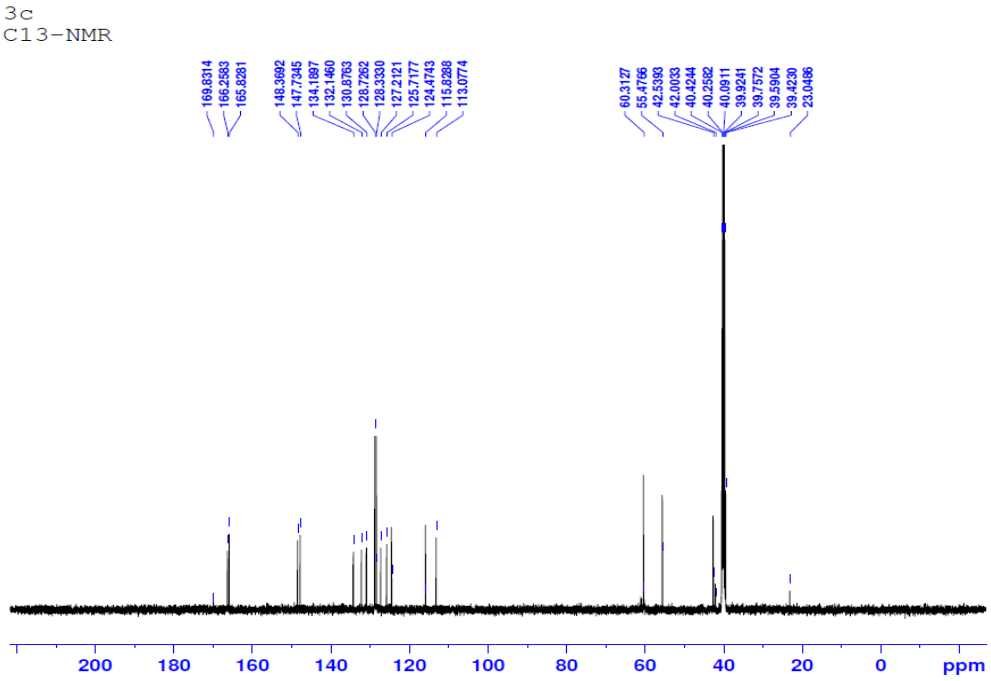

Figure B32

^{1}H NMR of (Z)-5-(4-hydroxy-3-methoxybenzylidene)-3-(2-(methylamino)ethyl)-2-phenyl-3,5-dihydro-4H-imidazol-4-one (3d)

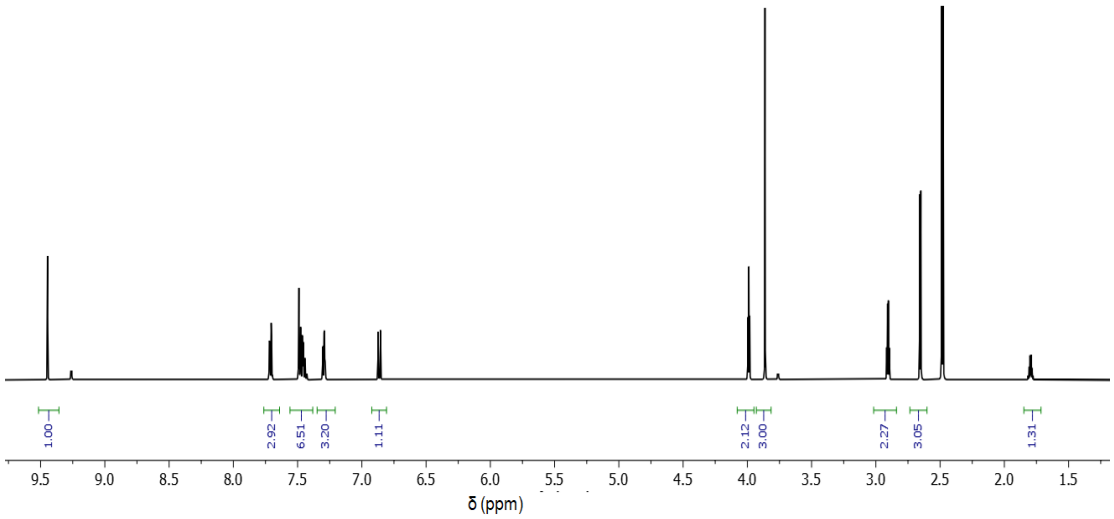

Figure B33

^{13}C NMR of (Z)-5-(4-hydroxy-3-methoxybenzylidene)-3-(2-(methylamino)ethyl)-2-phenyl-3,5-dihydro-4H-imidazol-4-one (3d)

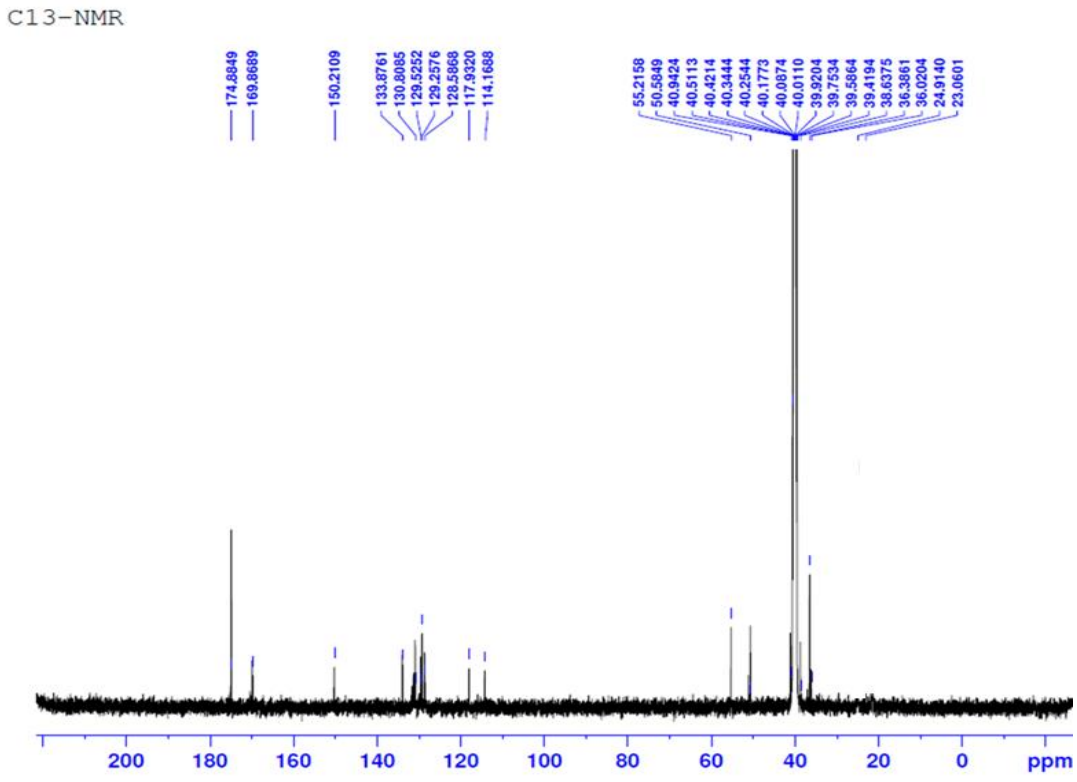

Figure B34a

^{1}H NMR of (Z)-3-butyl-5-(4-hydroxy-3-methoxybenzylidene)-2-phenyl-3,5-dihydro-4H-imidazol-4-one (3e)

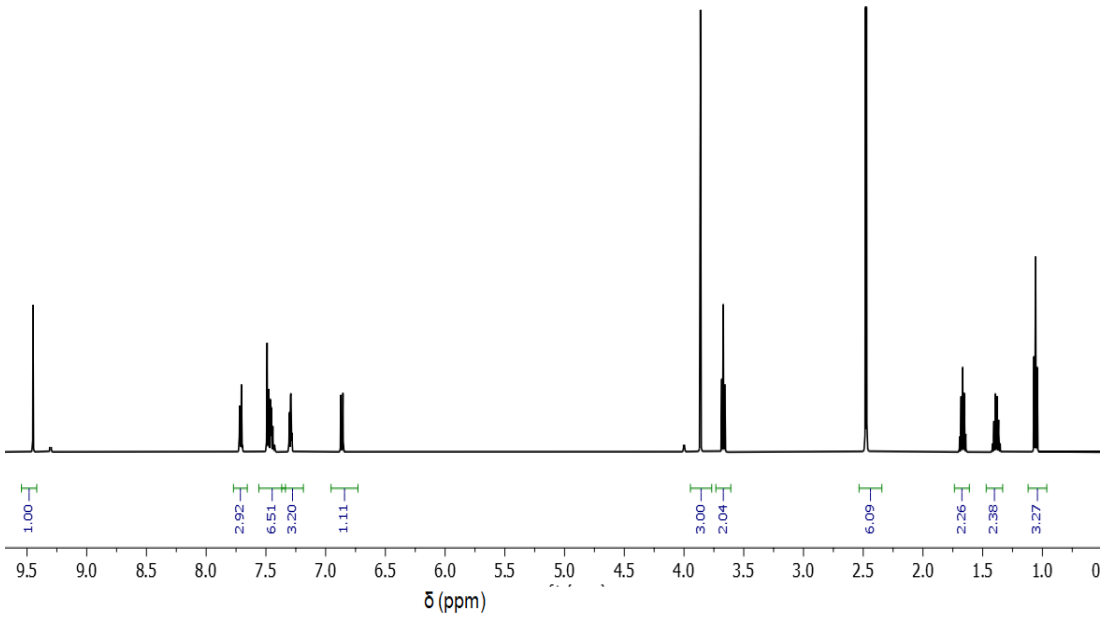

Figure B34b

^{1}H NMR of (Z)-3-butyl-5-(4-hydroxy-3-methoxybenzylidene)-2-phenyl-3,5-dihydro-4H-imidazol-4-one (3e)

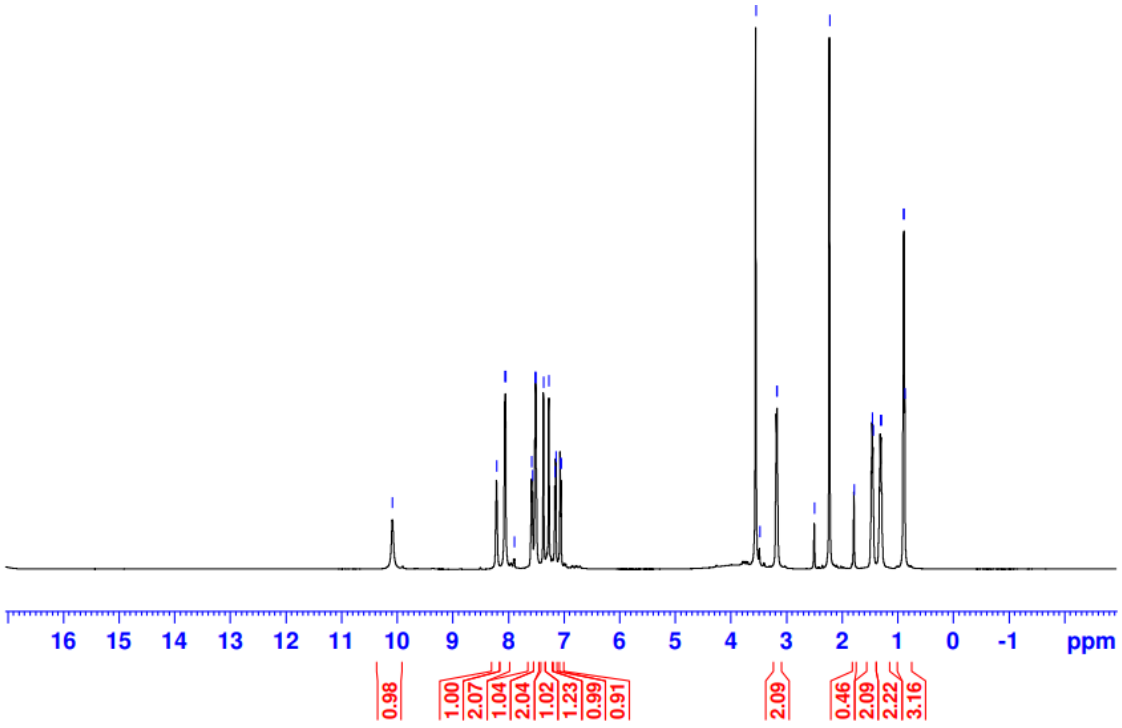

Figure B34c

[1]H NMR of (Z)-3-butyl-5-(4-hydroxy-3-methoxybenzylidene)-2-phenyl-3,5-dihydro-4H-imidazol-4-one (3e)

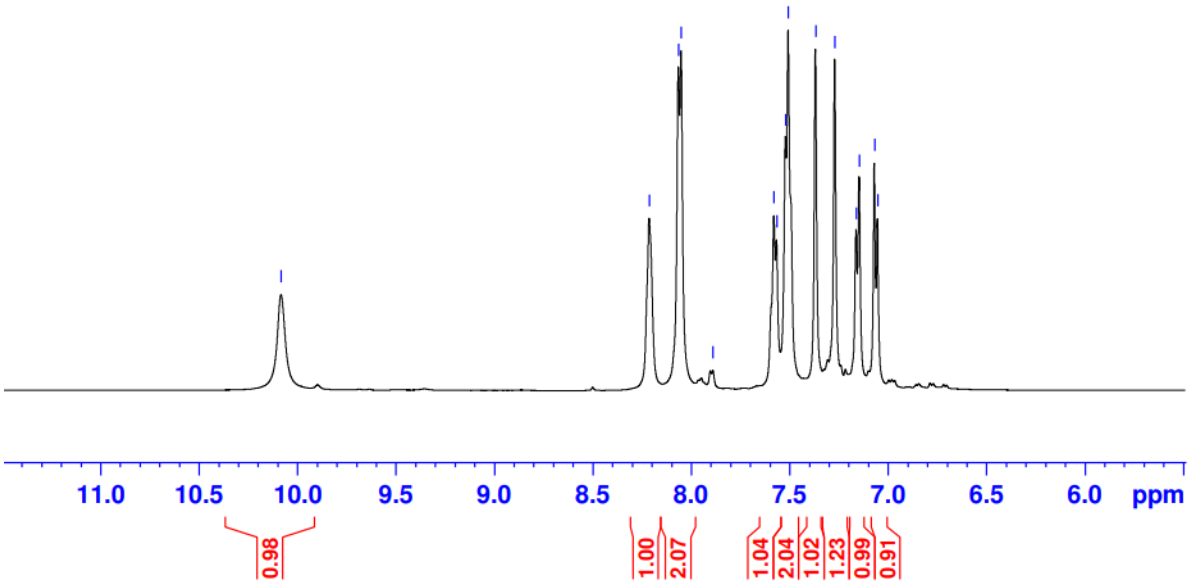

Figure B34d

[1]H NMR of (Z)-3-butyl-5-(4-hydroxy-3-methoxybenzylidene)-2-phenyl-3,5-dihydro-4H-imidazol-4-one (3e)

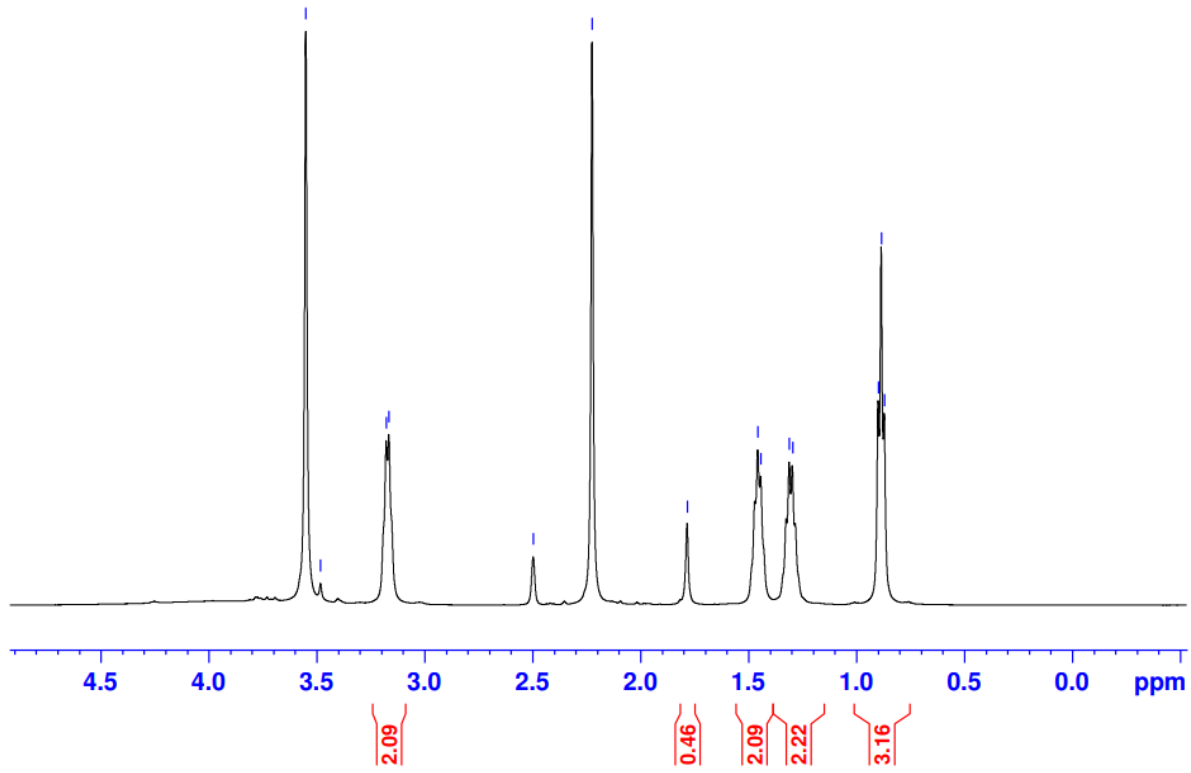

Figure B35

^{13}C NMR of (Z)-3-butyl-5-(4-hydroxy-3-methoxybenzylidene)-2-phenyl-3,5-dihydro-4H-imidazol-4-one (3e)

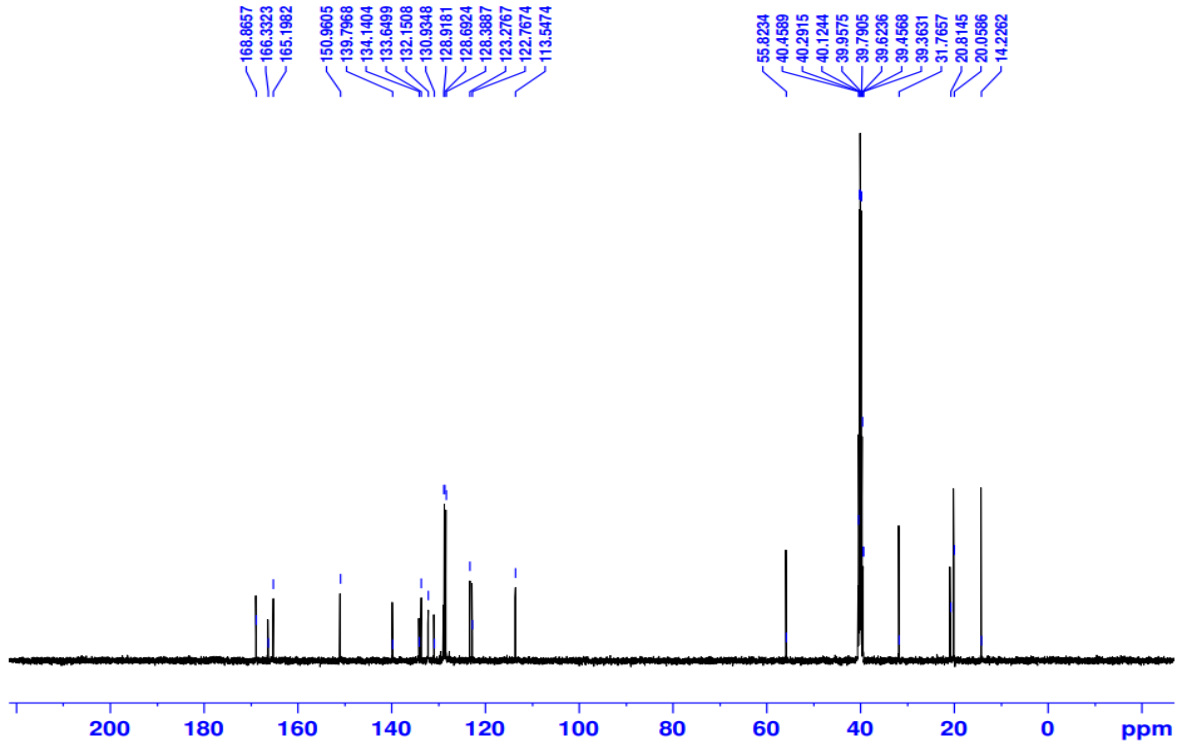

Figure B36a

^{1}H NMR of (Z)-3-dodecyl-5-(4-hydroxy-3-methoxybenzylidene)-2-phenyl-3,5-dihydro-4H-imidazol-4-one (3f)

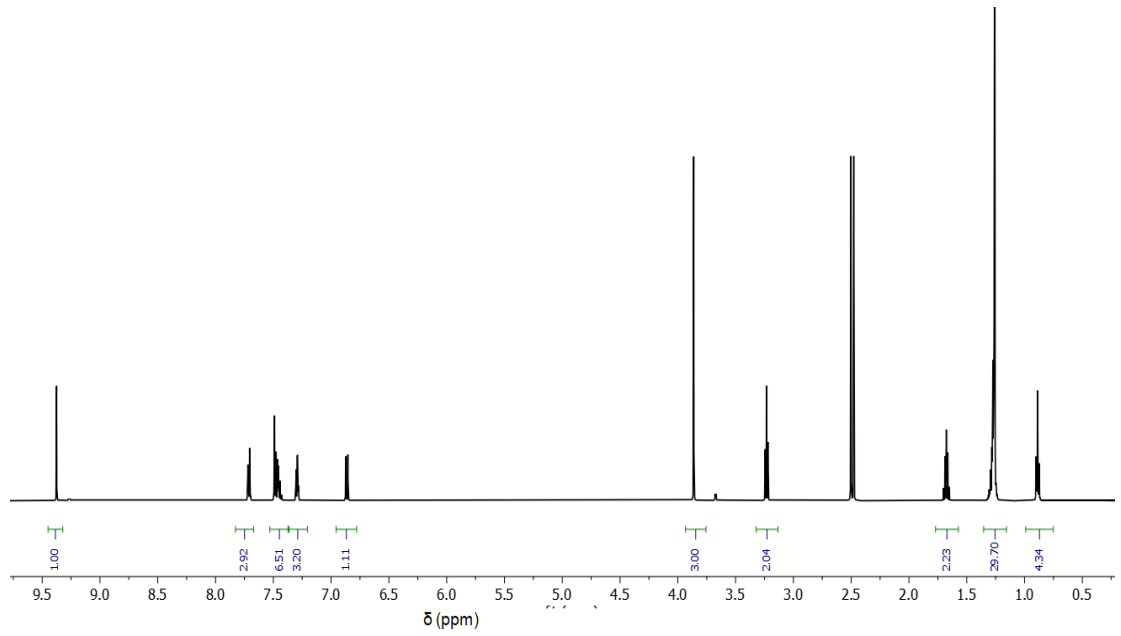

Figure B36b

^{1}H NMR of (Z)-3-dodecyl-5-(4-hydroxy-3-methoxybenzylidene)-2-phenyl-3,5-dihydro-4H-imidazol-4-one (3f)

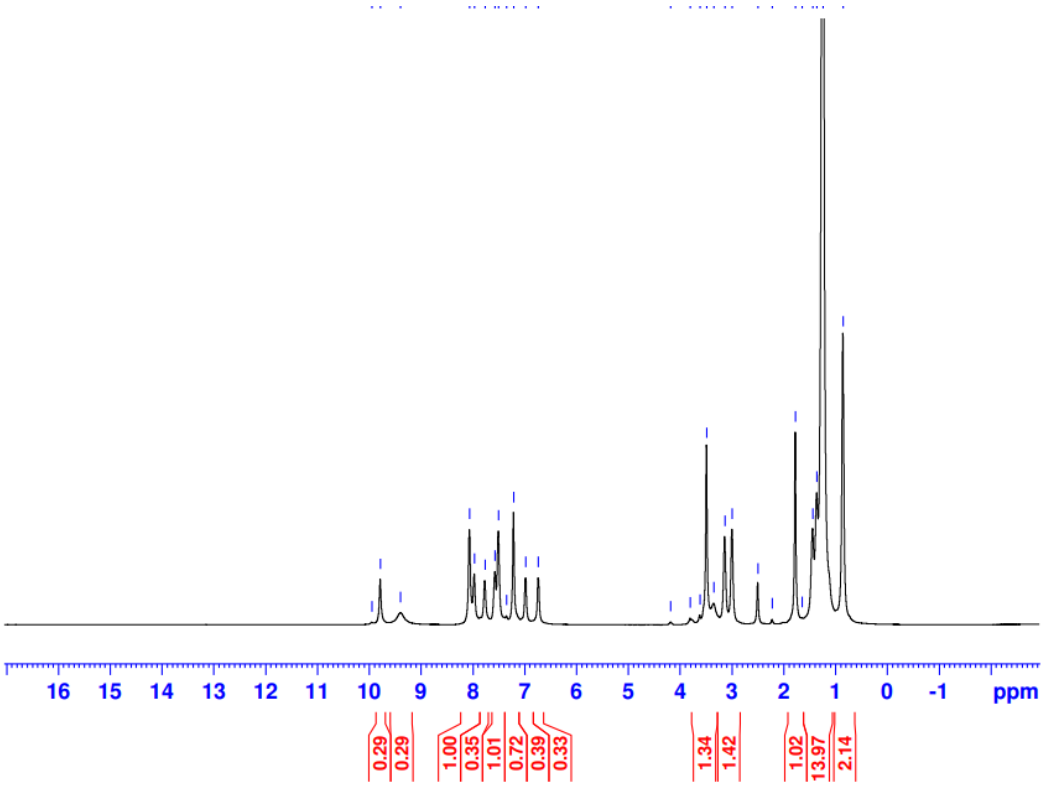

Figure B37

^{13}C NMR of (Z)-3-dodecyl-5-(4-hydroxy-3-methoxybenzylidene)-2-phenyl-3,5-dihydro-4H-imidazol-4-one (3f)

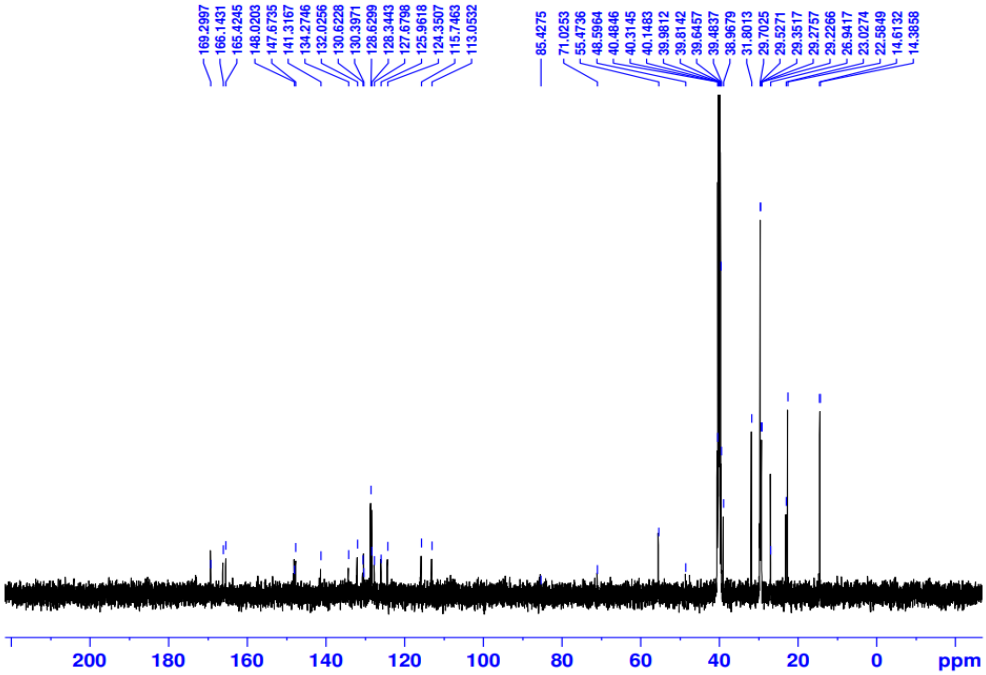

Figure B38

^{1}H NMR of (Z)-2-amino-5-((amino(4-(4-hydroxy-3-methoxybenzylidene)-5-oxo-2-phenyl-4,5-dihydro-1H-imidazol-1-yl)methyl)amino)pentanoic acid (3g)

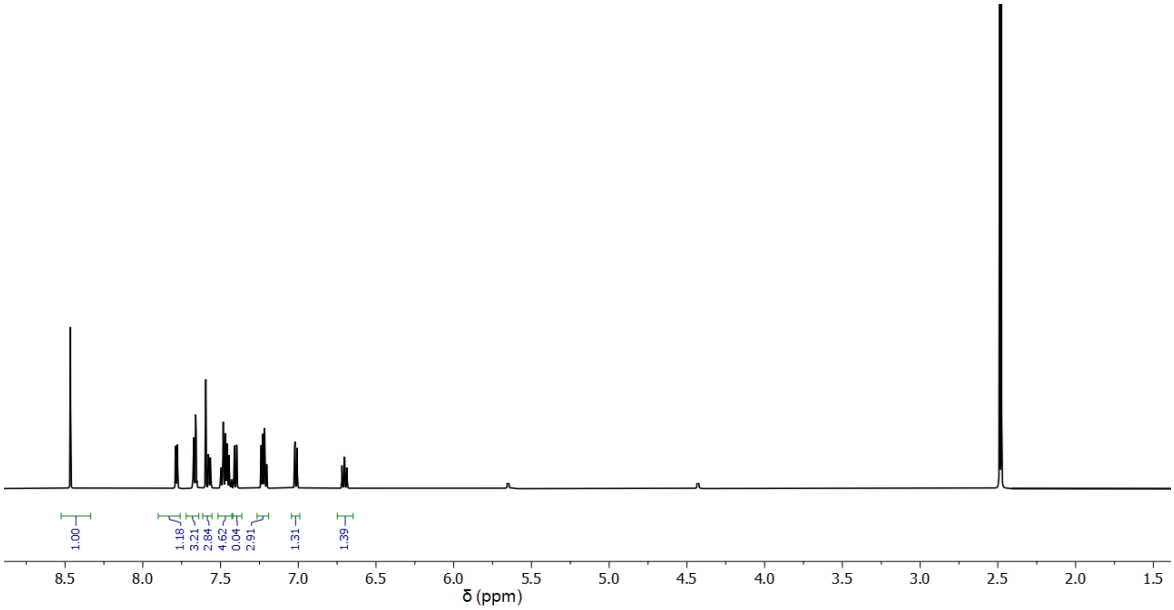

Figure B39a

^{1}H NMR of 2-thiophenecarbonylglycine (4)

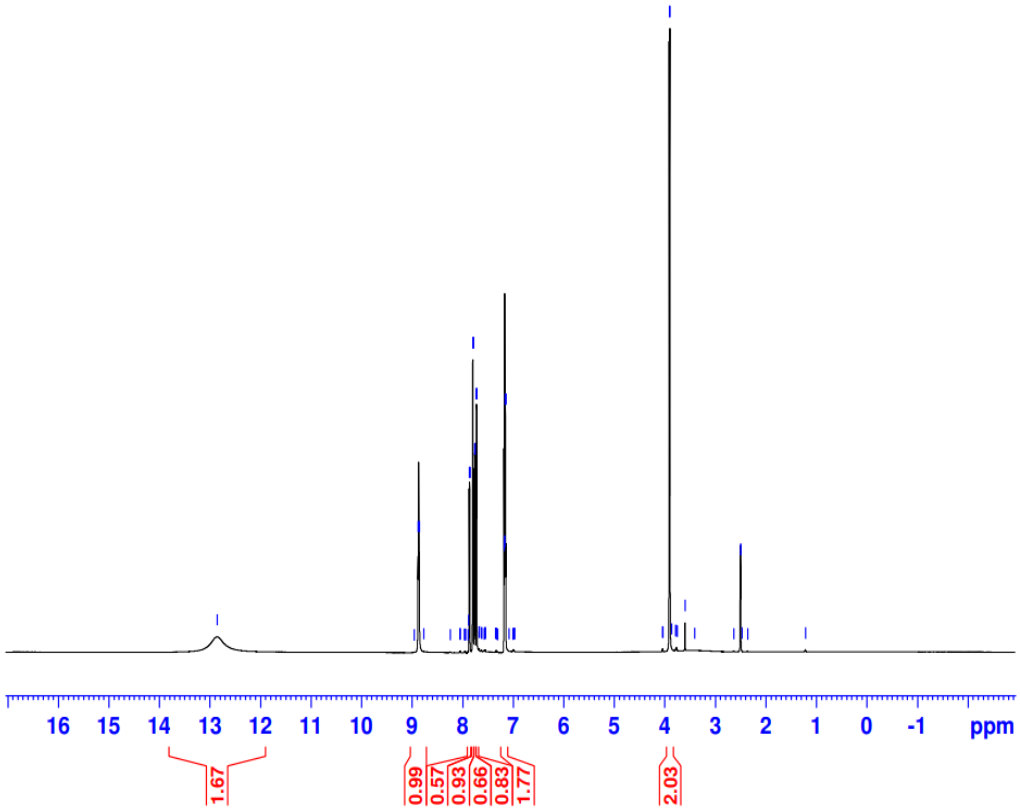

Figure B39b

[1]H NMR of 2-thiophenecarbonylglycine (4)

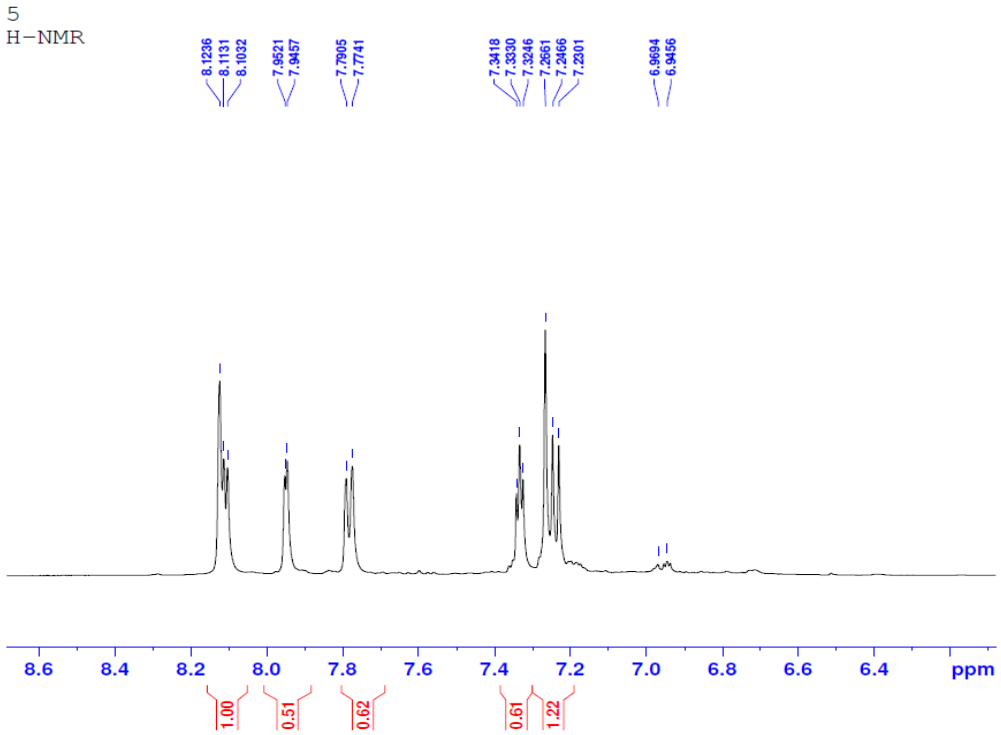

Figure B39c

[1]H NMR of 2-thiophenecarbonylglycine (4)

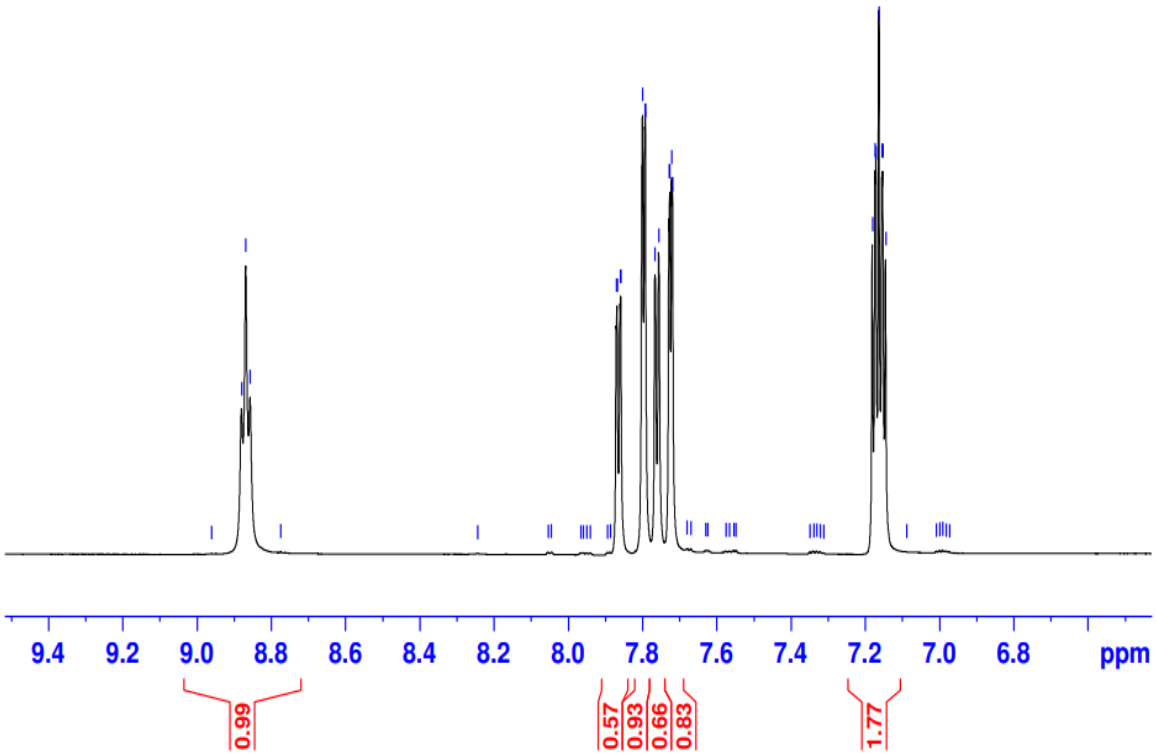

Figure B39d

[1]H NMR of 2-thiophenecarbonylglycine (4)

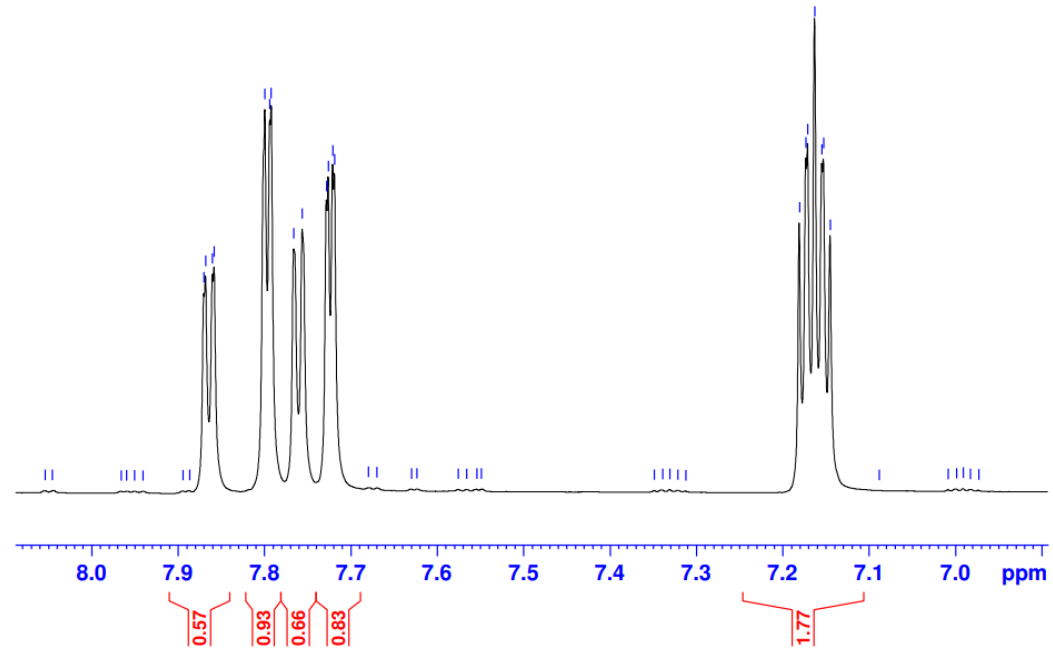

Figure B40a

[13]C NMR of 2-thiophenecarbonylglycine (4)

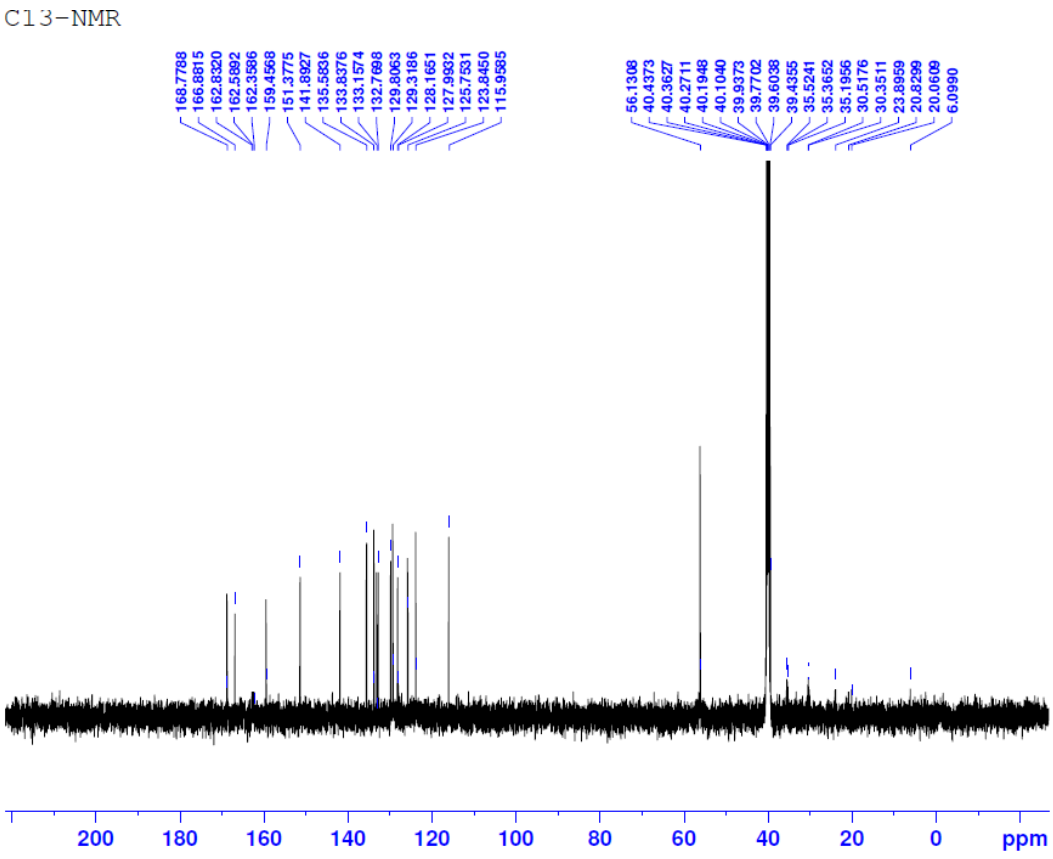

Figure B40b

^{13}C NMR of 2-thiophenecarbonylglycine (4)

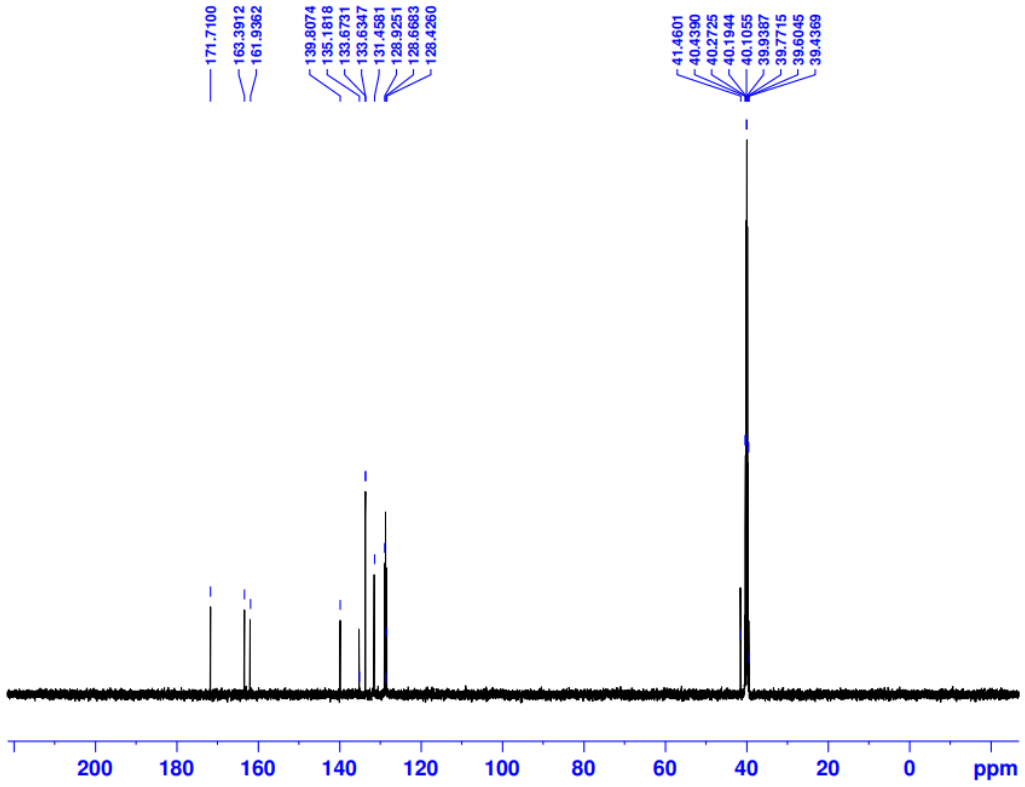

Figure B41a

^{1}H NMR of (Z)-3-((2-bromophenyl)amino)-5-(4-hydroxy-3-methoxybenzylidene)-2-(thiophen-2-yl)-3,5-dihydro-4H-imidazol-4-one (5a)

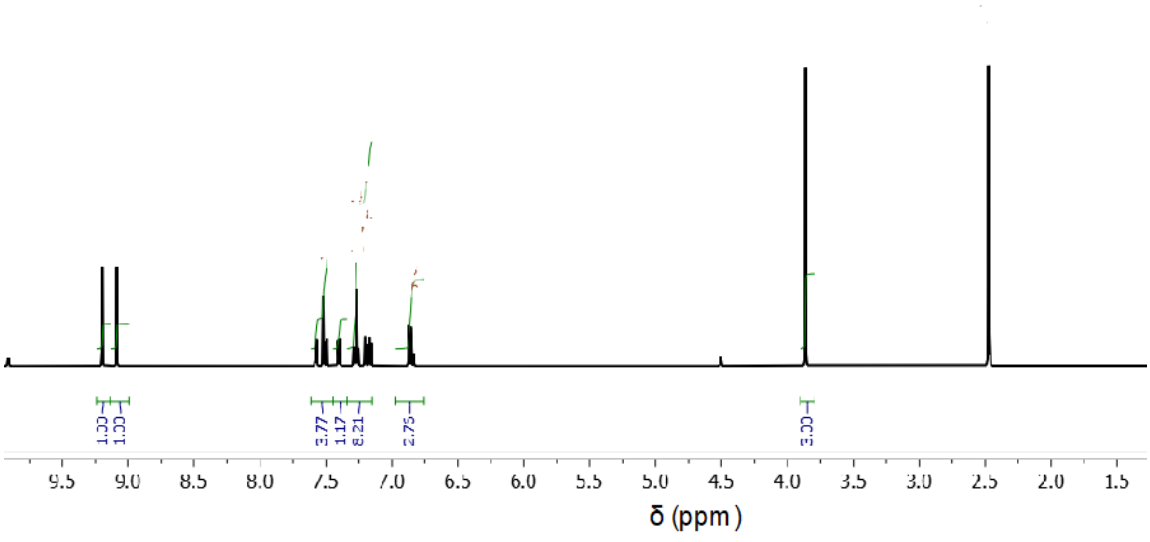

Figure B41b

^{1}H NMR of (Z)-3-((2-bromophenyl)amino)-5-(4-hydroxy-3-methoxybenzylidene)-2-(thiophen-2-yl)-3,5-dihydro-4H-imidazol-4-one (5a)

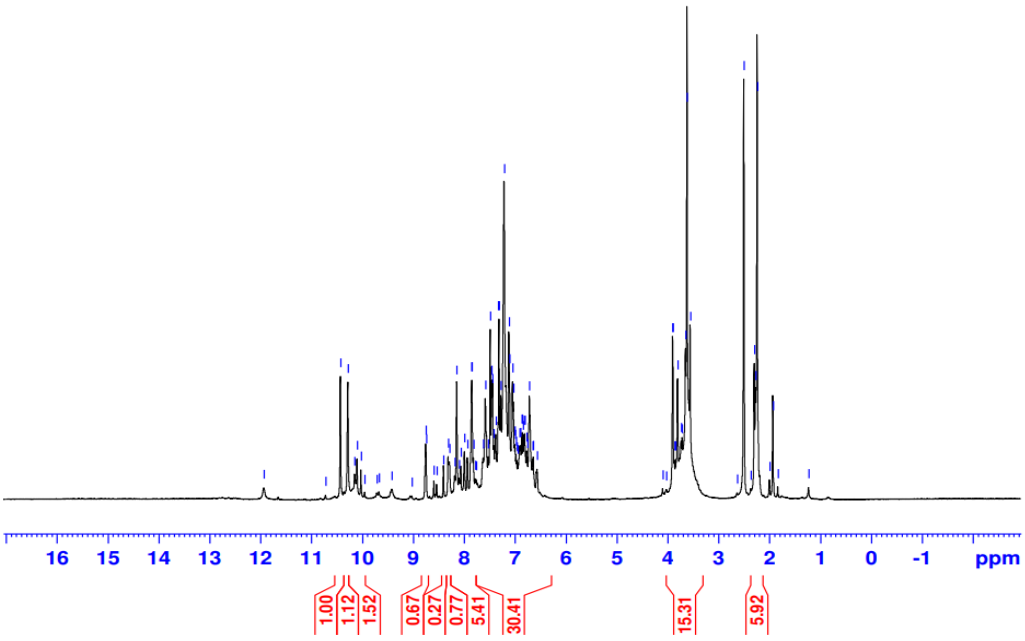

Figure B41c

^{1}H NMR of (Z)-3-((2-bromophenyl)amino)-5-(4-hydroxy-3-methoxybenzylidene)-2-(thiophen-2-yl)-3,5-dihydro-4H-imidazol-4-one (5a)

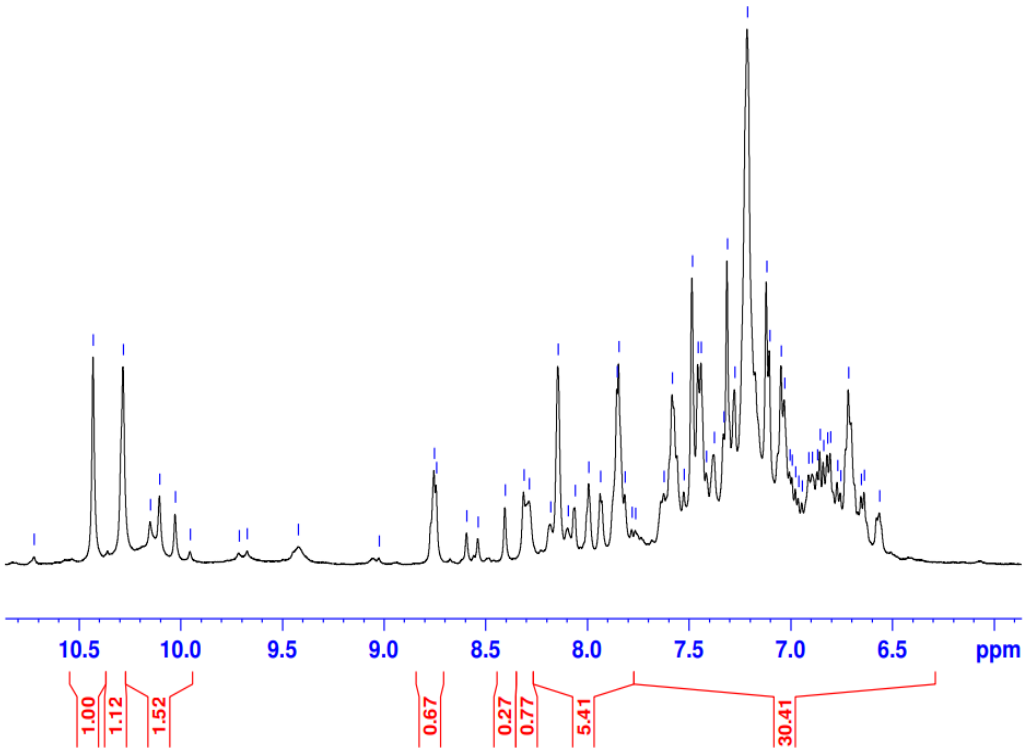

Figure B42a

^{1}H NMR of (Z)-3-((2-chlorophenyl)amino)-5-(4-hydroxy-3-methoxybenzylidene)-2-(thiophen-2-yl)-3,5-dihydro-4H-imidazol-4-one (5b)

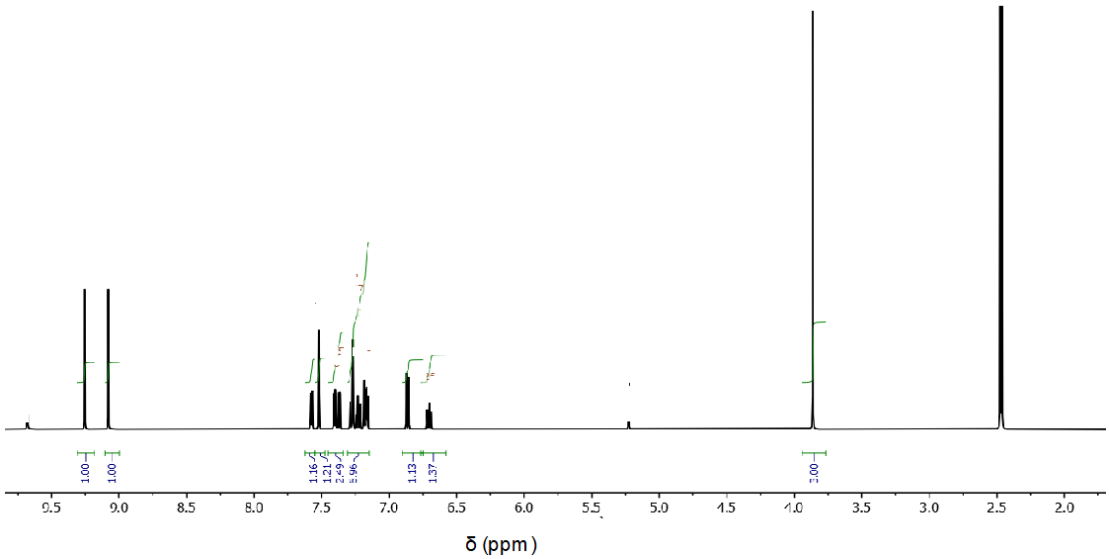

Figure B42b

^{1}H NMR of (Z)-3-((2-chlorophenyl)amino)-5-(4-hydroxy-3-methoxybenzylidene)-2-(thiophen-2-yl)-3,5-dihydro-4H-imidazol-4-one (5b)

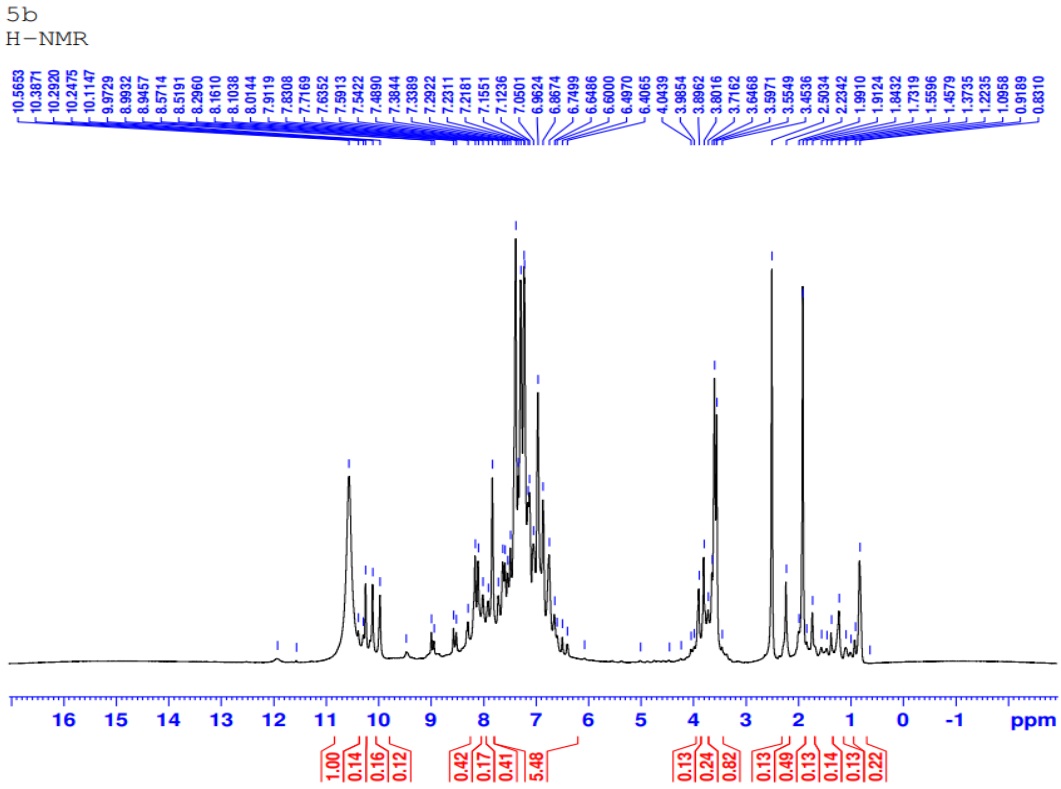

Figure B42c

^{1}H NMR of (Z)-3-((2-chlorophenyl)amino)-5-(4-hydroxy-3-methoxybenzylidene)-2-(thiophen-2-yl)-3,5-dihydro-4H-imidazol-4-one (5b)

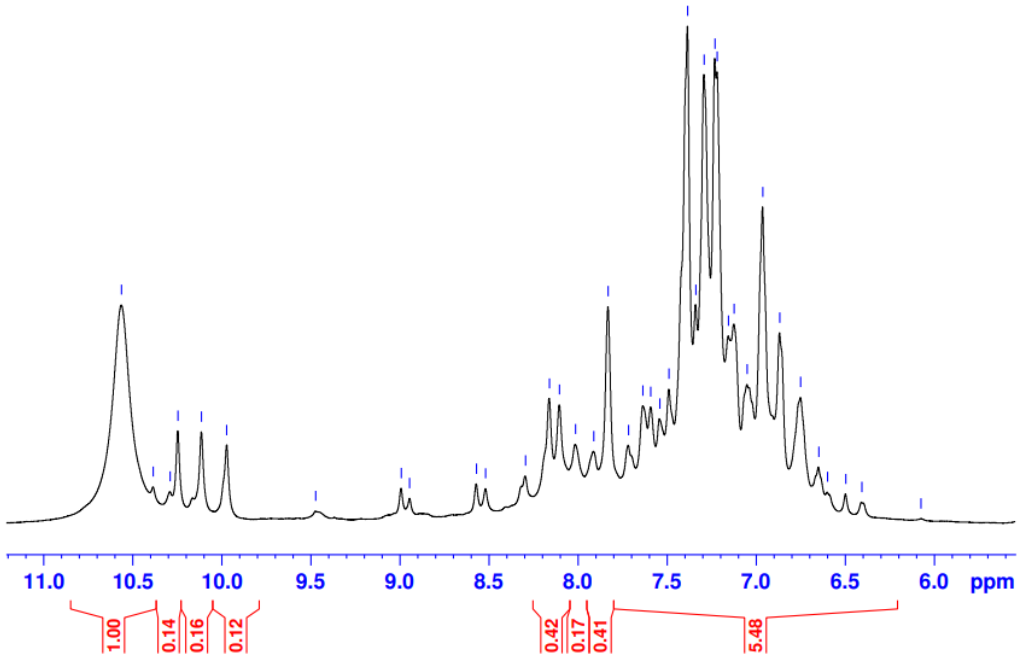

Figure B42d

^{1}H NMR of (Z)-3-((2-chlorophenyl)amino)-5-(4-hydroxy-3-methoxybenzylidene)-2-(thiophen-2-yl)-3,5-dihydro-4H-imidazol-4-one (5b)

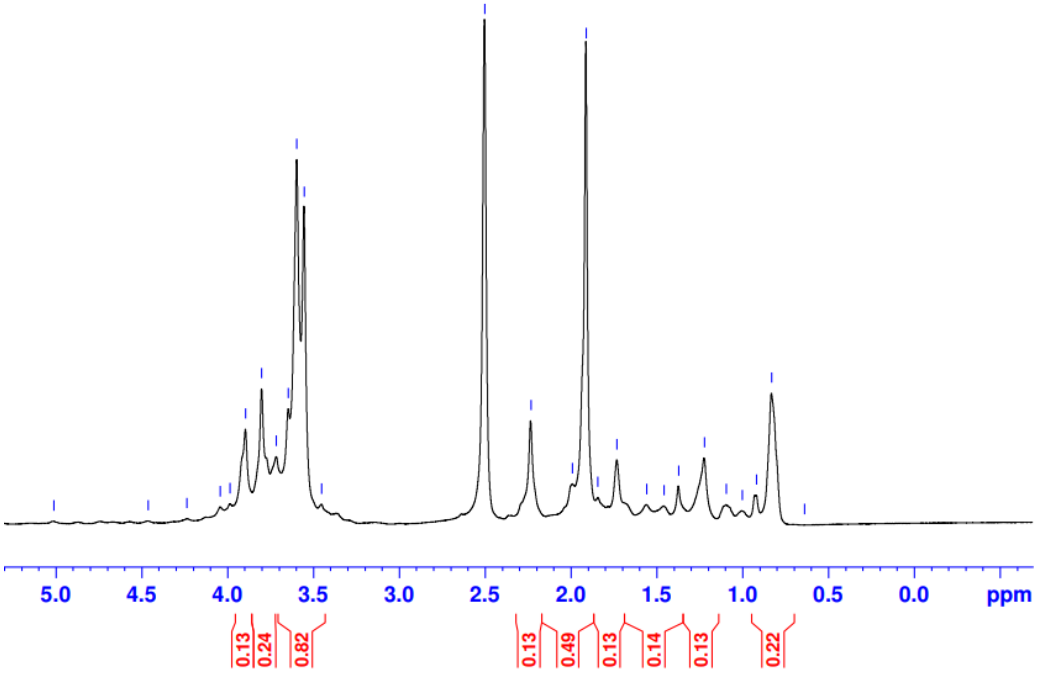

Figure B43

[1]H NMR of (Z)-5-(4-hydroxy-3-methoxybenzylidene)-3-(2-hydroxyethyl)-2-(thiophen-2-yl)-3,5-dihydro-4H-imidazol-4-one (5c)

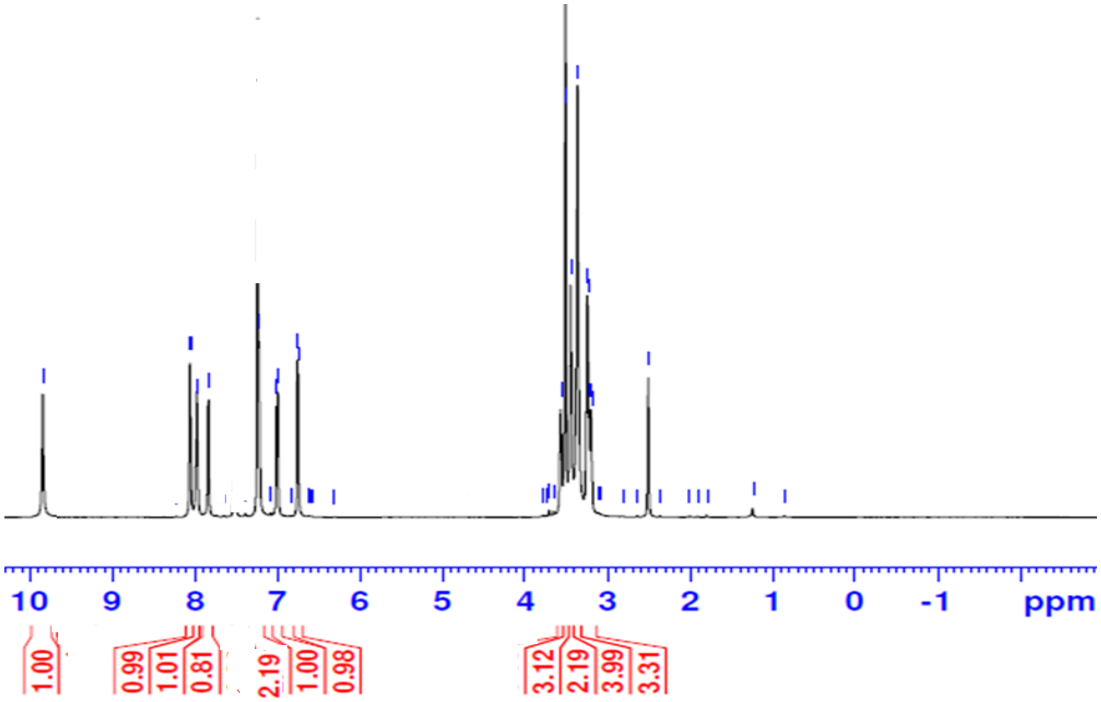

Figure B44

[13]C NMR of (Z)-5-(4-hydroxy-3-methoxybenzylidene)-3-(2-hydroxyethyl)-2-(thiophen-2-yl)-3,5-dihydro-4H-imidazol-4-one (5c)

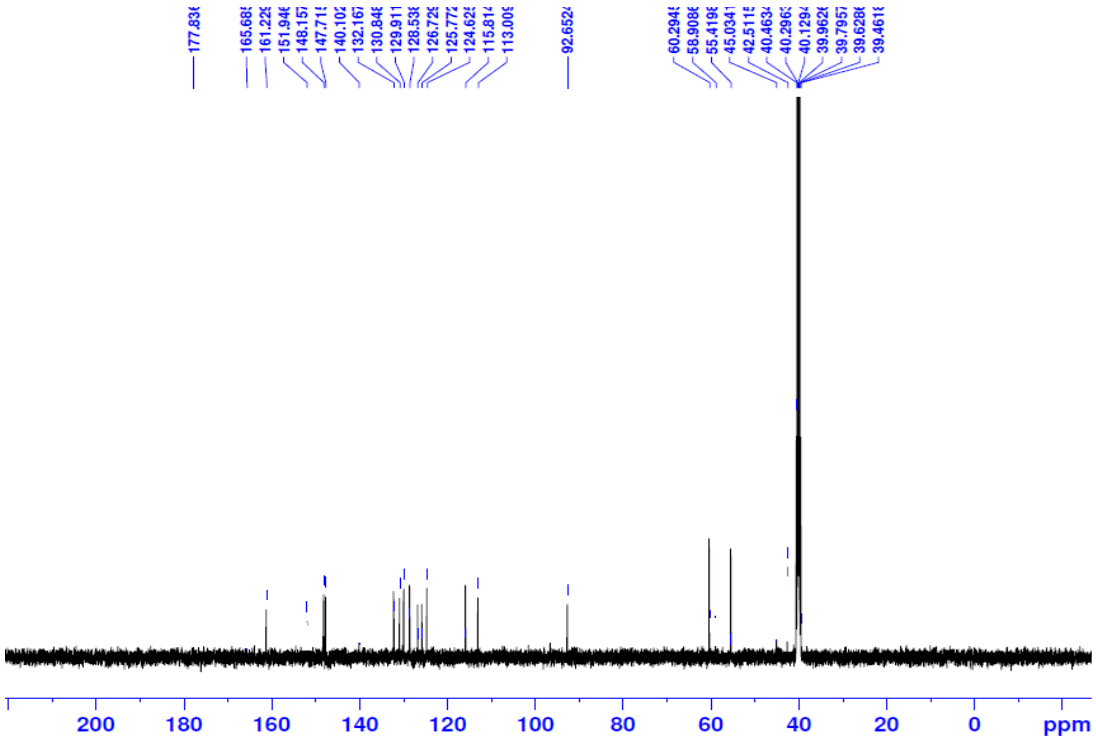

Figure B45a

^{1}H NMR of (Z)-5-(4-hydroxy-3-methoxybenzylidene)-3-(2-(methylamino)ethyl)-2-(thiophen-2-yl)-3,5-dihydro-4H-imidazol-4-one (5d)

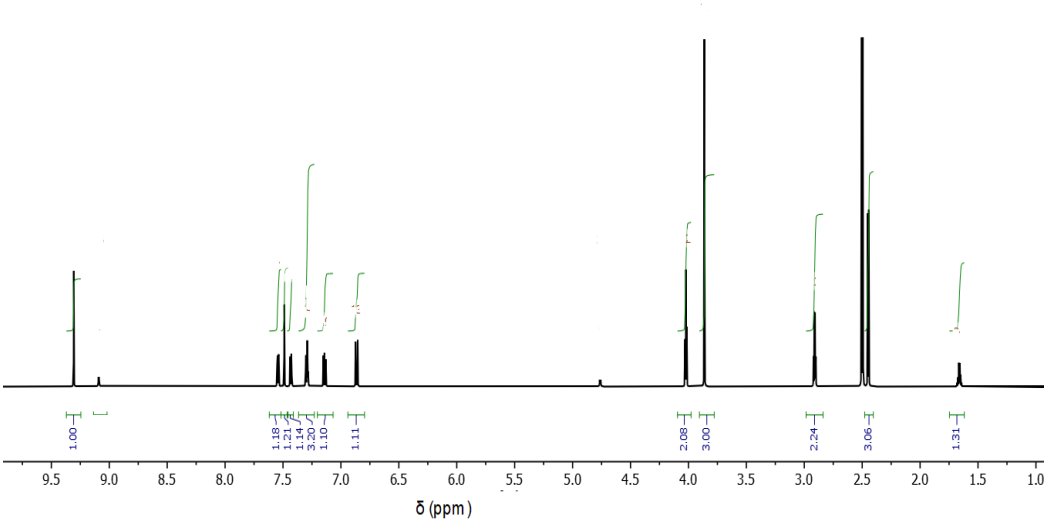

Figure B45b

^{1}H NMR of (Z)-5-(4-hydroxy-3-methoxybenzylidene)-3-(2-(methylamino)ethyl)-2-(thiophen-2-yl)-3,5-dihydro-4H-imidazol-4-one (5d)

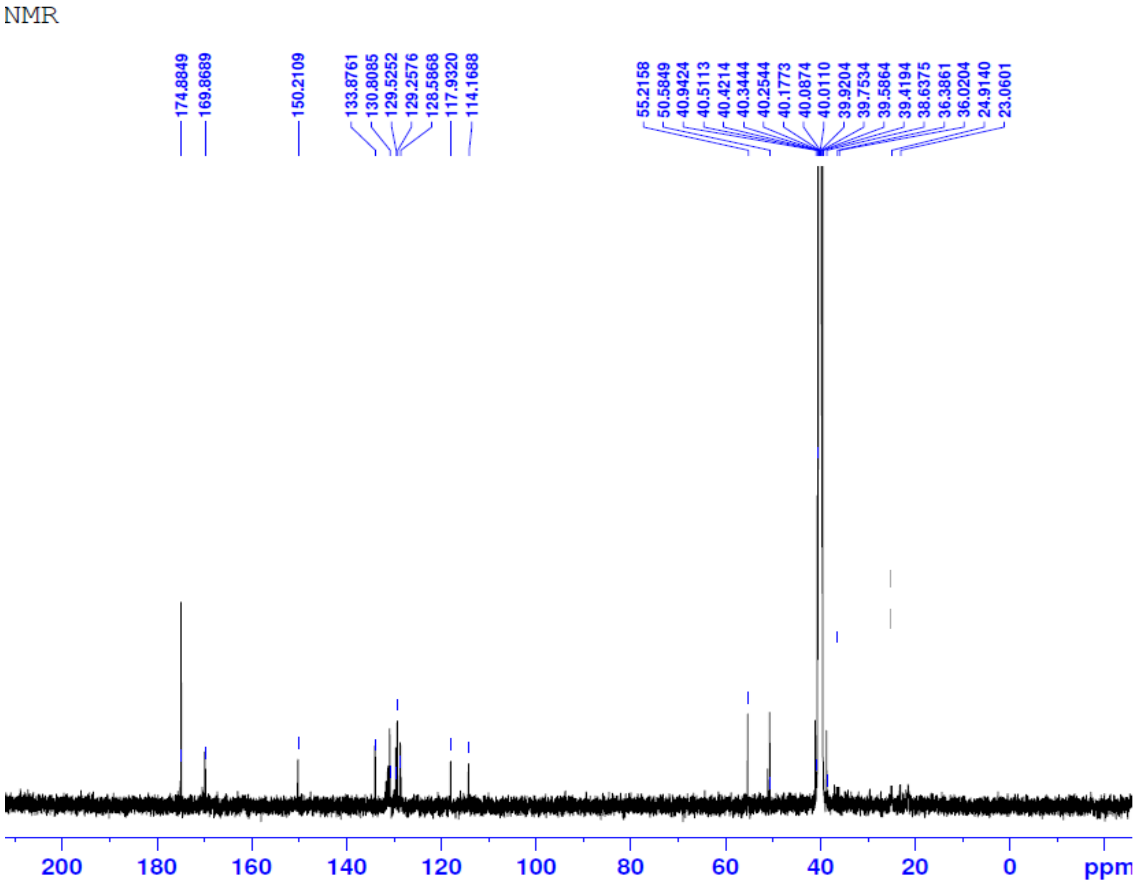

Figure B46

[1]H NMR of (Z)-3-butyl-5-(4-hydroxy-3-methoxybenzylidene)-2-(thiophen-2-yl)-3,5-dihydro-4H-imidazol-4-one (5e)

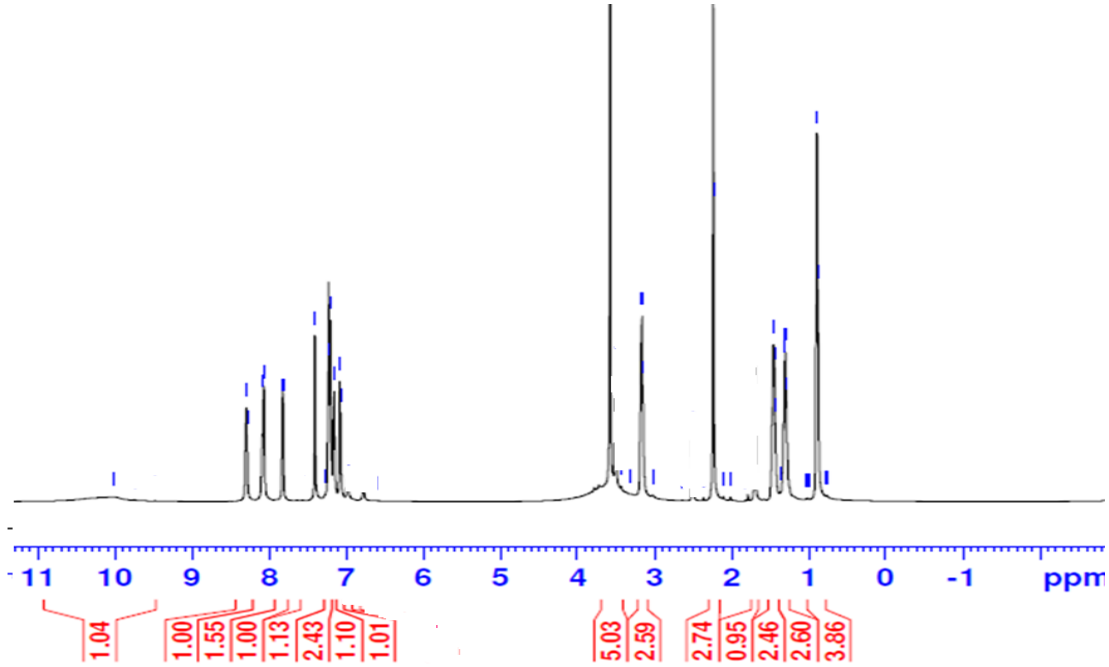

Figure B47

[13]C NMR of (Z)-3-butyl-5-(4-hydroxy-3-methoxybenzylidene)-2-(thiophen-2-yl)-3,5-dihydro-4H-imidazol-4-one (5e)

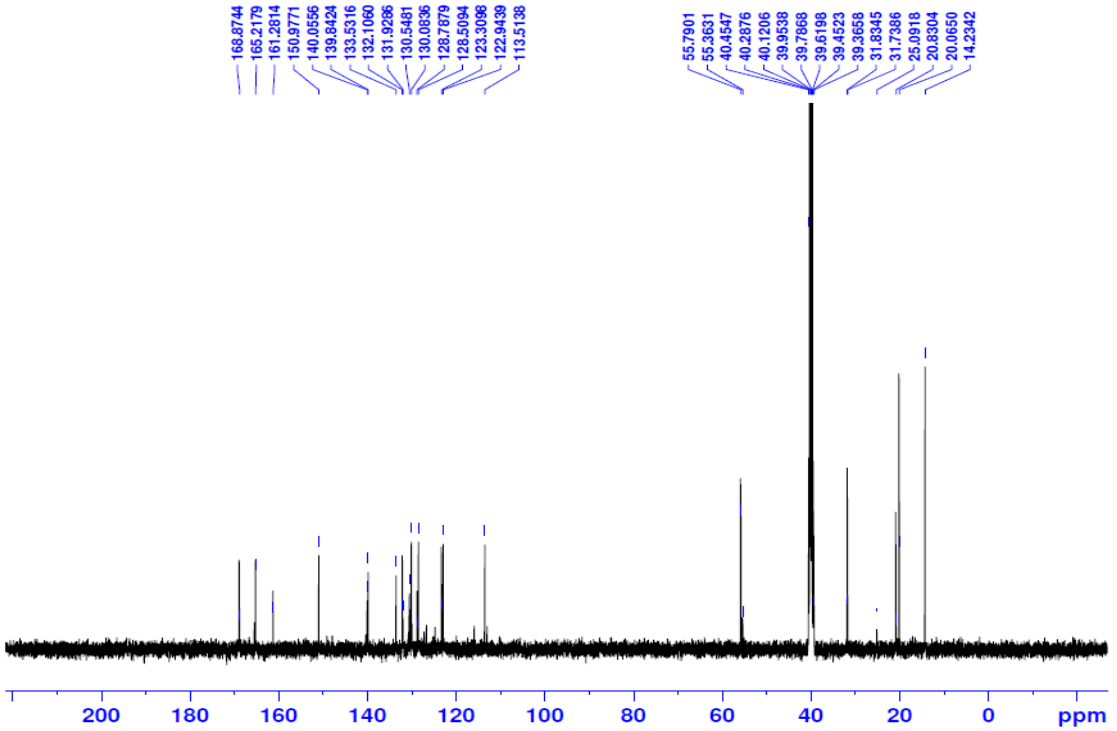

Figure B48

^{1}H NMR of (Z)-3-dodecyl-5-(4-hydroxy-3-methoxybenzylidene)-2-(thiophen-2-yl)-3,5-dihydro-4H-imidazol-4-one (5f)

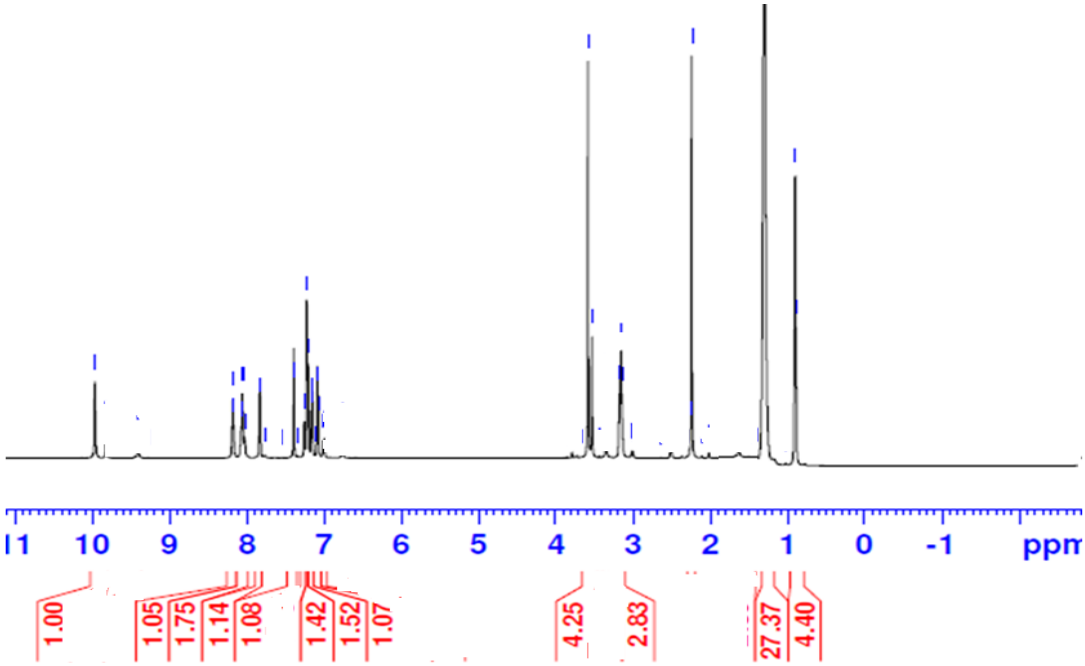

Figure B49

^{13}C NMR of (Z)-3-dodecyl-5-(4-hydroxy-3-methoxybenzylidene)-2-(thiophen-2-yl)-3,5-dihydro-4H-imidazol-4-one (5f)

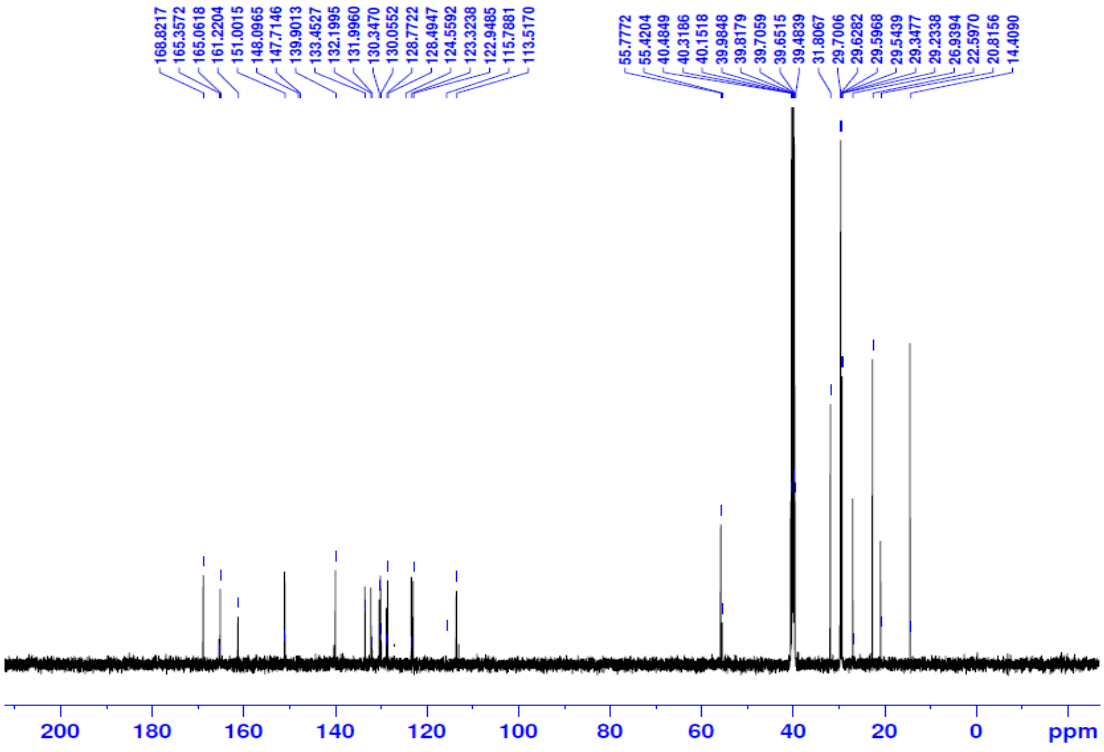

Figure B50

^{1}H NMR of (Z)-5-(4-hydroxy-3-methoxybenzylidene)-3-(pyridin-3-ylmethyl)-2-(thiophen-2-yl)-3,5-dihydro-4H-imidazol-4-one (5g)

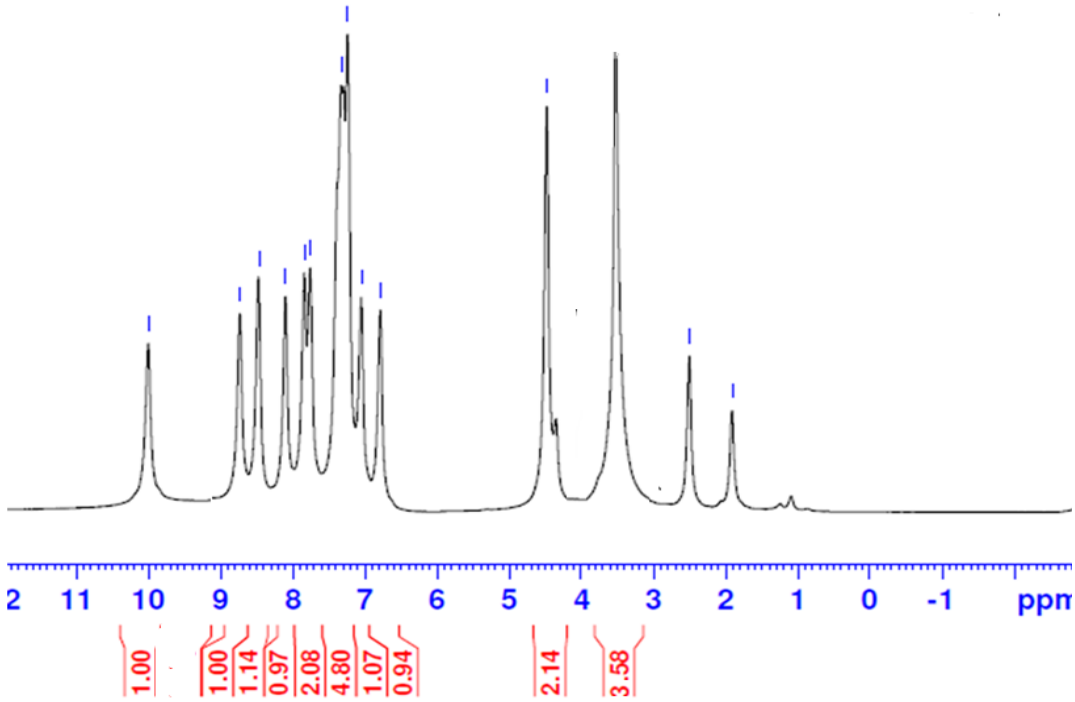

Figure B51

^{13}C NMR of (Z)-5-(4-hydroxy-3-methoxybenzylidene)-3-(pyridin-3-ylmethyl)-2-(thiophen-2-yl)-3,5-dihydro-4H-imidazol-4-one (5g

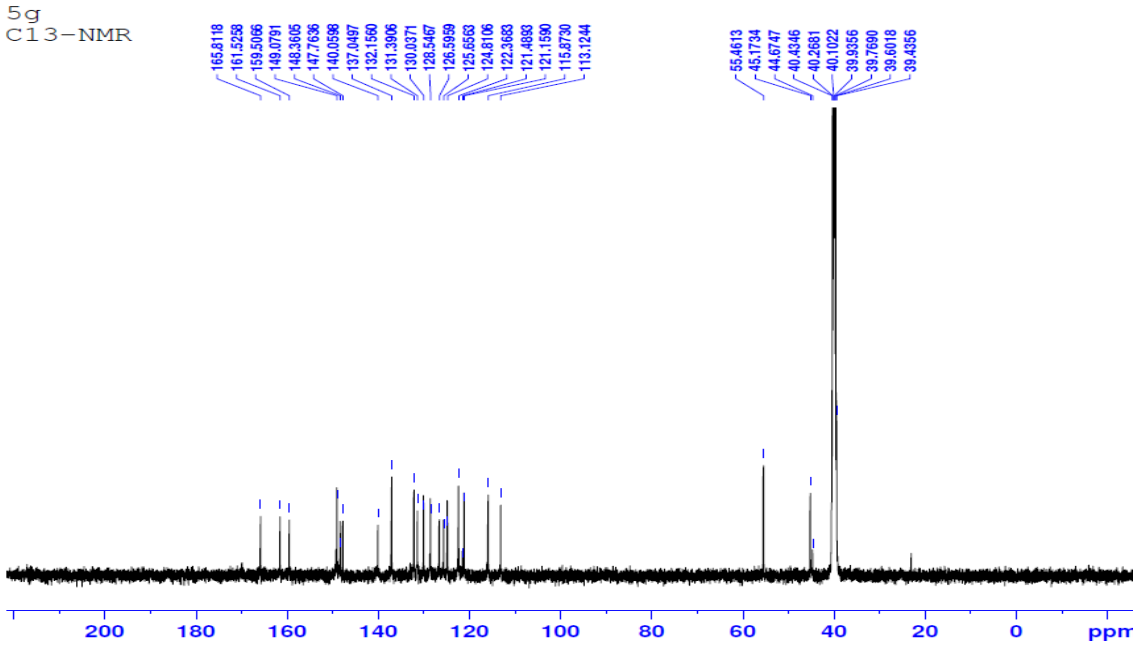

جـامعـــة النجاح الوطنية

كليـــة الدراســـات العليـــا

التصميم والتحضير والنشاط الحيوي والارساء الجزيئي لمشتقات الإيميدازولون المحتوية على مجموعات محبة للماء ومحبة للدهون

إعداد

أسوة مروان حسن فارس

إشراف

أ. د. عثمان حامد

قُدّمت هذه الأطروحة استكمالا لمتطلبات الحصول على درجة الدكتوراه في الكيمياء، من كلية الدراسات العليا، في جامعة النجاح الوطنية، نابلس– فلسطين.

2025

التصميم والتحضير والنشاط الحيوي والارساء الجزيئي لمشتقات الإيميدازولون المحتوية على مجموعات محبة للماء ومحبة للدهون

إعداد

أسوة مروان حسن فارس

بإشراف

أ. د. عثمان حامد

الملخص

أظهرت العلاجات الكيميائية المتوفرة حاليًا آثارًا جانبية سلبية تؤدي إلى تلف دائم في الأعضاء البشرية. لذلك، يُمثل إيجاد علاج فعال للسرطان بأقل آثار جانبية تحديًا كبيرًا. في هذا البحث، تم تصنيع سلسلتين جديدتين من مشتقات الإيميدازولون، إحداهما تحتوي على مجموعة فينيل (3a–g) والأخرى تحتوي على مجموعة ثيوفين (5a–g)، عن طريق التكثيف الحلقي لمشتقات الأوكسازولون القائمة على الفانيلين مع أمينات مختلفة.

تم تحليل النشاط المضاد للسرطان لمشتقات الإيميدازولون المُصنّعة ضد أربع سلالات مختلفة من الخلايا السرطانية: خلايا سرطان الكبد (HepG2)، وسرطان عنق الرحم (HeLa)، وسرطان القولون (CaCo-2)، وسرطان الثدي (MCF-7). أظهر إيميدازولون 3f الذي يحتوي على سلسلة دوديسيل أعلى نشاط مضاد للسرطان، حيث بلغت قيمة IC_{50} 3.2 ± 65.26 ميكرومولار ضد خلايا HepG2 و20.02 ± 3.5 ميكرومولار ضد MCF-7. وأظهر إيميدازولون g5 مع مجموعة الثيوفين والبيريديل أعلى كفاءة بين جميع المشتقات المختبرة، حيث بلغت قيمة 2.3 ± 18.44 IC50 ميكرومولار و5.96 ± 2.3 ميكرومولار ضد خلايا Hela و CaCo-2، على التوالي. أما إيميدازولون b5 مع مجموعة الكلوروفينيل، فقد بلغت قيمة 0.7 ± 2.18 IC50 ميكرومولار و5.51 ± 1.1 ميكرومولار ضد خلايا HepG2 و Hela، على التوالي.

تم تقييم الحركية الدوائية والقدرة المضادة للأورام لأكثر الإيميدازولونات نشاطًا من خلال تقنية ADME والالتحام الجزيئي. تؤكد خصائص ADME على تشابهها الدوائي الإيجابي وفقًا لإرشادات ليبينسكي، حيث تتراوح الأوزان الجزيئية بين 357.43 (5d) و468.65 غ/مول .(5f) تُظهر الجزيئات 3 g و3 f و5 fروابط هيدروجينية مثالية، وتوافرًا حيويًا معتدلًا (0.55)، ودرجات سهولة الوصول التركيبية بين 3.78 و4.76. تُبرز دراسات الالتحام مع بروتيني MAN 4 وHNJ 1 تفاعلات قوية مع 3 g و3 f و5f، حيث يُظهر الجزيء 3 g أفضل ارتباط مع MAN 4(−52.13 كيلو كالوري/مول) و5 fمع HNJ 1(−38.63 كيلو كالوري/مول). تُشير هذه النتائج إلى أن الإيميدازولونات 3 g و5 f مرشحان واعدان لعلاج السرطان المُستهدف.

بالإضافة إلى ذلك، تم فحص النشاط المضاد للبكتيريا للأوكسازولونات المُحضّرة. كان أوكسازولون 8، المحتوي على مجموعة 2−ثيوفينيل، الأكثر فعاليةً، بتركيز مثبط أدنى (MIC) قدره 500 ميكروغرام/مل، ضد جميع سلالات البكتيريا المُختبرة، بما في ذلك المكورات العنقودية الذهبية الأكثر مقاومة. يمكن لمزيج هذه الأوكسازولونات مع المضادات الحيوية التجارية أن يُعطي تأثيرًا تآزريًا يُثبّط نمو البكتيريا عند قيم (MIC) منخفضة.

الكلمات المفتاحية: فانيلين، مضاد للأورام، مضاد للميكروبات، محب للدهون، إيميدازولون، ثيوفين، الارساء الجزيئي.